

**Role of Notch-Delta Signalling in Cell Fate
Determination during Cutaneous Epithelial
Differentiation**

Mohamed A. Al Shuaili

A Thesis submitted in candidature for the degree of

Master of Philosophy in Medicine

(Dermatology)

School of Medicine, Cardiff University

MPhil (2011)

Table of Contents

Declaration.....	4
Acknowledgements.....	4
Abbreviation.....	5
List of Figures.....	7
List of Tables.....	11
Abstract.....	12
CHAPTER 1 – Introduction	16
1.1 Human Skin.....	16
1.1.1 Skin Structure.....	16
1.1.2 Stem Cells and Transit Amplifying (TA) Cells.....	17
1.1.3 Epidermal Differentiation (Keratinisation).....	21
1.1.4 Keratin Expression in the Epidermis.....	26
1.1.5 Calcium Regulation of Keratinocyte Differentiation.....	30
1.2 Notch Signalling Pathway.....	33
1.2.1 Historical Background.....	33
1.2.2 Notch Signalling in Epidermal Development.....	35
1.2.3 Structure of Notch Receptors and Ligands.....	42
1.2.4 Notch Signalling Pathways.....	44
1.2.5 Notch Transcriptional Regulation.....	50
1.2.6 Target Genes of Notch Signalling.....	55
1.2.7 HES and HERP Gene Families.....	56
1.2.8 Regulation of HES and HERP Gene Families in the Epidermis.....	59
1.2.9 Role of Notch Signalling in Epidermal Development:.....	61
CHAPTER 2: Materials and Methods	66
2.1 Keratinocyte Cell Culture Models.....	67
2.1.1 HaCaT Cells.....	67
2.1.2 Calcium-Induced Differentiation.....	71
2.2 Immunofluorescence (IMF).....	73
2.2.1 Tissue and Cell Preparation.....	75
2.2.2 Antibodies.....	76

2.2.3	<i>Labelling Procedure</i>	78
2.2.4	<i>Assessment of Results</i>	80
2.3	Total Protein Extraction and Analysis	80
2.3.1	<i>Extracting Proteins from Cultured Cells</i>	81
2.3.2	<i>SDS-Polyacrylamide Gel Electrophoresis</i>	83
2.4	RNA Extraction	85
2.5	Polymerase Chain Reaction (PCR)	87
2.5.1	<i>Reverse Transcription PCR (RT-PCR)</i>	88
2.5.2	<i>Standard PCR</i>	90
2.5.3	<i>Agarose Gel Electrophoresis</i>	96
2.5.4	<i>Quantitative Real Time PCR (QPCR)</i>	98
2.6	Cloning and Plasmid Extraction	105
2.7	Sequencing.....	118
CHAPTER 3: Expression of Keratin Genes (KRT14 and KRT10) in HaCaT Cell Culture Model		126
3.1	Introduction.....	127
3.2	Morphology of HaCaT Cells during Calcium-Induced Terminal Differentiation	130
3.3	Expression of K10 in HaCaT Cell Culture Model	132
3.4	Expression of K14 in HaCaT Cell Culture Model	157
CHAPTER 4: Expression of Notch Receptors, Ligands and Target Genes in HaCaT Cell Model		166
4.1	Introduction	167
4.2	Expression of Notch Receptors in HaCaT Cells	170
4.3	Expression of Notch Ligands (DLL1, JAG1 and JAG2) in HaCaT Cells.....	187
4.4	Expression of Notch Target Genes (HES and HERT) in HaCaT Cells	232
4.5	Summary	250
CHAPTER 5: Discussion and Conclusions		251
References		266

Acknowledgements

I would like to convey thanks to His Majesty Sultan Qaboos, Sultan of Oman, Diwan of the Royal Court and the Cultural Attaché at the Oman Embassy in London for providing my MPhil scholarship and the financial means to cover the necessary laboratory facilities. Also, this research would not have been possible without the support of many people. I owe my deepest gratitude to my lovely wife and to my beloved family for their understanding and endless love, through the duration of my studies. It is an honour for me to express gratitude to my supervisor, Dr. Paul E. Bowden who has been abundantly helpful and offered invaluable assistance, support and guidance from the very early stages of this research to the submission of this thesis. I would also like to thank my co-supervisor, Dr. Mark Lewis. Above all, thanks go to Mrs. Tammy Greaves (ne Easter) and Mrs. Fiona Rouge who provided unflinching encouragement at the bench and support in many ways, without which the study would not have been successful. I am indebted to many colleagues for supporting me, especially other members of the research group: Dr. Musheera Mohammad Ali, Dr. Marisa Taylor, Dr. Chantal Suthanathan, and Mary Cleaton for sharing literature and methodology. I must also forget to thank my best friends Dr. Ausama Abou Atwan and Dr. Clarence Beavers who were always there to help.

Abbreviations

ADAM	A Desintegrin and Metalloproteinase
bHLH	Basic Helix-Loop-Helix
BM	Basement Membrane
BMP	Bone Morphogenetic Protein
BMPR	Bone Morphogenetic Protein Receptor
CBF1	C-Binding Factor1
CCDK8	Complex of Cyclin C and Cyclin Dependent Kinase 8
cDNA	Complementary (Copy) Deoxyribonucleic acid
CSL	CBF1, Su (H) and Lag1
DSL	Delta, Serrate and Lag1
DLL1	Delta like 1
DMEM	Dulbecco's Modified Eagle's medium
DP	Dermal Papilla
ECM	Extracellular Matrix
EE	Epidermal Equivalent
EGF	Epidermal Growth Factor
EGFR	Epidermal Growth Factor Receptor
EPU	Epidermal Proliferation Unit
FA	Focal Adhesion
FACS	Fluorescence-Activated Cell Sorter
GFP	Green Fluorescent Protein
GRP58	Glucose-Regulated Protein 58
HaCaT	Human Keratinocyte Cell Line
hARP	Human Acidic Ribosomal Phosphoprotein
HERP	HES Related Repressor Protein
HES1	Hairy Enhancer of Split 1
IFE	Interfollicular Epidermis
IPTG	Isopropyl-thio-2-D-galactopyranoside
IRS	Inner Root Sheath
JAG	Jagged

K	Keratin
KCs	Keratinocytes
KHG	Keratohyalin Granules
MAML	Mastermind Like
MAPK	Mitogen Activator Protein Kinase
mRNA	Messenger Ribonucleic acid
N	Notch
NHK	Normal Human Keratinocytes
NICD	Notch Intracellular Domain
OFUT1	O-Fucosyl Transferase
ORS	Outer Root Sheath
PI3K	Phosphatidyl-Inositol-3-Kinase
PBS	Phosphate Buffered Saline
PCR	Polymerase Chain Reaction
PEST	Proline, Glutamic Acid, Serine, Threonine Rich Sequence
PPAR	Peroxisome Proliferators Activated Receptor
RBP-JK	Recombination Signal Binding Protein-J Kappa
RNA	Ribonucleic Acid
RPL13A	Ribosomal Protein Large 13 A
RTK	Receptor Tyrosine Kinase
SCs	Stem Cells
Su (H)	Suppressor of Hairless
TA	Transit Amplifying
TACE	Trans-Activating Converting Enzyme
TAD	Transcriptional Activator Domain
TBP	TATA- Binding Protein
TF	Transcription Factor
TF2H	Transcription Factor 2H
TNF	Tumour Necrotic Factor

List of Figures

Figure 1.1: Schematic Illustration of the Structure of Human Epidermis	23
Figure 1.2: Organization of Keratinocytes and Corneocytes in the Epidermis.....	26
Figure 1.3: Expression of Notch Receptors, Ligands and Target Genes in Human Epidermis.....	38
Figure 1.4: Schematic Structure of Notch receptor.....	40
Figure 1.5: Schematic Diagram of Notch Signalling Pathway in Drosophila.	
Figure 1.6: Schematic Diagram of Notch signalling Pathway in Mammals.	42
Figure 1.7: Schematic illustration of Notch Receptor and Ligand (Delta, Jagged) Structure.	43
Figure 1.8: Schematic of Canonical and Non-Canonical Notch Signalling Pathways.....	44
Figure 1.9: Schematic Illustration of Notch Signalling Pathway in Mammals.	48
Figure 1.10: Domain Structure of Notch Receptor Proteins.	50
Figure 1.11: Notch1 Function in Epidermis.....	56
Figure 1.12: Schematic of Notch Target Genes (HES, HERP and DEC).	59
Figure 2.1: Counting cells under Light Microscope using a Haemocytometer.	71
Figure 2.2: HaCaT Calcium Shift Assay.....	73
Figure 2.3 : Schematic Representation of Two Immunofluorescence Methods.	74
Figure 2.4: Schematic of Double Immunofluorescence.	75
Figure 2.5: Diagram Illustrating Oligo dT Primed Reverse Transcription of Poly A ⁺ mRNA.	90
Figure 2.6: Chart of Temperature Cycles during PCR.....	94
Figure 2.7: Graph of Three Stages in Standard PCR.	95
Figure 2.8: Analysis of PCR Fragments by Agarose Gel Electrophoresis.....	97
Figure 2.9: Binding of SYBR Green to DNA in Real Time PCR.	100
Figure 2.10: Graph of DNA Copy Number versus Cycle Number (qPCR).....	105
Figure 2.11: Schematic of Cloning a PCR Fragment into pGEM-T Easy.....	106
Figure 2.12: Diagram to Illustrate DNA Cleavage by EcoR1.	108
Figure 2.13: Analysis of Housekeeping Gene (<i>hARP</i>) Insert by Agarose Gel (1.5%) Electrophoresis.	114
Figure 2.14: Structure of pGEM-T Vector.	115
Figure 2.15: Standard View of a Sequence Chromatogram.....	121
Figure 2.16: Multi-Panel View of Sequence Chromatogram	122
Figure 2.17: Sequencing Chromatogram of Data from a Typical Sample.	123
Figure 2.18: Sequence of Notch 3 Insert.	123
Figure 2.19: Sequencing Chromatogram of pGEM-T vector and JAG2 insert.	124

Figure 3.1: Phase Contrast Micrographs of Early Passage HaCaT Cells.	132
Figure 3.2: Expression of K14 by SDS-PAGE and Western Blotting of Protein Extracts from HaCaT Cells Grown under Different Conditions.....	133
Figure 3.3: Expression of K10 by SDS-PAGE and Western Blotting of Protein Extracts from HaCaT Cells Grown under Different Conditions.....	134
Figure 3.4: Expression of K14 (Proliferation Marker) and Ki67 (Cell Division Marker) in HaCaT cells.	135
Figure 3.5: Expression of K10 (Differentiation Marker) in HaCaT cells.	136
Figure 3.6: Assessing Genomic DNA Contamination in Total RNA Extracts of HaCaT Cells.	138
Figure 3.7: Analysis of K14 PCR Products from HaCaT Cell cDNA by Agarose Gel Electrophoresis.	140
Figure 3.8: Analysis of K14 PCR Products from HaCaT Cell cDNA by Agarose Gel Electrophoresis.	141
Figure 3.9: Analysis of K10 PCR Products from HaCaT Cell cDNA by Agarose Gel Electrophoresis.	142
Figure 3.10: Analysis of K10 Plasmid Digests by Gel Electrophoresis.	143
Figure 3.11: Analysis of K14 Plasmid Digests by Gel Electrophoresis.	144
Figure 3.12: Analysis of Standard PCR with K10 Plasmid 5 Serial Dilutions.	146
Figure 3.13: Amplification Plot of K10 Plasmid Dilution Series.....	149
Figure 3.14: Standard Curve of K10 Plasmid Dilution Series.	150
Figure 3.15: K10 Gene Expression in HaCaT Cells during Calcium-induced Differentiation.....	155
Figure 3.16: K10 Gene Expression in HaCaT Cells during Calcium-induced Differentiation.....	156
Figure 3.17: Amplification Plot of K14 Plasmid Dilution Series.....	157
Figure 3.18: Standard Curve of K14 Plasmid Dilution Series.	158
Figure 3.19: Analysis of K14 Gene Expression (Copy Number) in HaCaT Cells during Calcium-induced Differentiation.	163
Figure 3.20: Analysis of K14 Gene Expression (Fold Change) in HaCaT Cells during Calcium-induced Differentiation.	163
Figure 3.21: Alterations in K14 and K10 Expression (Copy Number) in HaCaT Cells during Calcium-Induced Differentiation.	164
Figure 4.1: Expression of <i>NOTCH 1</i> during HaCaT Differentiation.....	173
Figure 4.2: Expression of <i>NOTCH 3</i> during HaCaT Cell Differentiation.	174
Figure 4.3: Expression of Notch 1 and Notch 3 in HaCaT Cell Differentiation.	175
Figure 4.4: Analysis of <i>Notch 1</i> Plasmid Digests by Gel Electrophoresis.	176
Figure 4.5: Analysis of <i>Notch 3</i> Plasmid Digests by Gel Electrophoresis.	176
Figure 4.6: PCR Reactions with Serial Dilutions of Notch 3 Plasmid 1 (N3plas1).....	179
Figure 4.7: Amplification Plot of Notch 3 Plasmid Serial Dilutions.	180
Figure 4.8: Standard Curve of Notch 3 Plasmid (Ct Value versus Original Copy Number).	181

Figure 4.9: Notch 3 Expression (Transcript Copy Number) in HaCaT Cells during Calcium-induced Differentiation.	186
Figure 4.10: Notch 3 Expression (Fold Change) in HaCaT Cells during Calcium-induced Differentiation.....	187
Figure 4.11: DLL1 PCR with cDNA from HaCaT Cells.	189
Figure 4.12: DLL1 PCR Products using gDNA and cDNA from HaCaT Cells (D4+10).	191
Figure 4.13: PCR with DLL1 Primers on cDNA from HaCaT Cell Cultures.	192
Figure 4.14: PCR with DLL1 Primers on cDNA from HaCaT Cells.....	193
Figure 4.15: PCR with DLL1 and DLL4 Primers on cDNA from Human Epidermis and Pancreas.	195
Figure 4.16: Analysis of PCR Products with DLL4 Primers.	196
Figure 4.17: Gel Analysis of Cloned Plasmids cut with EcoRI to Release the pGEM-T vector and DLL1 Insert.	198
Figure 4.18: Amplification Plot of <i>DLL1</i> Plasmid Serial Dilutions.....	200
Figure 4.19: Standard Curve of <i>DLL1</i> Plasmid Dilution Series.....	200
Figure 4.20: DLL1 Gene Expression in HaCaT Cells during Calcium-induced Differentiation.....	201
Figure 4.21: DLL1 Gene Expression in HaCaT Cells during Calcium-induced Differentiation.....	202
Figure 4.22: JAG1 Expression in HaCaT Cells.	206
Figure 4.23: JAG2 Expression in HaCaT Cells.	207
Figure 4.24: Analysis of JAG1 PCR Products (fully optimized) from HaCaT Cell cDNA by Agarose Gel Electrophoresis.	208
Figure 4.25: JAG2 PCR Products with cDNA from HaCaT Cells Analysed by Agarose Gel Electrophoresis.....	209
Figure 4.26: Analysis of JAG2 Plasmid Digests by Gel Electrophoresis.	210
Figure 4.27: Analysis of Standard PCR with JAG1 Plasmid 3 Serial Dilutions.....	211
Figure 4.28: Analysis of Standard PCR with JAG2 Plasmid 6 Serial Dilutions.....	213
Figure 4.29: Amplification Plot of JAG1 Plasmid Dilution Series.	214
Figure 4.30: Standard Curve of JAG1 Plasmid Dilution Series.	215
Figure 4.31: JAG1 Gene Expression in HaCaT Cells during Calcium-induced Differentiation.....	220
Figure 4.32: JAG1 Gene Expression in HaCaT Cells during Calcium-induced Differentiation.....	221
Figure 4.33: Immunoperoxidase (IMP) of Human Scalp Skin (frozen sections) to detect JAG1.	222
Figure 4.34: Amplification Plot of JAG2 Plasmid Dilution Series.....	223
Figure 4.35: Standard Curve of JAG2 Plasmid Dilution Series.	224
Figure 4.36: JAG2 Gene Expression in HaCaT Cells during Calcium-induced Differentiation.....	227
Figure 4.37: Expression of Jagged 2 (J2) and K10 (Differentiation Marker) in HaCaT Cells.....	229
Figure 4.38: Immunoperoxidase (IMP) of Human Scalp Skin (Frozen Sections).	230

Figure 4.39: Alterations in JAG1 and JAG2 Expression (Copy Number) in HaCaT Cells during Calcium-Induced Differentiation.	231
Figure 4.40: Expression of HES1 in HaCaT cell differentiation.	234
Figure 4.41: Analysis of HES1 Plasmid Digests by Gel Electrophoresis.	235
Figure 4.42: Amplification Plot of <i>HES1</i> Plasmid serial dilutions.	237
Figure 4.43: Standard Curve of HES1 Plasmid Dilution Series.	238
Figure 4.44: HES1 Gene Expression in HaCaT Cells during Calcium-induced Differentiation.	243
Figure 4.46: HES1 Gene Expression in HaCaT Cells during Calcium-induced Differentiation.	244
Figure 4.46: Immunoperoxidase (IMP) of the epidermis of human scalp skin (frozen sections).	245
Figure 4.47: HES5 Expression in HaCaT Cells.	246
Figure 4.48: Analysis of HES5 Plasmid Digested with EcoRI.	246
Figure 4.49: Gel Analysis of HES7 PCR Products from HaCaT Cell cDNA.	247
Figure 4.50: HEY1 Expression in HaCaT Cells.	248
Figure 4.51: HEY2 Expression in HaCaT Cell Cultures.	249
Figure 4.52: HEYL Expression in HaCaT Cells.	250
Figure 4.53: Expression of JAG1, JAG2, DLL1, HES1 and Notch3 in HaCaT Cells during Calcium-Induced Differentiation.	252
Figure 4.54: Expression Levels of <i>DLL1, K14, K10, JAG2, HES1 and NOTCH3</i> in HaCaT Cells during Calcium-Induced Differentiation.	253

List of Tables

Table 1.1: Characteristics of Immortalized and Normal Human Keratinocytes	32
Table 1.2: Notch Receptors, Ligands and Co-activators in Different Species.....	35
Table 1.3: Classification of Basic Helix-Loop-Helix (bHLH) Proteins.....	58
Table 2.1: Primary Antibodies used for IMF	77
Table 2.2: Secondary Polyclonal Antibodies used in IMF	78
Table 2.3: Preparation of 10% Resolving Gels (SDS-PAGE).....	83
Table 2.4: Preparation of 4% Stacking Gel (SDS-PAGE).....	84
Table 2.5: RT2 Components.....	89
Table 2.6: Typical PCR Reaction Mixture	92
Table 2.7: Stages in PCR Reaction and Timing	93
Table 2.8: Reaction Mixture for qPCR Experiment	101
Table 2.9: Typical Segment Settings for Real Time PCR	103
Table 2.10: Ligation Reaction Component.....	110
Table 2.11: Reagent List for Restriction Enzyme Digest of Cloned Plasmids.....	113
Table 2.12: Mass of <i>Notch 1 Plasmid 3</i> equivalent to Specific Copy Number	116
Table 2.13: Concentration of <i>Notch 1 Plasmid 3</i> DNA.....	116
Table 2.14: Dilution Series for N1plas3 Stock	118
Table 2.15: Different Primers used for Cloning	120
Table 3.1: Table of Primers for Standard PCR and qPCR with cDNA.	128
Table 3.2: Sequence of K14 Oligonucleotide Primers for PCR and qPCR	137
Table 3.3: Sequence of K10 Oligonucleotide Primers for qPCR	139
Table 3.4: Mass and Final Concentration of K10 Plasmid 5.....	145
Table 3.5: Serial Dilutions of K10 Plasmid 5 for qPCR	146
Table 3.6: Serial Dilutions of K14 Plasmid F for qPCR.....	147
Table 3.7: K10 Gene Expression (Copy Number) during HaCaT Cell Culture.....	151
Table 3.8: K10 Gene Expression (Fold Change) in HaCaT Cell Cultures	152
Table 3.9: Comparison of K10 Expression Levels (Copy Number) in Different HaCaT Cultures.....	153
Table 3.10: Comparison of K10 Expression Levels (Fold Change) in HaCaT Cultures..	154
Table 3.11: K14 Gene Expression (Copy Number) during HaCaT Cell Culture.....	159
Table 3.12: K14 Gene Expression (Fold Change) in HaCaT Cell Cultures	160
Table 3.13: Comparison of K14 Levels (Copy Number) in Different HaCaT Cultures...	161
Table 3.14: Comparison of K14 Expression Levels (Fold Change) in HaCaT Cultures..	162
Table 4.1: Table of Primers for Standard PCR and qPCR of Notch, Delta, Jagged, Hes and Hey	169

Table 4.2: Sequence of Notch Primers	171
Table 4.3: Agarose Gel Electrophoresis for PCR Products	172
Table 4.4: Dilution Series for N1plas3 Stock	178
Table 4.5: Dilution Series for N3plas1 Stock	179
Table 4.6: Raw qPCR Data for Notch 3 Gene Expression	183
Table 4.7: Raw qPCR Data for Notch 3 Gene Expression	184
Table 4.8: Statistical Comparison of Notch 3 Levels (Copy Number) at Different Stages of HaCaT Culture	185
Table 4.9: Statistical Comparison of Notch 3 Levels at Different Stages of HaCaT Culture (Fold Change)	185
Table 4.10: Sequence of Delta 1 like (DLL1) Primers	188
Table 4.11: Delta 1 like (DLL1) Primer Sequences	190
Table 4.12: Sequence of Delta Like 4 (DLL4) Primers.....	194
Table 4.13: Summary of <i>DLL1</i> and <i>DLL4</i> data experiments was conducted using standard PCR.	197
Table 4.14: Dilution Series for DLL1 Cloned PCR Product	199
Table 4.15: Statistical Analysis of DLL1 Expression Data.....	203
Table 4.16: Statistical Analysis of DLL1 Expression Data.....	203
Table 4.17: Sequence of Oligonucleotide Primers for JAG1 and JAG2.....	205
Table 4.18: Serial Dilutions of JAG1 Plasmid 3 for qPCR Standards.....	211
Table 4.19: Serial Dilutions of Jag 2 Plasmid 6 for qPCR Standards.....	212
Table 4.20: JAG1 Gene Expression (Copy Number) during HaCaT Cell Culture	216
Table 4.21: JAG1 Gene Expression (Fold Change) in HaCaT Cell Cultures.....	217
Table 4.22: Comparison of JAG1 Expression Levels (Copy Number) in Different HaCaT Cultures.....	218
Table 4.23: Comparison of JAG1 Expression Levels (Fold Change) in HaCaT Cultures.....	219
Table 4.24: JAG2 Gene Expression (Copy Number) during HaCaT Cell Culture	225
Table 4.25: JAG2 Gene Expression (Fold Change) during HaCaT Cell Culture	225
Table 4.26: Comparison of JAG2 Levels (Copy Number) in Different HaCaT Cultures.....	226
Table 4.27: Sequence of HES & HEY Primer Pairs.....	232
Table 4.28: Serial Dilutions of HES1 Plasmid 5 for qPCR	236
Table 4.29: HES1 Gene Expression (Copy Number) during HaCaT Cell Culture	239
Table 4.30: HES1 Gene Expression (Fold Change) in HaCaT Cell Cultures.....	240
Table 4.31: Comparison of HES1 Expression Levels (Copy Number) in Different HaCaT Cultures.....	241
Table 4.32: Comparison of HES1 Expression Levels (Fold Change) in HaCaT Cultures.....	242

Abstract

The notch signalling pathway is essential for the development and growth of all mammalian cells. The canonical pathway works by cell to cell communication and influences gene expression directly. Notch signalling plays an important role in cell differentiation processes in the embryo as well as in adult tissues. In *Drosophila*, signalling requires a single notch receptor and two ligands (delta and serrate). However, in mammals signalling is more complex and there are four notch receptors (NOTCH1-4), three delta like ligands (DLL1, DLL3, DLL4) and two jagged ligands (JAG1, JAG2). The interaction between a notch receptor at the cell surface and its ligand on a neighbouring cell, leads to sequential proteolytic cleavages which release the notch intracellular domain (NICD) from the cell surface receptor (*Estrach et al., 2008*). The NICD enters the nucleus and forms a complex with CSL and Mastermind to activate target genes (HES and HEY family members). Notch receptors have modified EGF-like repeats where fucose has been added to a serine or threonine residue and this O-linked fucose can be elongated by the action of an enzyme (*fringe*), enhancing or blocking ligand binding. There have been extensive studies on notch signalling in embryos but less is known in adult tissues, especially with regard to non-canonical pathways.

The aim of this project was to examine the expression of notch receptors, ligands and specific target genes during epidermal differentiation in human

skin. This was examined both in human epidermis (*in vivo*) as well as in culture models using HaCaT, a keratinocyte cell line. Examining notch signalling activity at different stages of keratinocyte differentiation could help to understand the precise role of notch signalling in cell fate determination during normal cutaneous epithelial cell growth and development, and may indicate what role, if any notch signalling might play in the pathology of skin disease.

Most of the work on delta ligands has been done in embryonic tissues with little work on adult skin. Thus, our approach focused on expression of DLL1, DLL3 and DLL4 in human epidermis and cultured HaCaT cells. DLL1 expression was confirmed (mRNA and protein level including sequence) but no convincing evidence of DLL3 or DLL4 expression was found. Evidence was also obtained for JAG1 and JAG2 expression in human epidermis and cultured cells, and there was some indication that differential expression might occur during terminal differentiation.

RT-PCR results indicated possible changes in notch ligand levels with calcium-induced differentiation in HaCaT cells and these were quantitated by real time PCR (qPCR). Expression levels could not be normalised to a housekeeping gene (β -Actin, human ARP, human TF2H, GRP58, B2H, RPL13 and TBP) as all those tested were not stable enough. Thus, cDNA probes for two notch receptors (N1 and N3), three ligands (DLL1, JAG1 and JAG2), six responsive genes (HES1,

HES5, HES7, HEY1, HEY2 and HEYL) and two keratin genes (KRT14, KRT10) were cloned and used to construct standard curves. This allowed quantitative estimation of expression levels in terms of copy number and fold change in both HaCaT cells and human epidermis. K14, Notch1 and DLL1 changed very little in HaCaT cells but K10, Notch3, JAG1, JAG2 and HES1 levels increased with differentiation. It was also concluded that signalling via Notch3 and JAG1 may influence the progress of terminal differentiation in human keratinocytes.

CHAPTER 1: Introduction

1.1 Human Skin

1.1.1 Skin Structure

Skin is the largest organ system in the human body and has three main components: an outer protective layer (epidermis), a central connective tissue matrix (dermis) and an inner subcutaneous layer of fat (adipose). Human epidermis is a keratinized stratified squamous epithelium that forms a semi-permeable physical barrier to the environment (*Hall and Watt, 1989; Watt, 1989*). Thickness varies according to body site, and epidermis is thickest on the palms of the hand and soles/heels of the feet (1.5 – 4.0 mm) but much thinner at other body sites (0.4- 1.5 mm).

A complex programme involving cell cycle arrest and terminal differentiation controls epidermal homeostasis, a process that involves complex co-ordinated changes in gene expression (*Chuong et al., 2002*). It is important to mention that the epidermis is a continuously self renewing stratified squamous epithelium and the stems cells that generate this tissue, reside in the basal layer. The skin appendages (pilosebaceous unit, nails and sweat glands) are epithelial structures that arise from the epidermis during embryonic development and are contiguous with the epidermis. They maintain their own

stem cell populations and have their own specialised differentiation pathways.

1.1.2 Stem Cells and Transit Amplifying (TA) Cells

In 1961, *Till and McCulloch* reported the first evidence of adult cells that can act as stem cells. This was identified after irradiation of the hematopoietic system and since this time, stem cells have been identified in many other tissues, including epidermis and the bulge area of hair follicles (*Potten and Loeffler, 1990*). The bulge stem cells can produce all the types of epithelial cell required to form all the different layers of the complex hair follicle including the hair shaft (*Taylor et al., 2000*). In the same way, the epidermal stem cell population produces the entire interfollicular epidermis that is necessary to maintain skin integrity.

Epidermal stem cells are considered a small undifferentiated cell population of self renewing basal keratinocytes. They can produce a population of transit amplifying (TA) cells that account for the majority of basal cells (*Bickenbach and Grinnell, 2004*). The relatively minor population of resident stem cells produce an impressive cell turnover rate to form this highly organized stratified tissue (*Mackenzie, 1970; Potten & Bullock, 1983; Morris et al., 1985*). Stem cells respond to multiple signalling networks that control their division, migration, proliferation and differentiation but precise mechanisms within human epidermis are not yet clear (*Fuchs and Horsley, 2008*). Moreover,

differences have been observed in relation to rates of basal cell proliferation versus stratification and differentiation, which vary considerably between embryonic and adult epidermal cells (*Fuchs and Horsley, 2008*). This can most easily be explained by the asymmetric division of stem cells and TA cells, a theory supported by *in vivo* cell kinetic assays (*Potten 1974; Mackenzie 1975; Jones et al., 1995 and Clayton et al., 2007*).

It has been known for several years that stem cells provide the proliferative potential of adult human epidermis and this small cell population resides in the basal cell layer (*Fuchs, 2008*). Several studies have estimated that basal cells are a mixture of stem cells (~10%) and TA cells (~90%). However, stem cells are difficult to define precisely and difficult to isolate for study. They are said to have the capacity to self renew indefinitely and to generate large numbers of proliferative basal cells (transit amplifying or TA cells) and this extensive capacity for cell renewal has been demonstrated *in vivo* (*Jones & Watt, 1993; Gambardella & Barrandon, 2003; Gallico et al., 1984 and Compton et al., 1989*).

In the mid 1970's, three different cell sub-populations were identified in the epidermal basal layer: stem cells, TA cells and cells committed to differentiation (*Potten, 1974; Christophers et al., 1974; Mackenzie, 1975, Potten and Morris, 1988*). In 1974, *Potten* introduced an idea about

epidermal stem cell units of specific structure and he defined a group of tightly packed proliferative cells (about 10) as an epidermal proliferative unit (EPU). The architecture of the epidermis was observed and this gave rise to the central stem cell theory, the need for TA cells, and the observation that daughter cells become committed to terminal differentiation as they move through the stratified epidermis as a vertical column. This architecture established the idea that stem cells sit at the centre of the EPU and continually renew themselves as well as producing sufficient daughter (TA) cells (*Potten, 1974; Mackenzie, 1997; Fuchs, 2008*). Meanwhile, stem cells also have a remarkable ability to give rise to differentiating cells (*Fuchs, 2008*). Based on previous observations *in vitro*, it was concluded that basal cells are likely to divide symmetrically giving rise to equal sized daughter cells (*Lowell et al., 2000; Lowell and Watt, 2001*). However, this debate carries on and more recent studies have suggested that basal cells divide asymmetrically *in vivo* (*Clayton et al., 2007*).

More recent research has been dedicated to identifying epidermal stem cells with molecular markers. Lowell and colleagues pointed out that the level of $\beta 1$ integrin (used as a cell surface marker) can distinguish stem cells from TA cells, as stem cells express 3-5 fold more than TA cells (*Lowell et al., 2000 and Kaur et al., 2004*). This was demonstrated earlier by *Jones and Watt (1993)* where $\beta 1$ integrin levels in cultured human foreskin determined over 2 weeks in culture were also found to be high. In addition, other investigators have

used different cell surface markers in an attempt to locate stem cells in situ. These include a small keratin (K19) which has been used as a stem cell marker in hair follicles (*Michel et al., 1996; Lyle et al., 1998*), whereas, p63 was used as a marker for interfollicular epidermis (*Pellegrini et al., 2001*). According to *Kaur et al (2004)*, there are no current assays that can adequately distinguish stem cells from their more committed progeny (TA cells), and that measurement of stem cell activity requires long-term assays to measure sustained epithelial regeneration. Nevertheless, researchers have so far failed to unequivocally establish if all the cells in the basal layer are stem cells or whether only a small number of stem cells exist (*Fuchs, 2008*). Although, distinct stem cells do serve different regions of skin, some do have the capacity to regenerate other regions when necessary. Thus, hair follicle bulge cells can regenerate interfollicular epidermis as well as the hair follicle, under the right conditions. However, it is not yet fully understood how stem cells are controlled so they can contribute to different levels of cell renewal at different times (*Kaur and Potten, 2011*).

It is important to point out that stem cells are regulated by signals from surrounding keratinocytes. This behaviour is defined by an orchestrated interaction between intrinsic transcriptional programmes and external signals from local tissues (*Fuchs et al., 2004; Watt and Driskell, 2010; Collins et al., 2011*). To execute different programmes of terminal differentiation, stem cells must be instructed by signal transduction at an early stage. However, the

nature of these signals remains unclear and the mechanism by which stem cell activity is regulated during tissue regeneration is still poorly understood (Lowell *et al.*, 2000; Fuchs *et al.*, 2004; Collins *et al.*, 2011). However, an emerging network of signalling pathways has established that one gene (p63) controls stem cells at a certain stage in their development and their later commitment to differentiation of the epidermis (Koster and Roop, 2008). This was proven by Lechler and Fuchs (2005) where the data suggested that p63 and β 1 α -catenin have a role in directing asymmetrical cell division in the epidermis. In addition, c-Myc also has an influence on stem cell fate where it stimulates stem cells to generate TA cells (suggested by Gandarillas and Watt, 1997).

1.1.3 Epidermal Differentiation (Keratinisation)

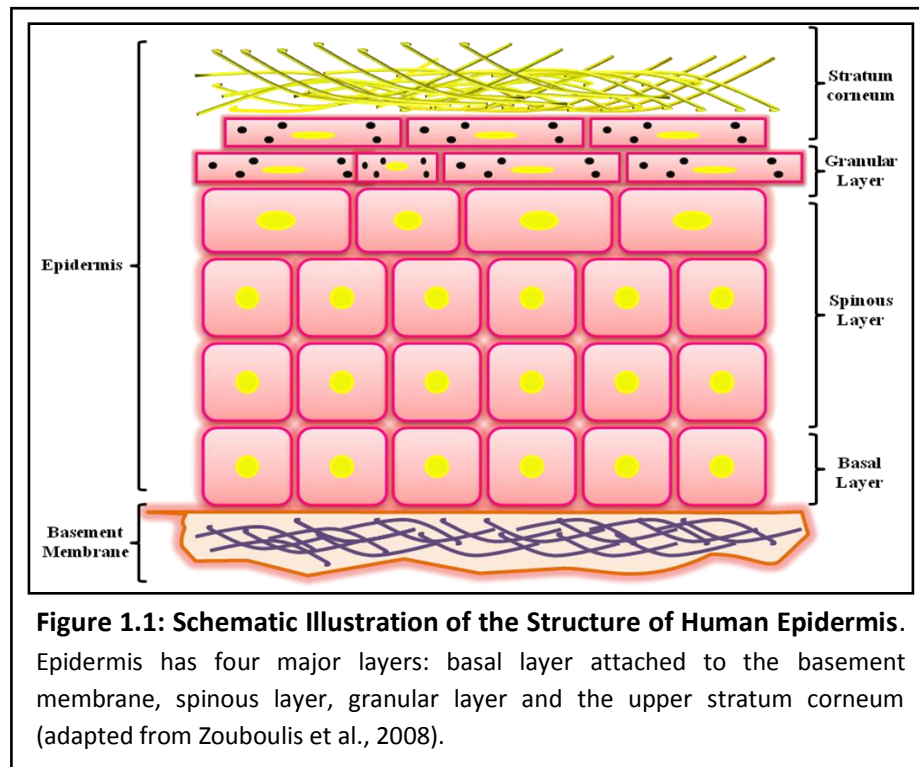
Keratinocytes are the most abundant cell type in the epidermis and considered to represent 80% of the total cell population. They are highly specialized epithelial cells that perform specific functions required for epidermal renewal, cellular cohesion, and barrier formation (Gambardella *et al.*, 2003). They are organized as four different layers (see **Figure 1.1**): basal, spinous, granular and corneum (Eckert and Rorke, 1989; Lee *et al.*, 2010). In thicker skin at some locations, a fifth layer (stratum lucidum) can also be seen. Other minor cell types are also present in the epidermis such as Merkel cells (associated with sensory nerve endings), Langerhan's cells (dendritic cells for

immune surveillance) and melanocytes (produce melanin to protect against UV damage).

Keratinocytes are attached to each other by adhesive intercellular junctions known as desmosomes. These structures can bind intermediate filaments to an inner plaque at the plasma membrane and adhere to each other using intercellular proteins, desmocollins and desmogleins, which are members of the cadherin super family of calcium dependent adhesion molecules (*Garrod and Chidgey, 2008*). The term was introduced by Josef Schaffer in 1920 and is derived from a Greek word (desmo) meaning bond and (soma) meaning body (*Delva et al., 2009*). Interestingly, they were first observed under the microscope by *Bizzozero* (1846-1901) and his insightful interpretation defined them as adhesive cell-cell contacts (*Matoltsy, 1975; Amagai and Stanley, 2011*). In the 1960's, *Odland* and his colleagues revealed that desmosome organization was more complex. Furthermore, *Matoltsy* (1974) isolated desmosomes from bovine nose epidermis using biochemical methods and defined several proteins.

As the epidermis endures many mechanical stresses, it is crucial for desmosomes to form strong anchoring junctions between keratinocytes. As intermediate filaments also attach to the inner plaque, these sites of intercellular adhesion form a supra-cellular network of scaffolding that can

facilitate and distribute mechanical forces throughout the epidermis (*Green and Simpson, 2007*).



This dynamic structure is critical for maintaining keratinocyte stability. In addition, there is evidence that desmosomes play a role in cellular process beyond that of cell adhesion (*Delva et al., 2009*). In fact, desmosomes appear to contribute to cell signalling, development and differentiation in various tissues including the skin (*Garrod and Chidgey, 2008; Petrof et al., 2011*). This means, they can participate in fundamental processes such as cell proliferation, differentiation and morphogenesis. In particular, desmosomal cadherins modulate intracellular signalling, control differentiation and may induce a switch from proliferation to differentiation upon stratification (*Ishii et al., 2001; Garrod and Chidgey, 2008; Petrof et al., 2011*). A similar related

structure, the hemidesmosome, anchors epidermal basal cells to the basement membrane zone. As the name suggests, this is a half-desmosome on the baso-lateral surface of the basal keratinocyte and a different set of specialised adhesion proteins connects this structure to the collagen fibres of the underlying dermis.

As cells move from the deeper basal layer outwards to form the spinous, granular and cornified layers, they become specialized and this is reflected by alterations in specific mitotic and synthetic properties as well as obvious changes in morphology. Early efforts by *Epstein and Maibach (1965)* calculated an accepted value of 28 days for normal human epidermis to turn over (from stem cell division to desquamation). This time includes stem cell division, TA cell amplification, programmed terminal differentiation, granular cell apoptosis, cornification and corneocyte desquamation.

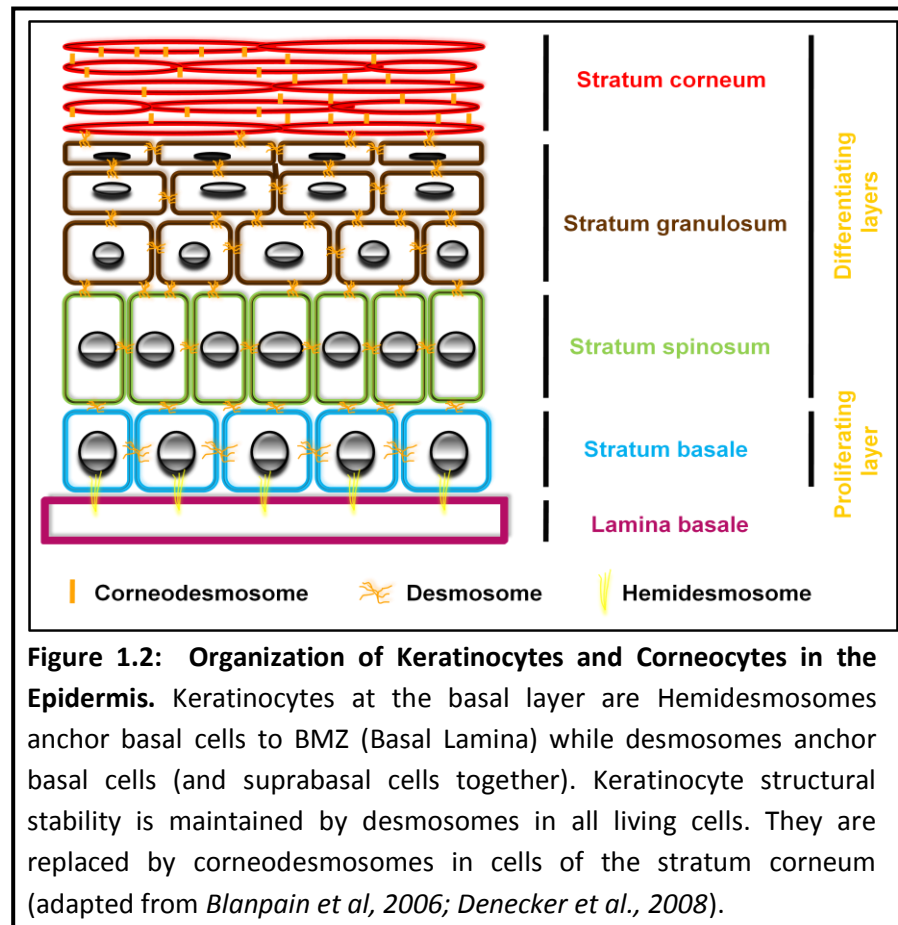
A series of genetic changes accompanied by specific metabolic events occur as the state of keratinocyte differentiation changes, a process called terminal differentiation or keratinisation (see **Figure 1.2**). Thus, keratinocytes have a relatively short life span in which they undergo a specific cycle of programmed cell death with rapid metabolism, growth and differentiation (*Schallreuter and Wood, 1995*). This process maintains structural stability of the epidermis and

is dynamic so that epidermal cell renewal is balanced by cell removal at the skin surface to maintain a constant thickness (homeostasis).

It is important to point out that during keratinisation, keratinocytes change size and shape accordingly. As soon as keratinocytes move into the supra-basal layer, the nucleus and cell body become larger and progressively assume a more flattened shape. In the granular layer below the stratum corneum, the nucleus breaks down, and organelles are removed. Lamellar bodies secreted by keratinocytes migrate towards the cell periphery, where they release their content of specialised lipids into the intercellular space in the form of hydrophobic cement. Finally, at the base of the stratum corneum, the “living” keratinocyte loses its nucleus and organelles to become a “dead” corneocyte. Corneocytes are not totally dead cells but they are unable to undergo any further gene transcription. However, the cells are full of structural proteins and have the enzymes required for desquamation. The epidermis therefore provides a waterproof barrier that is constantly renewed from the basal layer stem cells below.

At each stage of differentiation, epidermal cells become more specialized and alter both in structure and function. These changes in cellular differentiation are controlled by both extrinsic and intrinsic factors determined mainly at the

gene level, so studying the detailed molecular changes that occur will allow a more detailed understanding of the process of epidermal keratinisation.



1.1.4 Keratin Expression in the Epidermis

Intermediate filaments (IF) in epidermal keratinocytes are composed of keratin protein subunits. They form a 3D filament network around the cell and hold major organelles in place. However, there are several keratin proteins that form IF in the epidermis and their expression alters as cells proliferate

and differentiate (Bowden *et al.*, 1987). The filaments in basal cells are constructed from two keratins, K5 (a larger basic type II keratin) and K14 (a smaller acidic type I keratin). In addition, smaller amounts of K15 and K19 have also been reported in basal cells. However, as keratinocytes commit to terminal differentiation and move to a supra-basal position, they change their gene expression (Eckert and Rorke, 1989). K5 and K14 are specifically down-regulated and differentiation related keratins (K1 and K10) are up-regulated. Spinous cells contain all four keratins (K1, K5, K10 and K14) but as further growth and differentiation occurs, granular cells contain more K1 and K10 as K5 and K14 are progressively diluted out.

In addition, the cells of the upper spinous and granular cell layers express an additional keratin, K2. This is a marker of late differentiation and is believed to play a role in cornification. However, the precise role of K2 during late differentiation remains poorly understood (Collin *et al.*, 1992; Bikle, 2004; Sporn *et al.*, 2010).

No additional keratin gene expression occurs in the stratum corneum at the skin surface. However, the keratins here do not show the same biochemical profile as those in the lower living layers due to post-translational modification that removes the basic terminal sequences from these

differentiation-related keratins (K1, K10). This renders the proteins smaller and more acidic than the original gene products (Bowden *et al.*, 1984).

Keratin filaments terminate at desmosomes and anchor into the desmosomal plaque on the inner plasma membrane. They do not pass through the desmosome, the two halves of which are held together by intracellular interactions between desmocollins and desmogleins.

In addition to alterations in keratin gene expression, many other specific proteins are required for successful terminal differentiation and to hold the epidermis together. A few are synthesised in spinous cells (e.g. involucrin) but the majority are products of the granular cell (e.g. loricrin and filaggrin). Granular cells contain two types of keratohyalin granule (KHG): L-granules contain and release loricrin, a major component of the cornified envelope while F-granules contain and release filaggrin, essential for the close packing of keratin filaments in corneocytes. Granular cells also contain lamellar bodies (“membrane coating granules” or “Odland bodies”) which were first described by *George Odland* in 1964 (*Ro et al.*, 1964). Lamellar bodies contain various types of complex lipid including ceramides (*Blanpain and Fuchs, 2006*). These form complex intracellular lipid bilayers that fill the space between corneocytes with a lipid rich environment that prevents the passage of

aqueous molecules. This lipid barrier also prevents water getting out so prevents dehydration via the skin.

The other important part of the barrier is the cornified cell envelope. This is made by cross-linking a number of specialised proteins (e.g. loricrin, involucrin, envoplakin, periplakin, small proline-rich proteins, etc) to the transmembrane integrins of the granular cell by the action of transglutaminase. In this way, the cell membrane is significantly thickened and made impervious to water and small molecules. The envelope fills in the plasma membrane between the desmosomes and these are further modified to form corneodesmosomes so that the corneocytes are held firmly together at the skin surface. This protects the human body from external environmental factors (*Chu and Morris, 2005*). Once the cells reach the outer surface of the skin, the corneodesmosomes break apart under the influence of proteolytic enzymes and the outermost corneocytes are shed in a process called desquamation (*Hoath and Leahy, 2003; Barai et al., 2008*).

The integrins form another important family of structural molecules in the epidermis. Integrins are transmembrane proteins that act as cell surface receptors to transfer information between the outside and inside of the cell. They are very important for regulating epidermal growth, development and wound repair. They consist of two different glycoprotein subunits (alpha and

beta chains). Basal cells have a very specific profile of integrins ($\alpha 2\beta 1$, $\alpha 3\beta 1$, $\alpha 5\beta 1$ and $\alpha 6\beta 4$) and these alter with epidermal differentiation (*Jones et al., 1995; Deyrieux and Wilson, 2007*). The $\alpha 6\beta 4$ integrins occur on the basolateral surface and form part of the hemidesmosome. This keeps the basal cell firmly anchored to the basement membrane zone (BMZ). During epidermal differentiation $\alpha 6\beta 4$ integrin distribution becomes more diffuse and is part of the mechanism that releases cells from the BMZ. Suprabasal cells express $\alpha 2\beta 1$ and $\alpha 3\beta 1$ which are involved in sticking epidermal cells together in addition to the desmosomes. Interestingly, their function switches from contact between cells to contact with wound matrix molecules during wound repair. Finally, $\alpha 5\beta 1$ is expressed only in migrating cells shortly after wounding (*De Luca et al., 1994; Ginsberg et al., 2005*).

1.1.5 Calcium Regulation of Keratinocyte

Differentiation

During migration of cells from the basal layer to the stratum corneum, keratinocytes change dramatically both in terms of morphology and cellular biochemistry. In recent years, much progress has been made in relation to understanding some of the detailed molecular mechanisms behind this process.

Calcium is critical for controlling the balance of proliferation and differentiation in epidermal keratinocytes (*Eckert and Rorke, 1989*). Extracellular calcium suppresses proliferation and promotes differentiation of keratinocytes (*Yuspa et al., 1989*). Other studies have also shown that calcium signalling is important and a sustained increase in calcium levels is necessary for induction and maintenance of terminal differentiation (*Oda et al., 2000; Tu et al., 2001*). *Pillai et al (1990)* have shown that extracellular calcium can also act as a modulator and activator keratinocyte differentiation. This was examined by a comparative study with cultured keratinocytes, using both the HaCaT cell line (*Boukamp et al., 1988*) and normal human keratinocytes (NHK). Increasing the extracellular calcium concentration from 0.09 mM to 1.2 mM could induce morphological and biochemical changes in keratinocytes similar to those observed during differentiation *in vivo* (*Micallef et al., 2009*).

The effect of extracellular calcium on the induction of terminal differentiation in cultured keratinocytes can be followed using markers of differentiation such as keratins K1 and K10. These are only found in the spinous layer *in vivo* and are only expressed by differentiating cells in culture. The same is true for other markers of differentiation such as involucrin and filaggrin, which are localized to the upper spinous and granular cell layers *in vivo* and again only found in the more mature “differentiated” cells in culture (*Yuspa et al., 1989*).

Keratinocytes cultured in low calcium medium (0.05-0.20 mM) grow as a monolayer and exhibit properties of basal cells including continuous proliferation and expression of basal type keratins (K5 and K14). Adding calcium to the medium induces these cells to undergo terminal differentiation. A sudden increase in calcium concentration in the culture medium arrests cell growth and switches cells into terminal differentiation. The morphological and biochemical changes that occur in these cultured cells resemble those occurring in suprabasal cells *in vivo*. This is also accompanied by the expression of terminal differentiation markers such as K1, K10 and involucrin (Bikle *et al.*, 1996). There have been many studies of both primary keratinocytes (mouse and human) and various cell lines (e.g. HaCaT, Ntert) and a useful comparison illustrated below in **Table 1.1** was published recently (Micallef *et al.*, 2009).

Table 1.1: Characteristics of Immortalized and Normal Human Keratinocytes. A number of measures of proliferation and differentiation are compared (data from Micallef *et al.*, 2009).

Immortalized Human Keratinocytes	Normal Human Keratinocytes
↑ in proliferation at 20-30% in high Ca	↓ in proliferation at 20-30% in high Ca
Accumulation of S+G2 cells in high Ca	↓ S+G2 cells in high Ca
Delay in K1, K10, Involucrin in low and high Ca K1, K10 expressed on day 3 low and high Ca Involucrin expressed on day 6 low and high Ca	K1, K10, Involucrin expressed from day 1 (low Ca) K1, K10 and Involucrin ↑ gradually in high Ca

Organotypic cultures can also be used and here keratinocytes are grown at an air-liquid interface. These undergo more extensive differentiation and have been successfully used to study various aspects of keratinocyte growth and differentiation in the laboratory.

1.2 Notch Signalling Pathway

1.2.1 Historical Background

Notch was first described as a genetic trait in the fruit fly (*Drosophila melanogaster*) by an American geneticist and a Nobel Laureate (TH Morgan) in the early 20th century (*Morgan, 1917*). He described a mutated strain of fruit fly which had notches in the wing blades and attributed this to a lack of gene function (haploinsufficiency). However, the gene involved was not isolated, analysed and sequenced until the 1980s.

The initial characterization of notch mutants in *Drosophila* was done by Poulson while describing *drosophila* gut formation in the embryo (*Poulson, 1945*). During that time (1937-1945), he examined embryological effects of an extensive series of notch locus deficiencies and managed to identify several other defects in embryonic and adult tissues. Later work showed that the Notch pathway was not only essential for *Drosophila* development but was necessary for all animal tissues (*Wharton et al., 1985; Kidd et al., 1986; Fior*

and Henrique, 2009). Furthermore, this work indicated that notch mutants were not only involved in the development of the nervous system but also in many cell fate decisions that take place in other animal tissues (*Atravinas-Tsakonas, 1999*).

Interestingly, the observations by Poulson helped to clarify the importance of notch activity, and how the absence of notch genes can lead to hyperplasia of neural tissue at the expense of epidermis (*Lehmann et al., 1983; Fior and Henrique, 2009*). Also, the notch pathway was identified as a cascade of interacting neurogenic genes that function to control the formation of the fly nervous system (*Vassin et al., 1985*). The molecular analysis and sequencing of notch homologues was independently undertaken by *Wharton* and colleagues in the 1980's (*Wharton et al., 1985*). In the early 1990s, the four mammalian homologues of notch (Notch 1–4) were identified (*Hansson et al., 2004*). Ligands and co-receptors have now been identified in several species (**Table 1.2**).

Table 1.2: Notch Receptors, Ligands and Co-activators in Different Species
(data summarised from *Fior and Henrique, 2009*)

Species	Drosophila	C. elegans	Chick	Mammals
Receptor	Notch	Lin-12 glp-1	Notch1 Notch2	Notch1 Notch2 Notch3 Notch4
Ligands	Delta Serrate	Lag-2 Apx-1 arg-2 f16b122	Delta1 Delta4 Jagged1 Jagged2	Dll-1 Dll-3 Dll-4 Jagged1 Jagged2
CSL	Su(H)	Lag-1	CBF1/ RBPJK	CBF1/ RBPJK
MAM	Mam	Lag-3	Mam1 Mam2 Mam3	Mam1 Mam2 Mam3

1.2.2 Notch Signalling in Epidermal Development

Normal epidermal homeostasis requires a tight control of proliferation and differentiation programs within the epidermis. It is well known that notch signalling regulates epidermal cell adhesion and all the necessary components are expressed in epidermal keratinocytes (*Panelos and Massi, 2009*)

In recent years, there has been considerable progress in identifying the signalling pathway that regulates epidermal differentiation. It is important to

point out that movement of signals from outside to inside the cell is fundamental to many biological processes that take place in the skin and other tissues. This requires an interaction between two cells (a sending cell and a receiving cell) where specific signal transduction takes place. This means, cell growth or differentiation in the skin is somehow functioning in an integrative manner in which cellular processes are controlled (*Lefort and Dotto, 2004*).

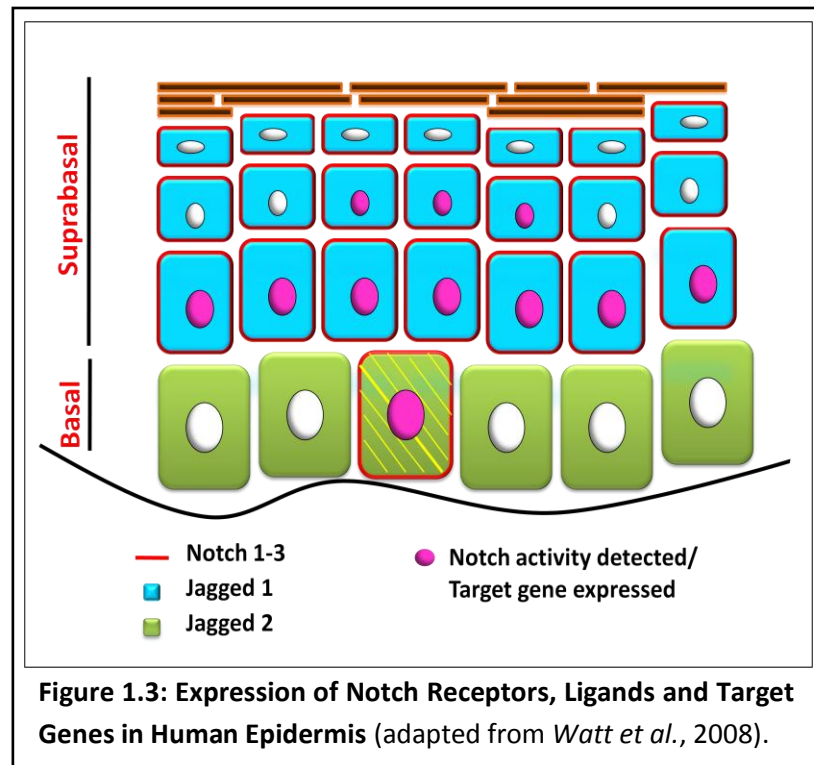
However, signal transduction can also be mediated by several other factors such as ion movements into and out of the cell and by modifying proteins by phosphorylation (*Iversen et al., 2005*). Thus, multiple signals from surrounding keratinocytes are involved in inducing the maturation of an individual epidermal cell. Several important signalling cascades have been implicated in the control of keratinocyte differentiation. These include the Wnt/ β -Catenin pathway (*Huelsken et al., 2001*), Sonic Hedgehog (Shh) (*Fan and Khavari, 1999; Hurlbut et al., 2007*), NF-Kappa B (*Seitz et al., 1998; Nickolof et al., 2002*) and c-Myc (*Gandarillas et al., 1997*). Homeobox (HOX) genes are also considered as a critical player in the embryologic development of skin (*Scott and Goldsmith, 1993*). In addition, bone morphogenetic protein (BMP) signalling is expressed throughout most of the developing skin epithelium and this appears to inhibit the early stages of hair follicle morphogenesis (*Andle et al., 2004; Blanpain and Fuchs, 2006*). Notch signalling has now been added to

the list of intercellular communication pathways that are involved in cell fate determination within the skin.

A broad spectrum of developmental processes is regulated by notch signalling (*Artavanis-Tsakonas et al., 1999*). There are a number of core players that participate and the initial interaction requires contact between two transmembrane proteins, a notch receptor on one cell and a delta-jagged family ligand on an adjacent cell (*Fortini, 2001*). However, there are 4 different notch receptors and 5 different ligands in human cells making interactions complex. Differential expression of notch receptors and ligands can vary in interfollicular epidermis and skin appendages, correlating with distinct cell fates and the control of different programmes of differentiation.

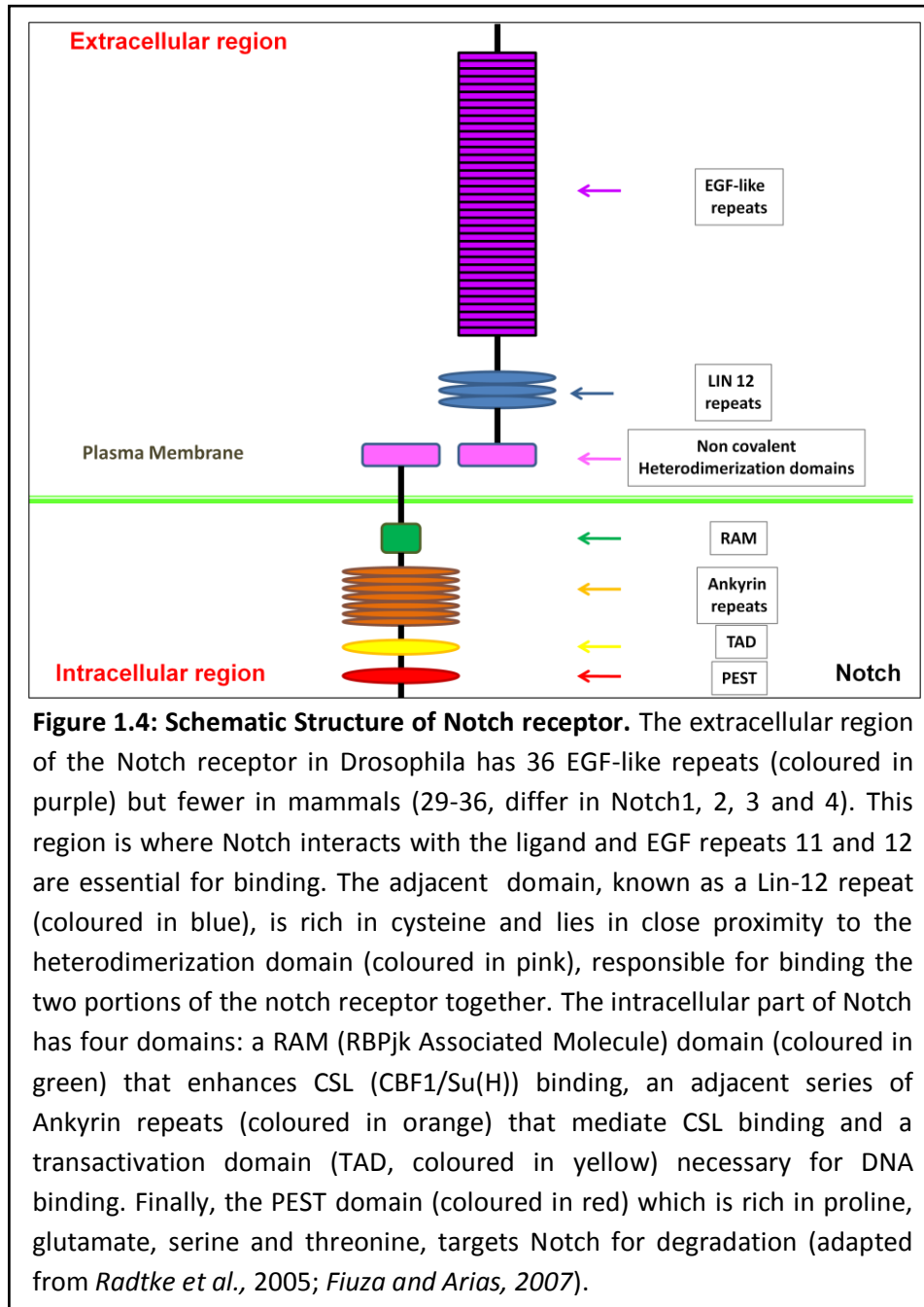
Several studies have established a dual role for notch-mediated changes in some cells. For example, Notch 1 allows basal cells to detach from the BMZ by down regulating integrins but at the same time, it promotes early up-regulation of differentiation markers such as keratins (K1 and K10) and involucrin. It also prevents the induction of loricrin and filaggrin in the lower epidermis so these molecules are only expressed in the granular layer.

Recently, it was shown by *Moriyama et al* (2008) that notch signalling induces granular cell differentiation and, simultaneously, prevents premature differentiation of spinous cells due to the simultaneous existence of both a transcriptional activator and repressor downstream of notch during epidermal development (**Figure 1.3**).



The original notch signalling pathway components (e.g. delta (DLL) and mastermind (MAM) genes) were isolated from neurogenic tissues of *Drosophila* (*Egan et al.*, 1998). The notch signalling pathway is a process of cell to cell communication that mediates short signals that are able to regulate cell fate decisions and maintain stem cell populations.

The notch gene encodes a single transmembrane receptor protein (**Figure 1.4**) that contains many EGF repeats and three membrane-proximal repeats (Lin12/Notch/Glp-1). The intracellular domain also has four distinctive regions: a RAM domain, ankyrin repeats, TAD and PEST domains (*Baron, 2003*). This polypeptide is synthesised in the endoplasmic reticulum, cleaved into two portions and these are linked in a non-covalent manner by the heterodimerization region.



In *Drosophila*, notch signalling only requires three gene products: a single notch receptor and two ligands (delta and serrate). In contrast, mammals have four different notch receptors (NOTCH1, NOTCH2, NOTCH3 and NOTCH4), three delta-like ligands (DLL1, DLL3 and DLL4) and two jagged ligands (JAG1 and JAG2). The number of notch receptors and ligands also

varies with species but despite this variation, notch signalling plays an essential role in several developmental processes common to all vertebrates (Louvi and Artavanis-Tsakonas, 2006) as shown in **Figures 1.5 and 1.6**.

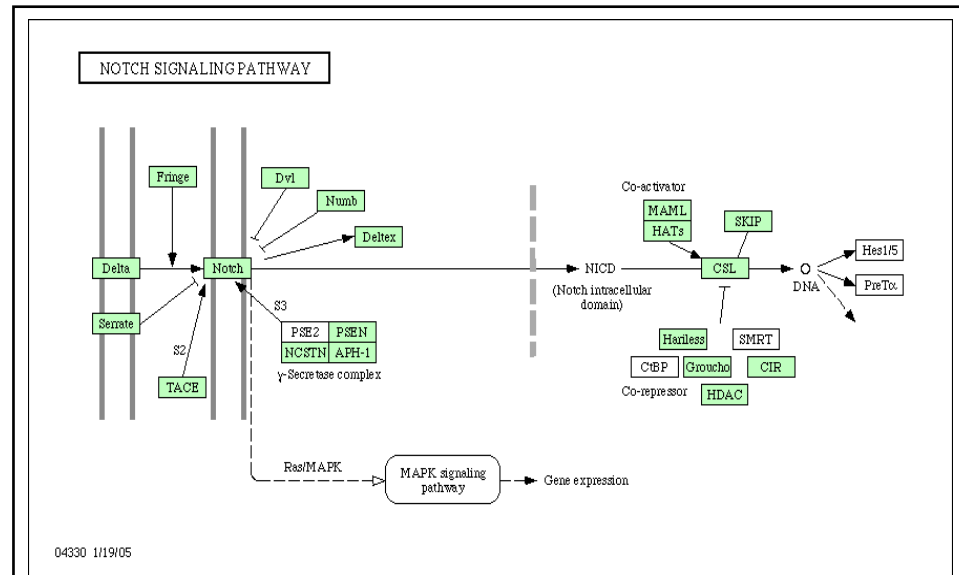


Figure 1.5: Schematic Diagram of Notch Signalling Pathway in *Drosophila*. Notch receptors are single-pass membrane molecules activated by Delta-like and Serrate family membrane-bound ligands. Notch is transported to the plasma membrane as two cleaved but otherwise intact polypeptides. Interaction with ligand leads to two proteolytic cleavages that free the intracellular domain (NICD). The NICD translocates to the nucleus, where it forms a complex with DNA binding proteins (CSL) and displaces a histone deacetylase (HDAC)-co-repressor (CoR) complex. Components of an activation complex, such as MAML1 and histone acetyltransferases (HATs), are recruited to the NICD-CSL complex and activate Notch target genes. Note: CBT and SMRT are not involved in target gene activation (adapted from the following website; http://www.genome.jp/keggbin/show_pathway?org_name=dme&mapno=04330).

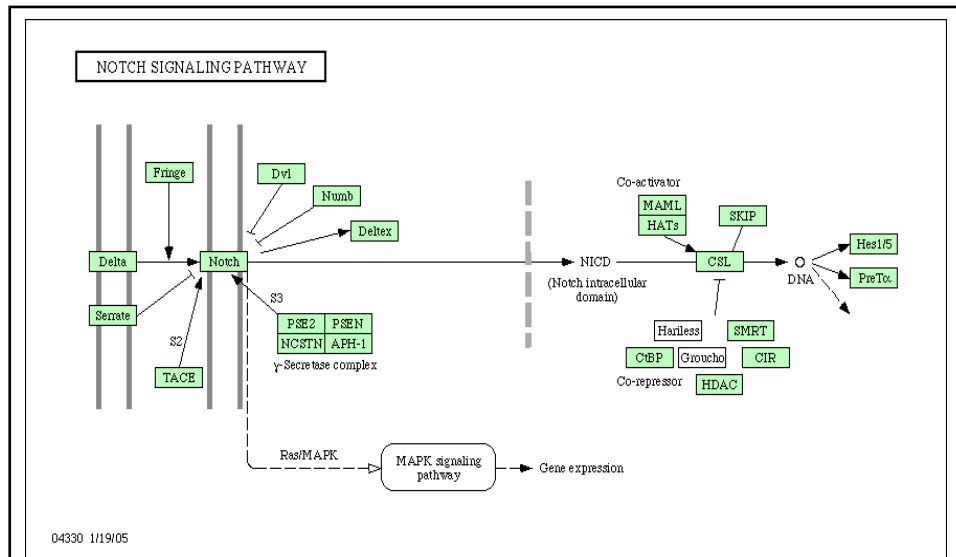


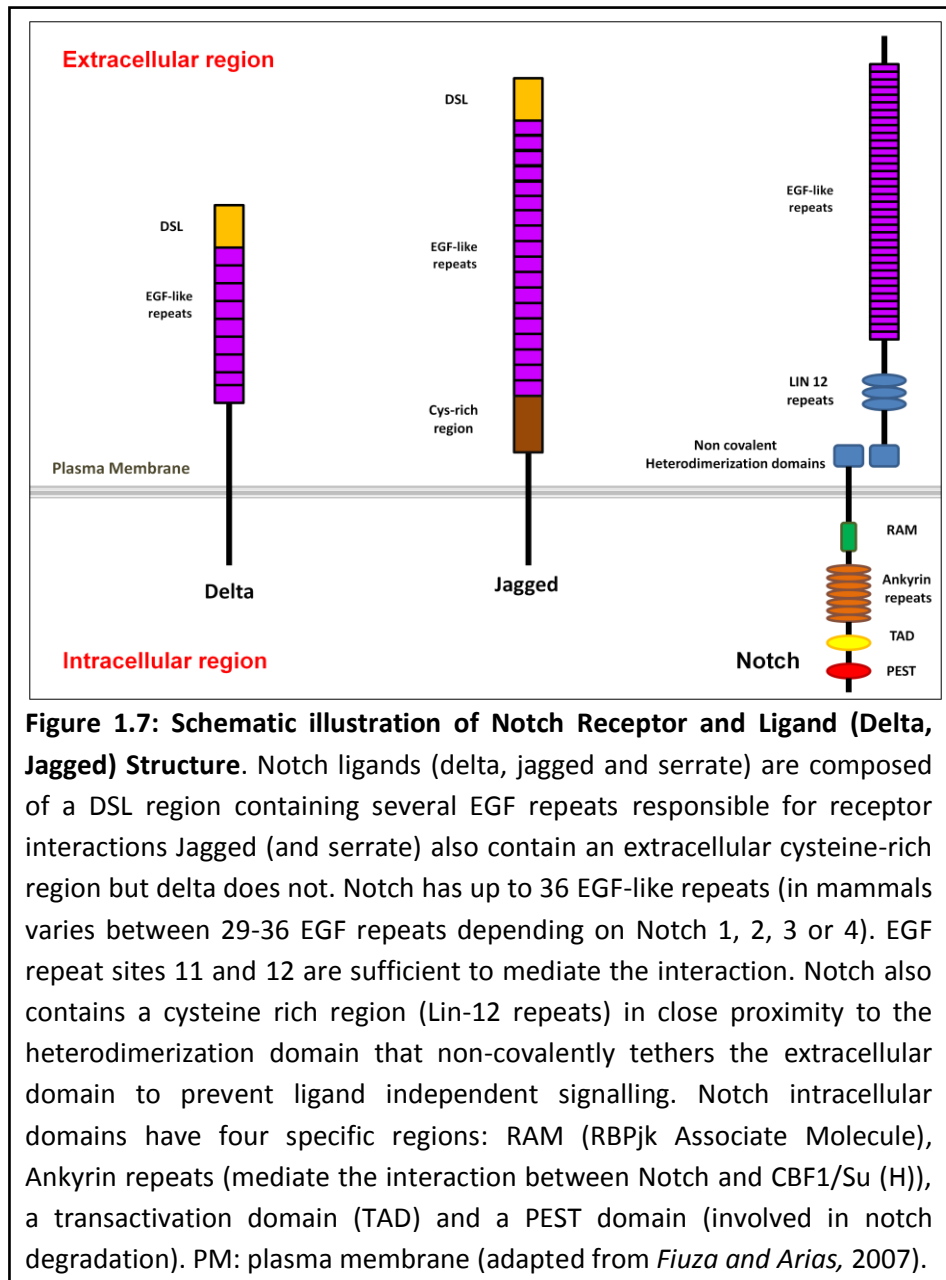
Figure 1.6: Schematic Diagram of Notch signalling Pathway in Mammals.

Notch proteins (Notch 1-4 in vertebrates) are single-pass membrane receptors activated by Delta and Jagged families of membrane-bound ligands. Notch is transported to plasma membrane as two polypeptides bound together at the cleavage site. Ligand interactions lead to two more proteolytic cleavages that release the intracellular domain (NICD). The NICD translocates to the nucleus, forms a complex with a DNA binding protein (CSL) and displaces the histone deacetylase (HDAC)-co-repressor (CoR) complex. Components of the activation complex, such as MAML1 and histone acetyltransferases (HATs), are recruited to the NICD-CSL complex, leading to activation of notch target genes. Note: Hairless and Groucho are not involved in target gene activation (adapted from <http://www.genome.jp/kegg/pathway/hsa/hsa04330.html>).

1.2.3 Structure of Notch Receptors and Ligands

There are two main differences in structure between delta and jagged (**Figure 1.7**). Firstly, jagged has 18 epidermal growth factor (EGF) repeats while delta only has 9. Secondly, the cysteine rich region within the extracellular portion of jagged is absent in delta (*Fiuza and Arias, 2007*). However, both are transmembrane receptors and have a cysteine rich called DSL (Delta-serrate-lig2). This is considered the most interesting region for notch signalling as it

mediates the interaction with the notch receptor EGF repeats (11-12 regions associated with ligand binding). Moreover, the N-terminal region is crucial for this interaction. The structure of the notch receptor and both ligands (delta and jagged) is shown in **Figure 1.7** below (*Fiuza and Arias, 2007*).



1.2.4 Notch Signalling Pathways

Notch signalling can occur via canonical or non-canonical pathways (Figure 1.8). The canonical pathway is notch cleavage dependent while non-canonical pathway does not require cleavage of the receptor.

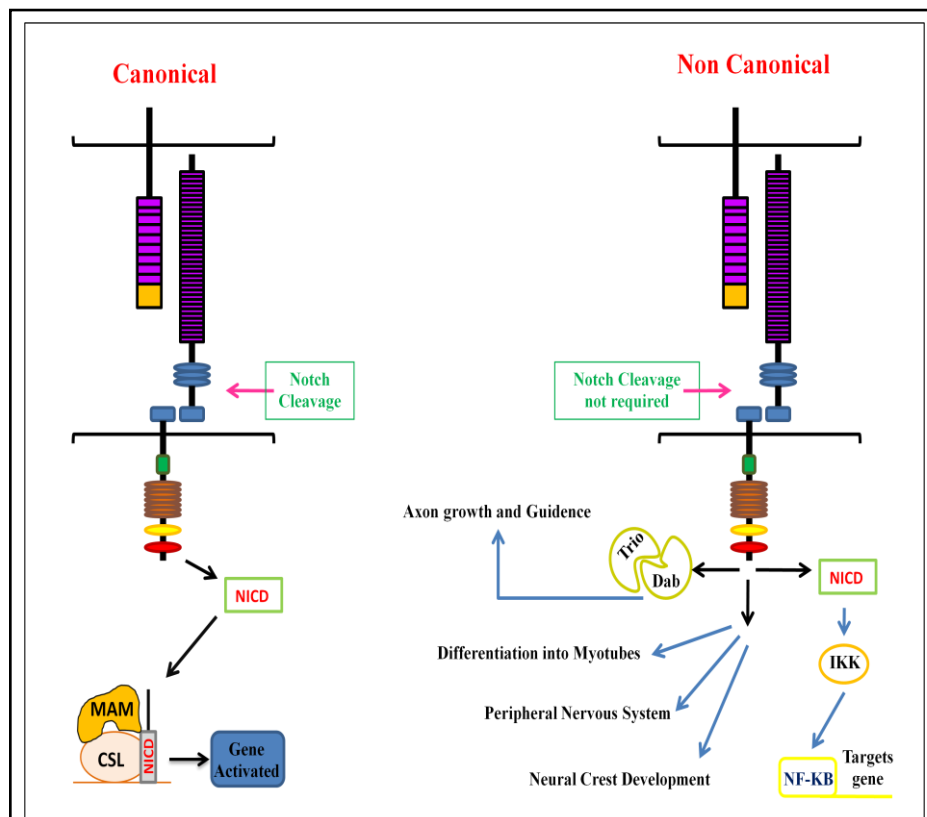


Figure 1.8: Schematic of Canonical and Non-Canonical Notch Signalling Pathways. Canonical notch signalling requires an interaction between receptor and ligand that releases the intracellular domain (NICD) by a series of proteolytic cleavages. This domain translocates to the nucleus, dislodges transcriptional co-repressors and enables gene activation. Non-canonical signalling does not require intra-membrane cleavage and interaction between the receptor and ligand signals via NICD, Trib/Dab or other signalling pathways can influence tissue development (adapted from Talora et al, 2008).

In 2002, *Okajima and Irvine* suggested that notch signalling via its ligands is positively regulated by a trans-golgi protein called OFUT1. However, when OFUT1 is over-expressed, it appears to inhibit notch signalling. This paradoxical effect was apparently due to increased removal of notch molecules from the cell surface (plasma membrane) and their entry into one of the protein degradation systems (e.g. the ubiquitin proteasome). This mechanism prevents excessive accumulation of notch receptors at the cell surface (*Sasamura et al., 2007*). Thus, how OFUT1 contributes to higher levels of notch activation during development is still not clear.

In general, notch signalling is triggered by cell to cell contact and this communication is essential for the correct patterning of animal tissues. Interestingly, the interaction between the notch receptor and its ligands is complex and both serrate and delta can act as signal activators or inhibitors in a concentration-dependent manner (*Fiuza et al., 2010*). The notch receptor is presented on the surface of one cell where it can then interact with ligands on neighbouring cells. The signalling pathway has several stages (**Figure 1.9**) and these can be defined according to a series of proteolytic cleavages (labelled S1 to S4).

S1 cleavage takes place in the trans-golgi in mammals during the transport of the notch receptor to the plasma membrane but that does not appear to be

the case in *Drosophila*. A study by *Kidd and Lieber (2002)* using a furin resistant receptor showed that S1 cleavage was not required for notch function in *Drosophila*.

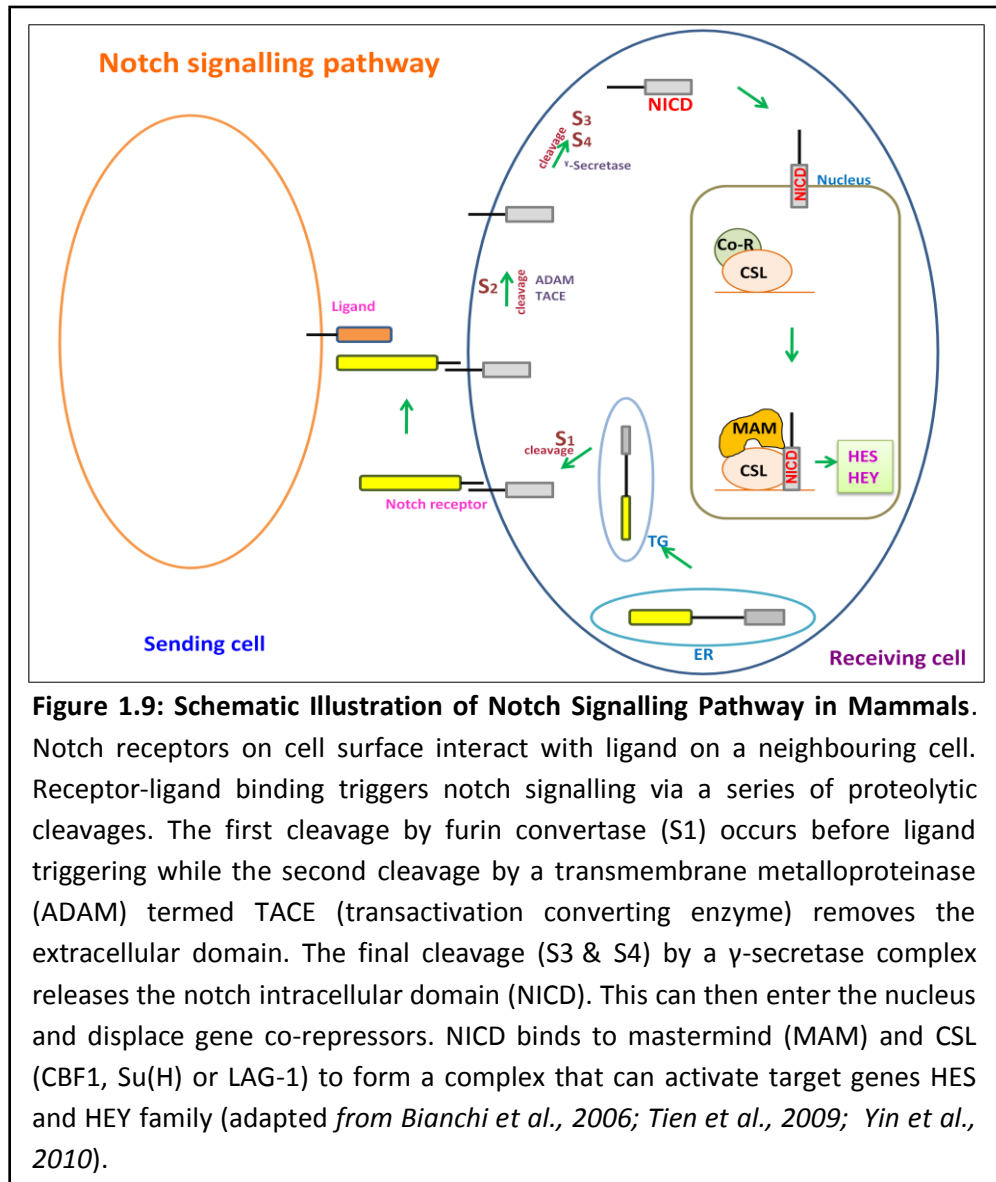
However, there is still no consensus concerning the role of S1 cleavage in notch function in mammals. Additionally, S1 cleavage appears to have different effects on the surface expression of N1 and N2 but is not required for pathway activation. Another observation was that ligand binding makes a conformational change in the NRR (negative regulatory region) and then metalloproteinase cleavage (S2) can remove the extracellular domain (*Gordon et al., 2009*).

The S1 cleavage site acts as a negative regulator of the receptor (NRR) to prevent notch activation in the absence of ligand (*Kopan and Ilagan, 2009*). This cleavage is done by an enzyme known as furin convertase within the Golgi complex during transport to the plasma membrane. This cleavage of mammalian notch receptors yields a non-covalently associated extracellular domain and transmembrane subunit which form a hetero-dimeric unit (*Rand et al., 2000*).

The second proteolytic cleavage (S2) takes place at the cell surface after an interaction between the receptor on one cell and a ligand (delta or jagged) on

a neighbouring cell. This cleavage is mediated by members of the ADAM family of metalloproteinases (*Gordon et al., 2009*). The interaction between receptor and ligand exposes an extracellular metalloproteinase sensitive site and the cleavage is done by an ADAM metalloproteinase such as TACE. This releases the extracellular domain (ECD) but the NICD still remains membrane tethered as this cleavage occurs external to the cell membrane. The cell membrane tethered NICD is the substrate for the next proteolytic step (S3 and S4).

In vivo studies in drosophila have shown that these two consecutive cleavages (S3 and S4) require presenilin proteins in order to release the NICD and activate notch signalling by translocation to the nucleus. In mammals, presenilin is associated with a large number of other proteins that make up the γ -secretase complex. S3 cleavage takes place within tethered NICD where presenilin and nicastrin release a soluble NICD. Interestingly, a recent report by *Taniguchi et al (2002)* suggests that presenilin may not be the protein that directly cleaves notch (*Baron, 2003*). The notch intracellular domain (NICD) once released from the plasma membrane can move to and enter the nucleus. A repression complex consisting of CSL and co-repressor proteins binds to DNA and keeps gene expression levels low (see **Figure 1.9**).



Therefore, in the absence of signalling, transcriptional repression of notch target genes occurs in the nucleus. However, once NICD is translocated to the nucleus, the RAM domain triggers structural changes in the co-repressor and this is displaced. RAM is an essential structure for the association of NICD and CSL. In mammals, C-Promoter binding factor 1 (CBF1) functions as the CSL unit and once the co-repressor has been displaced, MAM can bind to form a ternary complex that acts as a transcriptional activator. The MAM co-factor is very important in organizing this complex as it can recruit other proteins that play a role in the transcriptional up regulation of target genes (e.g. HES and HEY). However, it also recruits cyclin C and cyclin-dependent kinase 8 (CycC: CDK8) which can hyperphosphorylate the NICD so that it becomes a target for PEST-dependent degradation by Sel10 ubiquitin ligase (*Fryer et al., 2004*). This reduces nuclear levels of NICD and terminates activation of transcription, allowing a tight control of notch signalling (*Fior and Henrique, 2008*).

Notch receptors contain three highly conserved Lin12/Notch repeats and a heterodimerization domain (HD) that interacts to prevent premature signalling in the absence of ligand (see **Figure 1.10**). The EGF repeats can also be modified by adding various sugars and this allows enzymes such as Fringe to modulate receptor activity.

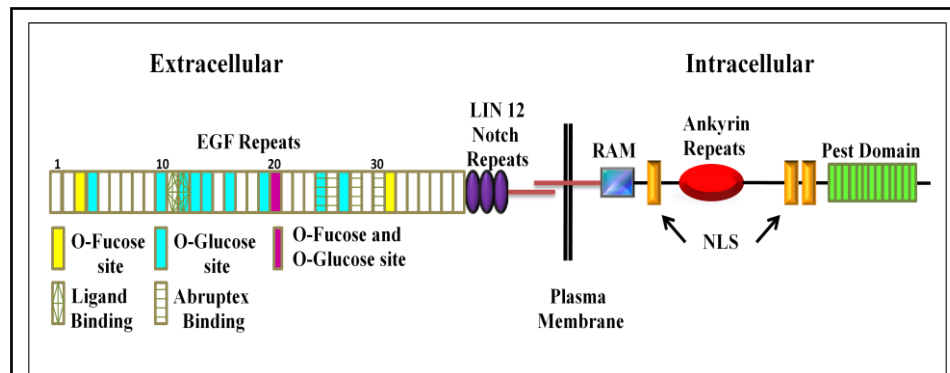


Figure 1.10: Domain Structure of Notch Receptor Proteins. Notch ligands bind to the extracellular domain (EGF repeats 11-12) of the receptor in a non-covalent manner. The intracellular domain detaches after a series of proteolytic cleavages that releases the NICD. LIN12 repeats modulate interactions between extracellular and intracellular domains. RAM (CBF1/RBPJ kappa (RBPJ κ)) associated molecule in mammals and the transactivation domain (TAD) aid release of NICD and allow activation of target genes in the nucleus. PEST = Proline-, Glutamic Acid-, Serine-, Threonine-rich and NLS = Nuclear Localisation Signal. Transcriptional activation domain (TAD) differs among the four notch receptors (adapted from *Haltiwanger and Stanley, 2002; Wu and Griffin, 2004; Radtke et al., 2005*).

1.2.5 Notch Transcriptional Regulation

Although the NICD is a short-lived transcription factor, it is possible that some notch target genes encode stable transcription factors that could produce a sustained activity of the pathway. Signalling depends on the amount of NICD inside the nucleus and this only appears to require a low concentration. However, in the absence of NICD, CSL will bind to co-repressors (e.g. SMRT, SPEN) and these will keep transcription silent.

Several mechanisms can regulate the notch signalling pathway. One important factor is the presence of the delta ligand. If there is *cis* interaction between the notch receptor and a delta ligand within the same cell, this can block interaction of the receptor with a ligand on a neighbouring cell. As a result, *cis* interactions down regulate notch signalling in cells where high levels of delta ligand occur on the cell surface (*Heitzler and Simpson, 1993*). A decade later, *Baron (2003)* showed biochemical data to suggest that delta has a direct inhibitory effect on notch receptors and can actively down regulate notch signalling in cells.

Another important factor is endocytosis of notch receptors or ligands. There is a strong possibility that NICD degradation keeps levels in the nucleus low. This mechanism is controlled by two domains: TAD (transactivation domain) and PEST (proline, glutamic acid, serine and threonine-rich) domain. The C-terminal region of the PEST domain is phosphorylated by CDK8, a cyclin-dependent kinase (*Fryer et al., 2004*) and such terminal phosphorylation targets the NICD for Fbw7/Sel10 ubiquitin ligase, a PEST-dependent degradation mechanism *in vivo*, that maintains low NICD levels in the nucleus.

Endocytosis is considered a major player in enhancing signalling between notch receptors and its ligands. In particular, notch receptor activation where ligand endocytosis is provoked by mono-ubiquitination which is mediated by

E3 ubiquitin ligases, neurilized and mindbomb (Le Borgne *et al.*, 2005 and Chitnis, 2006). In addition, Heuss *et al* (2008) proposed that endocytosis is not only required for ligand binding but also for recycling back to the plasma membrane and generating a new active ligand. Interestingly, it was found that endocytosis in other species is not always the same as in *Drosophila*. For example, endocytosis of DSL ligands is essential for notch signalling in mammals but not in *C. elegans* (Fortini, 2009).

In order for the ligand to be active, neurilized and mindbomb are required and work in close association with endocytosis, and are helped by the ubiquitin binding protein, epsin (Wang and Struhl 2004; Wang and Struhl, 2005; Bray, 2006).

It was found that notch signalling can be suppressed by high levels of ligand. In other words, the same ligand which interacts with notch in *trans* (cell to cell) in order to get activate signalling are also capable of interacting in *cis* to cause inhibitory effects (Del Alamo and Schweisguth, 2009; Fortini, 2009). Although the mechanism is not completely understood, this can be explained by a negative feedback loop in which cells receiving the signal down regulate ligand expression, thus reducing their ability to signal back, known as *trans* inhibition (Bray, 2006). Moreover, Miller and his colleagues presented new evidence suggesting that *cis* (within the cell) inhibition of Notch pathway by

delta in signal sending cells play a role where removal of E3 ubiquitin ligase is required for delta signalling at least during eye development (*Miller et al., 2009*). In addition, the inhibitory effect can potentially take place at any membranous compartment that contributes to developmental changes in the tissues and is not restricted to the cell surface.

Glycosylation was also found to play an important role in notch signalling. The extracellular domain of notch receptors and the DSL ligands contain a few potential sites for *N*-linked and *O*-linked glycosylation involving fringe glycosyltransferases, such as *O*-fucosyltransferase (*O*-fut1 in *Drosophila* and Pofut-1 in mammals) and Rumi (*Acar et al., 2008; Fortini, 2009*). These glycosyltransferases catalyse the elongation of *O*-fucose by adding N-acetylglucosamine to specific EGF-like repeats in the notch extracellular domain (*Bruckner et al., 2000*). This has a complex effect on notch signalling. Fringe increases the affinity between notch and its ligands and at the same time has an inhibitory effect on other ligands. For example, *O*-linked sites on the notch extracellular domain are more sensitive to delta than to serrate in the dorsal compartment of the *Drosophila* wing, so notch signalling will be higher via delta than via serrate.

The fringe family is more complex in mammals. There are three types of fringe proteins known as Manic, Radical and Lunatic. They are all notch signalling

modulators and are expressed in various restricted patterns but were found to have different effects. For example, delta induces notch 1 activity but jagged inhibits notch activity according to studies done *in vitro* and *in vivo* (Haines and Irvine, 2003; Fortini, 2009).

O-fucosyl-transferases also have an important role in notch signalling. Adding fucose to the EGF-like extracellular repeats of the notch receptor allows further modification and extension by fringe. In mammals, it was found that Pfovt-1 is required for the generation of notch receptors as it a requirement for transport of the notch receptors to the cell surface (Okajima *et al.*, 2005). On the contrary, Rumi was recently identified in *Drosophila* and it catalyzes the addition of *O*-glucose to specific residues of the notch extracellular domain in the endoplasmic reticulum. Its absence may lead to normal notch receptor transportation to the cell surface but receptor proteolysis failed in all tissues examined causing a severe notch signalling defect (Acar *et al.*, 2008).

Hubbard *et al* (1997) also suggested that other down regulators of notch signalling such as ubiquitin ligase play a significant role. Originally identified in *C. Elegans*, an E3 ubiquitin ligase component known as Sel-10 was found to interact with the NICD. It is thought that it may stimulate and trigger phosphorylation of the NICD and this consequently increases NICD turnover in the nucleus. On the other hand, it regulates the presence of notch receptors

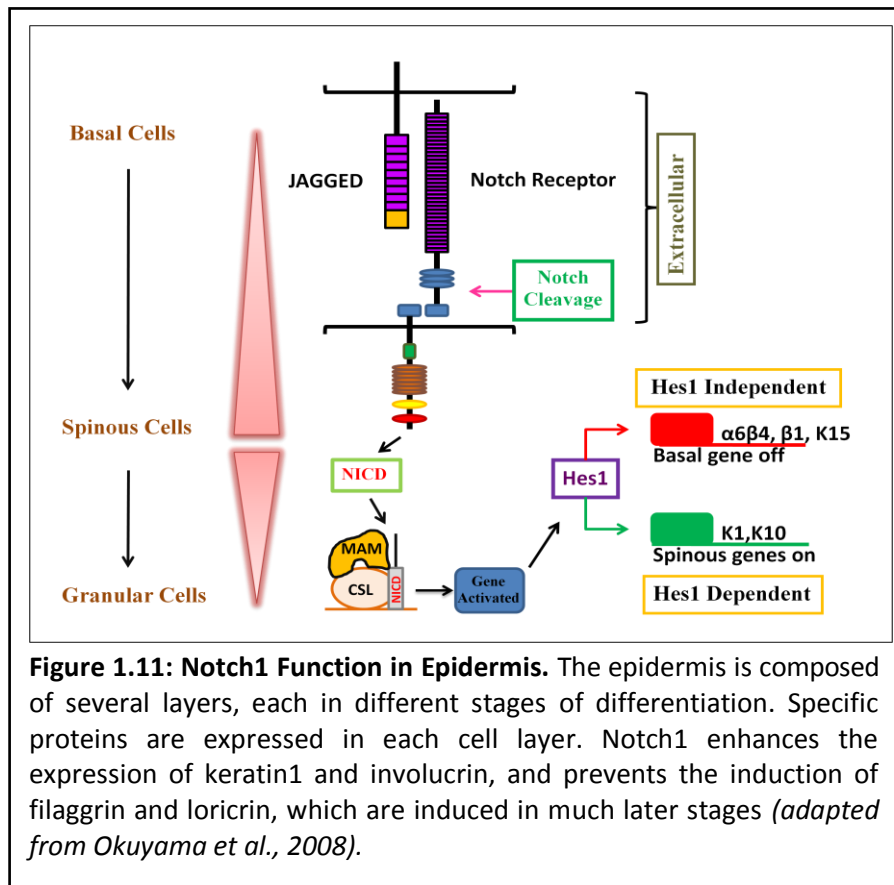
on the cell surface. For example, E3 ubiquitin-ligase (Nedd4 in *Drosophila*) targets notch molecules to the late endosome and subsequent degradation. Interestingly, Deltex (an E3 ubiquitin-ligase in *Drosophila*) is considered a positive regulator of notch but in mammalian cells it down regulates notch activity (*Izon et al., 2002; Le Borgne, 2006*). Thus, ubiquitin appears to control the availability of notch receptors at the cell surface as well as subsequently affecting signal strength and the duration of the signal (*Fior and Henrique, 2008*).

1.2.6 Target Genes of Notch Signalling

The main notch targets activated by the ternary nuclear complex belong to the HES and HERP gene families. These encode basic helix-loop-helix (bHLH) transcriptional repressors whose main function is to implement cell fate decisions mediated by notch signalling. In fact, HES and HERP families directly affect cell fate decisions as primary notch effectors (**Figure 1.11**).

Until recently, the HES gene family were the only known effectors of notch signalling in mammals. However, a new understanding of the notch signalling pathway was identified with the discovery of the HERP gene family. This discovery pointed out similarities between HES and HERP as transcriptional repressors. In particular, some amino acid sequences of HERP were closely related to those of HES family members (*Iso et al., 2003*). Despite the

similarity in the function of HES and HERP as transcriptional repressors for notch signalling, HERP family members employ a different repression mechanism (Iso *et al.*, 2002). Interestingly, HERP expression is detected in both HES expressing and non-HES expressing tissues (Iso *et al.*, 2003).



1.2.7 HES and HERP Gene Families

In *Drosophila*, Hairy and Enhancer of Split (E(spl)) genes are the primary targets of delta-notch signalling but in mammals, the target genes are termed HES. The HES family is a basic helix-loop-helix (bHLH) type C protein that can

modulate the transcriptional activity of target genes. A decade ago, another bHLH family member was identified and named HERP (HES-repressor protein) and this family had three members: HERP1, 2 and 3. However, the names have changed more recently: HEY (HEY2, HEY1, and HEYL), HESR (HESR2, 1 and 3), CHF (CHF1 and 2), HRT (HRT2, 1 and 3) and Gridlock. These are all crucial elements for the development of segmentation, myogenesis and neurogenesis and directly affect cell fate decisions in many tissues (*Iso et al., 2003; Fischer and Gessler, 2007*).

Interestingly, HERP was found to have similar domain characteristics to HES as well as a related amino acid sequence. Added to that, they are part of the larger family of basic helix–loop-helix (bHLH) proteins that regulate transcription by acting as repressors. They have a distinct domain structure including a specific hydrophobic domain that can form homo- or heterodimers. To date, more than 240 bHLH proteins have been identified in different species including many in man (*Massari and Murre, 2000*). They have a distinctive function that requires interaction with a specific DNA binding site. This interaction is closely mediated by contact between each basic domain and a specific half site of DNA consensus sequence (*Murre et al., 1994*).

Due to the bHLH structural and biochemical characteristics, they can be divided into three groups (A, B and C) as illustrated below (**Table 1.3**). Group C are characterized by an invariant proline residue at a specific site in the basic domain. Usually, they bind to class C sites (CACGNG) as well as N-box sequences (CACNAG). They are also known to bind class B sites to some extent but not to class A sites (*Fisher and Caudy, 1998; Iso et al, 2003*).

Table 1.3: Classification of Basic Helix-Loop-Helix (bHLH) Proteins.

Fisher & Caudy (1998)	Massari & Murre (2000)	Protein Type/Function
Class A	MyoD, Mash1	Transcriptional Activators
Class B	Myc, Max	bHLH-Leucine Zipper
Class C	HES, HERP VI VII	Transcriptional Repressors HLH Proteins lacking basic region bHLH-PAS Proteins

A major difference between HES and HERP is a specific proline residue in the basic helix-loop-helix region of HES and HERP has a glycine residue in the corresponding location. All HES members share the WRPW motif where as the HERP family has a YRPW motif or one of its variants: YQPW or YHSW (**Figure 1.12**). Additionally, the HERP family has an extra carboxyl terminal region

which is absent in HES family. Another difference is that the HERP gene plays a critical role in mediating notch effects in both HES and non-HES expressing tissues (*Iso et al., 2003*). The structural similarities and differences among HES and HERP protein families are shown below (**Figure 1.12**).

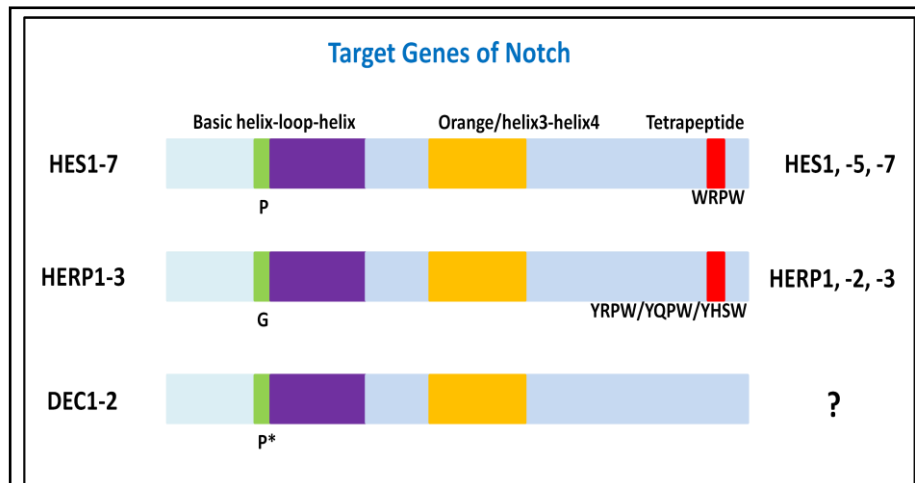


Figure 1.12: Schematic of Notch Target Genes (HES, HERP and DEC). Conserved domains are marked by distinct colours: The basic domain coloured in blue, the helix-loop-helix domain coloured in purple, the Orange domain coloured in orange, and the tetra peptide motif coloured in red. Potential target genes of Notch are listed on the right. DEC is shown because of its similarity to HES and HERP but there is no data supporting DEC as a Notch target (adapted from *Iso et al., 2003*).

1.2.8 Regulation of HES and HERP Gene Families in the Epidermis

Seven HES family members (HES1 to HES7) and three HERP family members (HERP1 to HERP3) have been described in mammals (*Zhong et al, 2000; Iso et al, 2002*). However, evidence has suggested that only three HES genes (HES1, HES5, HES7) but all three HERP genes are potential targets of the notch signalling pathway. However, this work was conducted in tissue culture

models that do not always reflect the situation *in vivo* (Iso *et al*, 2003). Also, while strong evidence that HES1, HERP1 and HERP2 were primary targets of notch in cultured cells was provided, only HES1 and HES5 are known to be true effectors of notch *in vivo* (Ohtsuka *et al*, 1999).

Furthermore, experiments in mice showed that notch signalling could affect HES and HERP genes differently. Some target genes appear to be independent, while a lack of notch signalling can cause a decrease in the expression of other target genes. This observation supports the supposition that HERP may be a physiological notch effector. Another observation is that HERP1 (also called HEY2, HESR2, CFH1 or HRT2) has intrinsic transcriptional effector activity and forms a heterodimer with HES1. However, these physiological observations still need to be tested directly on target gene promoters (Iso *et al*, 2003).

Another study showed that HES1 expression was not affected in the absence of notch. This raises a question as to whether there is an alternative pathway that can lead to target gene expression in the absence of notch signalling. According to Moriyama *et al* (2008), HES1 was expressed in undifferentiated embryonic stem cells, in foetal tissues, endothelial cells and regenerating liver (Katoh and Katoh, 2007).

An *in vivo* study using mice suggested that only HES1 plays an important role in the development of the epidermis. Nevertheless, it did show how crucial HES1 was for the generation and maintenance of spinous cells during epidermal development but the situation in postnatal tissues was not clear. At the same time, this indicates how important notch signalling is in the development of the nervous system and pancreas. While it is clear that HES1, HES5, and HES7 can be induced by notch signalling, it appears that HES2, HES3 and HES6 expression can be induced independent of notch signalling (*Moriyama et al., 2008*). However, the situation with HES4 is not clear as there is still insufficient data available. Other studies, suggested that HERP family members can be induced by notch signalling but results are also inconclusive.

1.2.9 Role of Notch Signalling in Epidermal Development:

Notch signalling is considered a highly conserved pathway essential for cell fate determination in embryonic development but less is known about the function in adult tissues. Human epidermis is regulated by notch signalling and this is required for the maintenance of stem cells, for proliferation and for differentiation into mature keratinocytes (*Blanpain et al, 2006*). However, some details of how this complex terminal differentiation programme is regulated in keratinocytes still remain unclear (*Nickoloff et al., 2002*). While

notch signalling in human epidermis may initially promote differentiation, loss of notch signalling in the skin may potentiate skin tumour development or result in a defect of interfollicular epidermal differentiation (*Rangarajan et al., 2001 and Nicolas et al., 2003*). It is important to point out that notch signalling is critically dependent of specific interaction with other signalling pathways with possible opposite roles in growth and development of different cell types.

It is now well demonstrated that notch signalling plays an important role in promoting human T-cell leukaemia. In fact, the proto-oncogenic function of notch signalling is also considered in human breast, ovarian cancer and melanoma. This was proven experimentally by *Lefort* and his team where suppression of notch signalling by either genetic or pharmacological manipulation was sufficient to observe oncogenic changes in primary human keratinocytes. Also, gene knockdown of ROCK1/2 and MRCK α *in vivo* showed that those kinases are critical targets in controlling human keratinocyte tumour formation through negative regulation by Notch1, and p53 which controls the expression of Notch1 in keratinocyte cell lines and tumours (*Lefort et al., 2007*).

In addition, suppression of Notch1 in primary human keratinocytes with activated *ras* causes aggressive squamous cell carcinoma (SCC) formation. A

major consequence of Notch1 deletion is impairment of skin barrier integrity and the defective barrier may promote tumorigenesis. According to *Demehri et al (2008)*, a reduction in notch signalling within keratinocytes impairs the ability to execute the terminal differentiation programme resulting in a defective skin barrier and death, if areas involved were large. Another observation was proposed using reduced notch expression as an experimental model suggested that the main effect of Notch1 loss is to provide a proliferative signal to initiated cells which can then form tumours and may even proceed to invasive carcinomas (*Demehri et al., 2009*).

Although, most SSCs harbour p53 mutations, additional tumour suppressors have been reported such as Notch1 mutations. It is well documented that Notch1 mutations occur in majority of T-cell lymphoblastic leukaemias/lymphomas. Yet, loss of Notch1 can produce basal cell carcinoma like cells or SCCs in mice. In fact current models suggest that Notch1 can act as a transcriptional down regulator due to p53 loss of function, which subsequently causes human epithelial malignancies. In addition, there is genetic evidence that non-canonical notch function in the skin may also contribute to carcinogenesis. Wang *et al* identified the presence of Notch1 and Notch2 mutations in 75% of cutaneous SCCs. This observation suggests that targeted inhibition of the notch pathway may induce squamous epithelial malignancies (*Wang et al., 2011*).

Several studies have examined notch signalling in human epidermis at the protein level. *Lowell et al* (2000) suggested that Notch1 was expressed in all living epidermal cells throughout differentiation but DLL1 was confined to the basal layer. On the other hand, *Wilson and Radtke* (2006) provided evidence that mRNA encoding Notch1-3 was expressed in the basal layer of human epidermis. *Estrach et al* (2008) also detected suprabasal expression of JAG1 and JAG2. In addition, *Powell et al* (1998) detected expression of Notch1 and JAG1 at the protein level in hair follicles with Notch1 expression in the bulb and ORS while JAG2 was restricted to the bulb and basal layer of the ORS.

A new insight presented by *Moriyama et al* (2008) suggested that the role of notch signalling was to either inhibit or promote differentiation depending on the exact cellular circumstances in which it was acting. This was proven in another study that highlighted a crucial role for notch signalling in the inhibition of epidermal development (*Blanpain et al., 2006*).

For example, absence of Notch1 in postnatal tissues causes hyperproliferation of basal keratinocytes. In contrast, absence of Notch1 during certain stages of epidermal development can result in hypoproliferation of the basal layer and loss of the granular layer (*Blanpain et al., 2006*). These contradictory functions of the notch signalling pathway in regulating keratinocyte proliferation and

differentiation raises questions about the precise role of notch signalling in embryonic development and in post-natal adult tissues. In addition, which notch signalling pathway (canonical or non-canonical) is active during the control epidermal keratinocytes (*Rangrajan et al., 2001*). However, there is still very little evidence of any dynamic regulatory function of notch signalling in terms of epidermal differentiation. In order to clarify some of these issues with regard to notch signalling and epidermal differentiation, a series of experiments have been conducted based on the HaCaT cell culture model of calcium-induced keratinocyte differentiation.

CHAPTER 2: Materials and Methods

Studying the expression of notch receptors, ligands and target genes and the control of the signalling pathway *in vivo* (i.e. in human skin) is not realistic, so it is important to have a model that resembles the skin as closely as possible. As we have focused on epidermal differentiation, a HaCaT cell culture model appeared to be the best option for conducting experiments that can mimic the differentiation-related changes observed in human epidermis. A number of different culture experiments were done as only a limited amount of material in terms of protein and total RNA can be produced per experiment and there is a need to test the reproducibility of such models. Also, in order to examine cultures using different techniques such as immunofluorescence (IMF), protein electrophoresis (SDS-PAGE) and western blotting, polymerase chain reaction (PCR and RT-PCR) and real time quantitative PCR (QPCR), more than one set of cultures would be required. Thus, cultures were set up in duplicate and sometimes triplicate so that total RNA could be extracted from one set, protein from another and IMF done on another so they all used the same cells. In addition, specific DNA probes of each signalling pathway intermediate were made from isolated total RNA and cloned into pGEM vectors to act as quantitation controls for QPCR.

2.1 Keratinocyte Cell Culture Models

Cell culture models are a valuable basic research tool and they have significantly helped molecular investigations into the structure and function of many different human tissues. For instance, in skin biology, studies of keratinocytes in monolayer culture have elucidated many functional and structural characteristics of the epidermis. These cells can stratify to produce the typical cell layers found *in vivo* and allow the study of keratinocyte differentiation and production of the cornified envelope (skin barrier). Furthermore, if used in raised organotypic cultures, differentiation proceeds even further and these models are now considered as an alternative to the use of laboratory animals, especially in the pharmaceutical and cosmetic industry.

2.1.1 HaCaT Cells

HaCaT cells are immortalized human keratinocytes that replicate indefinitely at low density but are able to differentiate at high density. Furthermore, high concentrations of calcium in the culture medium can increase the potential of these cells to differentiate. In low calcium (0.06 mM) medium, the cells are flat and spindle like with an absence of cell to cell adhesion. However, when the cells are exposed to high calcium levels (1.8 mM), they switch from proliferation to differentiation. The cells become cuboidal in shape and form compact organised groups with strong cell to cell adhesion via desmosome

junctional complexes. In addition, once they become confluent, they can also stratify forming several vertical layers of cells.

One advantage of using a HaCaT cell model is that these cells retain most of the features of normal epidermal cell morphogenesis and differentiation. At the same time, they can be encouraged to enter differentiation in a coordinate manner upon stimulation with calcium. Furthermore, these cells express markers appropriate to their state as well as undergoing noticeable structural changes as differentiation proceeds. This allows investigation of the signalling that underlies the calcium induced-differentiation in a laboratory setting. However, as these cells are immortalized, they can vary in growth rate and may respond to stimuli in a different way to normal keratinocytes, which can affect the validity of the experimental results obtained.

The HaCaT cell line was provided by Prof. N.E. Fusenig (Deutsches Krebsforschungszentrum [DKFZ], Heidelberg, Germany). Frozen HaCaT cells were stored in cryogenic ampoules in liquid nitrogen and the current research project used cells from passage 39-41. Stock cells were stored in a cryoprotective medium containing foetal bovine serum (FBS from Lonza, Slough, UK) and 10% dimethylsulphoxide (DMSO, Sigma Aldrich, Gillingham, UK). An aliquot of cells was thawed at room temperature (RT) and then re-suspended in 10ml of pre-warmed Dulbecco's Modified Eagle's Medium (DMEM from

Invitrogen, Paisley, UK) containing 10% FBS and antibiotics (100 units/ml of penicillin and streptomycin from Lonza, Slough, UK). All cell manipulations were performed under sterile conditions in an aseptic environment within a class 1 containment cabinet. HaCaT cells were grown in 75cm² culture flasks (Corning flasks supplied by Western Laboratory Solutions, Horndean, UK) with vented caps and incubated at 37°C in air containing 5% CO₂ (MCO-17AIC incubator, Sanyo, Loughborough, UK) until they reached 70-80% confluence. The DMEM medium was changed every other day and cells were passaged every 5-6 days.

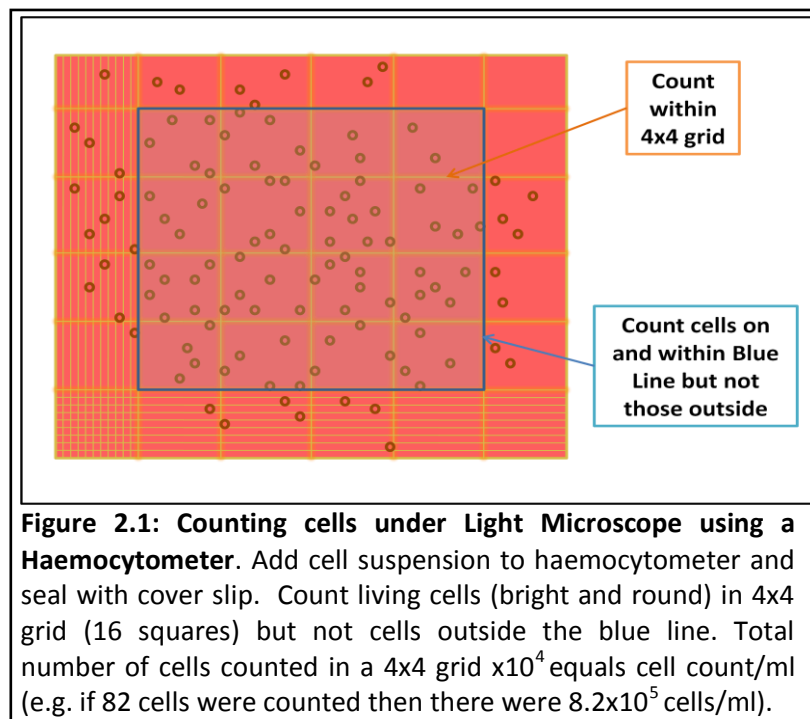
In order to passage the HaCaT cells, they were detached from the surface of the culture flask using trypsin. Initially, the cells were washed three times with sterile phosphate buffered saline (1x stock PBS from Lonza, Slough, UK) and then 5 to 10ml Trypsin-EDTA solution (0.5 mg/ml Trypsin, 0.2 mg/ml EDTA from Lonza, Slough, UK) was added to the culture flask. This was placed in an incubator at 37°C for 5-15 minutes depending on cell density. The cells were dislodged from the flask base by tapping the sides and then transferred to a 50 ml polypropylene tube containing 15ml of DMEM supplemented with 10% FBS. The tubes were centrifuged at 1500 rpm for 5 minutes at RT (Centra-4B centrifuge from IEC, Massachusetts, USA), the medium was carefully poured off and the cells were re-suspended in 5ml DMEM supplemented with 10% FBS and antibiotics (as detailed above). Three new flasks each containing 10 ml of DMEM containing 10% FBS and antibiotics were prepared and 1ml of the

re-suspended cells added to each flask to provide sub-cultures for subsequent experiments. The new flasks were labelled with the passage number and date, and then incubated for 3-5 days at 37 °C in 5% CO₂. Some of the generated HaCaT cultures are then frozen down for future use.

To freeze down HaCaT cells, they should initially be grown as usual in DMEM medium with 10% FBS until they are 80% confluent. Then the medium was poured off leaving the cells adhering to the plastic dish. The cells were then washed three times with 1ml of sterile 1x PBS and then incubated in Trypsin-EDTA (0.25% of Trypsin with 1mM EDTA) solution at 37°C for 5 minutes. Cells were dislodged from the flask by tapping the sides gently and then transferred into a 50ml tube containing 15ml DMEM + 10% FBS. The tubes were centrifuged for 5 minutes at 1500 rpm (RT) in a Centra-4B (IEC, Massachusetts, USA). The supernatant was removed and the cells re-suspended in 10 ml of freezing medium (FBS + 10% DMSO). The re-suspended cells were pipetted into a series of 1ml cryovials (Corning, NY, USA) labelled with the cell line, passage number and date. These were initially frozen in a -85°C freezer for 1-2 days and then transferred into a liquid nitrogen storage container (BIO36, Statebourne, Washington Tyne & Wear, UK) for long term storage.

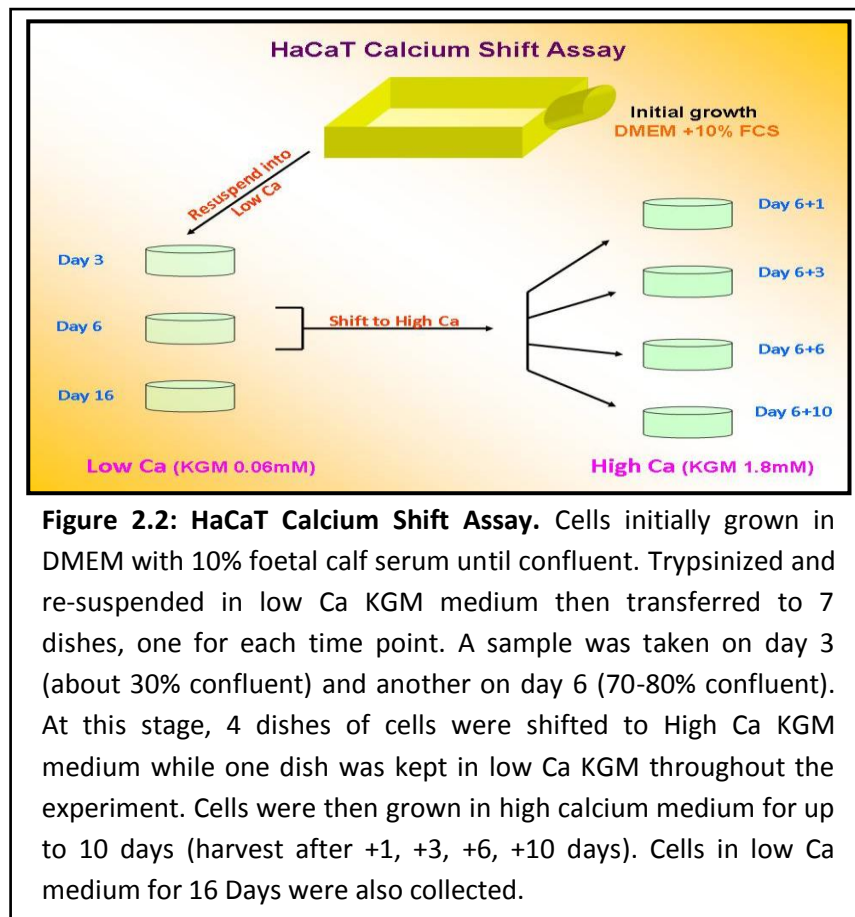
2.1.2 Calcium-Induced Differentiation

When HaCaT cells growing in DMEM reached 70-80% confluence, they were transferred to keratinocyte growth medium (KGM). Cells were washed with PBS and trypsinized as detailed above then centrifuged (1500 rpm, 5 mins, RT) and re-suspended in 5ml of KGM medium (Lonza, Slough, UK) containing 0.06mM CaCl₂ (low calcium medium), bovine pituitary extract (BPE), hEGF, insulin, hydrocortisone, genatmicin sulphate and amphotericin B. The cell density was assessed using a haemocytometer under a light microscope and the cell density of the original sample calculated as described below (See **Figure 2.1**).



Culture experiments required 7 large (10cm) petri dishes which were plated at a density of 4.5×10^5 cells per dish (in 6ml of medium), requiring a total of 3.15×10^6 cells ($7 \times [4.5 \times 10^5]$) in 42 ml (7×6 ml) of medium. For one experiment, cell counting results gave a density of 8.2×10^5 cells/ml so for seven dishes the total volume of cell suspension needed would be 3.84ml (31.5×10^5 divided by 8.2×10^5). This was then diluted to a total of 42.0 ml by adding 38.16 ml low calcium medium, mixing gently and then, adding 6ml of the cell suspension to each dish.

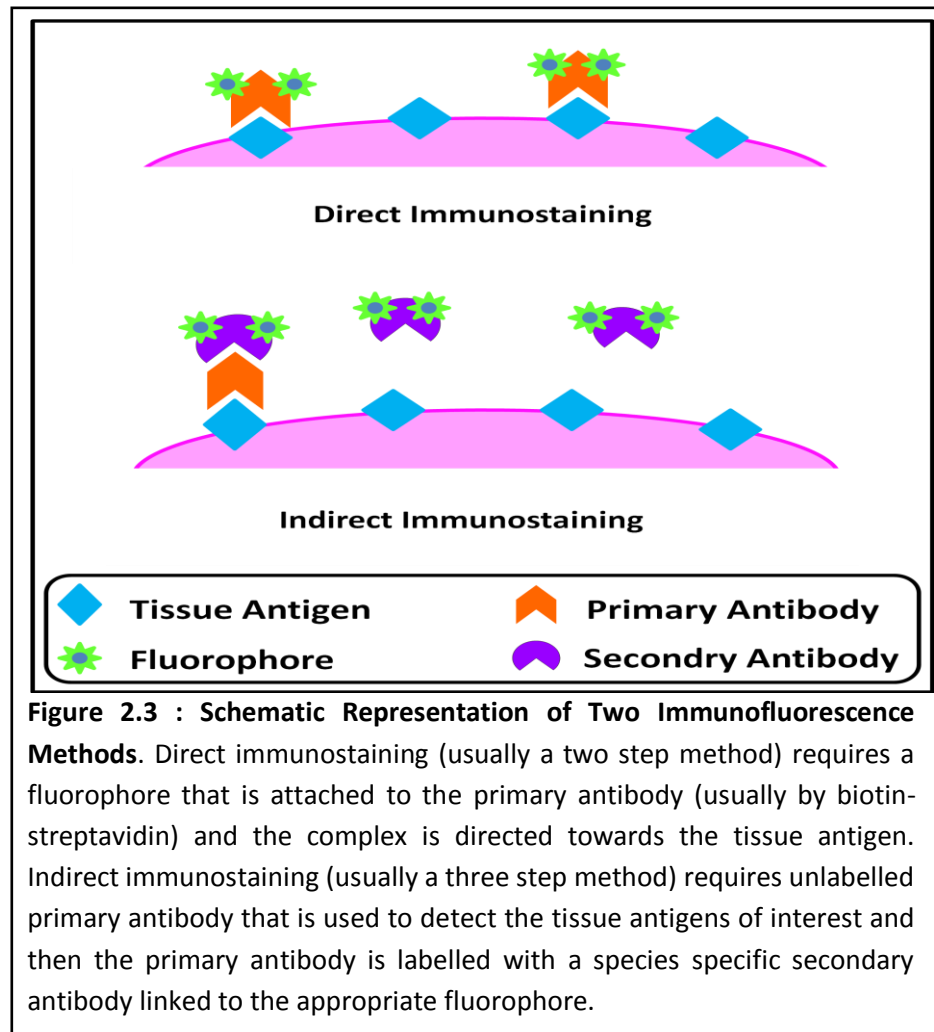
The larger 10cm dishes were seeded at a density of 450,000 (4.5×10^5) cells for RNA/protein extraction while smaller 3.5 cm dishes containing four cover slips used for IMF were seeded with 100,000 (1×10^5) cells, both in low calcium KGM medium. In order to assess HaCaT cells that were still proliferating and actively growing, one dish of cells was harvested at 3 days (about 30% confluent) and another dish at 5-6 days after plating (70-80% confluent). At this point, terminal differentiation was induced in the cells by altering the calcium level to 1.8 mM. A third dish was kept in low calcium medium for another 6 (or 10) days and then left to grow until the end of the experiment (harvested on day 12 or 16 depending on the experiment). Three sets of plates (four in some experiments) were grown for 5-6 days in low calcium medium and then switched to KGM medium containing high calcium (1.8 mM). These were also harvested at intervals (see **Figure 2.2**).



2.2 Immunofluorescence (IMF)

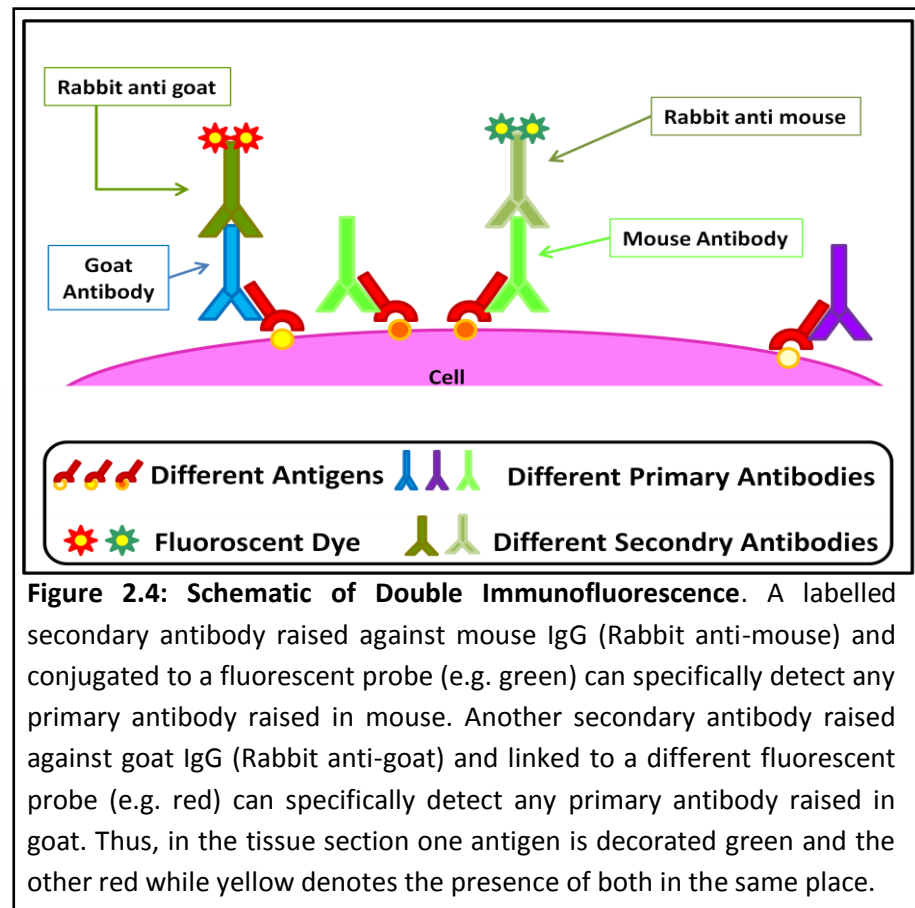
Proteins (or antigens) can be detected in tissues and cells using a technique called immunofluorescence (IMF) microscopy. There are two general approaches, direct or indirect. Direct immunofluorescence requires a fluorescent dye that is attached to the primary antibody, which can then be used to localize the respective antigen in a tissue or cell by fluorescence microscopy. Indirect immunofluorescence is more sensitive because this involves a three step rather than a two step method. Here, the fluorescent

dye is linked to a secondary antibody that is used to detect the primary antibody in a species specific manner (see **Figure 2.3**).



One advantage of immunofluorescence is that the technique can also be used to visualize two or more antigens within the same tissue or cell sample at the same time using different colour fluorescence. However, this requires that the primary antibodies are derived from different species and the secondary antibodies are species-specific so that no cross-reactivity occurs. A different

fluorescent dye can then be attached to each secondary antibody and so two different antigens can be localised in different colours (see **Figure 2.4**).



2.2.1 Tissue and Cell Preparation

Cultured cells grown on glass cover slips were treated with specific rabbit polyclonal or mouse monoclonal antibodies (see **Table 2.1**). For double immunofluorescence, the primary antibodies were either added as a mixture or added sequentially. However, each primary antibody should be used at its optimal concentration (usually diluted in 1x PBS). The primary antibodies were then detected by species-specific secondary antibodies (see **Table 2.2**) which are bound to a fluorescent dye: Alexa 488 (green) or Alexa 594 (red). These

dyes can be visualised under a fluorescence microscope and the location of antigens within the cells can be observed and digitally recorded.

2.2.2 Antibodies

Polyclonal and monoclonal antibodies are widely used in research as well as in medical diagnostics. They detect the presence of antigens in tissues or cells by reacting to various epitopes or regions of a specific antigen to which they were originally raised. They are also species specific and generally antibodies to human antigens are raised in mice, rabbits or goats. The epitopes can be linear or have a requirement for three-dimensional structure, characteristics that can limit their use. The optimum concentration for each antibody was established by testing serial dilutions. Despite polyclonal antibodies being sensitive, they are not always monospecific. This depends on the purity of the original antigen used and the response of the animal in which they were raised. Therefore, cross-reactivity can be experienced and is especially apparent in closely related antigens of the same protein family.

Keratin 10 is well documented as a marker of differentiation and expressed predominantly in suprabasal epidermal cells *in vivo*. A mouse polyclonal antibody (Ab24638-50) was commercially available from Abcam (**Table 2.1**). A keratin 14 (K14) mouse monoclonal antibody (LL002) was used as a marker of the proliferative compartment as K14 was expressed specifically in basal cells of epidermis *in vivo*. This antibody (LL002) was originally made in the London

Hospital by Prof. Irene Leigh but can now be purchased from Abcam. In addition, a rabbit polyclonal antibody to a nuclear marker found in dividing cells (Ki67) was purchased from Abcam (**Table 2.1**).

In order to detect Notch1 receptor expression in basal and/or suprabasal epidermal cells *in vivo* and in cultured keratinocytes, a rabbit polyclonal antibody (Ab5702) that was commercially available from Chemicon was purchased (**Table 2.1**). Jagged1, a Notch ligand was detected in human epidermal cells *in vivo* and in cultures with a goat polyclonal antibody (C-20) that was purchased from Santa Cruz (**Table 2.1**).

Table 2.1: Primary Antibodies used for IMF. The species, catalogue number, source company and working dilution are listed for each primary antibody.

Antibody	Species	Cat #	Company	Dilution	Amount
K14	Mouse	LL002	Abcam	1:5	10 µl in 50 µl
K10	Rabbit	Ab24638-50	Abcam	1:25	2 µl in 50 µl
Notch 1	Rabbit	Ab5702	Chemicon	1:25	2 µl in 50 µl
Ki67	Rabbit	Ab16667	Abcam	1:25	2 µl in 50 µl
Jagged 1	Goat	C-20	Santa Cruz	1:25	2 µl in 50 µl

There were two different Alexa Fluorescent dyes used in the IMF experiments. For instance, Alexa (type 594) which gives red fluorescence was used for the keratin 14 mouse antibody. On the other hand, Alexa (type 488) which gives a green fluorescence was used for Keratin 10, Ki67, Notch1 and Jagged1

antibody detection. Keeping in mind that this fluorescence depends on the species of the primary antibody whether it is a goat, rabbit or a mouse (see **Table2.2**).

Table 2.2: Secondary Polyclonal Antibodies used in IMF. Two different types of Alexa fluorescent secondary antibody were used: Alexa 594 (red fluorescence) and Alexa 488 (green fluorescence). These also differed in the species detected (use mouse, rabbit or goat depending on the species of primary antibody).

	Primary Antibody	Secondary	Species	Type	Dilution	Amount
1	K14	Alexa	Mouse	594	1:500	2 µl in 1ml
	K10, Ki67, Notch1	Alexa	Rabbit	488	1:500	2 µl in 1ml
2	K14	Alexa	Mouse	594	1:500	2 µl in 1ml
	Jagged1	Alexa	Goat	488	1:500	2 µl in 1ml

2.2.3 Labelling Procedure

Cultured cells (HaCaT) were grown on cover slips in 35mm petri dishes and were fixed using a mixture of ice-cold methanol/acetone (1:1). The fixed cells were then washed with 1x PBS and either processed directly for single or double immunofluorescence or left in 1x PBS overnight in the fridge (4°C).

Several 100µl aliquots of blocking solution (TBS + 5% BSA) were pipetted onto a piece of parafilm (Nescofilm, KARLAN Research Products, Arizona, USA). After fixation, cover slips were removed from the dish, dabbed on filter paper to remove excess liquid and then inverted (surface containing cells facing

down) onto an aliquot of blocking solution. These were incubated for 30 minutes at RT after which the cover slips were gently tapped on tissue to remove excess liquid. They were then placed face down on a 90 μ l aliquot of primary antibody diluted in PBS + 0.6% bovine serum albumin (see **Table 2.1** for list of primary antibody working dilutions). The cover slips were incubated overnight at 4°C in a humidified dish.

Secondary antibodies were diluted in PBS + 0.6% BSA (see **Table 2.2** for details) and 100 μ l aliquots added to a sheet of parafilm. The cover slips were washed three times with PBS (phosphate buffered saline) and after excess liquid had been removed, they were placed face down on the secondary antibody and allowed to incubate for 30 minutes at RT.

Finally, the cover slips were washed three times in PBS, dabbed dry and placed face down on a 70 μ l aliquot of DAPI solution (diluted to 1:1000 with PBS) for 5-10 seconds. Excess DAPI was removed and the cover slip placed face down on a 10 μ l aliquot of hydromount placed on a glass microscope slide. These were left for one hour until they were dry and then the cover slips were sealed onto the slide with clear nail polish. The slides were stored in the fridge at 4°C in the dark until examined under a fluorescent microscope with the appropriate filter.

2.2.4 Assessment of Results

A high resolution fluorescence microscope with a digital capture photographic system (Nikon Optiphot EFD-3 with Zeiss Axiocam system) was used to view the samples and provide images of the specimens studied. This microscope has a mercury light source, specific fluorescence optics (x20 and x40) and filters for FITC (green), TR (red) and DAPI (blue). These filters also work with the green (488) and red (594) Alexa dyes.

HaCaT cells were stained with selected pairs of primary antibodies linked to two different coloured fluorescent dye complexes (red or green) and counterstained with DAPI (stains nuclei blue). Each slide represents a different stage of HaCaT cell growth and differentiation. Individual images were taken for each cover slip under red, green or blue filters and recorded using the Zeiss Axiocam HRc system. Later, these images can be viewed by Axiovision software either as the individual colour images or any combination of the images (e.g. red and green, red and blue, green and blue or all three). These images were stored on a computer hard drive as both tiff and jpeg files.

2.3 Total Protein Extraction and Analysis

Total protein extraction is a method where the protein components of cultured cells or tissues (human, animal or plant) can be isolated from the

other macromolecules in the cells. As total RNA was also sought, a kit that was able to isolate both total protein and total RNA from the same sample was used (Norgen Biotek RNA/Protein purification kit, Norgen Biotek Corporation, Thorold, Canada). This made it possible to isolate both RNA and protein from a very small sample and use these extracts to study gene expression in a reliable way from a single sample of cells.

2.3.1 Extracting Proteins from Cultured Cells

Total RNA was extracted from HaCaT keratinocytes grown in 10cm petri dishes. The medium was removed from the dish and the cells were washed with 2ml PBS at RT. A 700µl aliquot of lysis solution supplied in the RNA/protein purification kit (Norgen Biotek Corporation, Thorold, Canada) was added to cells in the petri dish and a 1ml syringe was used to mix the cells and lysis buffer. The mixture was then placed in a sterile 1ml tube labelled with the extraction date and the tubes placed in a -80°C freezer until extracted.

In order to extract protein from the stored samples, they were first thawed on ice and then an equal volume of isopropanol was added and mixed. An aliquot of the lysate/alcohol mixture (up to a maximum of 600 µl) was applied to a separation column (from the Norgen Biotek RNA/Protein purification kit) and centrifuged (Sigma1-13, Buckinghamshire, UK) at 11,000 rpm for 1 minute at

RT. At this stage, the material eluted from the column can be used for protein extraction. The eluate (100µl) was placed into a fresh microcentrifuge tube (supplied in kit) and 475µl of molecular biology grade water containing 24µl of pH binding buffer was added. The contents of the tube were mixed well and up to a maximum of 600µl of pH adjusted protein was transferred into a new spin column with a new collection tube attached. This was centrifuged at 8,000 rpm for 2 minutes at RT. The spin column was inspected after centrifuging to ensure that the entire sample had passed into the collection tube. Then, flow through was discarded. Once the entire protein sample has been loaded onto the spin column, 500µl of protein wash buffer (supplied in the kit) was applied to the column and centrifuged at 8,000 rpm for 2 minutes at RT. The flow through was discarded and the spin columns were inspected for any residual liquid that did not pass into the collection tube. Neutralizer (9.3µl) was added to a 1.7ml elution tube (both supplied in the kit) and the spin column was transferred into this elution tube. Finally, 100µl of protein elution buffer was added to the spin column and centrifuged at 8,000 rpm for 2 minutes at RT to elute the bound proteins. The columns were discarded and the eluate in the collection tubes were transferred to new labelled 1.5ml tubes and stored at -20°C (short term) or -80°C for long term storage.

2.3.2 SDS-Polyacrylamide Gel Electrophoresis

Polyacrylamide gel electrophoresis in the presence of sodium dodecyl sulphate (SDS-PAGE) is a method of separating a protein mixture into its component polypeptides according to size. Separation of proteins of average size requires a gel of about 10% but resolving gels in the range of 7.5% to 17.5% can be used.

Gels were prepared in a plastic cassette held together with bulldog clips and sealed at the bottom. This was set up on a tray and the necessary reagents for two 10% resolving gels were mixed together (see **Table 2.3**) and pipetted into the cassette. This was filled to a point about 2 cm from the top and a layer of water was carefully applied to ensure a flat surface while the gel sets (takes about 30 minutes).

Table 2.3: Preparation of 10% Resolving Gels (SDS-PAGE).

Stock Components	Volume	Final Concentration
1.5M Tris pH 8.8	3.75 ml	0.375M
30% gel solution	5.00 ml	10%
dH₂O	6.025 ml	Not applicable
10% SDS	150 µl	0.1%
10% Ammonium persulphate	75 µl	0.05%
TEMED	7.5 µl	0.05%
Total Volume	15ml	

A stacking gel is added to the top of the resolving gel and this requires 5ml of a 4% gel mix prepared as shown below (**Table 2.4**). Once the resolving gel was set, the water was removed from the top and replaced with the stacking gel solution. A comb was then carefully placed into the top of the stacking gel mixture which was allowed to set for about 20-30 minutes.

Table 2.4: Preparation of 4% Stacking Gel (SDS-PAGE).

Stock Components	Volume	Final Concentration
0.5M Tris pH 6.8	1.25ml	0.125M
30% gel solution	0.66ml	3.9%
dH₂O	2.98ml	Not applicable
10% SDS	50µl	0.1%
10% Ammonium Persulphate	50µl	0.1%
TEMED	10µl	0.02%
Total Volume	5ml	

The sealing strip was removed from the bottom of the gel cassette (prevents liquid gel leaking from the cassette before setting occurs). However, the strip must be removed to allow the current to flow through gel. The two cassettes are placed onto the XCell II™ Module apparatus (Invitrogen, Paisley, UK) with the wells facing inwards and the gels locked into place.

Running buffer (80ml of 10x running buffer stock mixed with 720ml dH₂O) was poured into the apparatus and the protein samples and molecular weight

markers were carefully added to the wells. A sample of MagicMark™ XP Protein Standard (Invitrogen, Paisley, UK) and low molecular weight range marker were loaded first then the samples (15 µl of protein marker mix plus 5 µl 4x buffer was loaded per well).

Finally, the chamber between the gels was filled up to a point about half a centimetre above the wells. The gels were run at 150V (constant voltage) until the marker dye reached the bottom of the separating gel. At this point the power was turned off and the gels were unlocked. A novex spatula was used to crack the cassettes open from the sides and bottom. The stacking gel was removed from the cassette and one of the bottom edges of the resolving gel cut diagonally for identification. One gel was then stained with Coomassie blue R250 (Proteabio Europe, Nimes, France) and the duplicate gel was stored in the fridge (2°C) for western blotting.

2.4 RNA Extraction

Total RNA was extracted from HaCaT keratinocytes grown in 10cm petri dishes. The medium was removed from the dish and the cells were washed with 2ml PBS for few seconds at RT. The PBS was removed and 600µl lysis solution (RLT Plus buffer) from the RNeasy Plus Mini Kit (Qiagen Ltd., Crawley,

UK) was added to the petri dish and swirled around for about 1 minute to fully lyse the cells. A 1 ml syringe with 1" needle (25G) attached was used to extract cells from the dish and transfer them to a sterile 1ml tube. The cells were then passed through syringe needle 5-10 times to further lyse the cells and reduce the viscosity. Tubes were labelled with the extraction date and placed in a -80°C freezer until extracted. It is important to point out that the volume of RLT Plus required in the step above depends on the size of dish used in the tissue culture. For example, a petri dish smaller than 6 cm will need 350µl but more than 6 cm will need 700µl buffer.

In order to extract total RNA from the stored samples, they were first thawed on ice and then the tubes were placed in a bench centrifuge (Sigma Model 1-13, Newport Pagnell, UK) at maximum speed (13,000 rpm) for 3 minutes at RT. The homogenized lysate was then transferred to a gDNA Eliminator spin column fitted with a 2ml collection tube (Qiagen, Crawley, UK). The spin column was centrifuged at 11,000 rpm for 30 seconds at RT (Sigma 1-13, Newport Pagnell, UK). The column was discarded and 600µl of 70% ethanol was added to the eluate in the collection tube. The tube was mixed well by pipetting up and down. This eluate of the lysate/alcohol mixture (up to a maximum of 700 µl) was transferred to an RNeasy spin column fitted with a new 2ml collection tube (supplied in the kit) and centrifuged at 11,000 rpm for 15 seconds at RT (Sigma 1-13). An aliquot (700 µl) of RW1 buffer was added to the RNeasy spin column and this was centrifuged at 11,000 rpm for 15

seconds at RT. The eluate (flow through) was discarded and 500µl of RPE buffer was added to the column. This was centrifuged at 11,000 rpm for 15 seconds at RT and the eluate was again discarded. Another 500µl of RPE was added to the column which was centrifuged at 11,000 rpm for 2 minutes at RT and the eluate discarded. Finally, the RNeasy spin column was placed in a new 1.5ml collection tube (from the mini kit) and 50µl of RNase-free water (from the mini kit) was added directly to the spin column membrane. The column and collection tube were centrifuged at 11,000 rpm for 1 minute at RT and the total RNA in the labelled collection tubes were placed on dry ice before storage in a - 80°C freezer.

2.5 Polymerase Chain Reaction (PCR)

Polymerase chain reaction (PCR) is one of the fundamental methods in modern molecular biology. The PCR technique was developed in 1983 by *Kary Mullis*. He developed a method by which a desired gene or part of a gene can be amplified from a mixed DNA sample by adding a pair of short complimentary DNA oligonucleotides known as primers. They bind specific regions of cDNA or gDNA and DNA polymerase can copy the region between the primers. This enables researchers to produce millions of copies of a specific DNA sequence in few hours.

The major feature in PCR reactions is the temperature change during the reaction, which controls the annealing of the two DNA strands, the activity of the DNA polymerase and the binding of primers. However, in the early experiments, due to the use of high temperatures, the DNA polymerase had to be renewed at every cycle. This is expensive and time consuming. However, the discovery of a thermo-stable DNA polymerase (known as Taq polymerase) in hot spring bacteria such as *Thermus aquaticus* revolutionised the technique, as a single aliquot of Taq polymerase could be used for the whole process (up to 40 cycles).

PCR reactions have three major steps: denaturation of double stranded DNA, annealing of the primers to each single strand of DNA and extension of the sequence from the primer by Taq polymerase (copies single strand). These three operations are done at three different temperatures and are repeated for 30-40 cycles (outlined in detail below).

2.5.1 Reverse Transcription PCR (RT-PCR)

The process of RT-PCR requires two steps: reverse transcription of poly A⁺ mRNA to produce total cDNA and specific PCR amplification of a specific cDNA defined by the primers. This can be done separately or as a continuous reaction in a single tube. A dilution of isolated RNA was initially measured on a spectrophotometer (Pharmacia Gene Quant pro from Pharmacia GE

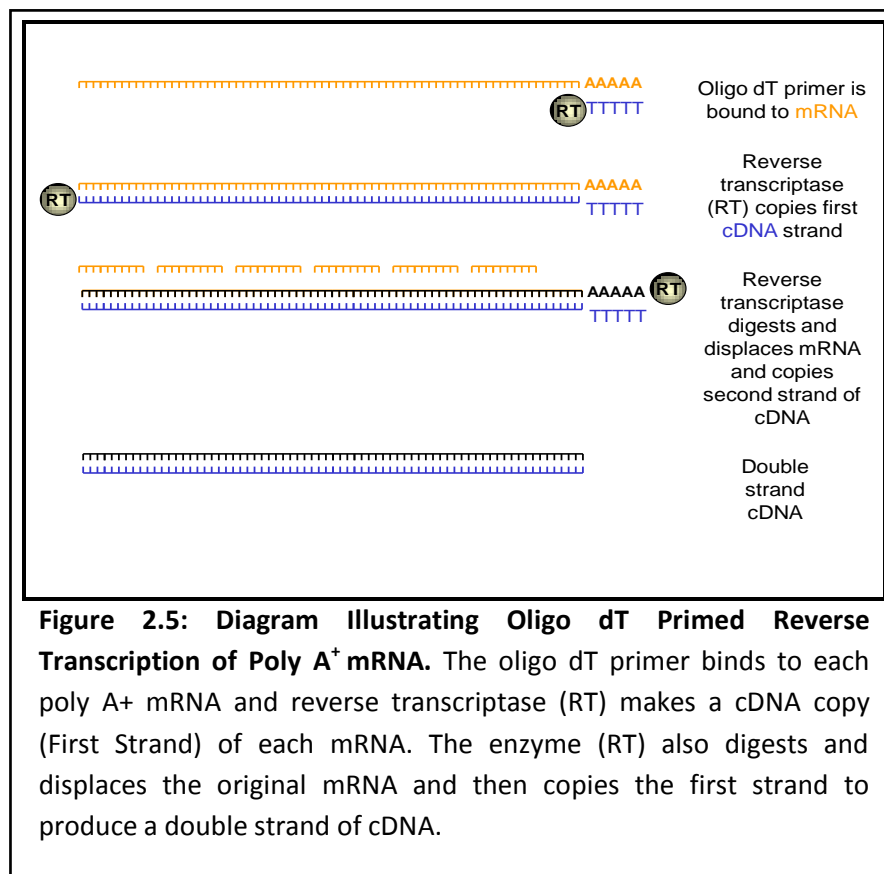
Healthcare, Little Chalfont, UK) to determine the concentration. The RNA concentration for each sample was equalised by adjusting the total volume to 10µl with sterile water. This mixture was then heated at 65°C for 10 minutes (hot start) in a PCR machine (ABI Gene Amp PCR System 9700 from Perkin Elmer, Norwalk, USA).

A master mixture of five reagents (Oligo dT, reverse transcriptase, dNTPs, RNase inhibitors) was prepared in nuclease free (NF) water (see **Table 2.5**). Immediately after the hot start reaction, 20 µl of the reagent master mixture was added to the mRNA in each tube. This was heated at 37°C for one hour allowing oligo dT to bind to the poly A tail of the mRNA templates. This initiates copying of the mRNA by reverse transcriptase (RT) to make the first single strand copy of DNA.

Table 2.5: RT2 COMPONENTS. Illustrates the second part of reverse transcription reaction mixture component where each sample of RNA (10µl) is mixed with 20 µl of mixture above post RT1. Note: all the reagents are placed on ice at all times.

Components	RT2 Mix 20µl Total
Oligo dT (Qiagen)	1µl
RNase (Qiagen)	0.2µl
dNTPs (Qiagen)	5µl
RT (Qiagen)	1µl
RT buffer (Qiagen)	6µl
dH ₂ O	6.8µl

The RT enzyme also displaces and digests the mRNA template (see **Figure 2.5**). Second strand synthesis then occurs using the first strand as a template to produce double stranded DNA. After one hour, the temperature was raised to 95°C to deactivate the RT enzyme and stop any further copying. Finally, the total cDNA concentration was quantified by spectrophotometer and then stored at -20°C for later experiments.



2.5.2 Standard PCR

Polymerase chain reaction (PCR) is a method of amplifying a defined section of DNA to produce a specified gene, cDNA or exon in huge copy numbers.

During the reaction, DNA polymerase activity and primer binding are controlled by changes in temperature. A heat-stable DNA polymerase is required (e.g. Taq polymerase) that can function at much higher temperatures (72°C) than normal (37°C optimum). PCR amplifies the target DNA over 30-40 cycles. The end point products can then be analysed by agarose gel electrophoresis and observed after staining with ethidium bromide (DNA intercalating agent that causes DNA to fluoresce under UV light).

PCR is a very sensitive technique so the risk of contamination while carrying out these experiments is high. Therefore, care must be taken to avoid contamination with other templates (RNA or DNA from the operator, from dust particles in the laboratory or contaminants in the reagents). Thus, when preparing a PCR master mixture, certified reagents were used including high quality nuclease free sterile water. The PCR master mix should be prepared in a single tube by mixing together sufficient reagents for the number of DNA templates to be amplified in the experiment (see **Table 2.6**). An aliquot (19µl) of the master mix was placed into each individual PCR tube and then 1µl of each different DNA template can be added. This makes all of the reactions identical apart from the differing DNA template. However, if the target gene differs in the experiment, individual master mixes containing the correct primers must be made. All manipulations must be carried out on ice and followed by gentle mixing (Vortex Genie 1 touch mixer from Scientific Industries, New York, USA) and centrifugation (Sigma1-13, Newport Pagnell,

UK). Each tube was then placed in the PCR machine (ABI Gene Amp PCR System 9700 from Perkin Elmer, Norwalk, USA) and the appropriate pre-programmed conditions for each specific gene selected for the run.

Table 2.6: Typical PCR Reaction Mixture. The level of template DNA varies according to the concentration so the water added is varied to always make a total of 20 μ l.

Components	Volume per 20 μ l Reaction
Water, nuclease free	9.9 μ l (Variable)
10X Hot Start PCR Buffer (Qiagen)	2 μ l
dNTPs (Qiagen) (200 μ M)	1 μ l
Q solution (Qiagen)	4 μ l
Hot Start Taq DNA Polymerase(Qiagen) (0.5 units/20 μ l reaction)	0.1 μ l
Primer Forward (0.05–1.0 μ M)	1 μ l
Primer Reverse (0.05–1.0 μ M)	1 μ l
Template DNA	1 μ l (Variable)

PCR has three main stages in each cycle. The first stage is denaturation, a process where the temperature is raised to 95°C to melt all double stranded DNA into single strands. This takes 2-4 minutes in the first cycle but only 1 minute in all subsequent cycles. In the second stage (annealing), the temperature is reduced to 55°C - 60°C depending on the primers used (see **Text box below**). As the reaction cools, the primers bind to the specified gene of interest. This binding can be weak or strong depending on the primer

sequence (particularly the GC content) and this affects the optimum temperature. Annealing proceeds for 45 seconds and during this time some DNA polymerase molecules may start copying a new DNA strand. Finally, the extension stage requires a temperature of 72°C, the optimum working temperature for Taq polymerase and the enzyme synthesizes a copy of each complementary strand (base for base) to generate two new single DNA strands (see **Table 2.7**).

Guidelines for Primer Design

- 15-30 nucleotides long
- Rich in GC content (40-60%) distributed uniformly
- Avoid placing more than 3 G or C at 3' end
- Place 3 conservative nucleotides at the 3' end
- Avoid primer dimers (binding to themselves)

Table 2.7: Stages in PCR Reaction and Timing. Three main stages: denaturation, annealing and extension. Initial denaturation at 95°C takes 2-4 minutes (one cycle) with subsequent denaturation only taking 1 minute. Annealing at 55-60°C (depending on primers) takes 45 seconds and then extension at 72°C for 1 minute. Repeat for 35 cycles (standard PCR) and then allow a final extension at 72°C for 10 minutes (one cycle).

Stage	Temperature	Time	Cycles
Initial Denaturation	95°C	2-4 minutes	1
Denaturation	95°C	1 minute	35
Annealing	55-60°C	45 seconds	
Extension	72°C	1 minute	
Final Extension	72°C	10 minutes	1

By the end of first cycle, there is one copy of each DNA strand. The PCR machine then runs a further 35 cycles and at each new cycle more DNA copies are produced. The number of cycles used in each PCR experiment depends on the amount of DNA template at the start and the efficiency of the reaction. Generally, starting with less than 10 copies of original template DNA requires approximately 40 cycles but as the amount of original template increases then fewer cycles (25-35) are sufficient (see **Figure 2.6**).

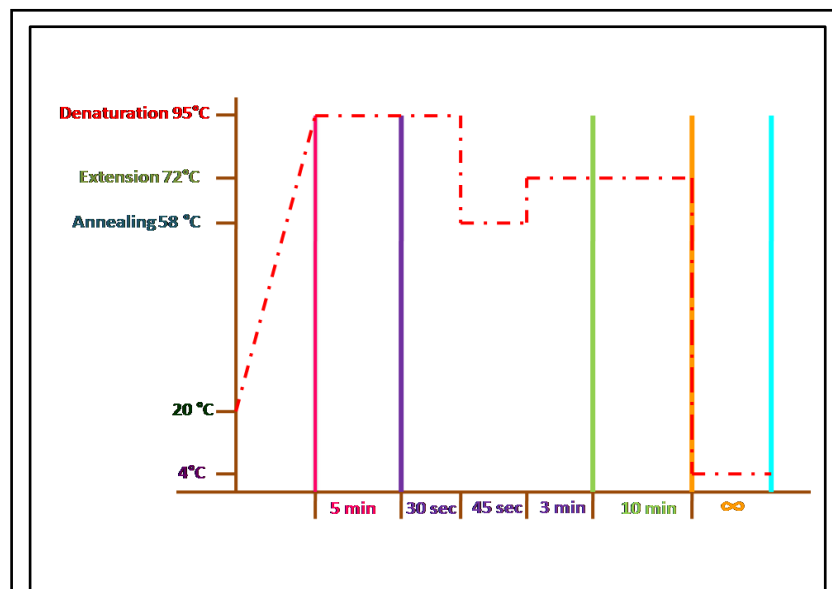


Figure 2.6: Chart of Temperature Cycles during PCR. Initial heating from RT (20°C) to 95°C can be done without Taq polymerase (Hotstart). Typical values for the main stages in a standard PCR are shown but actual values used can vary depending on the template DNA and primers.

As mentioned above, PCR is a technique that amplifies a single (or a few specific regions of DNA in multiplex reactions) to generate huge copy

numbers. However, standard PCR has limitations in terms of quantitating levels of gene expression. A graph of the PCR reaction can be divided into three regions (see **Figure 2.7**). The exponential portion of a PCR reaction is considered relatively low copy number and not ideal for measurements. Once copy numbers are increased, the PCR reaction becomes linear with time (cycles 15-30). At this stage, copies produced are proportional to the starting concentration. Later, PCR reaction then plateaus off and is again non-linear.

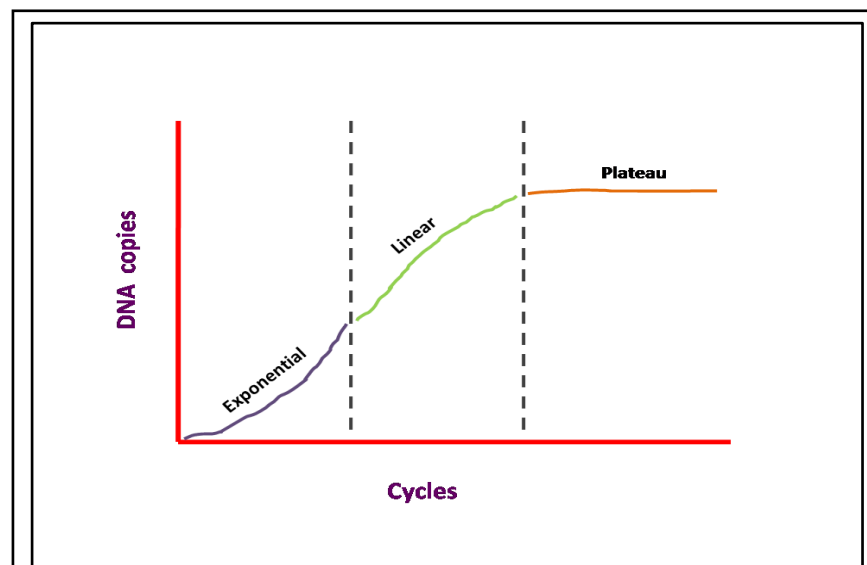


Figure 2.7: Graph of Three Stages in Standard PCR. The initial portion of a PCR reaction (Exponential) is relatively flat due to low copy number and not accurate for measurements. Once there is an increase in copy number become linear with time (cycles 15-30) then you can use this to quantitate as the copies produced are proportional to the starting concentration. Reaction then plateaus off and is again non-linear.

However, as the PCR reaction goes on, variability occurs and reagents are consumed at different rates. This slows down the reaction and causes a

plateau with a specific endpoint. Eventually, given enough time, the plateau area endpoint is reached in all reactions independent of the starting template concentration. Thus, this is good for generating material for further analysis (cloning, sequencing, etc) but not good for quantitating the level of gene expression in cells. An aliquot of the PCR reaction products can be analysed by agarose gel electrophoresis (0.7% - 1.5% gels) and visualised under UV light after treatment with an intercalating agent such as ethidium bromide (1µl of ethidium bromide for each 4µl of PCR sample). The rest of the sample can then be used for further analysis (cloning, sequencing, etc).

2.5.3 Agarose Gel Electrophoresis

PCR products are analysed by gel electrophoresis (horizontal quick screen gel electrophoresis unit from International Biotechnologies Inc., Iowa, USA). An aliquot of PCR product is combined with 5x Ficoll Tris-Acetate-EDTA (FTAE) buffer (Sigma-Aldrich, Gillingham, UK) at a ratio of 4:1 and run on a 1.5% agarose gel (Sigma-Aldrich, Gillingham, UK) for large (150-500 bp) products, a 1% agarose + 3% NuSieve (Lonza, Slough, UK) gel for medium-sized (100-300 bp) products or a 4% NuSieve (Lonza, Slough, UK) gel for small (50-150 bp) products (**Figure 2.8**).

All gels contained 0.0004% ethidium bromide (Sigma-Aldrich, Gillingham, UK) and were run in Tris-Acetate-EDTA (1x TAE) buffer (Sigma-Aldrich, Gillingham,

UK) at 90V and 50mA until the blue marker dye was in the centre of the gel (takes 30-45 minutes depending on several factors: gel density and ionic content of TAE buffer). The size marker used was ϕ X174 phage DNA cleaved with Hae III (New England Biolabs (UK) Ltd., Hitchin, UK) mixed with 5x FTAE buffer (4:1).

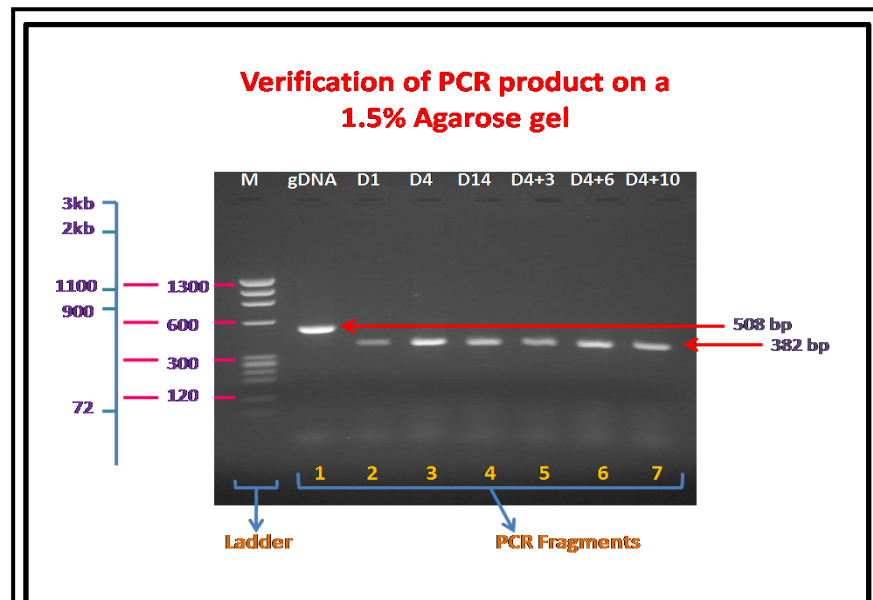


Figure 2.8: Analysis of PCR Fragments by Agarose Gel Electrophoresis. PCR products (4 μ l) were loaded on a 1.5% agarose gel containing ethidium bromide (1 μ l) and visualised under UV light. Lane 1: PCR fragment from genomic DNA (C19, 1:10) was 508 bp. Lanes 2-7: RT-PCR fragments of DLL1 (p1, p2R) were 382 bp (PCR over intron so that gDNA product larger). Samples from HaCaT cells grown in low calcium (D1, D4 and D14) or high calcium (D4+3, D4+6 and D4+10). Gel calibrated with a standard DNA marker (ϕ x174 +HaeIII), a mixture of DNA fragments of known size.

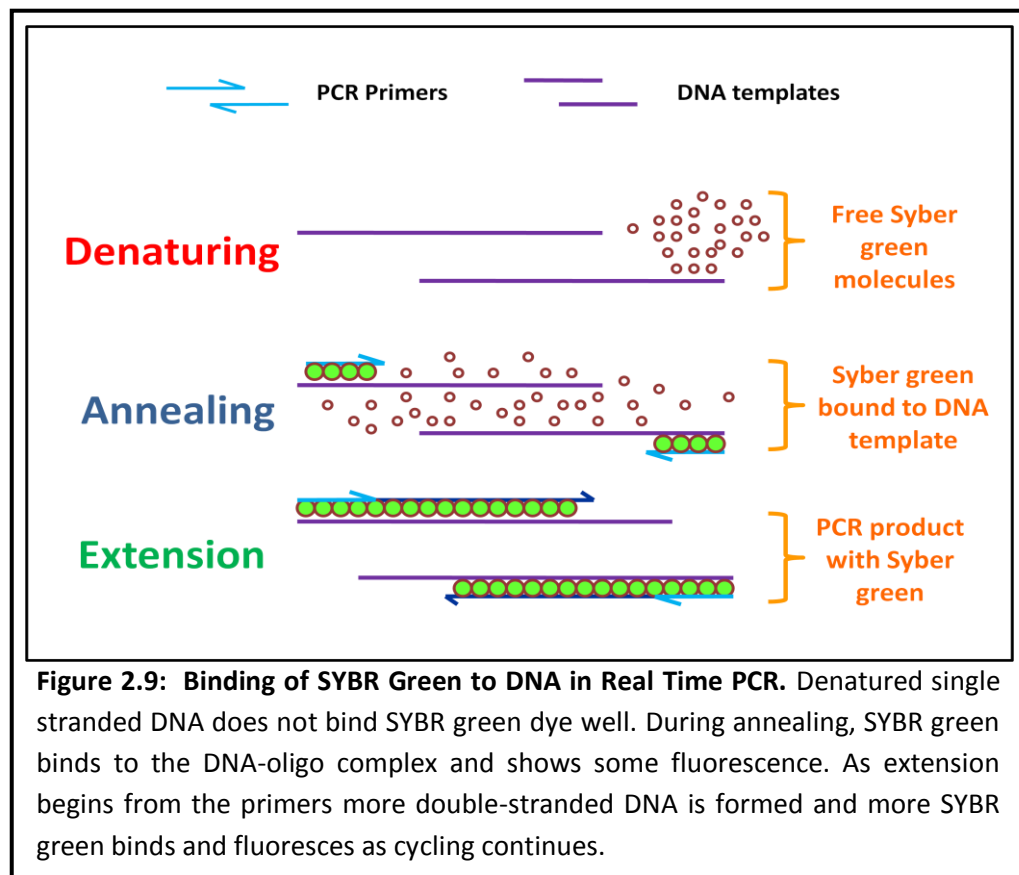
2.5.4 Quantitative Real Time PCR (QPCR)

Quantitative polymerase reaction (qPCR) measures PCR amplification in real time as it occurs. In other words, the data is collected during the PCR reaction as DNA copies are being produced. The technique is very sensitive and can detect a 2 fold change in original template level. However, the products must be kept small, so it is important to have a product size between 80 and 120 base pairs and not more than 150 base pairs.

Real time PCR is monitored by a laser and fluorescence detector after binding a fluorescent marker such as SYBR green (2x Brilliant II SYBR Green QPCR Master Mix from Agilent Technologies Inc, Edinburgh, UK) to the DNA. This marker emits fluorescence when bound to double-stranded DNA. The intensity of fluorescence increases as more copies are created as SYBR green has more double stranded DNA to bind. However, SYBR green dye does not bind to a specific gene product but will bind to any double stranded DNA including any primer dimers or secondary PCR products. Thus, it allows detection of DNA being amplified in real time.

SYBR green is considered one of the main fluorescent markers used to perform real time PCR analysis. It is a non-specific double stranded DNA binding dye so it is important that primer and DNA template levels are thoroughly optimized and that a single well defined product is produced.

During denaturation, the DNA template within the sample is melted into two single strands. SYBR green dye molecules do not bind to single-stranded DNA so they only fluoresce weakly and produce minimal background fluorescence. Once annealing begins, a few dye molecules start binding to double stranded DNA. Eventually, as more double stranded DNA is produced, the Syber green fluorescence signal increases proportionately. During extension the SYBR green dye binds to all the newly formed double-stranded DNA and so levels of fluorescence increase further as cycling continues. SYBR green fluorescence is measured at the end of each cycle and the intensity of the fluorescence above background level estimated. The point at which fluorescence increases above background is called the threshold cycle (known as Ct) and this point can be used to quantitate the starting amount of double-stranded DNA. Later, on completion of the extension phase, more dye binding to the newly synthesized DNA occurs and greater signals are apparent (see **Figure 2.9**).



A SYBR green master mix (Stratagene, Agilent Technologies, Edinburgh, UK) was used in each qPCR experiment and reagents were added in a specific order (see **Table 2.8** for details).

In addition, if there was more than one primer set required in an experiment, then a separate master mix was made up for each primer pair. Then, 21µl of master mix was added to a sufficient number of wells on a 96-well plate

(Qiagen Ltd., Crawley, UK) for the experiment. However, the first well should contain 25µl sterile water as a negative control.

Table 2.8: Reaction Mixture for qPCR Experiment (25 µl total).

Component	Volume for 25 µl Mix
Water (nuclease free)	6.5µl
SYBR green master mix	12.5 µl
Primer Forward (200nM-400nM)	1 µl
Primer Reverse (200nM-400nM)	1 µl
DNA Template (low and high Ca HaCaT cells)	4 µl each

A no template control (NTC), to determine if any primer dimers or secondary PCR products are produced, for each primer pair was also included and this contained 21µl of master mix plus 4µl of sterile water (instead of DNA template). The master mix was added to the other wells and 4µl of each DNA template was added to the sample wells but not to the water or NTC control wells. Later, the 96-well plate was placed in a centrifuge (Mistral 3000 from MSE (UK) Ltd., London, UK) and spun at 1,000 rpm for 5 minutes at RT.

The Mx3000P real time PCR machine was allowed to warm up for 20 minutes before use to attain the correct starting temperature. The correct settings must be selected on the menu at start up. Initially, a SYBR green assay was selected and then each well for the experiment was assigned the correct well label (e.g. water control, no template control or sample well). SYBR green dye was chosen as the fluorescence type.

To minimize error, each sample was run in triplicate and these were grouped together in the software. The thermal profile was then set up before initiating the run. The annealing temperature was selected depending on the primers used and the size of target gene product (generally <150 bp). The SYBR green assay contained 3 segments: an initial hot start, standard cycle, and finally a dissociation cycle (see **Table 2.9**). A dissociation curve is obtained by heating the products to 95°C for 1 minute, cooling to 55°C and then increasing the temperature incrementally by 1°C back up to 95°C. As the temperature rises the double-stranded DNA melts into single stranded DNA causing the SYBR Green to dissociate and decrease the fluorescence. The change in fluorescence is plotted against temperature and the resulting graph can be used to determine if any primer dimers or secondary PCR products are present as each product will have its own melting point.

Finally, all the experimental data was saved on the attached PC (hard drive).

Run times are typically two and half hours and results can be viewed and

analysed on any PC using MXPro software.

Table 2.9: Typical Segment Settings for Real Time PCR.

Initial denaturing occurs at high temperature for 1 cycle and then the standard cycle of denaturing, annealing and extension runs for 40 cycles. The final cycle is used to generate a dissociation curve.

Segment	Temperature	Duration	Cycles
Segment 1	95°C	10 minutes	1 st cycle
Segment 2	95°C	30 seconds	40 cycles
	60°C	One minute	
	72°C	30 seconds	
Segment 3	95°C	One minute	One cycle
	55°C	30 seconds	
	95°C	30 seconds	

Rea-time qPCR is more sensitive, accurate and quantitative than standard PCR. All samples run to the same end point in standard PCR (plateau generated as materials become exhausted) and differences between initial DNA concentrations cannot be detected. However, with qPCR, product levels are measured continuously in the exponential and linear phases giving data that is proportional to the DNA concentration at the start. The graph below shows an example in terms of four samples representing a serial dilution which gave very different levels of product in the early stages but eventually all attain the same plateau end point as in a standard PCR. Thus, qPCR detected the purple sample first at 20 cycles in the exponential phase while the green sample (with less starting DNA) was not detected until 25 cycles

were reached. Similarly, the pink sample was not detected until 30 cycles were completed and the blue sample required 35 cycles. This data can then be used to construct a standard curve of DNA starting concentration versus the initial point of detection or threshold, called the Ct value (see **Figure 2.10**).

Standard curves should include at least five points using a serial dilution of pure DNA or cloned plasmid DNA. Each point should be run in triplicate. The MXPro software can then produce a graph of the log of each known concentration against the Ct to produce a standard curve determining the efficiency, linearity and sensitivity of qPCR assay. Using the standard curve the DNA concentration (or copy number) in unknown samples run under the same conditions can be calculated from their Ct values and this can produce data on the level of gene expression in cells and tissues.

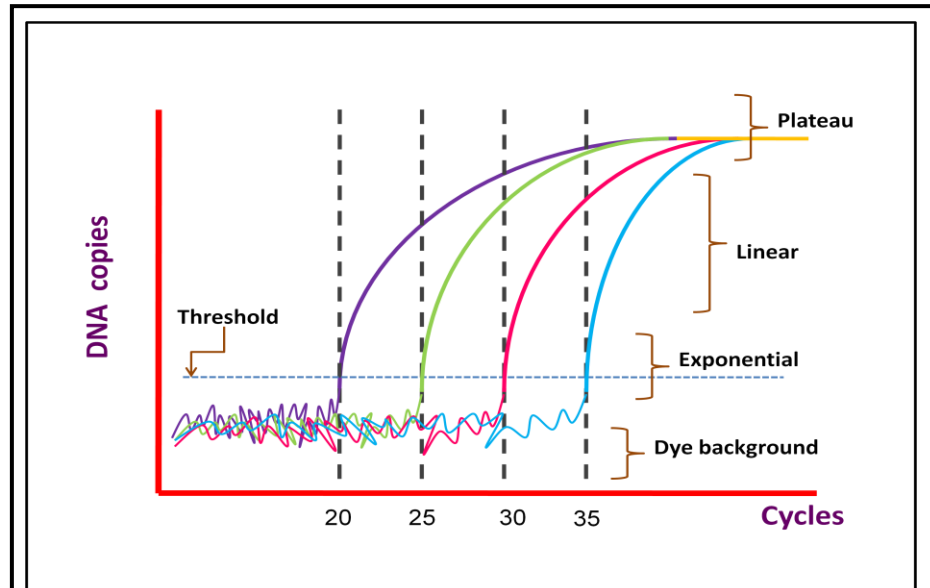


Figure 2.10: Graph of DNA Copy Number versus Cycle Number (qPCR). Purple increase above background at 20 cycles, green at 25 cycles, pink at 30 cycles and blue at 35 cycles. Eventually, all four samples reach a plateau where no further DNA copies are produced. qPCR can show precisely when each DNA sample was detected and this is proportional to the starting DNA concentration.

2.6 Cloning and Plasmid Extraction

Cloning is a way of producing large quantities of a single gene product and this can be achieved using genomic DNA or cDNA depending on the subsequent experimental requirements. Generally, a purified PCR product is used and this is inserted into carrier DNA, called a vector. For amplification in a bacterial host a number of bacterial plasmids have been constructed and we have used pGEM-T Easy (Promega, Southampton, UK) as the vector system in our experiments. The host bacterial cells used were a competent strain of *E. coli* (Stratagene Top10 cells from Agilent Technologies UK Ltd, Stockport, UK).

The human cDNA or gDNA (insert) must be ligated into a vector and the whole plasmid inserted into host bacterial cells. The plasmid is then replicated as the bacteria divide, and thousands of identical copies are produced. Generally, vectors smaller than 10 kb in size are cloned in bacterial plasmids while larger vectors that contain inserts up to 20 Kb in size, require different host systems such as bacteriophages or mammalian viruses. Bacterial plasmids consist of a circular molecule of DNA with a transcription initiation site, known primer binding sites and a multiple cloning site. They are able to multiply independently inside the host bacterial cells (see **Figure 2.11**).

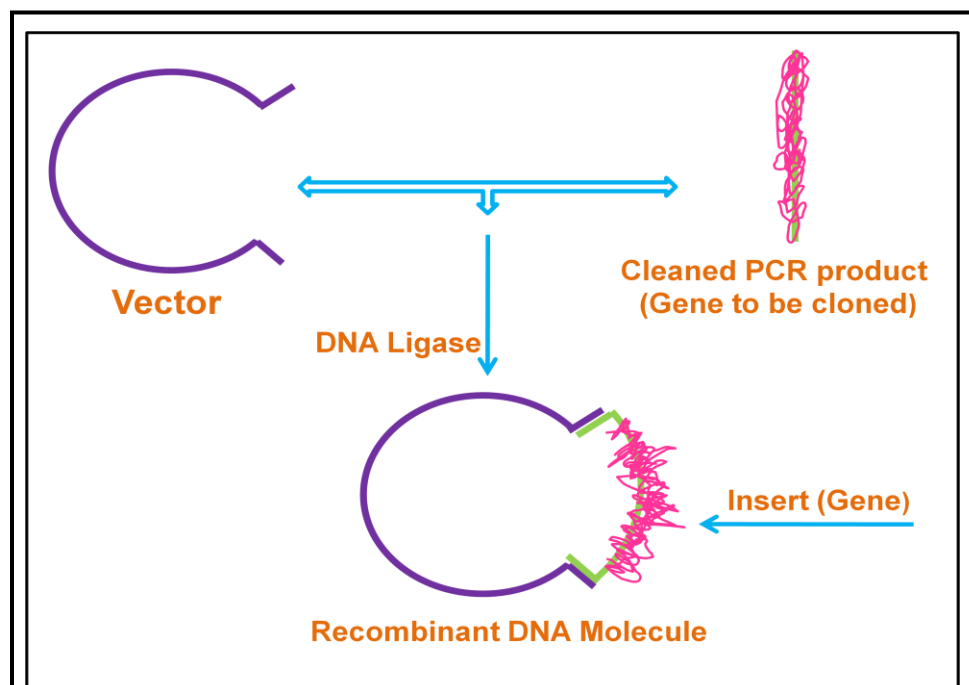


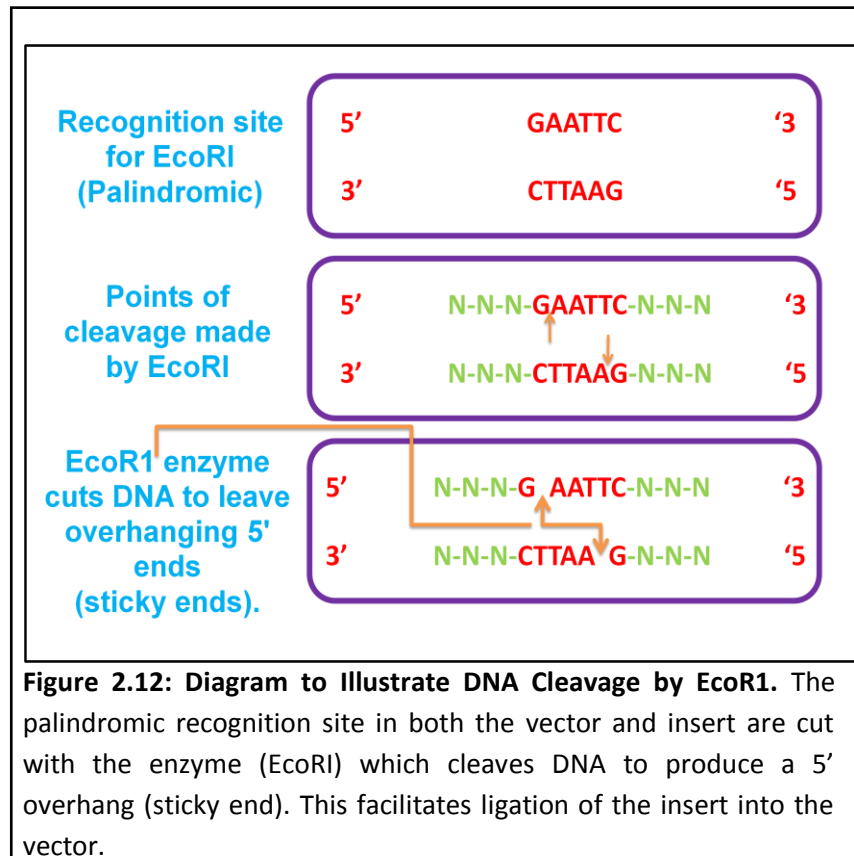
Figure 2.11: Schematic of Cloning a PCR Fragment into pGEM-T Easy. The PCR fragment is ligated into the vector at specific restriction enzyme sites (e.g. EcoRI) and then inserted into *E. coli* by bacterial transformation.

The pGEM-T Easy vector carries an ampicillin resistance gene and a lac Z gene required for clone selection. It is 3,015 bp in size and has binding sites for SP6 and T7 promoter primers on either side of a multiple cloning site (a string of restriction enzyme sites). Both the vector and the insert of interest must have the same restriction endonuclease sites at the ends in order to be successfully ligated into the cut plasmid. Also, it is an advantage to use different enzyme sites at each end and then the orientation of cloning can be controlled rather than being random.

Furthermore, the insert and vector must not contain an internal restriction enzyme site the same as that used for cloning. In other words, the vector must be cleaved at a single position in the circular DNA molecule. An example is shown below (see **Figure 2.12**) where a restriction enzyme called EcoR1 has been used for cloning. This enzyme produces sticky ends on the vector and insert which promote ligation.

Once the insert has been ligated into the bacterial vector then the plasmid must be inserted into Top 10 cells, a process known as transformation. Luria broth (LB) plates containing ampicillin were prepared in advance. A premix of LB already containing agar (LB Agar Powder from Invitrogen, Paisley, UK) was used (10g Peptone 140, 5g Yeast extract, 5g Sodium Chloride and 12g Agar).

LB Agar mix (3.2 g) was mixed into 100 ml of dH₂O and autoclaved for two hours at 120°C.



The medium was then cooled down to about 50°C prior to adding 200µl of ampicillin (50mg/ml stock diluted 1:500 giving final concentration of 100µg). The medium was then poured into 10 cm petri-dishes making sure that the bottom of the dish was completely covered and the lids were placed at an angle leaving an air gap so condensation does not form. The plates were allowed to set and then were stored up-side-down at 4°C until used.

For blue-white colony selection, indicator plates must be made by adding 4 μ L IPTG (Isopropyl-thiogalactoside) (0.1mM) and 40 μ L X-Gal (5-bromo-4-chloro-3-indoyl β -D galactopyranoside) (300 μ g/ml) to the LB Amp plates. This was spread over the agar surface and the plates were then placed in a 37°C incubator (Weiss-Gallenkamp, Leicestershire, UK) for 15 minutes. The plates were then stored in the fridge until used to grow the cloned bacteria.

The PCR products were cleaned by precipitation with polyethylene glycol (PEG). Initially, PEG solution (26% PEG 8000, 6.6mM MgCl₂, 0.6M NaOAc, pH 5.2) was mixed by inversion and then 20 μ l was added to remaining PCR product (16 μ l) and the DNA allowed to precipitate at RT for 10 minutes. The tubes were centrifuged at 13,000 rpm for 25 minutes at RT (Heraeus Biofuge 13 from Fisher Scientific Loughborough, UK) during which time oligonucleotide dilutions were made (7 μ l of stock primer at 10pmol/ μ l plus 13 μ l of dH₂O giving 3.5 pmol/ μ l final).

The supernatant was carefully pipetted off and 200 μ l of ice cold 70% ethanol was added. The tubes were mixed by careful inversion and then centrifuged at 11,000 rpm for two minutes at 4°C (Microfuge R from Beckman Coulter Inc., High Wycombe, UK). The ethanol wash was repeated, the supernatant pipetted off and the sample left to dry on the bench (invert on clean tissue). Later, the dried sample was re-suspended in 16 μ l nuclease free water (store

at 4°C). The cleaned DNA was added to a reaction tube containing T4 DNA ligase (Invitrogen, Paisley, UK), 2x rapid ligation buffer (Invitrogen, Paisley, UK), pGEM-T easy vector and nuclease free water (see **Table 2.10**).

Table 2.10: Ligation Reaction Component. Composition of a standard ligation reaction using cleaned PCR products and pGEM vector.

Reaction Component	Standard Reaction Volumes
2X Ligation Buffer	5 μ l
pGEMT-Easy Vector	1 μ l
PCR product	3 μ l
T4 DNA Ligase	1 μ l
Total Volume	10 μ l

The reaction components were gently mixed and incubated overnight at 4°C. The ligation mix can then be used immediately or stored at -20°C for future use. One vial of Top 10 cells was thawed on ice and divided into two (1.5 ml) tubes (25 μ l in each tube). An aliquot (5 μ l) of the ligation mix was added to the cells, gently mixed and incubated for 30 minutes on ice. The cells were then given heat shock treatment by heating in a 42°C water bath (Grant Instruments Ltd, Cambridge, UK) for 30 seconds and then returned to ice for 2 minutes. An aliquot (250 μ l) of SOC medium (2% (w/v) Tryptone (pancreatic digest of casein), 0.5% (w/v) Yeast extract, 8.6mM NaCl, 2.5mM KCl, 20mM MgSO₄ and 20mM Glucose from Sigma-Aldrich, Gillingham, UK) was brought up to RT and then added to the cells. Samples are mixed gently and then placed in an orbital incubator for one hour at 37°C (set shaking at

230 rpm). After incubation, the whole mixture was added to an LB/Amp/IPTG/X-Gal plate and spread over the agar surface using sterile spreader. The plates were then incubated at 37°C overnight after which blue and white colonies should appear (blue colonies contain empty vector while white colonies contain vector plus insert). Bacteria that have no vector cannot grow because of the ampicillin (vector contains an ampicillin resistance gene).

After overnight incubation, a colony selector was used to pick a single white colony from each plate which was placed into 3 ml LB medium plus 6 µl ampicillin (50 mg/ml) in a sterile 15 ml plastic tube. The tubes were incubated at 37°C overnight (shaking set at 230 rpm). The following day, 500 µl of each culture was added to a labelled cryovial containing 0.5 ml of 80% glycerol and stored at -85°C (stock culture). The rest was transferred into 1.5ml tubes and centrifuged at 13,000 rpm for 5 minutes (Sigma 1-13). The supernatant was removed (dispose as biological waste) and the pellets (containing the bacteria) were extracted using a Qiaprep Spin Miniprep kit protocol for plasmid DNA purification (QIAprep®Miniprep Handbook, Qiagen Ltd., Crawley, UK).

All plasmid DNA purification was done at room temperature as stated in the manufacturers guide (QIAprep®Miniprep Handbook, Qiagen Ltd., Crawley, UK). Initially, the pellets were re-suspended in 250µl P1 buffer using vortex

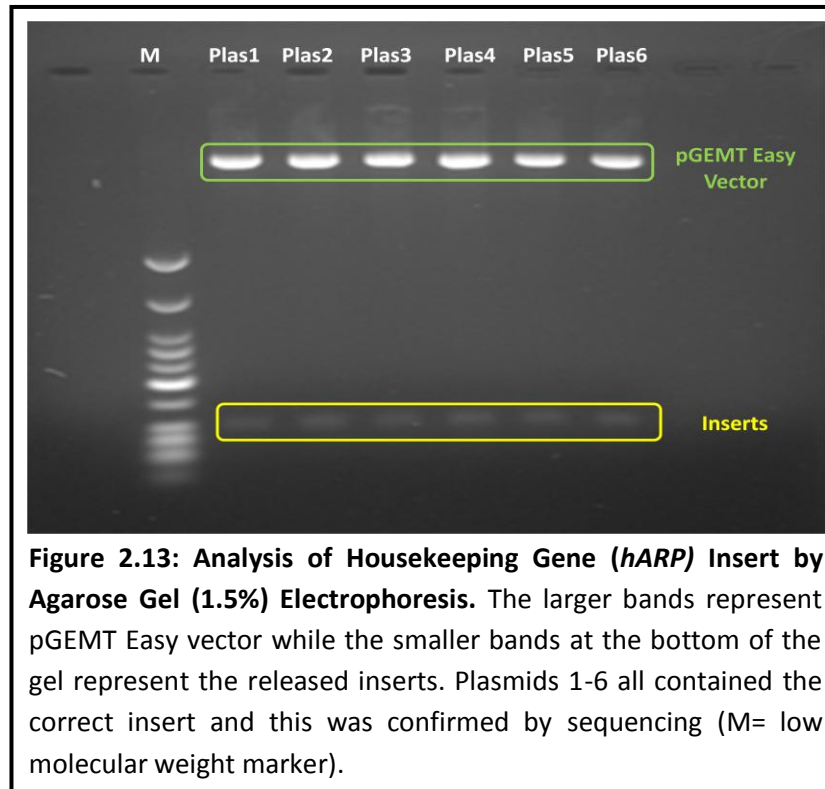
(Vortex Genie 1 from Scientific Industries, New York, USA) and transferred into a microcentrifuge tube supplied in the kit. An aliquot (250 µl) of P2 buffer was added and mixed thoroughly by inverting the tube 4 to 6 times. Then, 350µl of N3 buffer was added and mixed immediately by tube inversion. This was followed by centrifugation at 13,000 rpm for 10 minutes at RT (Sigma 1-13 Centrifuge). The supernatants were added to a QIAprep spin column (supplied in the kit) by pipette and this was centrifuged at 13,000 rpm for 60 seconds at RT. The flow-through (eluate) was discarded and the spin column was washed by adding 0.5ml PB buffer and centrifuged at 13,000 rpm for 60seconds at RT. Again, the spin column flow-through was discarded and further washed with 0.75ml PE Buffer and centrifuged at 13,000 rpm for 60 seconds at RT. An additional centrifuge step for 1 minute at the same speed was recommended after discarding the flow through to remove any residual wash buffer. The QIAprep spin column was then placed in a clean 1.5ml microcentrifuge tube (supplied in the kit) and 50µl of EB Buffer was added to the centre of each spin column, allowed to stand for 1 minute and then centrifuged at 13,000 rpm for 1 minute at RT.

Once plasmids were extracted, inserts were checked by digesting with EcoR1, the insert enzyme (New England Biolabs (UK) Ltd., Hitchin, UK) and analysing the fragments on an agarose gel (for details of digest see **Table 2.11**).

Table 2.11: Reagent List for Restriction Enzyme Digest of Cloned Plasmids. . Plasmid was treated with EcoRI to cleave the insert DNA from the pGEM-T vector.

Component	Volume Added
Plasmid DNA	3 μ l
EcoRI (NEB) (1Unit/20 μ l)	1 μ l
EcoRI 10x Buffer (NEB)	2 μ l
dH ₂ O (not available)	14 μ l
Total volume	20 μ l

All digests were incubated in a 37°C water bath (Grant Instruments Ltd., Shepreth, UK) for 1 hour. Later, the samples were moved to a 70°C water bath (Grant Instruments Ltd., Shepreth, UK) for another 20 minutes to denature the enzyme and stop digestion. The digests were then loaded on a 1.5% agarose gel with a low molecular weight marker to verify the presence of inserts. As EcoRI was used to cut the original plasmid for ligation of the insert, the digest should then release the insert from the vector. Each lane on the agarose should have two bands, the top band is the vector and the bottom band theoretically represents the released insert (see **Figure 2.13**). To ensure that inserts were the gene of interest, all inserts were sequenced. It is important to point out that pGEMT vector has a multiple cloning site (see **Figure 2.14**) and all inserts were sequenced using the SP6 promoter primer.



This was followed by preparing serial dilutions of each insert with the correct sequence. For example, plasmid 3 containing a Notch 1 insert (N1plas3) was selected for preparing serial dilutions. The concentration of the stock plasmid DNA was determined by spectrophotometric analysis (580 ng/ μ l or 5.8e-7 g/ μ l). Initially, this stock was diluted serially (3 x 1 in 100) down to a more manageable 1 in 10^6 giving a concentration of 5.8e-13 g/ μ l. In order to calculate the dilution required to produce 300,000 copies in 5 μ l, a series of calculations were performed.

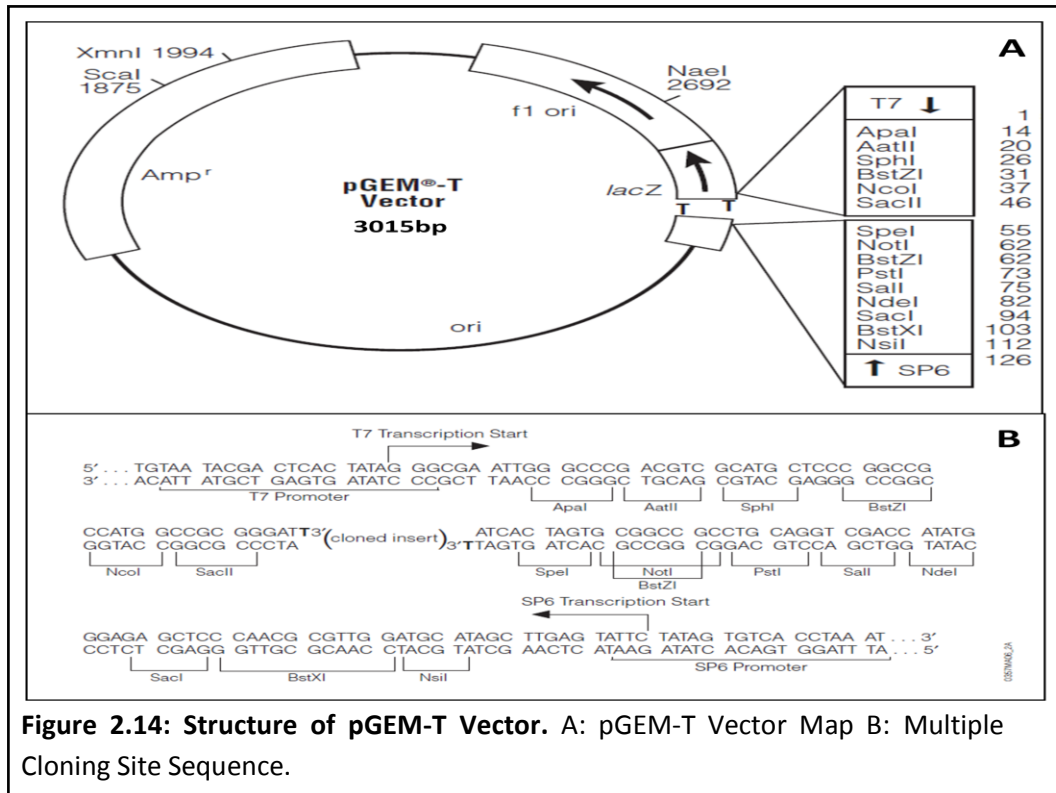


Figure 2.14: Structure of pGEM-T Vector. A: pGEM-T Vector Map B: Multiple Cloning Site Sequence.

Initially, the mass of a single plasmid molecule (vector plus insert) was calculated from the following equation:

$$m (\text{mass}) = n (\text{vector} + \text{insert bp}) \times 1.096 \times 10^{-21} \text{g}$$

$$n = \text{Total bp (pGEM-T easy} + \text{probe insert size)}$$

$$= 3,015 \text{ bp} + 142 \text{ bp}$$

$$= 3,257 \text{ bp}$$

Thus,

$$m = 3,157 \times 1.096 \times 10^{-21} \text{ g}$$

$$= 3.46 \times 10^{-18} \text{ g}$$

The calculated mass of a single molecule of N1plas3 ($3.46 \times 10^{-18} \text{ g}$) was then used to determine the mass equivalent of the number of desired copies (from

300,000 to 30), a product of the mass of a single molecule and the copy number required (see **Table 2.12**).

Table 2.12: Mass of Notch 1 Plasmid 3 equivalent to Specific Copy Number

Copy #		Mass of N1 Plasmid (g)
300,000		1.038e-12
30,000	X 3.46e-18 g	1.038e-13
3000		1.038e-14
300		1.038e-15
30		1.038e-16

As the plasmid is dispensed in a 5µl volume per PCR reaction then the concentration of the solution required (g/µl) was calculated by dividing the mass equivalent of plasmid by 5 (see **Table 2.13**).

Table 2.13: Concentration of Notch 1 Plasmid 3 DNA required to achieve Copy # Stated.

Copy #	Mass of N1 Plasmid DNA (g)		Final Concentration of N1 Plasmid DNA (g/µl)
300,000	1.038e-12	Divide by 5	2.076e-13
30,000	1.038e-13		2.076e-14
3000	1.038e-14		2.076e-15
300	1.038e-15		2.076e-16
30	1.038e-16		2.076e-17

As the plasmid concentration equivalent to a fixed number of vector copies has been calculated and the stock plasmid concentration known, the required

dilution to make 500 μl of standard containing 300,000 copies can be calculated as follows:

$$C_1V_1 = C_2V_2$$

Where C_1 = Initial concentration of stock used ($\text{g}/\mu\text{l}$)
 V_1 = Volume of stock plasmid DNA needed (μl)
 C_2 = Final concentration of plasmid required ($\text{g}/\mu\text{l}$)
 V_2 = Final Volume of plasmid DNA solution (μl)

$$V_1 = \frac{C_2 \times V_2}{C_1} = \frac{2.076\text{e-}13 \times 500}{5.8\text{e-}13} = 179\mu\text{l stock N1plas3}$$

$$\text{Volume of Diluent} = 500\mu\text{l} - 179\mu\text{l} = 321 \mu\text{l Sterile Water}$$

This example showed how to prepare a standard solution containing 300,000 copies of the N1plas3 vector and insert. All manipulations were done under sterile conditions and making sure that pipetting was precise. All the plasmids obtained from cloning including the ones used for making serial dilutions were stored at -20°C .

A full range of serial dilutions for the N1plas3 cloned insert are shown below. Initially, the stock was diluted from $5.8\text{e-}7 \text{ g}/\mu\text{l}$ down to a more manageable $5.8\text{e-}13 \text{ g}/\mu\text{l}$ by three serial dilutions of 1:100 (total 1 in 10^6). The calculated dilution (described above) was then used to derive a standard working solution containing 300,000 copies of the plasmid and all other working solutions made from this by serial 1:10 dilutions (**Table 2.14**).

Table 2.14: Dilution Series for N1plas3 Stock. Sterile nuclease free water was used as the diluent and dilutions 4-8 were used for qPCR.

	Source of plasmid DNA for dilution	Initial Conc. (g/ μ l) C_1	Volume of Plasmid DNA (μ l) V_1	Volume of Diluent (μ l)	Final Vol. (μ l) V_2	Final conc. (g/ μ l) C_2	Copy #
1	Stock	5.8e-7	10 μ l	990 μ l	1000 μ l	5.8e-9	N/A
2	Dilution1	5.8e-9	10 μ l	990 μ l	1000 μ l	5.8e-11	N/A
3	Dilution2	5.8e-11	10 μ l	990 μ l	1000 μ l	5.8e-13	N/A
4	Dilution3	5.8e-13	179	321	500 μ l	2.076e-13	300,000
5	Dilution4	2.076e-13	10 μ l	90 μ l	100 μ l	2.076e-14	30,000
6	Dilution5	2.076e-14	10 μ l	90 μ l	100 μ l	2.076e-15	3000
7	Dilution6	2.076e-15	10 μ l	90 μ l	100 μ l	2.076e-16	300
8	Dilution7	2.076e-16	10 μ l	90 μ l	100 μ l	2.076e-17	30

2.7 Sequencing

Automated sequencing used Big Dye v3.1 chemistry followed by analysis on an ABI310 DNA analyzer (Cardiff University, School of Medicine, Central Biotechnology Services).

To confirm that the inserts were correct, the isolated plasmids were sequenced using an SP6 primer in one direction and a T7 primer in the opposite direction. A 4 μ l aliquot of the plasmid mix, 1 μ l primer (1 μ M), 2 μ l Big Dye v3.1, 2 μ l of 5x Big Dye buffer and 1 μ l of sterile H₂O were mixed together and placed in the PCR machine (ABI 9700 Gene Amp PCR system from Perkin Elmer Norwalk, USA). The Big Dye programme (25 cycles at 96 °C for 10 sec, 50°C for 5-10 sec, 60°C for 4 min, then ramp down to 4°C and hold) was used (two and a half hour run). The tubes were removed from PCR machine, 1 μ l of

3M NaOAc added followed by 25µl ice cold 95% ethanol. Mix and then leave on dry ice for 10 minutes. The tubes were then centrifuged at 13,000 rpm for 30 minutes at 4°C (Microfuge R, Beckman Coulter Inc., High Wycombe, UK) and then carefully decant the supernatant. Add 180µl of ice cold 70% ethanol and mix by inversion. The tubes were then centrifuged at 11,000 rpm for 2 minutes at 4°C and the supernatants were removed with a pipette without disturbing the pellet. Another 180µl ice-cold 70% ethanol was added the tubes centrifuged again at 11,000 for 2 minutes at 4°C. The supernatant was removed by pipette and 10µl ice cold 70% ethanol was added. All samples were then taken to CBS (Central Biotech Services) for sequence analysis on an ABI 310 DNA Sequencer (Life Technologies Ltd., Paisley, UK). This was repeated for several other inserts required for this research project as shown below (See **Table 2.15**).

Finally, standard dilutions of each plasmid covering the range from 300,000 copies to 30 copies were prepared and 20 µl aliquots of each dilution were stored at -20°C (freezer) for use in real time PCR experiments.

Table 2.15: Different Primers used for Cloning by Inserting a DNA Fragment into a Bacterial Cell Plasmid (Vector).

Primers	PCR	CLONING	SEQUENCE	No. PLASMIDS
HK14 (p55, p57R)	Good	Done	Correct	3
HK10 (p22, p5R)	Good	Done	Correct	3
DLL1 (p7, p8R)	Good	Done	Correct	3
NOTCH1 (p7, p6R)	Good	Done	Correct	3
NOTCH3 (p1, p4R)	Good	Done	Correct	3
JAG1 (p11, p12R)	Good	Done	Correct	3
JAG2 (p14, p11R)	Good	Done	Correct	3
HES1 (p1, p2R)	Good	Done	Correct	3
HES5 (p1, p2R)	Good	Done	Correct	3
HES7 (p1, p2R)	No Band	Failed	Not Done	Not Done
HEY1 (p3, p4R)	Weak	Failed	No Good	Not Done
HEY2 (p3, p4R)	Weak	Failed	No Good	Not Done
HEYL (p1, p2R)	Weak	Failed	No Good	Not Done

A number of commercial and non-commercial software packages to analyse sequencing were available. Some had advantages in which they could trim low-quality DNA traces automatically. For that reason, resulting sequence chromatograms of the genes were first displayed using Finch TV (Free Download: Software Version 1.4.0, Geospiza Inc., Washington, USA). This

application was used to easily view, define and edit sequences chromatograms.

The sequencing data was returned as two files per sample (an electrophoretogram and a linear sequence as text). Finch TV software can display the sequence electrophoretogram either as a single panel (requires continuous scrolling) or in a multiple panel view where the chromatogram is wrapped round (see **Figures 2.15 and 2.16**).

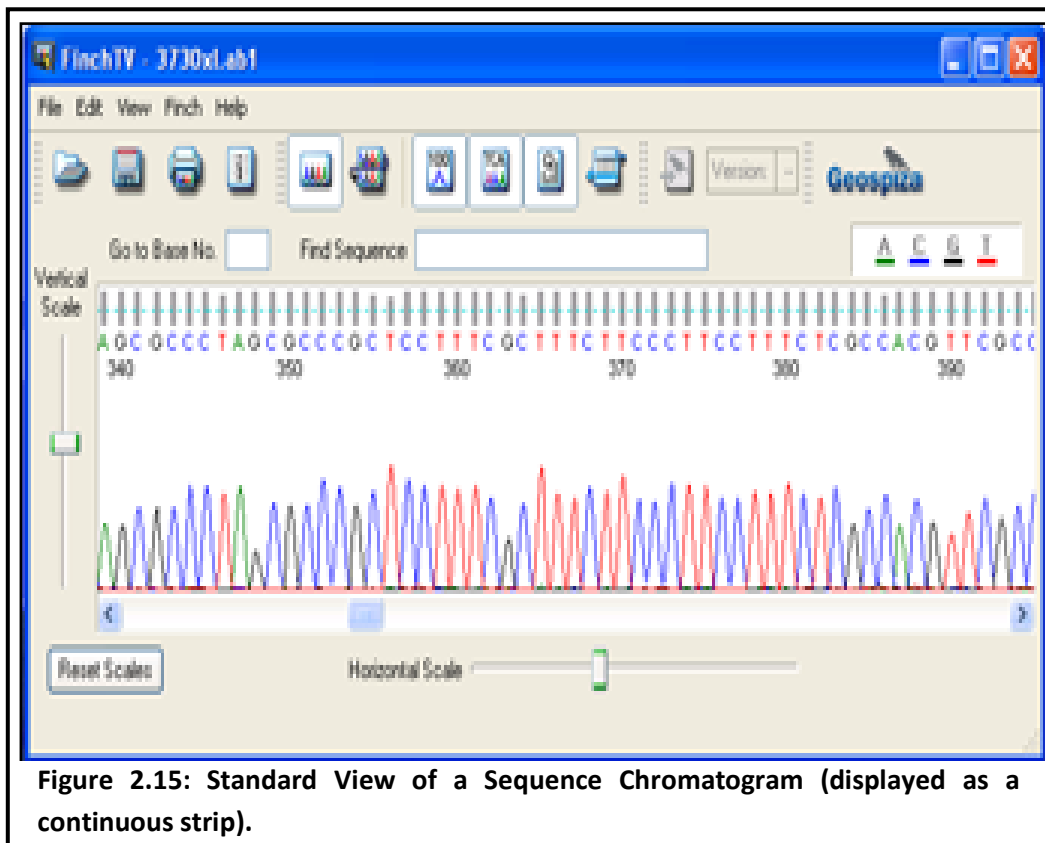


Figure 2.15: Standard View of a Sequence Chromatogram (displayed as a continuous strip).

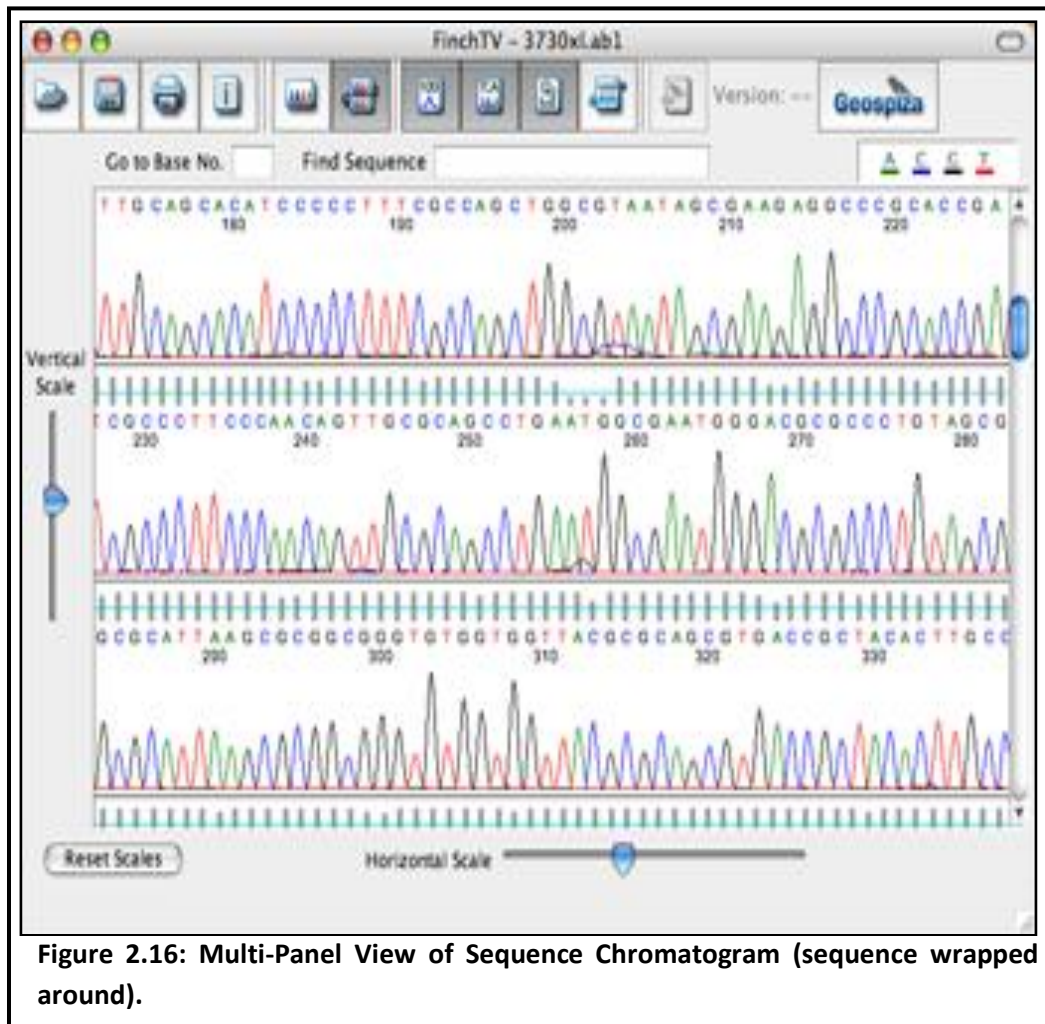
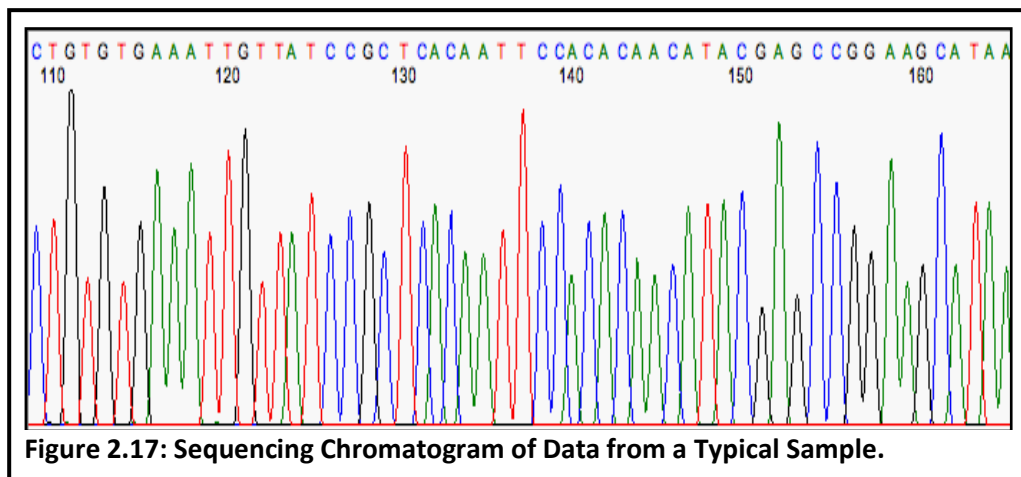
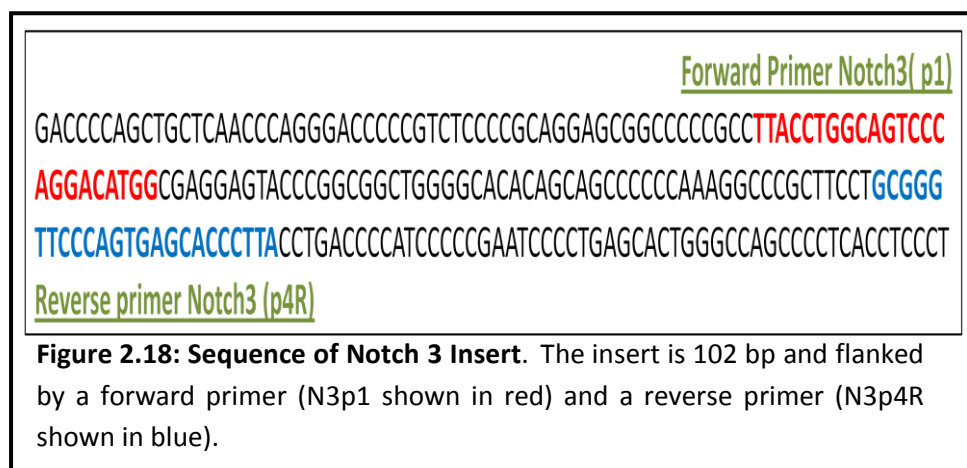


Figure 2.16: Multi-Panel View of Sequence Chromatogram (sequence wrapped around).

The sequencing data was viewed as a group of fluorescent peaks (chromatogram) representing the four DNA bases (**A**denine, **T**hymine, **G**uanine, and **C**ytosine) in four different colours (Green = A, Blue = C, Black = G and Red = T) the single letter base code is given above the trace and all bases are numbered from the start. For better visualization of peaks, the chromatogram can be scaled vertically and horizontally. At each point there is only a single clean peak with no overlap of the other bases (low noise baseline) meaning the sequencing chemistry is very clean (see **Figure 2.17**).



In addition, the peaks should be spaced evenly. Sometimes artefacts and errors are present on a chromatogram. For instance, misplaced peaks where a real gap is misinterpreted as a real nucleotide. Also, if the error rate becomes higher, the data is considered not reliable and the sequence should be repeated using different primers if necessary. Chromatograms can also be displayed as a text sequence (**Figure 2.18**).



The text sequences can then be further analysed by other software packages such as Geneious version 4.8.3 (**Figure 2.19**). They can also be matched against a reference database from National Center for Biotechnology Information using the Blast feature available at the following web address (<http://www.ncbi.nlm.nih.gov/nucore>).

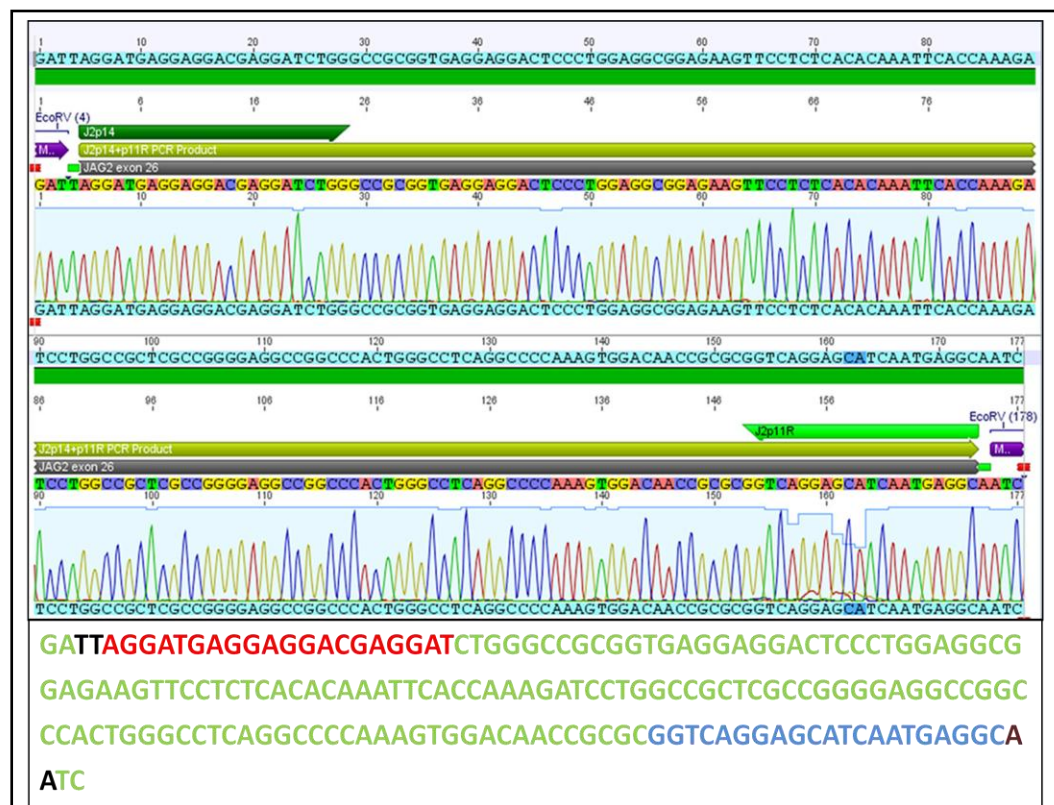


Figure 2.19: Sequencing Chromatogram of pGEM-T vector and JAG2 insert. The JAG2 insert size is 168bp (shown in green) and lies within the pGEM-T vector (3015 bp). The insert was flanked by the forward primer (JAG2p14 shown in red) and the reverse primer (JAG2p11R shown in blue). TT and AA (shown in black) represent the partial EcoR1 sites in pGEM-T where the JAG2 probe was inserted.

In summary, a wide variety of methodologies were included in this chapter. This range of research tools may be considered descriptive in a way. In addition, it includes statistics of data collected throughout the experiments. In other words, it covers different aspects of research topic by using different methods to see if it will be similar or not. For instance, testing the expression of gene of interest by optimizing it and processing through PCR and qPCR is considered informative. The following chapters will demonstrate results in two parts (3, 4). It will also outline the main component of each Notch receptors, ligands and target genes expression in cultured models. This will be followed up by discussion which will compare findings in the research and whether it agrees or disagree with other research work done earlier.

CHAPTER 3: Expression of Keratin Genes (KRT14 and KRT10) in HaCaT Cell Culture Model

3.1 Introduction

Examining notch signalling in human skin (*in vivo*) was proving to be difficult so a model system was required where the signalling process and its response to the differentiation status of the cell could be assessed. The HaCaT tissue culture model was chosen because this was already established in the laboratory and terminal differentiation could be induced using a calcium shift technique. Thus, a number of experiments were set up to examine cells growing over a 4-7 day period, altering the calcium levels to induce terminal differentiation and allowing further growth for another 6-10 days. Sufficient numbers of HaCaT cells were then produced so that total RNA and total protein could be extracted for analysis of both the state of proliferation and differentiation as well as investigating the level of notch signalling. In order to assess gene expression levels, both standard and real time PCR were done using various primer combinations (see **Table 3.1** below). Where possible, primers pairs were designed over intron boundaries so that the genomic PCR product (amplicon) was approximately 500 bp larger than the cDNA amplicon, providing an internal control for genomic contamination.

A set of HaCaT cells that had been cultured for different lengths of time in low calcium medium and then shifted to high calcium medium (see Methods Chapter for details) were prepared. Total RNA was extracted from the cultures

at each time point and stored at -85°C. A small aliquot was subjected to a standard PCR with genomic DNA (gDNA) primers (intron primers do not bind to RNA or cDNA) to detect gDNA contamination. If no bands were detected on the agarose gel, this would suggest that the total RNA preparation from the HaCaT cells was not contaminated with gDNA. This screen was also repeated after reverse transcription of HaCaT total RNA to total cDNA, and if gDNA products were found in anything other than trace amounts, the cDNA was discarded. It is important to point out that approximately 21 days were required to collect a complete set of HaCaT cell cultures at all time points, assuming the cultures grew as expected.

Table 3.1: Table of Primers for Standard PCR and qPCR with cDNA.

Gene	Primers for Standard PCR	Primers for Q-RT-PCR
Human Keratin 14 (KRT14)	p55, p56R (Product = 266bp)	p55, p57R (Product = 112bp)
Human Keratin 10 (KRT10)	p20, p23R (Product = 136 bp)	p22, p24R (Product = 111 bp)

Once total RNA had been extracted from the HaCaT cells harvested at different times, cDNA was generated by reverse transcription and a standard PCR carried out for each gene of interest (KRT14, KRT10, Notch receptors, ligands and target genes). The PCR products were analysed on 1.5% agarose gels and the resulting product sizes compared with the anticipated theoretical size. PCRs were carried out according to a rigorous protocol to minimize errors such as contamination by other DNA, primer dimers and products of incorrect

size. Ideally, the PCR products should show strong bands on a gel. As only an aliquot of the whole PCR reaction is tested, the remainder can then be sequenced to verify the precise identity of the product.

Standard PCR reactions are limited in terms of the estimation of specific gene expression levels and it can be difficult to distinguish between PCR samples containing 10 copies or 50 copies on a gel. Thus, when there are small differences in expression level, this is best estimated by quantitative real time PCR (qPCR).

In order to get an absolute level of quantitation in a dynamic cell system, levels of gene expression must be related to a housekeeping gene that is stable through the cellular changes of a typical experiment. This is an important control in qPCR experiments. However, levels of the housekeeping genes examined (β -actin, TF2H, TBP and RPLA13) were not stable as HaCaT cells altered from proliferation to differentiation. Thus, none of these molecules were considered as a stable housekeeping gene in the HaCaT cell culture model.

Primers designed for real time PCR should generate a product size of 80-120bp and not be more than 150bp. Therefore, set of primers were

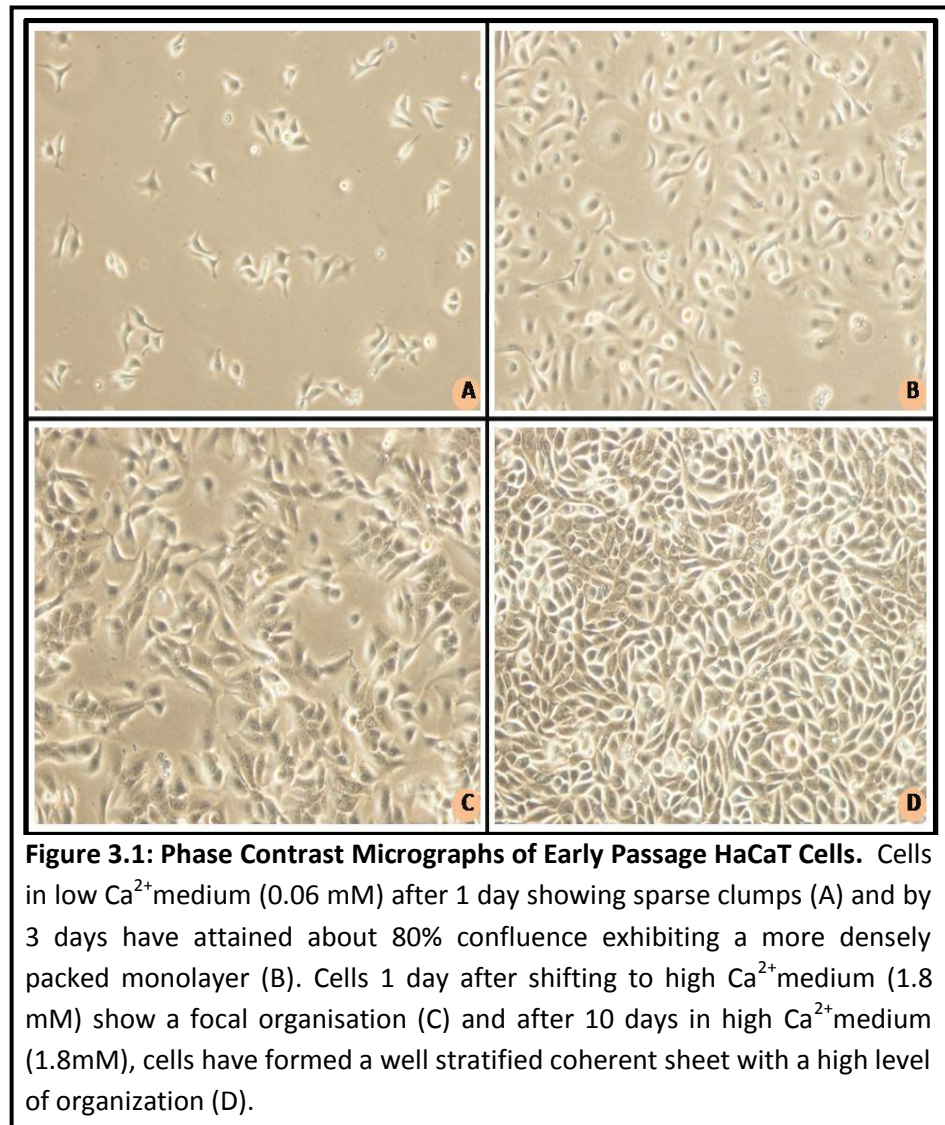
specifically designed for qPCR although some of the primers designed for standard PCR could be used because where the size of the product was suitable (see **Table 3.1**). This was followed by estimating the level of gene expression from the qPCR data. This was calculated using a standard curve measuring the efficiency of the qPCR reaction and CT value.

To establish the expression level of the gene of interest, the qPCR data was analyzed using the standard curve of efficiency and CT value and each gene was tested in triplicate using same set of HaCaT cells to minimize variation.

3.2 Morphology of HaCaT Cells during Calcium-Induced Terminal Differentiation

HaCaT cell culture was found to be the best *in vitro* model of human keratinocyte function. In fact, it represents a reliable and convenient model for keratinocyte proliferation and differentiation (*Deyrieux and Wilson, 2007*). At the same time, manipulation of HaCaT cell conditions by adjusting calcium levels (shift from low to high Ca^{2+}) demonstrates many of the actual morphological changes taking place in primary human keratinocytes and provides a reasonable representation of the *in vivo* situation.

HaCaT cells were initially grown in DMEM containing 10% foetal calf serum (FCS). The cells were then transferred to keratinocyte growth medium (KGM) containing low levels of Ca^{2+} (0.06 mM). During this stage, these cells appear as individual small clusters of spindle shaped cells which round up as they divide. They tend to stay apart from one another and coat the base of the dish in a monolayer. There are few if any flat cornified cells and few if any cells that are K10 positive. Thus, they generally represent a homogenous group of loosely associated rapidly dividing basal cells. HaCaT cells continue to proliferate and remain as monolayer during early expansion of cells numbers (*Boukamp et al., 1988*). In contrast, HaCaT cells in high Ca^{2+} medium showed extensive organisation and a typical stratified epithelium resulted with coherent sheets of corneocytes on the surface. In addition, the cells formed a prominent densely packed polygonal structure with proliferating cells in the middle and differentiating cells to the periphery. However, some cells do continue to proliferate but at a lower rate (see **Figure 3.1**). It should also be noted that cells left in low calcium for 16 days do terminally differentiate due to contact inhibition of growth at high density, but these cells are not so well organised.



3.3 Expression of K10 in HaCaT Cell Culture Model

Proliferation and terminal differentiation in the HaCaT cell culture model can be defined by the expression of different keratins and by markers of proliferation such as Ki67. Keratins K5 and K14 are expressed by basal keratinocytes undergoing proliferation. Gene expression is switched to suprabasal keratins (K1 and K10) as cells are committed to terminal

differentiation. This was demonstrated at the protein level using two techniques. Total proteins were extracted from the HaCaT cultures at different times, separated by SDS-PAGE, transferred by western blotting and reacted with either K14 or K10 antibodies. K14 levels were found to be approximately equal over the whole culture period, although less expression was observed in the early cultures (**Figure 3.2**).

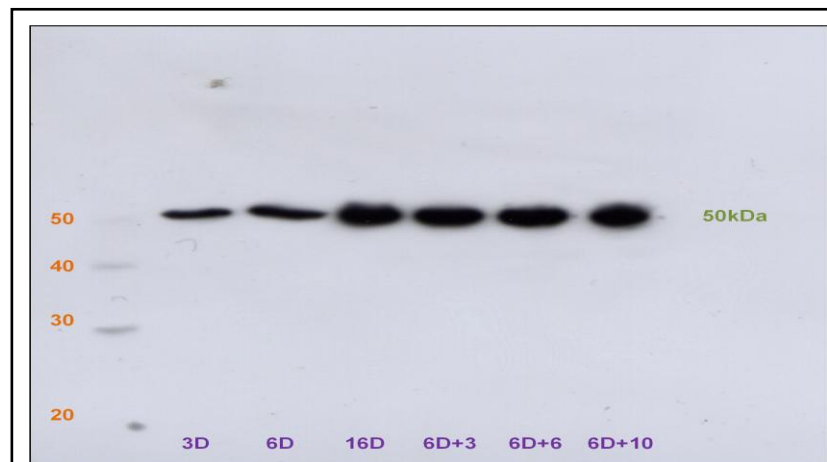
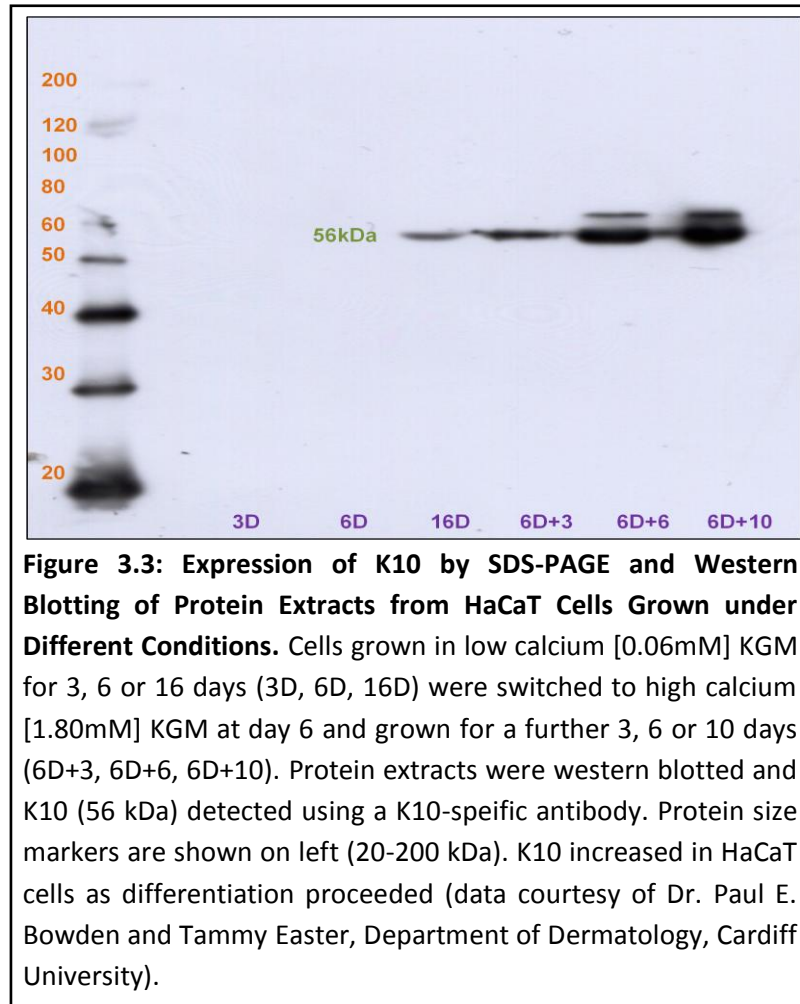


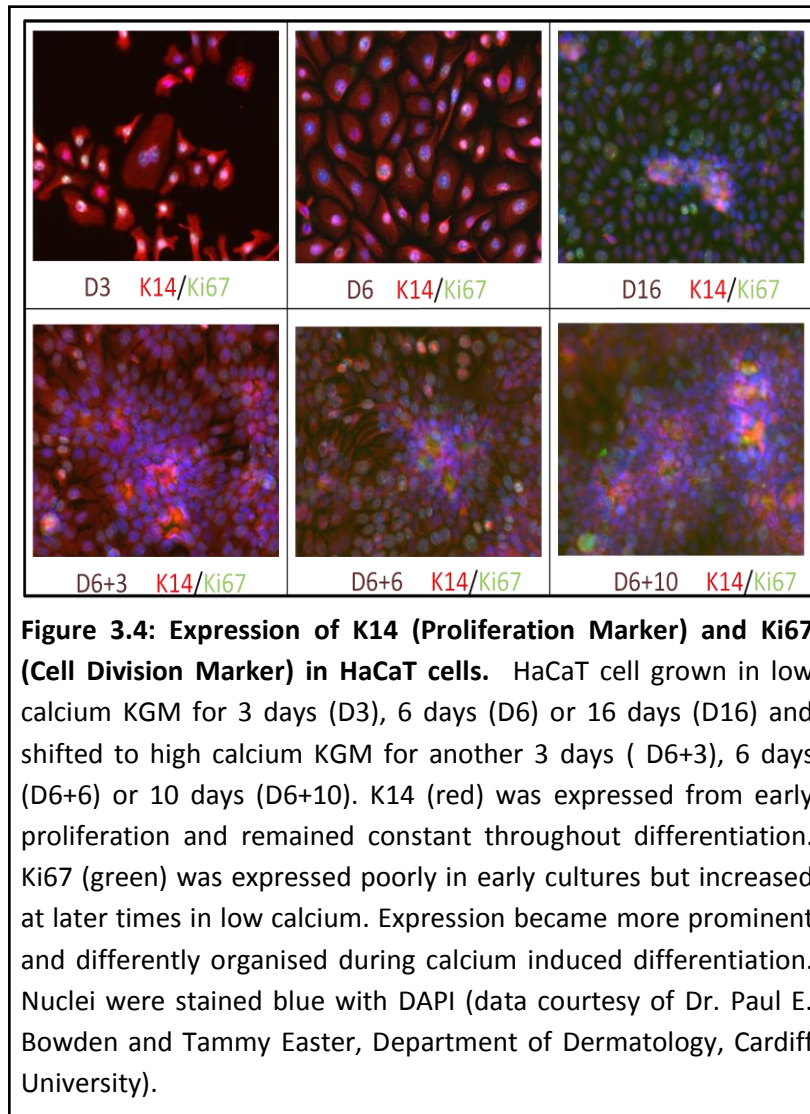
Figure 3.2: Expression of K14 by SDS-PAGE and Western Blotting of Protein Extracts from HaCaT Cells Grown under Different Conditions. Cells grown in low calcium [0.06mM] KGM for 3, 6 or 16 days (3D, 6D, 16D) were switched to high calcium [1.80mM] KGM at day 6 and grown for a further 3, 6 or 10 days (6D+3, 6D+6, 6D+10). Protein extracts were western blotted and detected using a K14 antibody (LL002). Protein size markers are shown on left (20-50kDa). Note constant K14 levels throughout HaCaT cell differentiation (data courtesy of Dr. Paul E. Bowden and Tammy Easter, Department of Dermatology, Cardiff University).

However, when K10 was examined (**Figure 3.3**), expression was low to virtually absent in early proliferating cultures (3D, 6D), increased in low

calcium at 16 days and increased dramatically in cells induced to differentiate with high calcium.



Keratin 14 (K14) expression was also examined in the cells by indirect immunofluorescence (**Figure 3.4**). While levels overall did remain constant, the amount of K14 in the proliferating cells appeared higher but at later times, the cell density was much higher but the cell content appeared lower. Ki67 expression also varied throughout the culture.



K10 expression was found to be a good marker for terminal differentiation both *in vivo* (data not shown) and in HaCaT cultures (**Figure 3.5**). This was generally absent in early low calcium cultures (Days 3 and 6) but was found in any cells that formed organised clumps. However, by day 16 in low calcium, the cell density was high and so cell-cell contact induced K10 expression at several locations. However, after calcium induction, the cells became more organised and K10 expression was switched on in all cells that attained a suprabasal position (mimicking the *in vivo* situation).

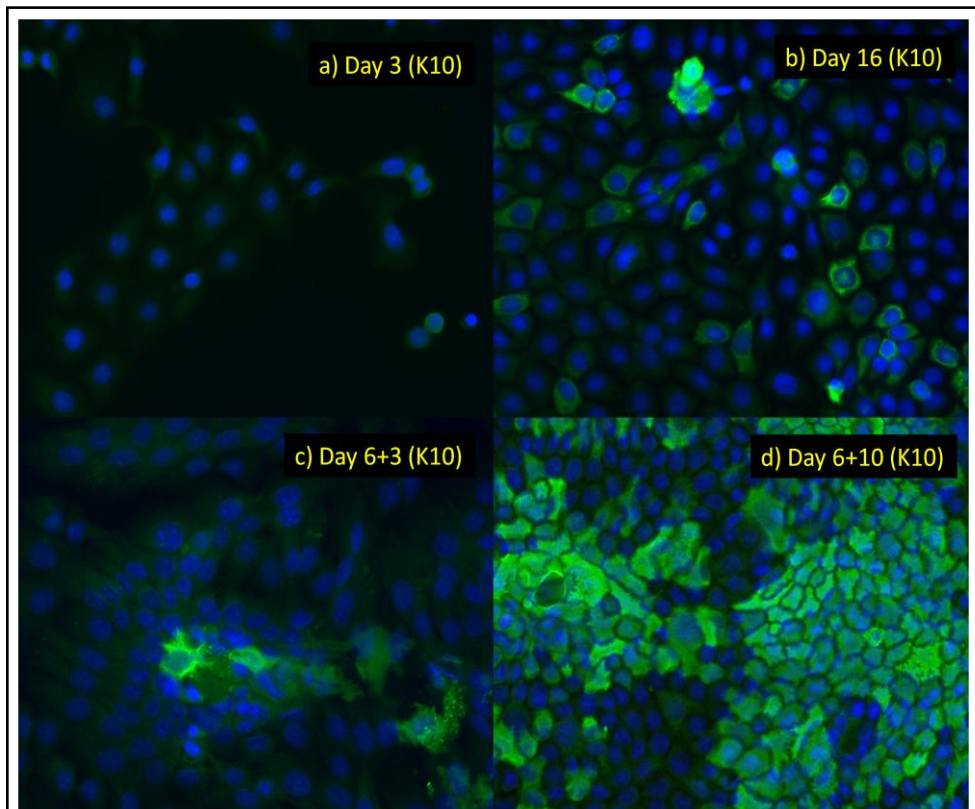


Figure 3.5: Expression of K10 (Differentiation Marker) in HaCaT cells. HaCaT cells were grown in low calcium KGM for 3 days, 6 days or 16 days and shifted to high calcium KGM at day 6 and grown for another 3 days (Day 6+3), 6 days (Day 6+6) or 10 days (Day 6+10). Data is shown for Day3 and Day 16 in low calcium and for Day 6+3 and 6+10 in high calcium. K10 (green) was not expressed in early proliferating low calcium cultures but low levels were found at day 16. After calcium induction, cells were more organised and expressed K10 in much larger amounts. Nuclei were stained blue with DAPI (data courtesy of Dr. Paul E. Bowden and Tammy Easter, Department of Dermatology, Cardiff University).

Thus, cellular levels of K10 and K14 are good indicators of the state of cultured cells. Therefore, before notch receptors, ligands and target genes could be evaluated in terms of altered gene expression during terminal differentiation, K10 and K14 expression had to be evaluated in more quantitative terms. Thus, mRNA (cDNA) levels measured in the HaCaT cell culture model and the effect on differentiation was investigated.

Human K10 and K14 primer pairs generally work well and in addition to quantitating levels in cell cultures, they have been generally used in PCR reactions as controls. They can indicate if the DNA in any reaction was intact and they are also useful to test for genomic contamination, as long as primer pairs are located over an intron. Also the expression of other genes can be related to K14 expression as this was stable over the whole time period of a HaCaT cell culture experiment (similar use to a housekeeping gene in qPCR).

Keratin primers were used to test HaCaT RNA quality and look for any genomic contamination. One primer pair (HK14p55 and p56R) was used to detect the K14 gene (KRT14) and this was designed across intron 7 to produce an amplicon of 830 bp with gDNA but a smaller amplicon (266 bp) with cDNA. However, this was too big for use in qPCR so another primer was made (HK14p57R) in exon 8 producing a smaller fragment (112 bp) with cDNA (Table 3.2).

Table 3.2: Sequence of K14 Oligonucleotide Primers for PCR and qPCR.

Note: reverse complement primers are designated "R". One pair was used for standard PCR (p55 and p56R) and another for qPCR (p55 and p57R).

Primers	Sequence
K14 p55	[5'- CTG GAT CGC AGT CAT CCA GAG ATG -3']
K14 p56R	[5'- GAT AAT GAA GCT GTA TTG ATT GCC -3']
K14 p57R	[5'- TGG TGC GAA GGA CCT GCT CGT GGG -3']

The K14 primer set was used to investigate gDNA contamination of total RNA extracts from HaCaT cells in culture. The K14 PCR was designed across intron 7 so cDNA products are smaller (266 bp) than genomic DNA products (830 bp). When run with a set of RNA samples, there are no products in the absence of gDNA contamination so the only product found was in the sample containing the control genomic DNA (gDNA). Here a single band of 830 bp was observed with the K14 primers on a 1.5% agarose gel, confirming the lack of genomic contamination (**Figure 3.6**).

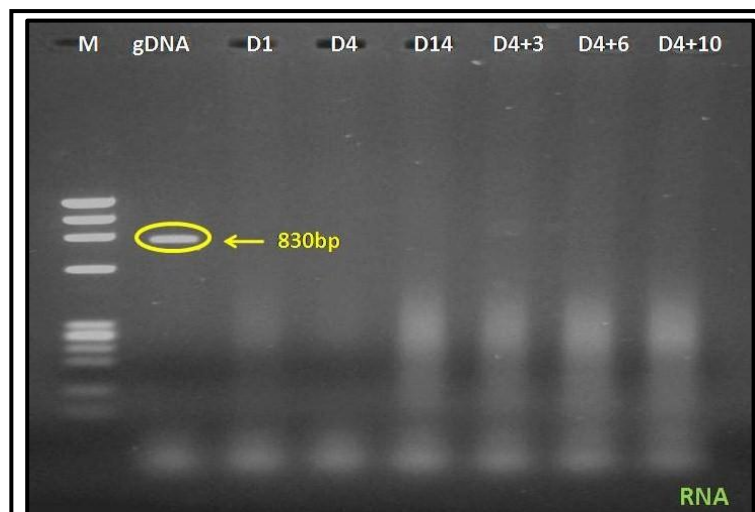


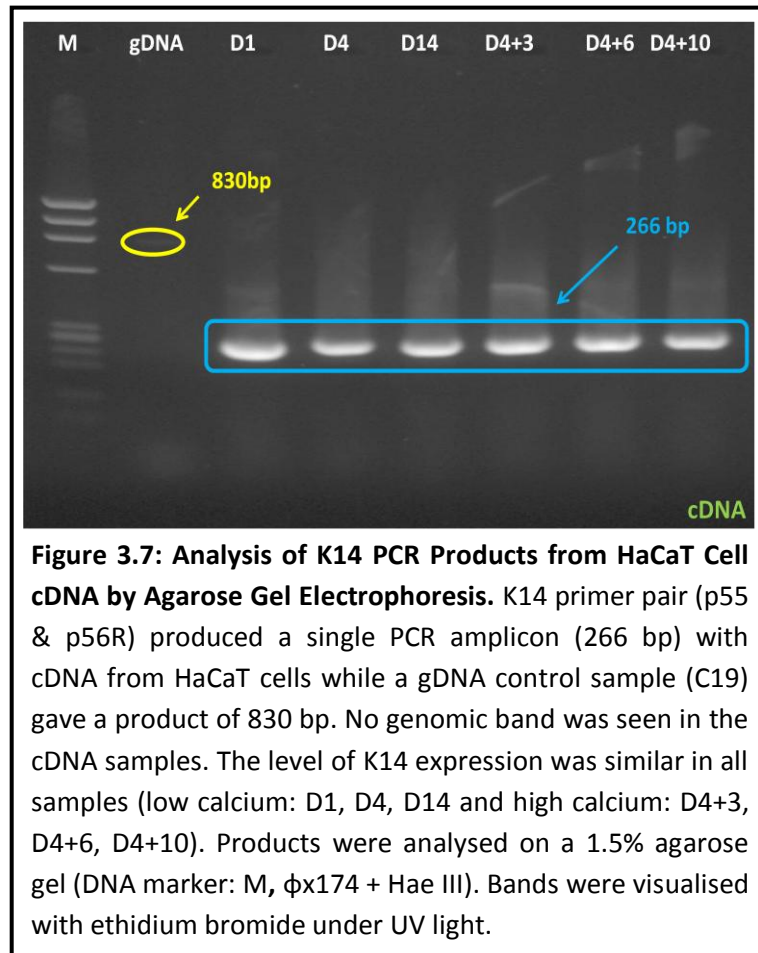
Figure 3.6: Assessing Genomic DNA Contamination in Total RNA Extracts of HaCaT Cells. PCR with K14 primers (p55, p56R) on a genomic DNA (gDNA) sample (C19) and a series of total RNA extracts from HaCaT cells (D1, D4, D14, D4+3, D4+6, D4+10). The K14 PCR product (830 bp) was only found in the tube with control gDNA showing that there was no gDNA in the RNA extracts. M= ϕ x174 DNA +Hae III marker.

The K10 primers used for standard PCR also generated a fragment that was too large for qPCR. Thus, two specific primers were designed in the 3' non-coding region of the gene (HK10p22 and p24R) to give an amplicon of 111 bp on cDNA and gDNA. Another pair (HK10p20 and p23R) were also made over intron 7 (304 bp) that produced an amplicon of 136 bp on cDNA and 440 bp on gDNA (**Table 3.3**).

Table 3.3: Sequence of K10 Oligonucleotide Primers for qPCR. Note that reverse complement primer was designated "R".

Primers	Sequence
HK10p20	[5'- CTC CAG CGG AGG CCA CAA GTC CTC -3']
HK10p23R	[5'-GAT GAA AGA ACT CTA CCG TCG GGC -3']
HK10 p22	[5'- TGC ATC AAG AGG AAA GAG TCT CCC-3']
HK10 p24R	[5'- AAG GTC TAT TTC CAT AGA CCA TCA AGA CAG-3']

After reverse transcription of HaCaT total RNA to total cDNA using a poly A+ primer, the K14 oligonucleotide primer pair (K14p55, p56R) were used under standard PCR conditions (58°C annealing and 35 cycles). The PCR products were run on a 1.5% agarose gel (**Figure 3.7**) and their identity was confirmed by sequence analysis. The PCR resulted in uniform strong bands (at 266 bp) throughout HaCaT cell proliferation and differentiation and appeared independent of the amount of calcium in the medium. In addition, there were no larger bands (830 bp) except in the gDNA control tube.



The K14 primer pair optimized for quantitative PCR was initially tested on total cDNA from HaCaT cells using a standard protocol. Again a single strong band (at 112 bp) was observed on the 1.5% agarose gel (**Figure 3.8**) and the identity of the product was confirmed by direct sequencing. It is important to point out that the total RNA samples from each HaCaT cell culture time point were quantified and adjusted to the same concentration to ensure that the cDNA generated was as representative of mRNA expression as possible. This step reduces some of the inherent variation and helps to produce more reliable qPCR results.

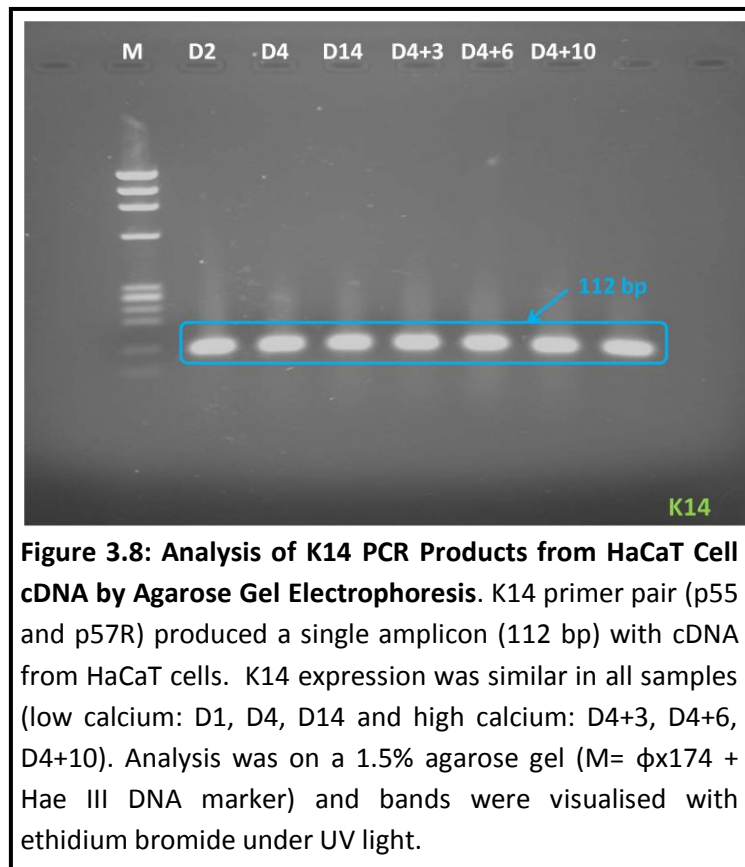


Figure 3.8: Analysis of K14 PCR Products from HaCaT Cell cDNA by Agarose Gel Electrophoresis. K14 primer pair (p55 and p57R) produced a single amplicon (112 bp) with cDNA from HaCaT cells. K14 expression was similar in all samples (low calcium: D1, D4, D14 and high calcium: D4+3, D4+6, D4+10). Analysis was on a 1.5% agarose gel (M= ϕ x174 + Hae III DNA marker) and bands were visualised with ethidium bromide under UV light.

This was also repeated for the K10 primer pair (K10p22 and p24R) designed for qPCR, which produced a small amplicon (111 bp) from the 3' non-coding region of the gene (and cDNA). It was tested on cDNA from HaCaT cells using standard PCR conditions (58°C annealing and 35 cycles) and analysed on a 1.5% agarose gel (**Figure 3.9**). K10 showed relatively consistent expression throughout the HaCaT cell period in culture and little difference was observed between low calcium and high calcium conditions. This was not expected as there was very little if any K10 protein expression in early cultures (day 1-4) while cells were proliferating and a much more dramatic increase in K10 levels in differentiating cells. Thus, it may be that the conditions used in the PCR were causing all reactions to reach a maximum plateau independent of the

original starting conditions as long as there were a least a few molecules of K10 mRNA present. This also highlighted the need for qPCR.

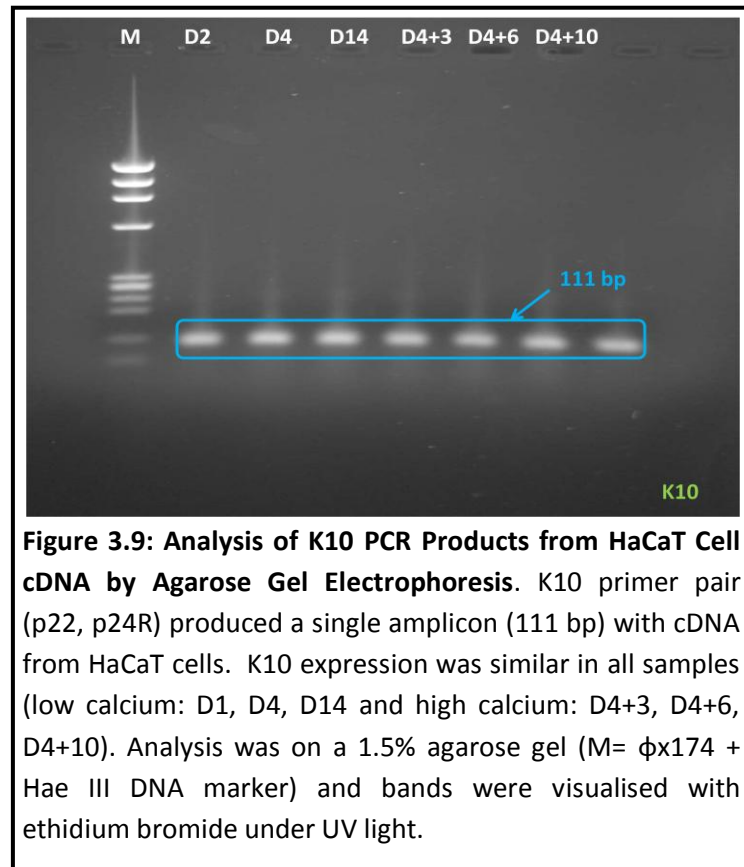


Figure 3.9: Analysis of K10 PCR Products from HaCaT Cell cDNA by Agarose Gel Electrophoresis. K10 primer pair (p22, p24R) produced a single amplicon (111 bp) with cDNA from HaCaT cells. K10 expression was similar in all samples (low calcium: D1, D4, D14 and high calcium: D4+3, D4+6, D4+10). Analysis was on a 1.5% agarose gel (M= ϕ x174 + Hae III DNA marker) and bands were visualised with ethidium bromide under UV light.

K10 and K14 PCR amplicons were sequenced to confirm their identity and then they were inserted into separate pGEM-T easy vectors and cloned (see methods chapter for details).

Once ligated into the pGEM-T easy vectors and cloned, the relevant bacterial clones were grown in batch culture and the plasmid carrying the vector and

insert isolated. Six clones were selected for each insert and the plasmids were extracted using a Qiagen mini plasmid kit (details in methods chapter). The K10 and K14 inserts were released from the pGEM-T easy vectors by digestion with Eco RI, and the products were run on a 1.5% agarose gel (**Figures 3.10 and 3.11**).

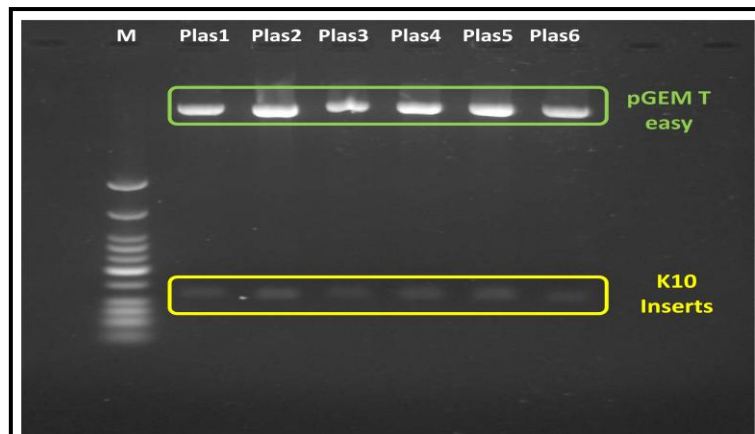
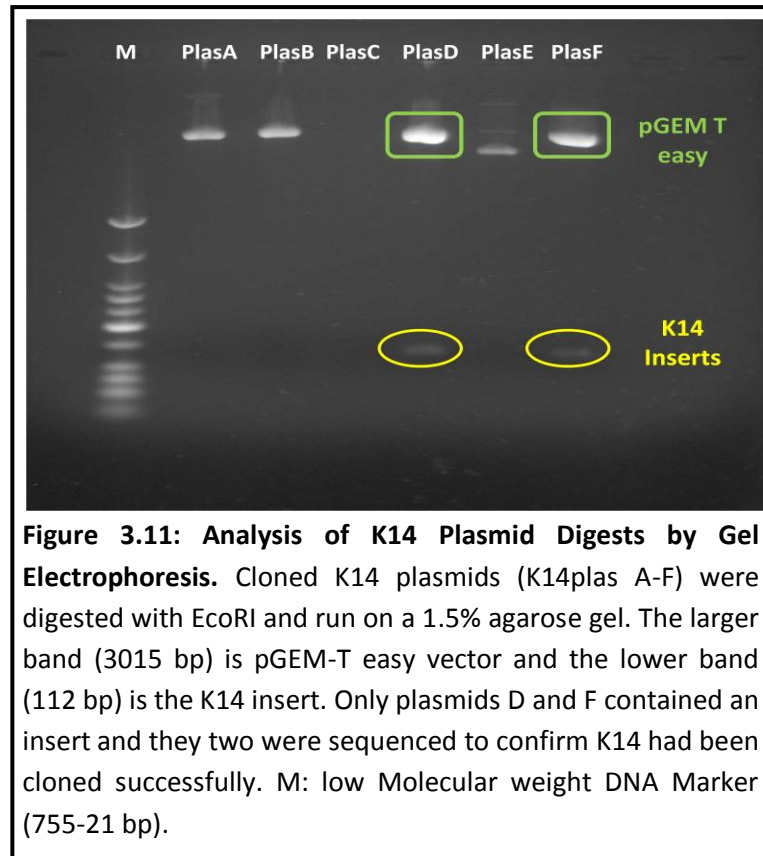


Figure 3.10: Analysis of K10 Plasmid Digests by Gel Electrophoresis. Cloned K10 plasmids (K10 Plas1-6) were digested with EcoRI and run on a 1.5% agarose gel. The larger band (3015 bp) is pGEM-T easy vector and the lower band (111 bp) is the K10 insert. All inserts were sequenced to confirm K10 had been cloned successfully. M: low molecular weight DNA marker (755-21 bp).

The clones that contained plasmids with inserts were stored as glycerol stocks at -80°C and isolated plasmid DNA was stored at -20°C. One plasmid was then selected based on the quality of the insert and a set serial dilutions was made. Plasmid 5 was selected for K10 and plasmid F for K14 and serial dilutions

(300,000 to 30 copies) were made for use in qPCR experiments (see methods Chapter for details).



In brief, the DNA concentration of the stock plasmid solution was measured by spectrophotometry (180 ng/ μ l for K10 plasmid 5). This was then diluted 1 in 10^6 to produce a working K10 plasmid 5 working solution (1.8e-13 g/ μ l). The length of the plasmid (3126 bp) was calculated from the size of the vector (3015bp) and insert (111 bp) and the mass of a single copy calculated from the following equation (where m=mass (g), n = number of base pairs):

$$m = n \times 1.096e^{-21} \text{ g/bp}$$

This gives a value of 3.426e-18 g for the mass of a single K10 plasmid. In order to calculate the mass of a fixed number of molecules, multiply the mass of a single molecule by the number of molecules required. As this was delivered in a 5 µl aliquot then the mass data must be divided by 5 to obtain the final concentration (**Table 3.4**).

Table 3.4: Mass and Final Concentration of K10 Plasmid 5 containing between 300,000 and 30 copies in a 5 µl Aliquot

Copy #	Mass of K10 Plasmid DNA (g)	Final Concentration of K10 Plasmid DNA in 5 µl (g/µl)
300,000	x 3.426e-18g	1.028e-12
30,000		2.06e-13
3000		2.06e-14
300		2.06e-15
30		2.06e-16

These values can then be used together with the stock concentration to work out the dilutions necessary to obtain the correct copy number using the following equation:

$$C_1V_1=C_2V_2$$

Where C_1 = Initial plasmid DNA concentration (g/µl)
 V_1 =Volume of stock plasmid solution needed (µl)
 C_2 = Final plasmid DNA concentration (g/µl)
 V_2 = Final volume of working plasmid solution (µl)

So for the dilution containing 300,000 copies the following applies and all other dilutions can be made at 1 in 10 from this stock (**Table 3.5**):

$$V_1 = \frac{C_2 \times V_2}{C_1} = \frac{2.06e^{-13} \times 100}{1.8e^{-13}} = 11.43 \mu\text{l}$$

$$\text{Volume of diluent} = 100 \mu\text{l} - 11.43 \mu\text{l} = 88.57 \mu\text{l}$$

Table 3.5: Serial Dilutions of K10 Plasmid 5 for qPCR. Sterile nuclease free H₂O was used as the diluent.

Dilution	Source of plasmid DNA for dilution	Initial Conc. (g/μl)	Volume of K10 Plasmid DNA (μl)	Volume of Diluent (μl)	Final Vol (μl)	Final Conc (g/μl)	Copy #
		C ₁	V ₁		V ₂	C ₂	
1	Stock	1.8e-7	10μl	990μl	1000μl	1.8e-9	N/A
2	Dilution 1	1.8e-9	10μl	990μl	1000μl	1.8e-11	N/A
3	Dilution 2	1.8e-11	10μl	990μl	1000μl	1.8e-13	N/A
4	Dilution 3	1.8e-13	11.43	88.57	100μl	2.06e-13	300,000
5	Dilution 4	2.06e-13	10μl	90μl	100μl	2.06e-14	30,000
6	Dilution 5	2.06e-14	10μl	90μl	100μl	2.06e-15	3000
7	Dilution 6	2.06e-15	10μl	90μl	100μl	2.06e-16	300
8	Dilution 7	2.06e-16	10μl	90μl	100μl	2.06e-17	30

The serial dilutions of K10 plasmid were initially tested by standard PCR and analyzed on a high definition (3% NuSieve and 1% agarose) gel (**Figure 3.12**).

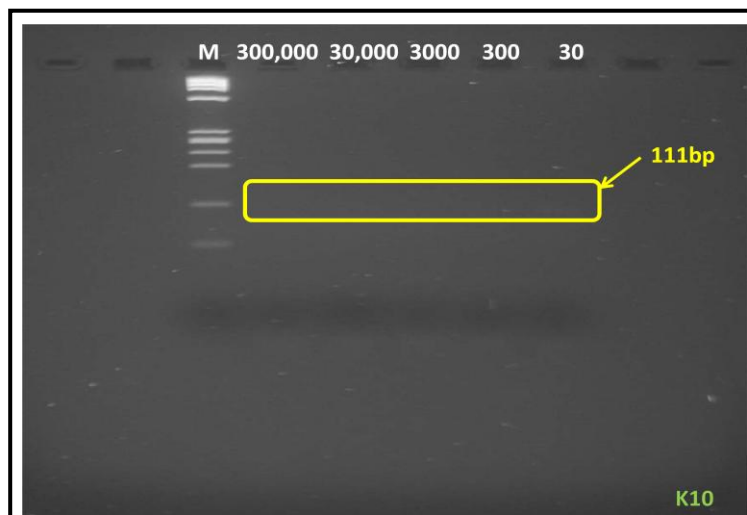


Figure 3.12: Analysis of Standard PCR with K10 Plasmid 5 Serial Dilutions. *K10* plasmid 5 dilutions (300,000 copies to 30 copies) were run by standard PCR (58a35c) using K10 primers (HK10p22, p24R). Products were analysed on a 3% NuSieve + 1% agarose gel and only very faint bands (not clear) were seen (M = DNA marker: φx174 + Hae III).

Plasmid F containing the K14 insert was selected for qPCR and a set of serial dilutions made in the same way. The stock K14 plasmid DNA concentration was 400 ng/ μ l and this was diluted 1 in 10^6 ($4e-13$ g/ μ l). The mass of a single plasmid was calculated as $3.42e-18$ g and the mass of 300,000 copies was calculated as $1.028e-12$ g. This is equivalent to $2.056e-13$ g/ μ l in a 5 μ l aliquot. Thus, the initial plasmid working solution containing 300,000 copies of K14 vector and insert was made by adding 51.41 μ l of stock plasmid DNA to a tube containing 48.59 μ l sterile water. The other working plasmid solutions were made by diluting this initial solution by 1 in 10 (**Table 3.6**).

Table 3.6: Serial Dilutions of K14 Plasmid F for qPCR. Sterile nuclease free H₂O was used as diluent.

Dilution	Source of Plasmid DNA for dilution	Initial Conc (g/ μ l) C_1	Volume of K14 Plasmid DNA (μ l) V_1	Volume of Diluent (μ l)	Final Vol (μ l) V_2	Final Conc (g/ μ l) C_2	Copy #
1	Stock	$4e-7$	10 μ l	990 μ l	1000 μ l	$4e-9$	N/A
2	Dilution 1	$4e-9$	10 μ l	990 μ l	1000 μ l	$4e-11$	N/A
3	Dilution 2	$4e-11$	10 μ l	990 μ l	1000 μ l	$4e-13$	N/A
4	Dilution 3	$4e-13$	51.41	48.59	100 μ l	$2.056e-13$	300,000
5	Dilution 4	$2.056e-13$	10 μ l	90 μ l	100 μ l	$2.056e-14$	30,000
6	Dilution 5	$2.056e-14$	10 μ l	90 μ l	100 μ l	$2.056e-15$	3000
7	Dilution 6	$2.056e-15$	10 μ l	90 μ l	100 μ l	$2.056e-16$	300
8	Dilution 7	$2.056e-16$	10 μ l	90 μ l	100 μ l	$2.056e-17$	30

K10 expression was measured in HaCaT cultures by qRT-PCR and both the copy number of cDNA (and mRNA by inference) and also the fold change relative to the initial culture conditions (Day 1-3, varies between difference experiments) were estimated.

The K10 standard dilution series was run at the same time as the experimental samples and this data was used to calculate the copy number from the individual sample Ct values (number of cycles to reach the threshold). The K10 dilution series data was analysed first and a standard curve drawn.

The amplification plot (**Figure 3.13**) of the K10 dilution series showed 5 evenly spaced curves (fluorescence vs cycle number) and these were shown in different colours for each dilution (blue = 300,000; red= 30,000; green = 3,000; grey = 300 and yellow = 30 copies). As the dilution increased, the threshold copy number (Ct value) increased and this data can be used to calculate a standard curve of Ct value versus copy number (**Figure 3.14**). The copy number of experimental (unknown) samples can then be estimated from their Ct values.

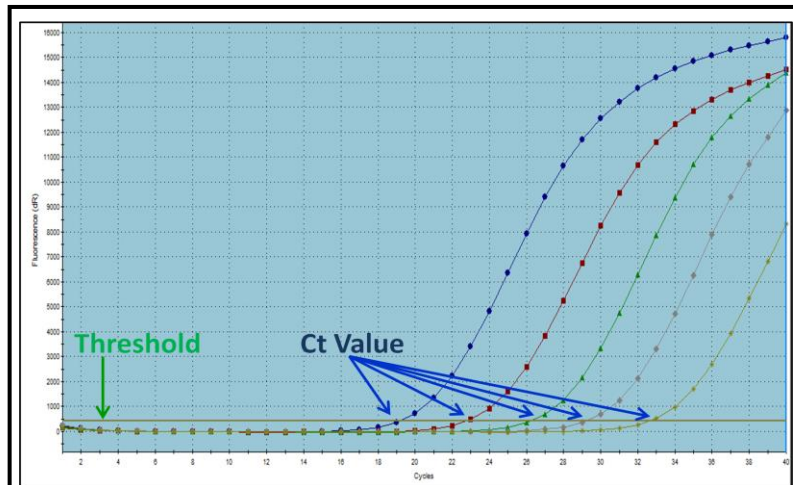


Figure 3.13: Amplification Plot of K10 Plasmid Dilution Series. Amplification plots were calculated by qPCR MxPro Software. Each colour represents the fluorescence values for a different K10 plasmid dilution: blue 300,000 copies; red 30,000; green 3,000; grey 300 and yellow 30. The distance between each fluorescence amplification plot was approximately constant (3-4 cycles starting at 18 cycles) and the Ct values measured as the lines cross the threshold. Note: The data represents an average of 3 separate measurements (triplicate samples).

The Ct values for the K10 dilution series ranged from 19 to 33 and this produced a linear plot (**Figure 3.14**) with an efficiency of 99.2% (ideal = 100%), an R^2 value of 0.999 (ideal = 1.000) and a slope of -3.342 (ideal = -3.2 to -3.6). This represents a very good standard curve for K10 and this was used to estimate the copy number in experimental samples from the measured Ct value.

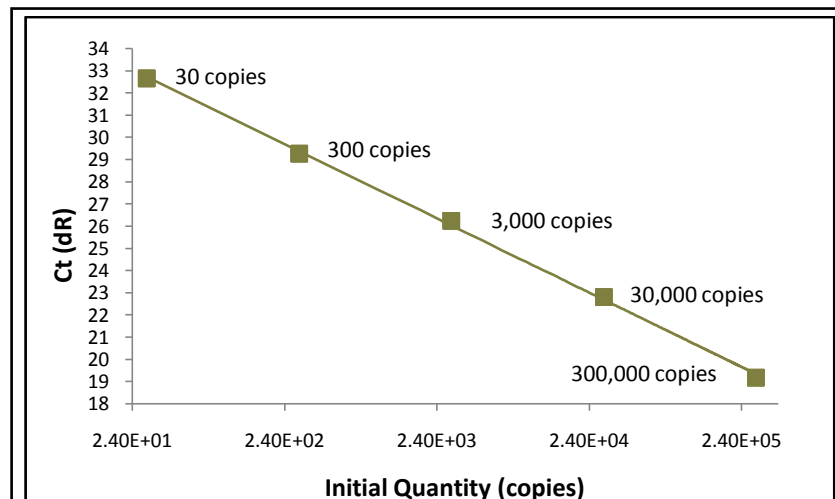


Figure 3.14: Standard Curve of K10 Plasmid Dilution Series. The Ct value was plotted against copy number and the efficiency of the PCR reaction estimated as 99.2% (calculated from the slope which was -3.342). The Rsq value was 0.999 indicating the data is a close fit to the linear line as plotted. The scale on the x-axis does not signify the copy number at each data point. It is important to note that the standard curve may only be used to interpolate, not extrapolate, the quantity of the unknown sample. This is because the assay may not be linear outside the range covered by the standard tested.

The qPCR data from 3 consecutive experiments (triplicate experiments) were then analysed using the K10 standard curve and INSTAT software. The raw qPCR data was analysed using different statistical methods such as Tukey-Kramer Multiple Comparison Test and One-way Analysis of Variance (ANOVA). This software was used to analyse the K10 experimental data in two different ways: initially calculating the level of K10 expression in relation to copy number and then calculating the fold change in expression.

Proliferating cultures (3 days and 6 days in low calcium medium) did have a low copy number (188,500 – 366,100) of K10 transcripts (**Table 3.7**) even though very little if any K10 protein was observed in these cells. However, the cultures that showed distinct stratification and cornification (16D in low calcium and all high calcium cultures) showed a large increase in K10 copy number (834,400 – 2,372,000). All the data represents an average value of three separate experiments (**Table 3.7**).

Table 3.7: K10 Gene Expression (Copy Number) during HaCaT Cell Culture. Data for 3 experiments showed the same general trend with an increase in K10 expression as the cultures differentiated. There was a significant increase in copy number as cells differentiated (16D, 6D+3, 6D+6, 6D+10) relative to proliferating cultures (3D, 6D). **Note:** sample values were outside standard curve range (see Figure 3.13) so the cDNA was diluted 1:10 to bring them into range (30-300,000 copies) and the numbers below represent the original undiluted cDNA.

Experiment	3D	6D	16D	6D+3	6D+6	6D+10
1	262,300	354,800	1,316,000	834,400	2,372,000	1,892,000
2	188,500	326,100	1,367,000	1,014,000	2,224,000	1,959,000
3	238,500	366,100	1,352,000	998,000	2,187,000	1,929,000
Average	229,767	349,000	1,345,000	948,800	2,261,000	1,926,667

In terms of fold change, the increase in K10 expression during differentiation represented a 3.18 (min) to 13.92 (max) fold increase over the level observed in day 3 cultures (**Table 3.8**).

Table 3.8: K10 Gene Expression (Fold Change) in HaCaT Cell Cultures. K10 gene expression only increased slightly while cells were proliferating (1.83 fold max) but much larger increases were seen as cells differentiated (3.18-13.92 fold). Fold change data relative to 3D culture levels and average values of 3 experiments are shown in blue.

Experiment	3D	6D	16D	6D+3	6D+6	6D+10
1	1.00	1.35	5.02	3.18	9.04	7.21
2	1.00	1.73	7.25	5.38	11.80	10.39
3	1.00	1.83	9.86	7.21	13.06	13.92
Average	1.00	1.64	7.38	5.26	11.30	10.51

Comparisons were then made between levels of K10 expression at each time point in the HaCaT culture experiments using the Tukey-Kramer Multiple Comparison Test (**Table 3.9**). Here, values of q greater than 5.628 were just significant ($p < 0.05$) while larger values of q (>13.175) were very significant ($p < 0.001$). In all cases when comparing cultures that showed signs of differentiation with proliferating cultures (either 3D or 6D), the increases were significant. There was no significant difference between K10 levels in 3D and 6D cultures (both low calcium) but 16D cultures in low calcium did stratify due to contact inhibition and the levels of K10 were significantly higher. The cultures that differentiated the longest (6D+10) had lower K10 levels than 6D+6 which appeared to be the optimum time in this model.

Table 3.9: Comparison of K10 Expression Levels (Copy Number) in Different HaCaT Cultures. The mean difference in copy number between the cultures compared was calculated and a q value assigned. Where the value of Q was >5.628, the data was significant (values shown in red). **Note:** sample values were outside standard curve range (see Figure 3.13) so the cDNA was diluted 1:10 to bring them into range (30-300,000 copies) and the numbers below represent the original undiluted cDNA.

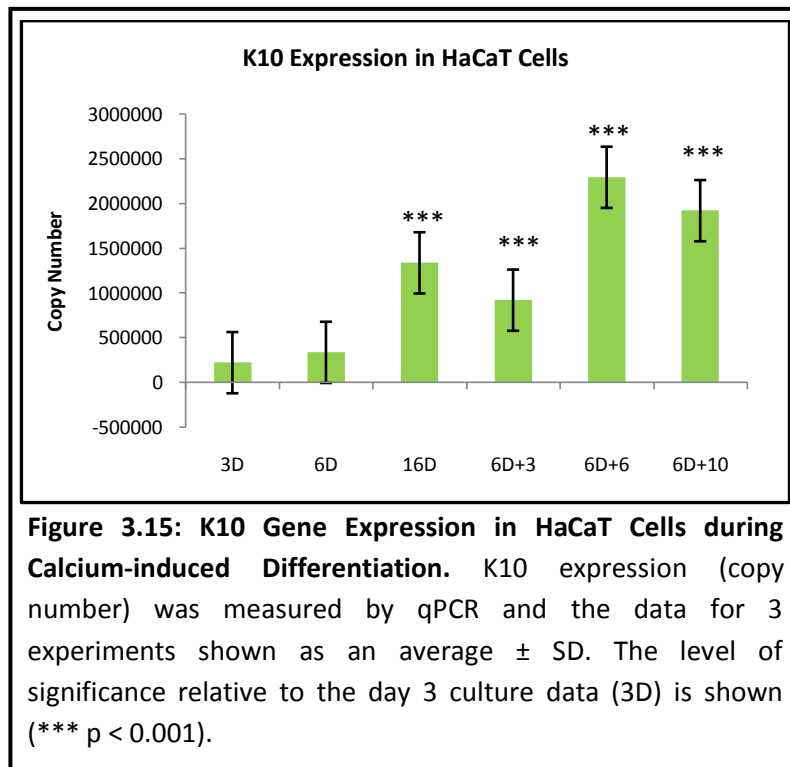
Comparison	Mean Difference	Q	P value
3D vs 6D	-115050	2.169	ns P>0.05
3D vs 16D	-1116100	21.042	*** P<0.001
3D vs 6D+3	-698800	13.175	*** P<0.001
3D vs 6D+6	-2072600	39.075	*** P<0.001
3D vs 6D+10	-1700100	32.053	*** P<0.001
6D vs 16D	-1001050	18.873	*** P<0.001
6D vs 6D+3	-583750	11.006	** P<0.01
6D vs 6D+6	-1957550	36.906	*** P<0.001
6D vs 6D+10	-1585050	29.883	*** P<0.001
16D vs 6D+3	417300	7.868	* P<0.05
16D vs 6D+6	-956500	18.033	*** P<0.001
16D vs 6D+10	-584000	11.010	** P<0.01
6D+3 vs 6D+6	-1373800	25.901	*** P<0.001
6D+3 vs 6D+10	-1001300	18.878	*** P<0.001
6D+6 vs 6D+10	372500	7.023	* P<0.05

Interestingly, the data expressed as fold change in K10 expression levels was not as significant as the copy number data (**Table 3.10**). This was also analysed using the Tukey-Kramer Multiple Comparison Test and values of q was greater than 5.628 were significant ($p < 0.05$). The only data that remained significant were the comparisons between proliferating cultures in low calcium (3D and 6D) and late differentiating cultures in high calcium (6D+6 and 6D+10).

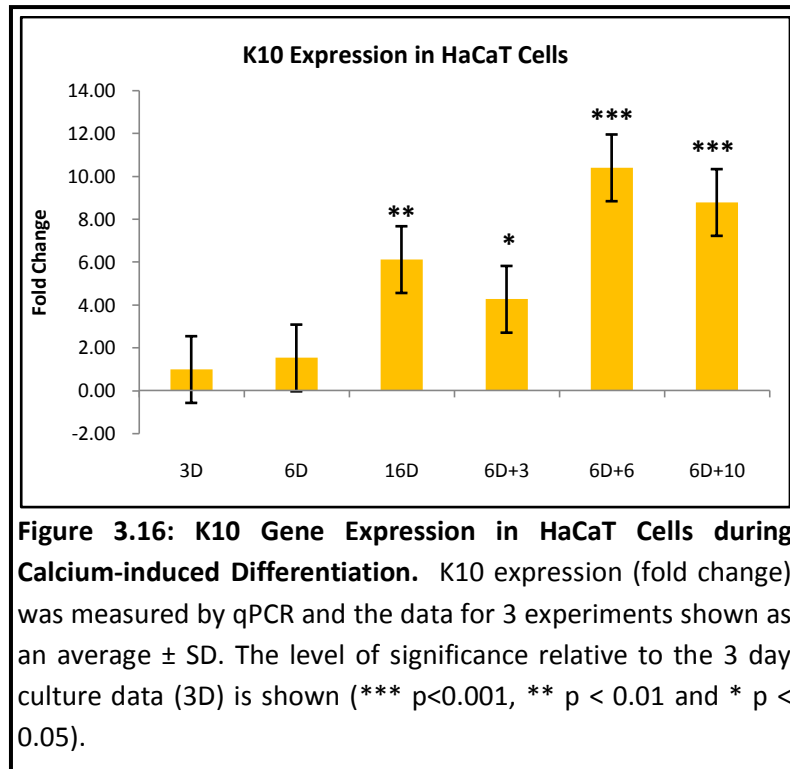
Table 3.10: Comparison of K10 Expression Levels (Fold Change) in HaCaT Cultures. The mean difference in K10 fold change between certain cultures was compared and where the value of Q was greater than 2.60, the difference was significant ($p < 0.05$ or more).

Comparison	Mean Difference	Q	P value
3D vs 6D	-0.5400	0.5028	ns $P > 0.05$
3D vs 16D	-5.135	4.781	** $P < 0.01$
3D vs 6D+3	-3.280	3.054	* $P < 0.05$
3D vs 6D+6	-9.420	8.770	*** $P < 0.001$
3D vs 6D+10	-7.800	7.262	*** $P < 0.001$
6D vs 16D	-4.595	4.278	** $P < 0.01$
6D vs 6D+3	-2.740	2.551	ns $P > 0.05$
6D vs 6D+6	-8.880	8.268	*** $P < 0.001$
6D vs 6D+10	-7.260	6.759	*** $P < 0.001$
16D vs 6D+3	1.855	1.727	ns $P > 0.05$
16D vs 6D+6	-4.285	3.989	** $P < 0.01$
16D vs 6D+10	-2.665	2.481	ns $P > 0.05$
6D+3 vs 6D+6	-6.140	5.717	** $P < 0.01$
6D+3 vs 6D+10	-4.520	4.200	** $P < 0.01$
6D+6 vs 6D+10	1.620	1.508	ns $P > 0.05$

The copy number data for K10 expression in different HaCaT cultures was made into a bar chart and the standard deviation (SD) was shown for each bar as well as the significance relative to the 3D cultures (**Figure 3.15**). Low levels of K10 expression were found in early cultures in low calcium medium (3D & 6D) and K10 expression was increased significantly in all cultures that had differentiated and stratified (16D, 6D+3, 6D+6, 6D+10).



Expressing the K10 data as fold change produced a bar chart with the same overall trends but lower levels of significance (**Figure 3.16**). The only increases that were significant were those in late differentiation (6D+6 and 6D+10) as these were greater than 10 fold over the level seen in the 3D cultures (p < 0.01 and p < 0.05 respectively).



These observations agreed with previous work done in the laboratory and agreed with the data obtained at the protein level. Thus, K10 appears to be expressed in some cells in early low calcium cultures and the small amounts of cDNA probably represent a few cells that have clumped together and begun differentiating due to contact inhibition of growth. K10 expression was much more apparent in the cultures that had been left in low calcium for 16 days. However, cultures exposed to high calcium are much more organised, stratify better and express a significantly higher level of K10. While there may be a slight discrepancy between K10 mRNA and protein levels in early cultures, this can be explained either by levels of detection in the different methods used or may be a consequence of blocking K10 translation in proliferating cells.

3.4 Expression of K14 in HaCaT Cell Culture Model

Unlike K10, the levels of K14 did not change so dramatically as HaCaT cells differentiated. The same experimental procedure and MxPro software were used for analysis by qRT-PCR. This required cloning a segment of K14 into pGEM-T easy, constructing a set of serial dilution standards of known copy number and then relating the sample fluorescence and Ct value back to the starting copy number. The amplification plot data for the serial dilutions was not quite as good as K10 with some variation in the Ct values between dilutions (**Figure 3.17**).

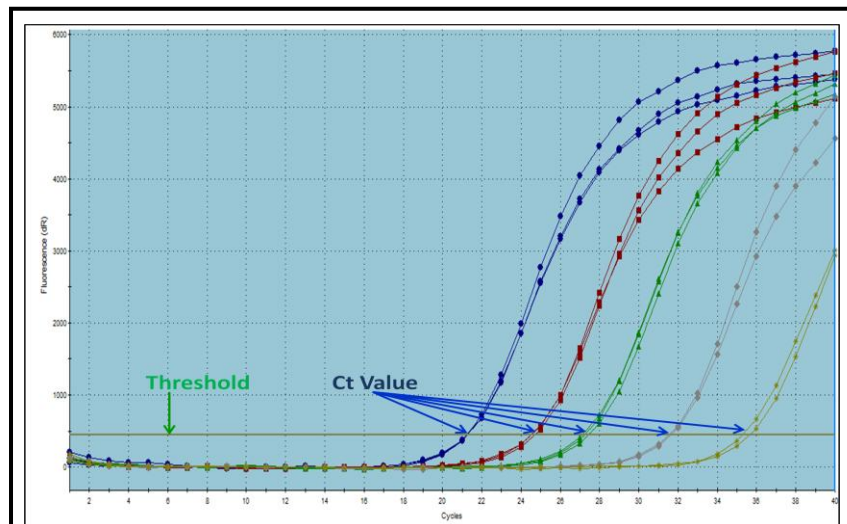
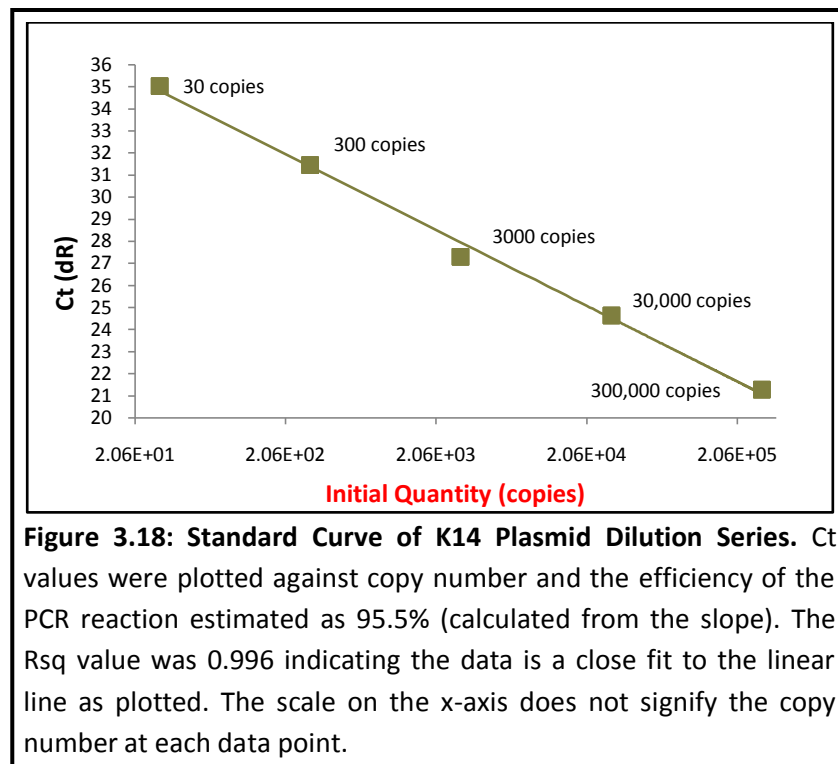


Figure 3.17: Amplification Plot of K14 Plasmid Dilution Series. Amplification plots of qPCR data were calculated by MxPro Software. Each colour represents the fluorescence values for a different K14 plasmid dilution: blue 300,000 copies; red 30,000; green 3,000; grey 300 and yellow 30. The distance between each fluorescence amplification plot was approximately constant (3-4 cycles starting at 21 cycles) and the Ct values measured as the lines cross the threshold. Note: This is an average of 3 measurements (triplicate).

The Ct values for the K14 dilution series ranged from 21 to 36 and this produced a linear plot (**Figure 3.18**) with an efficiency of 95.5% (ideal = 100%), an Rsq (R^2) value of 0.996 (ideal = 1.000) and a slope of -3.434 (ideal = -3.2 to -3.6). This represents a reasonable standard curve for K14 and this was used to estimate the copy number in experimental samples from the measured Ct value.



The qPCR data from 3 consecutive experiments (triplicates) was then analysed using the K14 standard curve and INSTAT software. This analysed the raw qPCR data using different statistical methods such as Tukey-Kramer Multiple Comparison Test and One-way Analysis of Variance (ANOVA). This software was used to analyse the K14 experimental data, initially calculating the level of

K14 expression in relation to copy number (The original cDNA was diluted into 1 in 100, to get the data in range for qPCR) and then calculating the subsequent fold change. K14 levels increased in early proliferating cultures (6 day cultures almost 4 fold higher level than 3 day cultures) after which the level of K14 reduced (**Table 3.11**). This data was not related to the amount of starting cellular material so the initial increased K14 expression probably reflected the 4 fold increase in cell density typically seen between 3 and 6 days and the subsequent reduction in K14 levels as cellular material increased further reflected a fall in K14 expression in real terms.

Table 3.11: K14 Gene Expression (Copy Number) during HaCaT Cell Culture. Data for 4 experiments showed the same general trend with an increase in K14 expression as the cultures initially proliferated and then a subsequent decrease as cells differentiated. An average value for the four experiments is shown in blue. **Note:** sample values were outside standard curve range (see **Figure 3.18**) so the cDNA was diluted 1:100 to bring them into range (30-300,000 copies) and the numbers below represent the original undiluted cDNA.

Experiment	3D	6D	16D	6D+3	6D+6	6D+10
1	526,200	1,899,000	943,200	943,000	879,400	784,800
2	542,300	1,657,000	925,100	708,300	652,200	646,600
3	316,015	1,228,335	610,598	777,741	602,446	582,537
4	256,580	1,377,011	684,505	586,466	530,225	505,857
Average	410,274	1,540,336	790,851	754,877	666,068	629,949

The initial increase in K14 expression during proliferation was equivalent to a 3.98 fold change while the K14 level in differentiating cells was almost 2 fold above the levels observed in 3D cultures (**Table 3.12**).

Table 3.12: K14 Gene Expression (Fold Change) in HaCaT Cell Cultures. K14 gene expression increased almost 4 fold in early proliferating cultures and then decreased as cells differentiated (1.95 to 1.62 fold). Fold change data relative to 3D culture levels and average values of 4 experiments are shown in blue.

Experiment	3D	6D	16D	6D+3	6D+6	6D+10
1	1.00	3.61	1.79	1.79	1.67	1.49
2	1.00	3.06	1.71	1.31	1.20	1.19
3	1.00	3.89	1.93	2.46	1.91	1.84
4	1.00	5.37	2.67	2.29	2.07	1.97
Average	1.00	3.98	1.95	1.96	1.71	1.62

The level of K14 expression at each time point in the HaCaT culture experiments was analysed using the Tukey-Kramer Multiple Comparison Test. Here, values of q greater than 4.495 were just significant ($p < 0.05$) while larger values of q (>8.241) were very significant ($p < 0.001$). Large differences were only obtained when comparing 6D cultures to all others and the data was in general highly significant in all cases ($p > 0.001$). This was true whether the data was expressed in terms of copy number (**Table 3.13**) or fold change (**Table 3.14**).

Table 3.13: Comparison of K14 Levels (Copy Number) in Different HaCaT Cultures. The mean difference in K14 copy number between the cultures as listed (comparison) was calculated and a Q value assigned. Where the value of q was >4.495, the data was significant (actual p values shown in red). **Note:** sample values were outside standard curve range (see **Figure 3.18**) so the cDNA was diluted 1:100 to bring them into range (30-300,000 copies) and the numbers below represent the original undiluted cDNA.

Comparison	Mean Difference	Q	P value
3D vs 6D	-1130063	10.652	*** P<0.001
3D vs 16D	-380577	3.587	ns P>0.05
3D vs 6D+3	-131428	1.239	ns P>0.05
3D vs 6D+6	-255794	2.411	ns P>0.05
3D vs 6D+10	-219675	2.071	ns P>0.05
6D vs 16D	749486	7.064	** P<0.01
6D vs 6D+3	998635	9.413	*** P<0.001
6D vs 6D+6	874269	8.241	*** P<0.001
6D vs 6D+10	910388	8.581	*** P<0.001
16D vs 6D+3	249149	2.348	ns P>0.05
16D vs 6D+6	124783	1.176	ns P>0.05
16D vs 6D+10	160902	1.517	ns P>0.05
6D+3 vs 6D+6	-124366	1.172	ns P>0.05
6D+3 vs 6D+10	-88247	0.8318	ns P>0.05
6D+6 vs 6D+10	36119	0.3404	ns P>0.05

Apart from the day 6 data (6D), comparison between day 3 cultures in low Ca²⁺ (3D) and other time points (6D, 16D, 6D+3, 6D+6 and 6D+10) showed no significant difference. This was also true of the other comparisons independent of how the data was expressed.

Table 3.14: Comparison of K14 Expression Levels (Fold Change) in HaCaT Cultures. The mean difference in K14 fold change between certain cultures was compared and where the value of Q was greater than 4.495, the difference was significant ($p < 0.001$).

Comparison	Mean Difference	Q	P value
3D vs 6D	-2.983	11.187	*** P<0.001
3D vs 16D	-1.025	3.845	ns P>0.05
3D vs 6D+3	-0.9625	3.610	ns P>0.05
3D vs 6D+6	-0.7125	2.673	ns P>0.05
3D vs 6D+10	-0.6225	2.335	ns P>0.05
6D vs 16D	1.958	7.343	*** P<0.001
6D vs 6D+3	2.020	7.577	*** P<0.001
6D vs 6D+6	2.270	8.515	*** P<0.001
6D vs 6D+10	2.360	8.852	*** P<0.001
16D vs 6D+3	0.06250	0.2344	ns P>0.05
16D vs 6D+6	0.3125	1.172	ns P>0.05
16D vs 6D+10	0.4025	1.510	ns P>0.05
6D+3 vs 6D+6	0.2500	0.9378	ns P>0.05
6D+3 vs 6D+10	0.3400	1.275	ns P>0.05
6D+6 vs 6D+10	0.09000	0.3376	ns P>0.05

The K14 data from individual experiments was also analysed by the INSTAT statistical software as an overall average. This was presented as a bar chart showing mean plus standard deviation and the p values where they were significant. This was expressed both in terms of total copy number (**Figure 3:19**) and fold change (**Figure 3:20**).

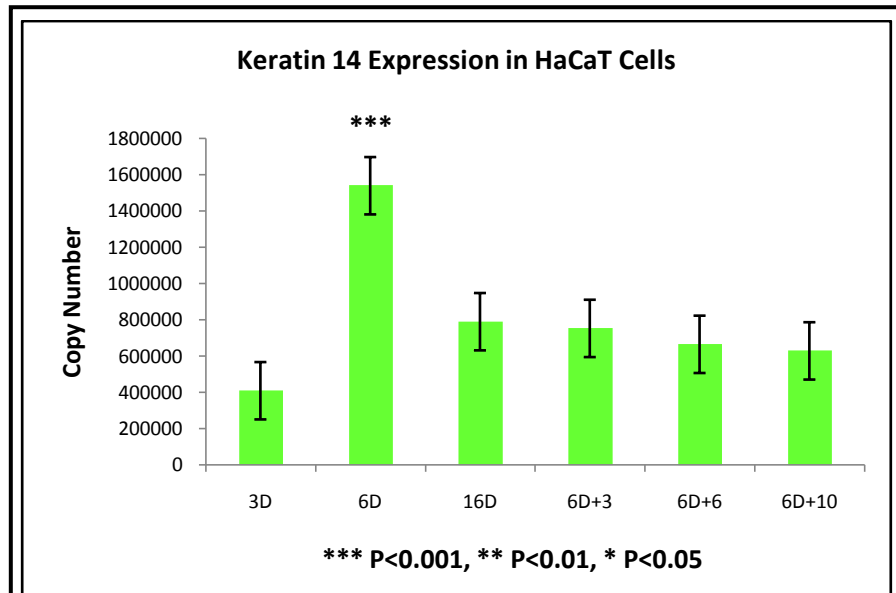


Figure 3.19: Analysis of K14 Gene Expression (Copy Number) in HaCaT Cells during Calcium-induced Differentiation. K14 copy number was estimated by qPCR in HaCaT cultures at different stages of proliferation and differentiation. Green bars show the mean of 3 different experiments together with standard deviation (black bars). The only significant data relative to day 3 was an increase at day 6 ($p < 0.001$).

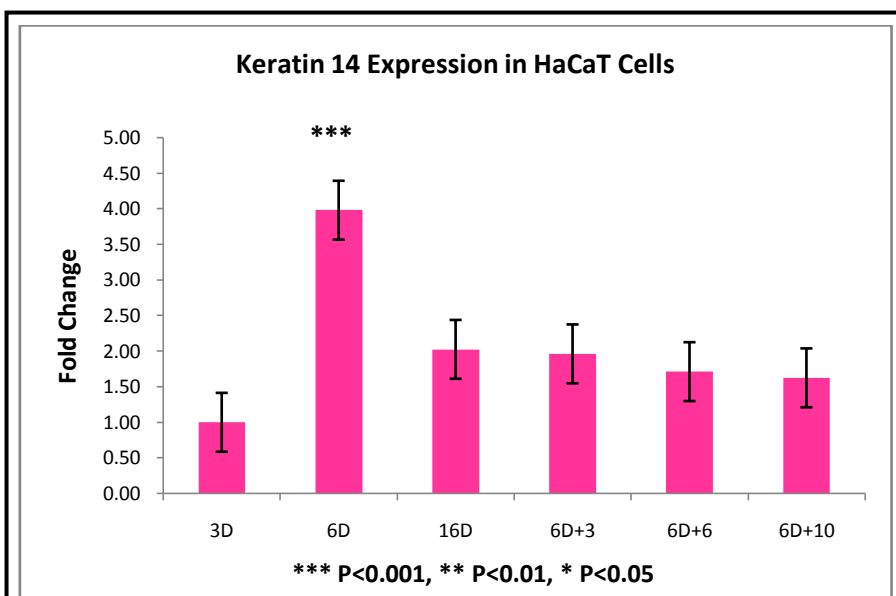


Figure 3.20: Analysis of K14 Gene Expression (Fold Change) in HaCaT Cells during Calcium-induced Differentiation. The fold change in K14 expression was estimated by qPCR in HaCaT cultures at different stages of proliferation and differentiation. Pink bars show the mean of 3 different experiments together with the standard deviation. The only significant data relative to 3D was the increase at 6D ($p < 0.001$).

In conclusion, K14 expression levels increased significantly during early proliferation (between 3 and 6 days in low calcium culture) when the cells were increasing in mass. After calcium induced differentiation, K14 levels reduced almost back to the initial 3D culture level. As the cell volume continued to increase, then a reduction in K14 expression per unit cell seemed likely, agreeing with the reduction seen as cells differentiated *in vivo*.

In general, the change over from a majority of K14 expression to a majority of K10 expression can be seen by comparing the copy number data on the same bar chart (Figure 3.21).

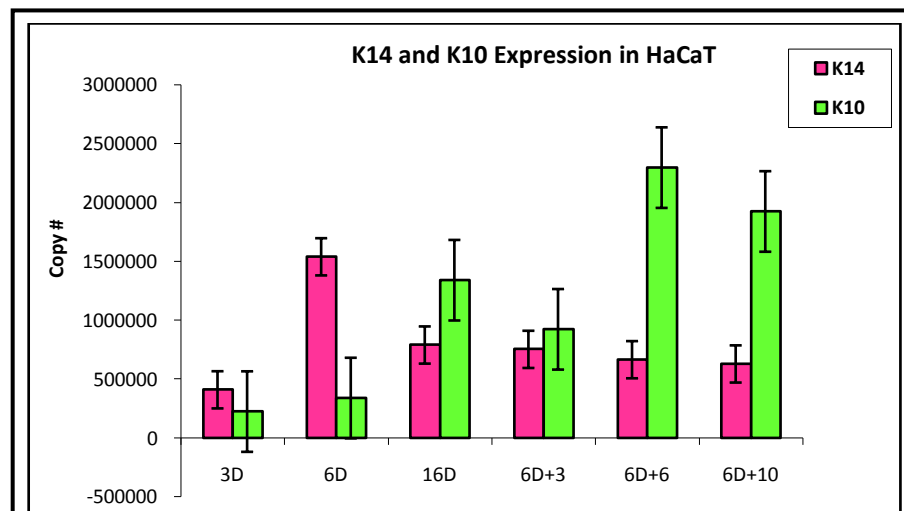


Figure 3.21: Alterations in K14 and K10 Expression (Copy Number) in HaCaT Cells during Calcium-Induced Differentiation. K14 (pink) and K10 (green) expression (copy number) was measured by qPCR and analysed using MxPro software. The K14 gene expression was increased in low calcium medium (3D, 6D) but then reduced again as cells differentiated (16D). The same reduction was also seen during calcium-induced differentiation (6D+3, 6D+6 and 6D+10). The opposite was true for K10 where levels are low in proliferating cultures and these increase as cells differentiate.

The observations of K10 and K14 expression, together with the Ki67 IMF data, showed that HaCaT cells in culture were broadly similar to human epidermis *in vivo* in terms of the commitment to terminal differentiation and that this model was sufficient to study alterations in notch signalling during epidermal differentiation *in vitro*.

CHAPTER 4: Expression of Notch Receptors, Ligands and Target Genes in HaCaT Cell Model

4.1 Introduction

Investigating notch signalling in human skin (*in vivo*) was proving to be difficult and a model system was sought so that the signalling process and its response to the differentiation status of the cell could be assessed. The HaCaT tissue culture model was chosen because this was already established in the laboratory and terminal differentiation can be induced reproducibly using the calcium shift technique. In brief (see Chapter 2 for details), the cells were grown over a 4-7 day period until they reach 70-80% confluence and then the calcium level in the medium is increased and the cells are allowed to grow for another 6-10 days. Sufficient numbers of HaCaT cells were then produced so that total RNA and total protein could be extracted for analysis of both the state of cellular proliferation and extent of terminal differentiation. Once the model was reproducibly shifting into terminal differentiation after increasing calcium levels, then notch signalling could be evaluated and experiments designed to investigate the effect of notch signalling on the process. In order to assess gene expression levels, both standard and real time qPCR were done using various primer combinations (see **Table 4.1** below). Where possible, primer pairs were designed over intron boundaries so that any genomic PCR product (amplicon) was larger than the cDNA amplicon, providing an internal control for genomic contamination.

Once total RNA had been extracted from HaCaT cell cultures harvested at different times, cDNA was generated by reverse transcription and a standard PCR carried out for each gene of interest (notch receptors, ligands and target genes). PCR products were analysed on 1.5% agarose gels to estimate the size of each amplicon. PCRs were carried out according to a rigorous protocol to minimize errors such as contamination by other DNA, primer dimers and products of incorrect size. Ideally, the PCR products should show strong single bands on the agarose gel. As only an aliquot of the whole PCR reaction was tested, the remainder can then be sequenced for identity verification (see Chapter 2 for details).

Standard PCR reactions are limited in terms of the estimation of specific gene expression levels and it can be hard to accurately distinguish PCR samples that contain 20 copies or 50 copies on a gel. Thus, when there are small differences in expression level, quantitative real time PCR (qPCR) is required.

In order to get an absolute level of quantitation in a dynamic cell system, levels of gene expression must be related to a housekeeping gene that is stable through the cellular changes of a typical experiment. This is an important control in qPCR experiments. However, the levels of the housekeeping genes examined (β -actin, TF2H, TBP and RPLA13) in the HaCaT cell culture model were not stable and levels changed as HaCaT cells changed

from proliferation to terminal differentiation. Thus, none of these molecules were considered as a stable housekeeping gene in the HaCaT cell culture model. Thus, in order to estimate the copy number of a given gene product in the HaCaT cells, a probe for each gene was cloned and sufficient cDNA generated to make a gene specific standard curve. This would relate absolute levels to Ct values and therefore gene copy number in the experimental samples could be estimated from the Ct values obtained.

Primers for real time PCR were arranged to generate an optimum product size of 80-120bp and should not be more than 150bp. Some of the primers designed for standard PCR were of a suitable size for use in qPCR but where this was not the case, primers were designed specifically for qPCR (**Table 4.1**).

Table 4.1: Table of Primers for Standard PCR and qPCR of Notch, Delta, Jagged, Hes and Hey.

Gene	Primers for PCR	Primers for qPCR
Notch 1 receptor	N1p7, N1p6R	
Notch 3 receptor	N3p1, N3p4R	
Delta like 1	DLL1p1, DLL1p2R	DLL1p7, DLL1p8R
Jagged 1	Jag1p11, Jag1p12R	
Jagged 2	Jag2p14, Jag2p11R	
Hes 1	Hes1p1, Hes1p2R	
Hes 5	Hes5p1, Hes5p2R	
Hes7	Hes7p1, Hes7p2R	
Hey1	Hey1p3, Hey1p4R	
Hey2	Hey2p3, Hey2p4R	
HeyL	HeyLp1, HeyLp2R	

Each gene was tested in triplicate using the same set of HaCaT cells to minimize variation in the results. To establish the expression level of each gene, qPCR results were analyzed using standard curve and CT values established for each gene.

4.2 Expression of Notch Receptors in HaCaT Cells

As HaCaT cells undergo calcium-induced terminal differentiation, many changes in gene expression occur and some of these involve notch-delta signalling. Thus, we initially wanted to investigate which notch receptors were present in HaCaT cells and if they altered expression during a calcium shift experiment. Thus, were notch receptor levels of expression different in proliferating and differentiating HaCaT cells. Expression levels measured by standard PCR were not accurate and before we could proceed with qPCR, a functional primer pair had to be designed and tested to generate a notch receptor specific cDNA probe that could be cloned and used to make a qPCR standard curve.

However, as the optimum size of primers for standard PCR were generally larger (300-600 bp) than those used for qPCR (150bp or less), in some cases it was necessary to make at least two sets of primers. All of the primers were

designed by my supervisor (Dr. P.E. Bowden, Cardiff University) and those for amplifying the notch 1 and notch 3 gene fragments are shown below (**Table 4.2**).

Table 4.2: Sequence of Notch Primers. All oligonucleotide primers were designed by Dr. P.E. Bowden (Dermatology Dept, Cardiff University) and supplied by Sigma-Aldrich Company Ltd (Poole, UK). Reverse primers were designated 'R'.

Primer Name	Primer Sequence
Notch 1 (N1p7)	[5'- ACC TTC CGC ACG CGG ATT AAT TTG -3']
Notch 1 (N1p6R)	[5'- TGC ACT CTT GGC ATA CAC ACT CCG -3']
Notch 3 (N3p1)	[5'- TTA CCT GGC AGT CCC AGG ACA TGG -3']
Notch 3 (N3p4R)	[5'- TAA GGG TGC TCA CTG GGA ACC CGC -3']

Notch 1 and notch 3 expression were investigated in HaCaT cells during proliferation (1-6 days in low Ca²⁺ KGM) and terminal differentiation (1-10 days after shift to high Ca²⁺ KGM). Total RNA was extracted from the relevant HaCaT cells and cDNA prepared by reverse transcription (see **Chapter 2** for details). The PCR reactions were prepared in ice-cold tubes and Taq polymerase was added last. Samples were run at an optimal annealing temperature for the oligonucleotide pairs chosen (60°C in this case) and run for 35 cycles. The PCR products were analysed by flat bed electrophoresis using a combination gel (3% NuSieve and 1% agarose) for better resolution of smaller fragments of DNA. The gel was run for about 45 minutes (conditions

summarized in **Table 4.3**) and the DNA was visualised under UV light (gel contained ethidium bromide).

Table 4.3: Agarose Gel Electrophoresis for PCR Products.

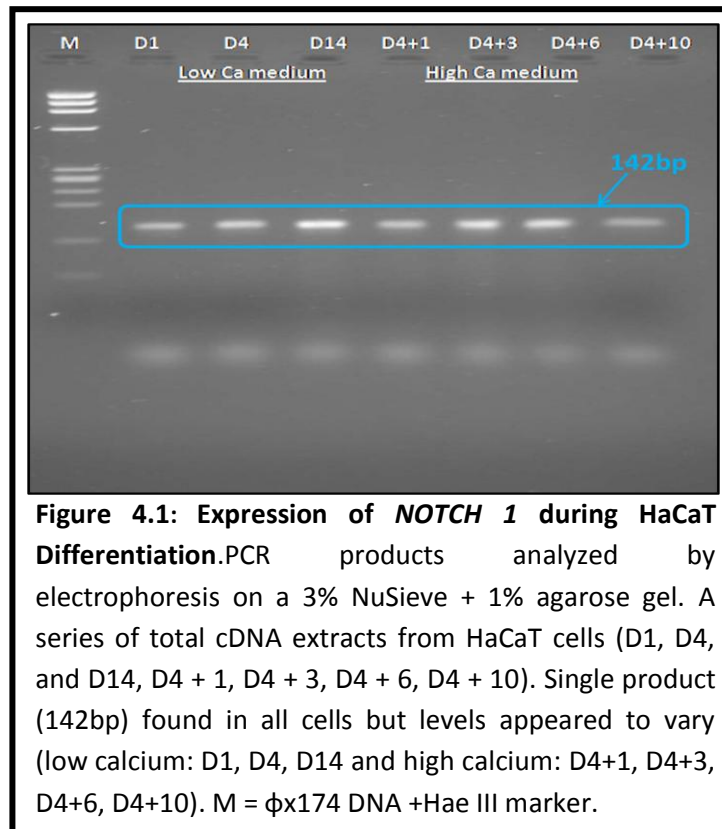
Experimental conditions for analysis of PCR products generated with Notch 1 and Notch 3 primer sets using agarose gel electrophoresis.

Experiment	Notch 1 & Notch 3
Gel Composition	3% NuSieve + 1% Agarose
Electrophoresis Buffer	Tris-Acetate-EDTA
Power pack Setting	90V (current 50mA)
Running Time	45 minutes
Sample Preparation	4 µl sample plus 1 µl glycerol/BPB mix
Marker Preparation	Low MW (ϕX174 + HaeIII)

Notch 1 amplicons (142 bp) showed strong bands across the whole gel, changing very little throughout the experiment (**Figure 4.1**). Thus, the levels appeared to be similar in proliferating HaCaT cells (low Ca²⁺ KGM) and differentiating HaCaT cells (high Ca²⁺ KGM). The amplicons were sequenced to confirm their identity as products of the notch 1 gene (**data not shown**).

In contrast, Notch 3 was expressed predominantly during cell differentiation (in all high Ca²⁺ cultures and at day 14 in low Ca²⁺ medium) and only weak expression was observed during cell proliferation in early low calcium cultures

(see **Figure 4.2**). The PCR products were confirmed as notch 3 by sequencing. However, in different sets of HaCaT cell cultures, the results were variable and it was difficult to get a consistent expression of Notch 1 and 3. This was explained, at that time, due to the low level of expression therefore difficult to detect.



It is important to point out that PCR conditions for notch 1 and 3 were not fully optimized at this stage for use in RT-qPCR. However, since notch 1 and 3 primers gave a product of the correct size, it was only necessary to optimize the conditions for qPCR.

In order to clone the notch inserts generated for use as a qPCR standard, the optimum PCR was chosen for each notch reaction. The Notch 1 amplicon (142 bp) was strongest in Day 14 cultures in low calcium medium (**Figure 4.1**) and the Notch 3 amplicon (102 bp) was strongest in day 4+6 cultures in high calcium medium (**Figure 4.2**).

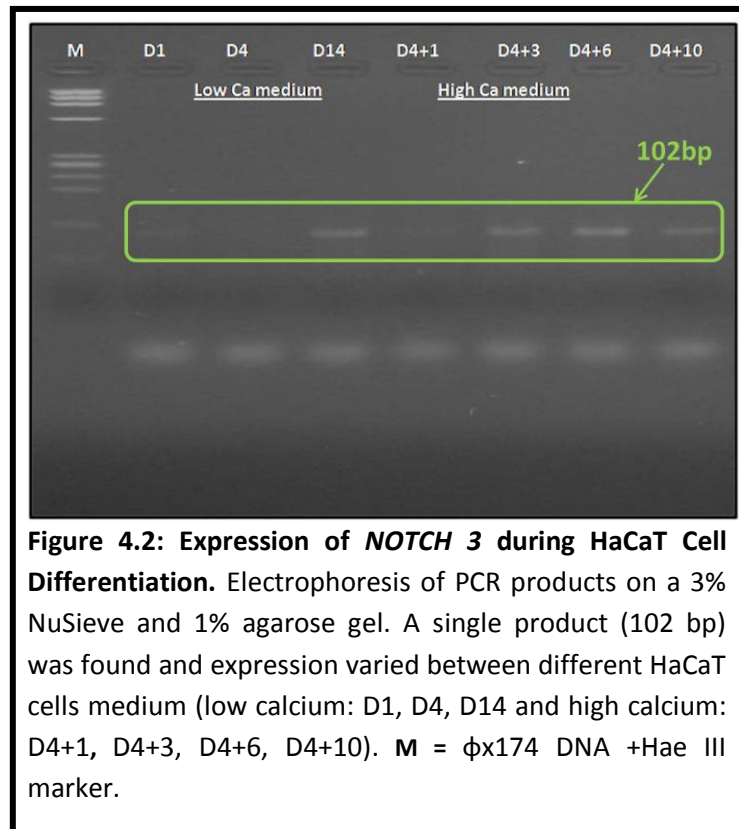


Figure 4.2: Expression of *NOTCH 3* during HaCaT Cell Differentiation. Electrophoresis of PCR products on a 3% NuSieve and 1% agarose gel. A single product (102 bp) was found and expression varied between different HaCaT cells medium (low calcium: D1, D4, D14 and high calcium: D4+1, D4+3, D4+6, D4+10). **M** = ϕ x174 DNA +Hae III marker.

These observations were considered as optimum levels and chosen as the starting point for cloning the Notch 1 and Notch 3 specific PCR products for use as qPCR standards. Both were run on the same gel to obtain a direct comparison of the size of each amplicon (**Figure 4.3**). This was followed by sequencing the products using standard automated sequencing protocols.

Once the sequence was confirmed, the Notch 1 and Notch 3 PCR products were cloned into pGEM-T easy vectors (see **Chapter 2** cloning procedure).

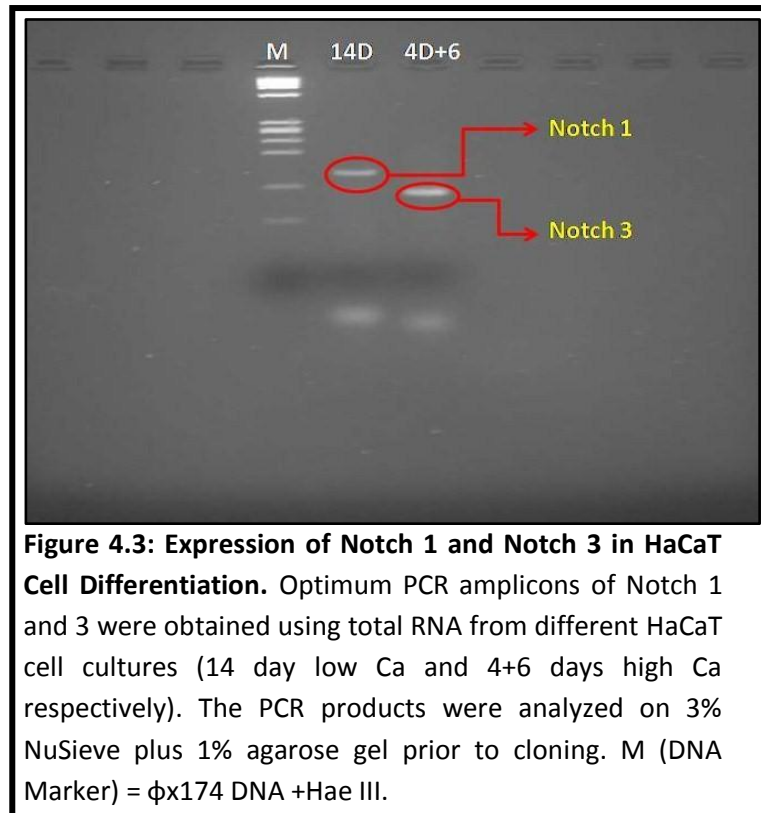


Figure 4.3: Expression of Notch 1 and Notch 3 in HaCaT Cell Differentiation. Optimum PCR amplicons of Notch 1 and 3 were obtained using total RNA from different HaCaT cell cultures (14 day low Ca and 4+6 days high Ca respectively). The PCR products were analyzed on 3% NuSieve plus 1% agarose gel prior to cloning. M (DNA Marker) = ϕ x174 DNA +Hae III.

PCR fragments were cleaned prior to ligation into the bacterial plasmid (pGEM-T easy vector system). Once the PCR fragments have been inserted into the plasmids, these are inserted into bacteria by transformation and the clones generated examined. The best clones were then selected and grown in bulk. The plasmids from each clone were extracted using a Qiagen plasmid miniprep kit and the inserts (Notch 1 or Notch 3) were released from the vector by restriction enzyme digestion (Eco RI) and then analysed by electrophoresis on 1.5% agarose gels (**Figures 4.4 and 4.5**). To ensure that

inserts did represent the gene of interest, they were all sequenced and checked against the human genome database (**data not shown**).



Figure 4.4: Analysis of *Notch 1* Plasmid Digests by Gel Electrophoresis. Cloned *Notch 1* plasmids (Plas 1-6) were digested with EcoRI and run on a 1.5% agarose gel. The pGEM-T easy vector is the larger band (3015 bp) and the lower band (142 bp) is the *Notch 1* insert. M: DNA Marker = 100 bp Ladder. Plasmid 1, 3, 4, 5 contained inserts of the correct size and their identity was confirmed by sequencing.

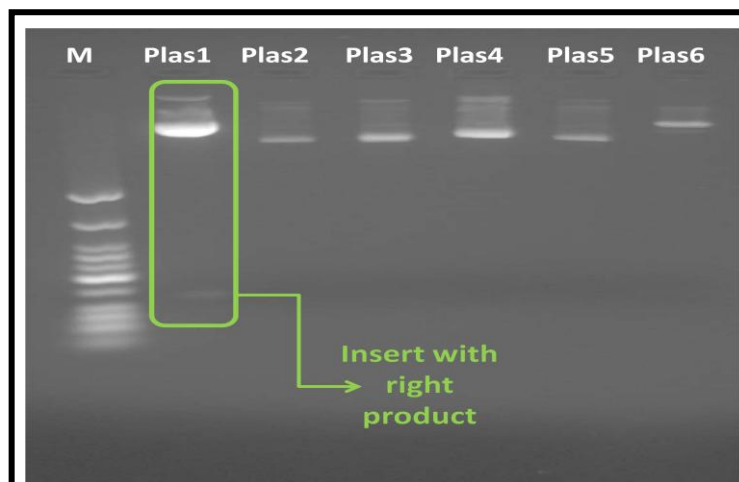


Figure 4.5: Analysis of *Notch 3* Plasmid Digests by Gel Electrophoresis. Cloned *Notch 3* plasmids (Plas 1-6) were digested with EcoRI and run on a 1.5% agarose gel. The pGEM-T easy vector is the larger band (3015 bp) and the smaller band (102 bp) is the *Notch 3* insert. Only Plas1 had an insert of the correct size and the identity was confirmed by sequencing. M: DNA Marker (100 bp Ladder, NEB). Plasmids 2-6 showed incomplete digestion of the vector and no product was released.

Once the inserts had been confirmed by sequencing, then stocks of three isolated plasmids for each PCR generated insert were stored at -80°C . Sufficient amounts of plasmid could then be generated to make serial dilutions of each gene probe of interest. Serial dilutions were calculated based on the combined size (bp) of the pGEM-T vector and the PCR generated insert. The equations were based on the average mass of a single base pair ($1.096\text{e-}21$ g) derived from the dividing the gram molecular weight of 1 bp (660 g) by Avogadro's number ($6.023\text{E}23$), the number of molecules per mole (see **Chapter 2** for details).

Serial dilutions of the appropriate Notch 1 (N1plas3) and Notch 3 (N3plas1) plasmid DNA were made for the qPCR experiments. The concentration of stock N1plas3 DNA was determined by spectrophotometric analysis (580 ng/ μl or $5.8\text{e-}7$ g/ μl). Initially, this stock was diluted serially (three times by 1 in 100) to a more manageable 1 in 10^6 (concentration $5.8\text{e-}13$ g/ μl). The mass (m) of a single plasmid molecule (vector plus insert) was calculated from the size ($3,015$ bp + 142 bp), so that $n = 3,157$ bp and $m = 3157 \times 1.096\text{e-}21$ g, a value of $3.46\text{e-}18$ g. The calculated mass of a single molecule of N1plas3 ($3.46\text{e-}18$ g) was then used to determine the mass equivalent of 300,000 copies ($1.038\text{e-}12$ g) which is equivalent to a concentration of $2.076\text{e-}13$ g/ μl in a 5 μl aliquot (as used for the PCR reaction). The stock plasmid was $5.8\text{e-}13$

g/μl so the dilution required to contain 300,000 copies in 500 μl was calculated as 179μl of stock N1plas3 diluted with 321 μl of sterile water. This 300,000 copy number stock can then be used to make a serial dilution series (1:10) to generate working solutions that contain 30,000, 3,000, 300 and 30 copies in 5 μl (**Table 4.4**).

Table 4.4: Dilution Series for N1plas3 Stock. Sterile nuclease free water was used as the diluent and dilutions 4-8 were used for qPCR.

Dilution	Source of plasmid DNA for dilution	Initial Conc. (g/μl) C ₁	Volume of Plasmid DNA (μl) V ₁	Volume of Diluent (μl)	Final Vol (μl) V ₂	Final Conc (g/μl) C ₂	Copy #
1	Stock	5.8e-7	10μl	990μl	1000μl	5.8e-9	N/A
2	Dilution1	5.8e-9	10μl	990μl	1000μl	5.8e-11	N/A
3	Dilution2	5.8e-11	10μl	990μl	1000μl	5.8e-13	N/A
4	Dilution3	5.8e-13	179	321	500μl	2.076e-13	300,000
5	Dilution4	2.076e-13	10μl	90μl	100μl	2.076e-14	30,000
6	Dilution5	2.076e-14	10μl	90μl	100μl	2.076e-15	3000
7	Dilution6	2.076e-15	10μl	90μl	100μl	2.076e-16	300
8	Dilution7	2.076e-16	10μl	90μl	100μl	2.076e-17	30

The same calculations were repeated for the Notch 3 plasmid (N3plas1). The N3plas1 DNA stock had a concentration of 500 ng/μl (5e-7 g/μl) and this was also diluted 1 in 10⁶ (5e-13 g/μl). The insert was 102 bp so the mass of a single molecule of plasmid was calculated as before (3.416e-18 g). The mass equivalent of 300,000 copies would be 1.0248e-12 g and the concentration of plasmid required in a 5 μl aliquot would 2.0496e-13 g/μl. Thus, the dilution required to make 500 μl of a standard stock solution containing 300,000 copies of plasmid would be 205 μl of stock diluted with 295 μl sterile water. Again, this solution can then be diluted 1:10 to make a set of working serial dilutions (**Table 4.5**).

Table 4.5: Dilution Series for N3plas1 Stock. Sterile nuclease free H₂O was used as the diluent and dilutions 4-8 used for qPCR.

Dilution	Plasmid DNA Dilutions	Initial Conc. (g/μl) C ₁	Plasmid DNA Volume (μl) V ₁	Volume of Diluent added (μl)	Final Vol. (μl) V ₂	Final Conc. (g/μl) C ₂	Copy #
1	Stock	5e-7	10μl	990μl	1000μl	5e-9	N/A
2	Dilution 1	5e-9	10μl	990μl	1000μl	5e-11	N/A
3	Dilution 2	5e-11	10μl	990μl	1000μl	5e-13	N/A
4	Dilution 3	5e-13	205	295	500μl	2.049e-13	300,000
5	Dilution 4	2.0497e-13	50μl	450μl	500μl	2.049e-14	30,000
6	Dilution 5	2.0497e-14	50μl	450μl	500μl	2.049e-15	3000
7	Dilution 6	2.0497e-15	50μl	450μl	500μl	2.049e-16	300
8	Dilution 7	2.0497e-16	50μl	450μl	500μl	2.049e-17	30

Initially, an aliquot of each diluted plasmid was run in a standard PCR reaction and analyzed on a high resolution gel (3% NuSieve and 1% agarose). The Notch 3 dilution series was analysed as an example (**Figure 4.6**) but only the high copy number standards resulted in a clearly visible product and the amplicons progressively disappeared as the starting material was serially diluted.



Figure 4.6: PCR Reactions with Serial Dilutions of Notch 3 Plasmid 1 (N3plas1). Reactions were analysed on a 3% NuSieve plus 1% agarose gel. The Notch 3 amplicon is 102 bp (yellow arrows) and this represents a dilution series from 300,000 copies to 30 copies as starting material. M (Marker) = ϕ x174 DNA +Hae III.

These standardised serial dilutions of cloned Notch 1 and Notch 3 PCR fragments were analysed by qPCR and a standard curve constructed from the data using MxPro software (MX3000P Real Time PCR Machine). The Notch 3 data was reasonable and the individual amplification plots from the separate wells containing different levels of cloned Notch 3 plasmid (300,000 to 30 copies) all showed a good sigmoid curve and all attained a plateau of approximately equal height (**Figure 4.7**). Also, the different dilutions gave equally spaced plots providing Ct values about 4 cycles apart. When plotted as a standard curve (**Figure 4.8**), the N3plas1 data showed an efficiency value of 101.8 % (reproducible over the triplicate repeats).

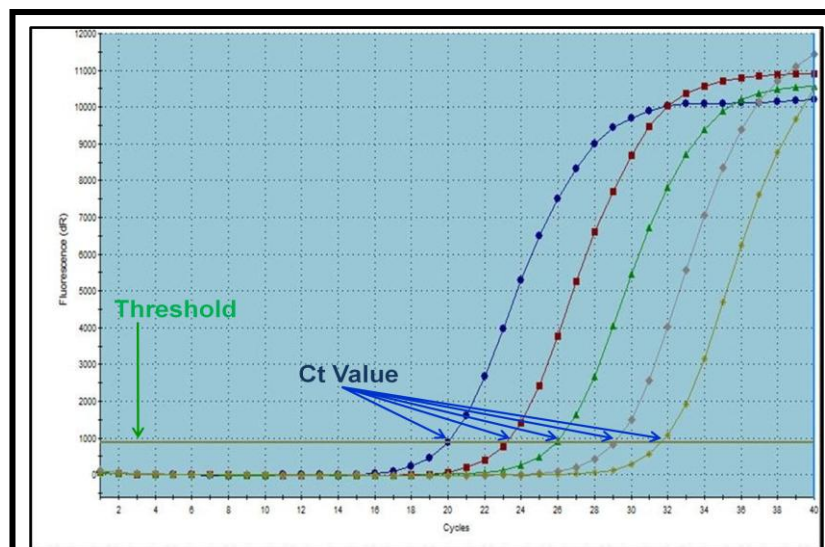
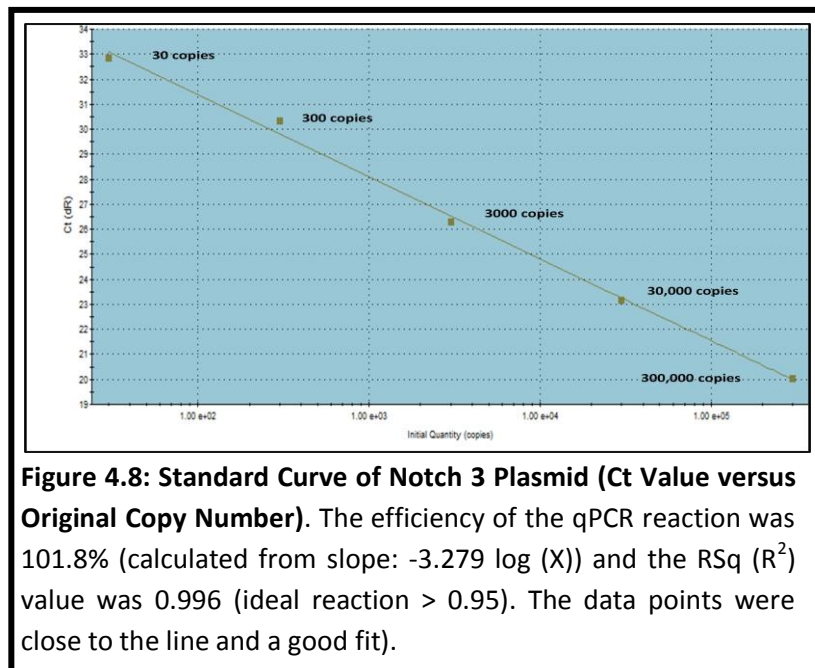


Figure 4.7: Amplification Plot of Notch 3 Plasmid Serial Dilutions.

Fluorescence data from MxPro software showing the amplification from different starting levels of Notch 3 plasmid in different colours: Blue represents 300,000 copies, red (30,000 copies), green (3,000 copies), grey (300 copies) and yellow (30 copies). A constant distance (4 cycles) between each fluorescence amplification plot indicated a good serial dilution.



This data showed a good relationship between the starting copy number in the serial dilutions and the fluorescence obtained in qPCR. This was then used to calculate the relative copy number in unknown experimental samples from the Ct values obtained. The standard curve for Notch 1 was similar (data not shown).

A series of qRT-PCR experiments were run using mRNA extracted from HaCaT cultures grown under different conditions for different lengths of time (see **Chapter 2** for details). These were run together with a standard dilution series of cloned Notch 1 or 3 plasmids of known copy number. Experiments were conducted in triplicate and different sets of HaCaT cultures used as the level of differentiation in any given culture was variable. The data were analysed

with MxPro software and different statistical packages (including Tukey-Kramer Multiple Comparison Test and One-way Analysis of Variance or ANOVA).

Overall, Notch 1 was expressed at a constant level in keratinocyte cultures and there were no significant differences between levels during cell proliferation and terminal differentiation. Thus, few changes in Notch 1 expression were detected during calcium-induced HaCaT cell differentiation in culture. This broadly agreed with early results obtained by standard PCR and protein chemistry (Paul E. Bowden, unpublished data). However, previous experiments using Notch 1 antibodies (for immunofluorescence and western blotting) produced variable results and consistently poor data, probably due to low levels of expression and the fact that only poor antibodies were available. Thus, we concluded that there were few changes in Notch 1 levels of expression during keratinocyte differentiation in HaCaT cultures.

However, the data for Notch 3 did show some alterations during the culture period. The qPCR experimental data was analyzed by INSTAT software in two different ways. The level of expression was initially calculated in relation to copy number and then any alterations in expression level were calculated as fold change relative to the starting point (day 3 culture). This produced

different levels of significance in the data but the trend remained the same (Tables 4.6 to 4.8).

The copy number varied between the different experiments but the data was reasonable between triplicates done within a single experiment (data not shown). In general, Notch 3 levels increased as calcium-induced differentiation proceeded with levels being much higher after calcium shift (samples 6D+3, 6D+6 and 6D+10). While cultures left for 16 days in low calcium did show induced differentiation (due to contact inhibition), levels of Notch 3 were not as high as those seen in the presence of calcium (Table 4.6).

Table 4.6: Raw qPCR Data (Copy Number) for Notch 3 Gene Expression. Data obtained from qPCR experiments run four times and each samples was run in triplicate using same cDNA of HaCaT cells. Data expressed as copy number relative to the standard dilution series of cloned Notch 3 PCR product. Notch 3 levels generally rise with calcium-induced differentiation but the data was variable between different cultures.

Experiment	3D	6D	16D	6D+3	6D+6	6D+10
1	1,280	765	4,864	9,312	7,998	5,554
2	8,787	785	6,880	23,970	16,190	10,640
3	4,465	644	2,935	15,410	11,510	9,751
4	4,347	947	2,130	16,600	10,790	20,690
Average	4,719	785	4,202	16,323	11,622	11,659

The data was also expressed as fold change relative to day 3 (3D) cultures (Table 4.7) and Notch 3 levels varied from 1.21 to 7.28 fold higher in differentiating cultures. However, this did vary from culture to culture.

Table 4.7: Raw qPCR Data for Notch 3 Gene Expression.

Data obtained from qPCR experiments run four times (each qPCR sample in triplicate using cDNA of HaCaT cells). Fold change of Notch 3 expression levels during calcium-induced differentiation of HaCaT cell cultures. All data is relative to the expression level at day 3 in low calcium (3D).

Experiment	3D	6D	16D	6D+3	6D+6	6D+10
1	1.00	0.60	3.8	7.28	6.25	4.34
2	1.00	0.09	0.78	2.73	1.84	1.21
3	1.00	0.14	0.66	3.45	2.58	2.18
4	1.00	0.22	0.49	3.84	2.48	4.76
Average	1.00	0.26	1.43	4.33	3.29	3.12

The raw copy number data of all four experiments shown in **Table 4.6** was analysed statistically using the Tukey-Kramer Multiple Comparison Test and a comparison done between day 3 (low Ca^{2+}) cultures (3D) and cultures at all other time points (6D, 16D, 6D+3, 6D+6 and 6D+10), as well as some other additional comparisons were made (**Table 4.8**). The increase in Notch 3 expression was highly significant ($p < 0.001$) when comparing 6D (6 days in low Ca^{2+}) to 6D+3 (3 days after switch to high Ca^{2+}). The data was less significant when comparing Notch 3 levels in day 3 or day 16 low calcium cultures compared to any cells in high Ca^{2+} (6D+3, +6, +10). This suggested that Notch 3 levels were initially high, decreased as cells proliferated and then increased again as cells terminally differentiated (**Table 4.8**). The derived fold change data was also analysed using the Tukey-Kramer Multiple Comparison Test. Changes in Notch 3 expression were even less significant (**Table 4.9**) and in fact, only the comparison between 6D and 6D+3 gave a significant change (4 fold, $p > 0.05$).

This data was then plotted as a bar chart to summarize changes in Notch 3 levels that occurred during the HaCaT cell culture experiments (**Figures 4.9 and 4.10**).

Table 4.8: Statistical Comparison of Notch 3 Levels (Copy Number) at Different Stages of HaCaT Culture. Values of Q > 4.495 are significant (p < 0.05, coloured in red) and asterisks designate significance level.

Comparison	Mean Difference	Q	P value
3D vs 6D	3934.5	1.899	ns P>0.05
3D vs 16D	517.50	0.2498	ns P>0.05
3D vs 6D+3	-11623	5.611	** P<0.01
3D vs 6D+6	-6902.3	3.332	ns P>0.05
3D vs 6D+10	-6939.0	3.350	ns P>0.05
6D vs 16D	-3417.0	1.650	ns P>0.05
6D vs 6D+3	-15558	7.511	*** P<0.001
6D vs 6D+6	-10837	5.232	* P<0.05
6D vs 6D+10	-10874	5.249	* P<0.05
16D vs 6D+3	-12141	5.861	** P<0.01
16D vs 6D+6	-7419.8	3.582	ns P>0.05
16D vs 6D+10	-7456.5	3.600	ns P>0.05
6D+3 vs 6D+6	4721.0	2.279	ns P>0.05
6D+3 vs 6D+10	4684.3	2.261	ns P>0.05
6D+6 vs 6D+10	-36.750	0.01774	ns P>0.05

Table 4.9: Statistical Comparison of Notch 3 Levels at Different Stages of HaCaT Culture (Fold Change). Values of Q > 4.495 are significant (p < 0.05, coloured in red).

Comparison	Mean Difference	Q	P value
3D vs 6D	0.7375	0.9811	ns P>0.05
3D vs 16D	-0.4325	0.5753	ns P>0.05
3D vs 6D+3	-3.325	4.423	ns P>0.05
3D vs 6D+6	-2.288	3.043	ns P>0.05
3D vs 6D+10	-2.122	2.823	ns P>0.05
6D vs 16D	-1.170	1.556	ns P>0.05
6D vs 6D+3	-4.062	5.404	* P<0.05
6D vs 6D+6	-3.025	4.024	ns P>0.05
6D vs 6D+10	-2.860	3.805	ns P>0.05
16D vs 6D+3	-2.893	3.848	ns P>0.05
16D vs 6D+6	-1.855	2.468	ns P>0.05
16D vs 6D+10	-1.690	2.248	ns P>0.05
6D+3 vs 6D+6	1.037	1.380	ns P>0.05
6D+3 vs 6D+10	1.203	1.600	ns P>0.05
6D+6 vs 6D+10	0.1650	0.2195	ns P>0.05

Initially, the levels of Notch 3 decreased as the cultures proliferated and expanded. However, even in the absence of calcium, levels of Notch 3 returned to day 3 levels in 16 day cultures that were confluent, stratified but disorganised. Levels were significantly higher in all cells that had differentiated in the presence of high calcium levels, cultures that showed a much higher level of cellular organisation.

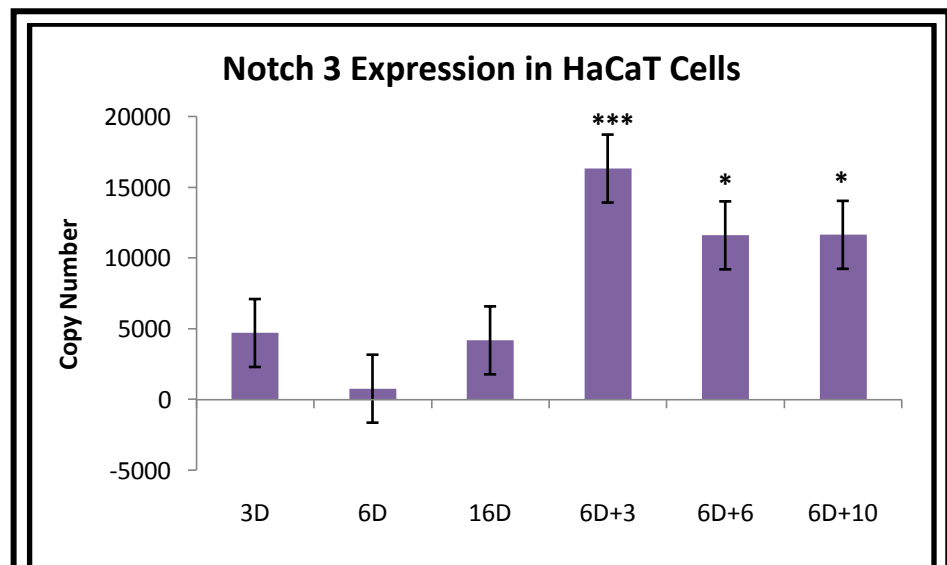


Figure 4.9: Notch 3 Expression (Transcript Copy Number) in HaCaT Cells during Calcium-induced Differentiation. No significant changes occurred in low calcium medium (3D, 6D, 16D) but significant increases were observed in differentiating cells (6D+3, 6D+6, 6D+10) especially at 3 days after introduction of high calcium (significance relative to 3D: * = $p < 0.05$ and *** = $p < 0.001$).

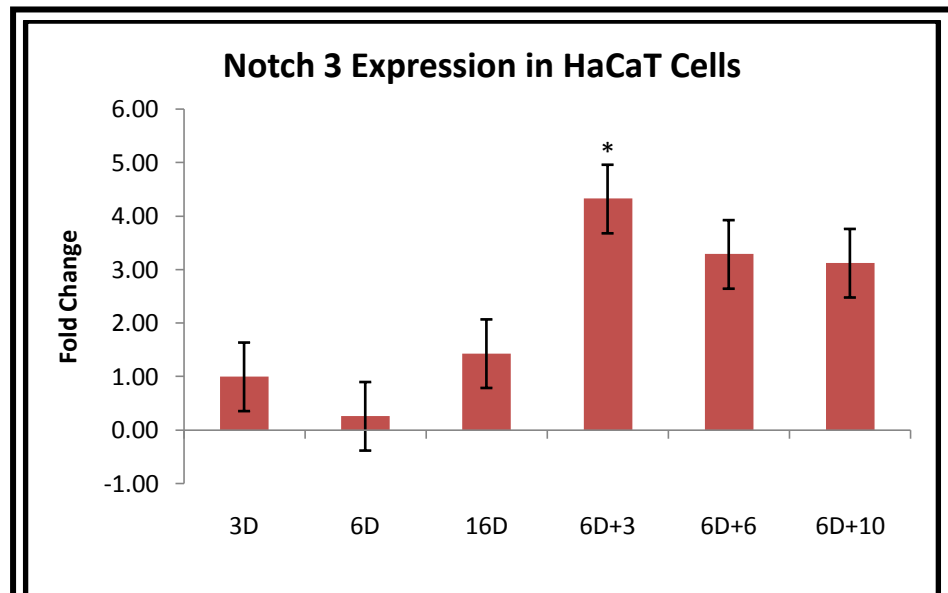


Figure 4.10: Notch 3 Expression (Fold Change) in HaCaT Cells during Calcium-induced Differentiation. No significant changes in copy number were detected in low calcium medium (3D, 6D, 16D) and the only significant increase observed in differentiating cells occurred 3 days after the switch to high calcium medium (* p<0.05).

4.3 Expression of Notch Ligands (DLL1, JAG1 and JAG2) in HaCaT Cells

The expression of three Notch ligands (DLL1, JAG1 and JAG2) was investigated in the HaCaT cell culture model. Cells were induced to differentiate with high calcium levels and the expression between proliferating cells and terminally differentiating cells compared using PCR and qPCR.

Initially, several DLL1 primers were designed and tested in the laboratory so that an optimum set could be developed (see **Table 4.10**). Several experiments were done to obtain PCR products from the different DLL1 primer pairs using both genomic DNA (gDNA) and cDNA obtained by reverse transcription of total RNA from the relevant HaCaT cell cultures. Standard PCRs with all primer pairs were run at 58°C (annealing temperature) and 35 cycles.

Table 4.10: Sequence of Delta 1 like (DLL1) Primers. Initially, three primer pairs were designed and synthesised (p1, p3 and p5 forward primers and p2R, p4R and p6R reverse primers). Product sizes were: 382 bp for p1+p2R, 267 bp for p3+p4R and 254 bp for p5+p6R.

Primers	Sequence
DLL1 p1	[5'- AGA CGG AGA CCA TGA ACA AC -3'] Exon 9
DLL1 p2R	[5'- TCC TCG GAT ATG ACG TAC AC -3'] Exon 10
DLL1 p3	[5'- GCC GCT GTT CTA AGG AGA GA -3'] Exon 1
DLL1 p4R	[5'- TGG CCT GGT AGT GCT TGA GG -3'] Exon 2
DLL1 p5	[5'- TAT CCG CTA TCC AGG CTG TC -3'] Exon 6
DLL1 p6R	[5'- CTC CCT CCG TTC TTA CAA GG -3'] Exon 7

Earlier work with two DLL1 primer pairs (p3, p4R and p5, p6R) on cDNA from proliferating HaCaT cells (D3 and D6) showed that two bands of different size were obtained with both primer sets while the K14 control primers gave a single band (**Figure 4.11**). All samples were sequenced and both products were from the correct region of DLL1. However, the upper band was amplified from gDNA and included intron sequences while the lower band was amplified from cDNA. This indicated that the total RNA preparations of HaCaT cells were

contaminated with some gDNA. However, the K14 control did not produce a gDNA band but a single band of the correct size for cDNA even though the primers were across an intron. The only possible explanation is that K14 mRNA (and therefore cDNA) was abundant in the samples and the cDNA binds the primers well, so there would be little chance of binding to gDNA. DLL1 primers on the other hand bind poorly to cDNA and levels were low so binding to gDNA was more likely.

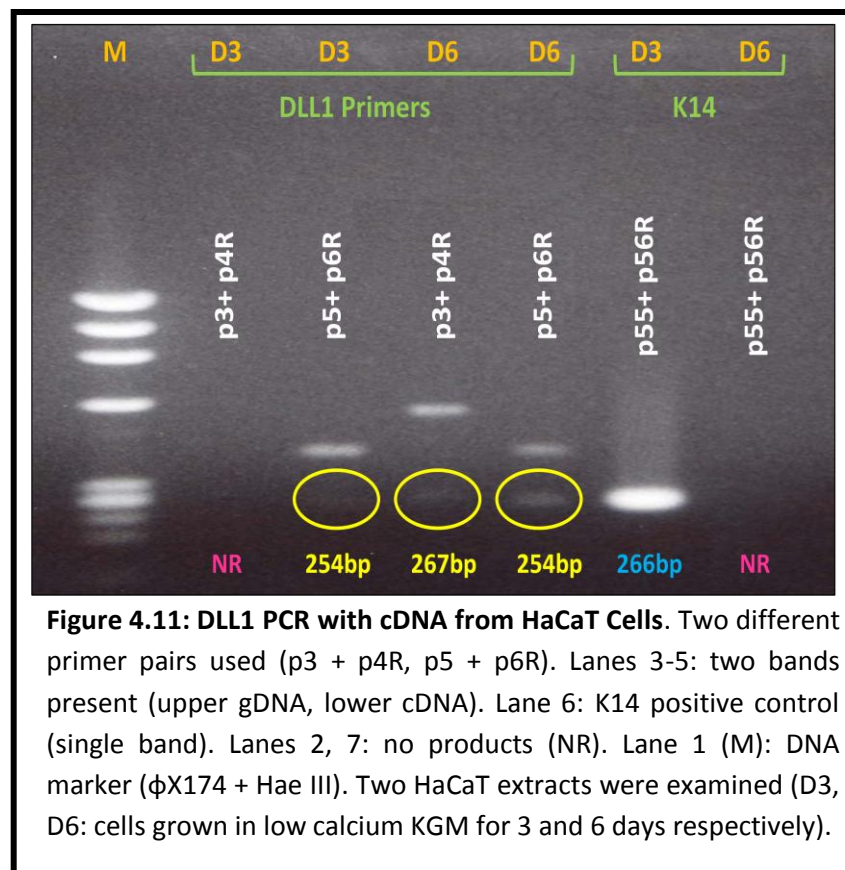


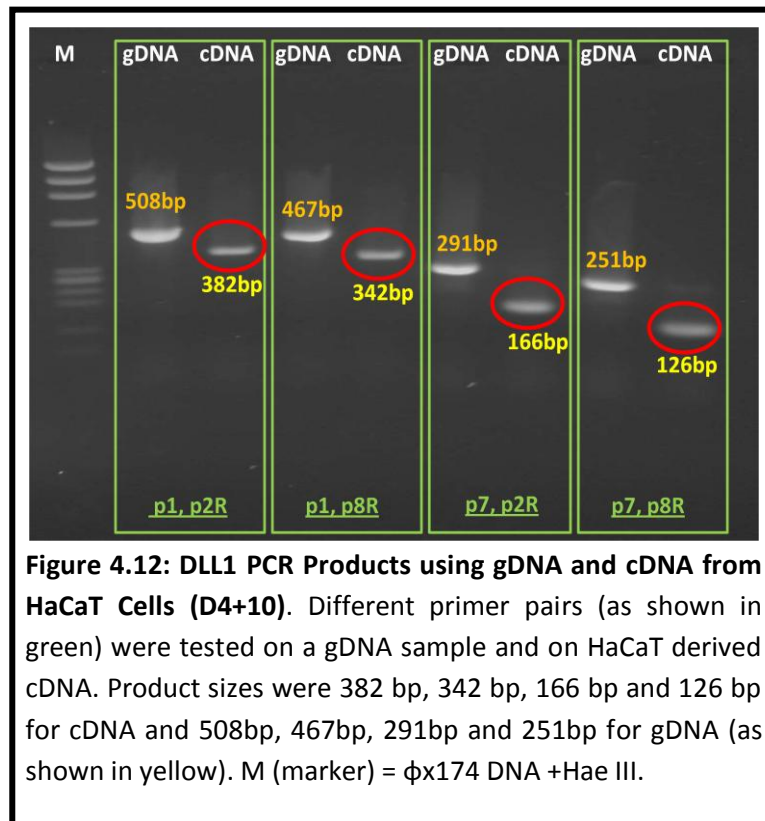
Figure 4.11: DLL1 PCR with cDNA from HaCaT Cells. Two different primer pairs used (p3 + p4R, p5 + p6R). Lanes 3-5: two bands present (upper gDNA, lower cDNA). Lane 6: K14 positive control (single band). Lanes 2, 7: no products (NR). Lane 1 (M): DNA marker (ϕ X174 + Hae III). Two HaCaT extracts were examined (D3, D6: cells grown in low calcium KGM for 3 and 6 days respectively).

These early total RNA extracts from HaCaT cells were discarded due to genomic DNA contamination and later extracts were treated with DNase to remove any genomic DNA. The stock RNA samples together with the derived cDNA samples were then quality tested by PCR with K14 primers before use (see **Chapter 3, Figures 3.6 & 3.7**).

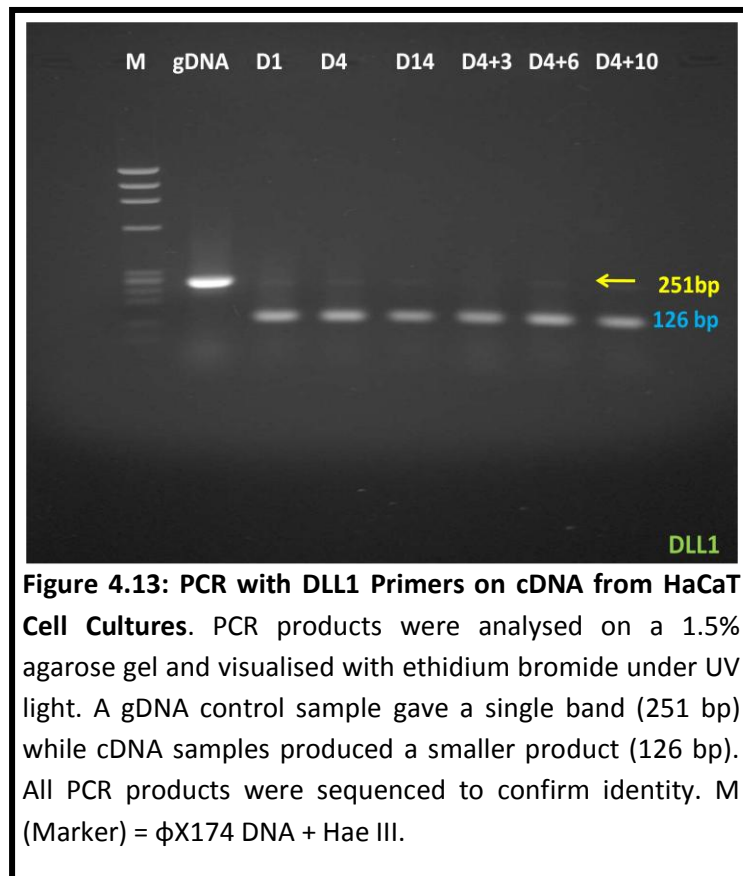
A second problem was that the sizes of standard PCR products were too big for qPCR, so another set of primers was made and tested (**Table 4.11**). Several combinations of DLL1 primers were tested using the new primers and the original primers (**Figure 4.12**) on a sample of cDNA from differentiating HaCaT cells (6D+10). Two combinations gave products that were still too large for qPCR (p1+p8R: 342 bp and p7+p2R: 166 bp) but p7 and p8R gave a single product (126 bp) ideal for qPCR. This experiment also included a sample of genomic DNA that produced a larger band in each case due to the presence of intervening introns. Generally, very little gDNA contamination was noted in the cDNA samples but a faint band could be seen with the new primer pair (p7, p8R).

Table 4.11: Delta 1 like (DLL1) Primer Sequences. DLL1p7 is a forward primer in exon 9 while DLL1p8R is a reverse primer in exon 10. The product size generated was 126bp (all primers designed by Dr. P.E Bowden, Cardiff University).

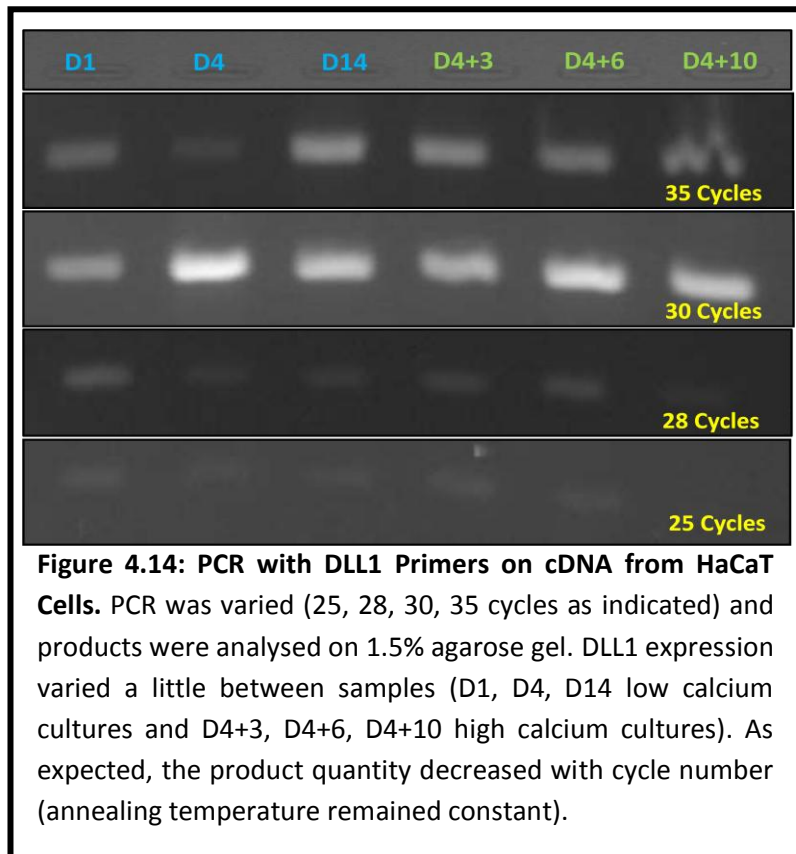
Primers	Sequence
DLL1 p7	[5'- ACA GCA AGC GTG ACA CCA AGT GCC -3'] Exon 9
DLL1 p8R	[5'- TTG AAG TTG AAC AGC CCG AGT CCG -3'] Exon 10



The new primer pair (DLL1p7, p8R) was then used for PCR with a full set of HaCaT cDNA samples, representing all stages of the culture model from proliferation to differentiation. A single sample of gDNA was also used as a control for genomic contamination. The PCR was run at 58°C (annealing) and 35 cycles after which the samples were analysed on a 1.5% agarose gel (**Figure 4.13**). DLL1 amplicons appeared to be uniform throughout the samples and little difference was observed between levels during proliferation (low calcium) and differentiation (high calcium). The cDNA product (126 bp) was predominant but low levels of a gDNA product (251 bp) were visible indicating a very low level of gDNA contamination.



The effect of altering the PCR cycle number (35, 30, 28 and 25 cycles) was then examined using the another DLL1 primer set (p1 and p2R: cDNA product size 382 bp). The expression was variable at all cycle levels tested and as expected the amount of total product faded as the cycle number reduced (**Figure 4.14**). This was repeated with the smaller primer set (p7, p8R) but unfortunately the products were too faint to see (**data not shown**).



Previous studies on DLL4 suggested that it was not expressed in human epidermis and a standard PCR was conducted to confirm this earlier observation. Several DLL4 primer pairs had been designed for earlier research projects in the department (**Table 4.12**) and one pair (DLL4p5 and p6R) was selected for the experiment.

Table 4.12: Sequence of Delta Like 4 (DLL4) Primers. Three sets of primers were made for DLL4 (p1 + p3R, p4 + p2R, p5 + p6R). The product sizes were 241bp, 257bp and 522bp respectively. All primers were designed by Dr. P.E. Bowden (Cardiff University) and synthesised by Sigma.

Primers	Sequence
DLL4 p1	[5'- TGA CCA CTT CGG CCA CTA TG -3'] Exon 4
DLL4 p3R	[5'- CAC AAG TAC ATT GCC AGG GAG TGC -3'] Exon 6
DLL4 p4	[5'- AAG CTA CAC CTG CAC CTG TCG -3'] Exon 7
DLL4 p2R	[5'- AGT TGG AGC CGG TGA AGT TG-3'] Exon 8
DLL4 p5	[5'- TAC ACC GAC CTC TCC ACA GAC ACC -3'] Exon 9
DLL4 p6R	[5'- ACA CAG ACT GGT ACA TGG AGT CCC -3'] Exon 10

DLL1 and DLL4 were only weakly expressed in human epidermis so in order to clone a strong PCR product, a good source of cDNA was sought. As DLL1 was strongly expressed in human pancreas, PCR reactions were done with DLL1 and DLL4 primer pairs on cDNA from both pancreas and human epidermis (pancreatic cDNA was purchased and epidermal cDNA made in the laboratory). The products were run on a 1.5% agarose gel together with a K14 control (**Figure 4.15**). The DLL1 product was the same size for both epidermal and pancreatic cDNA (382 bp) but the latter was cleaner. The products from the DLL4 PCR were not the same size, the epidermal product (230 bp) being smaller than the pancreatic product (522 bp).

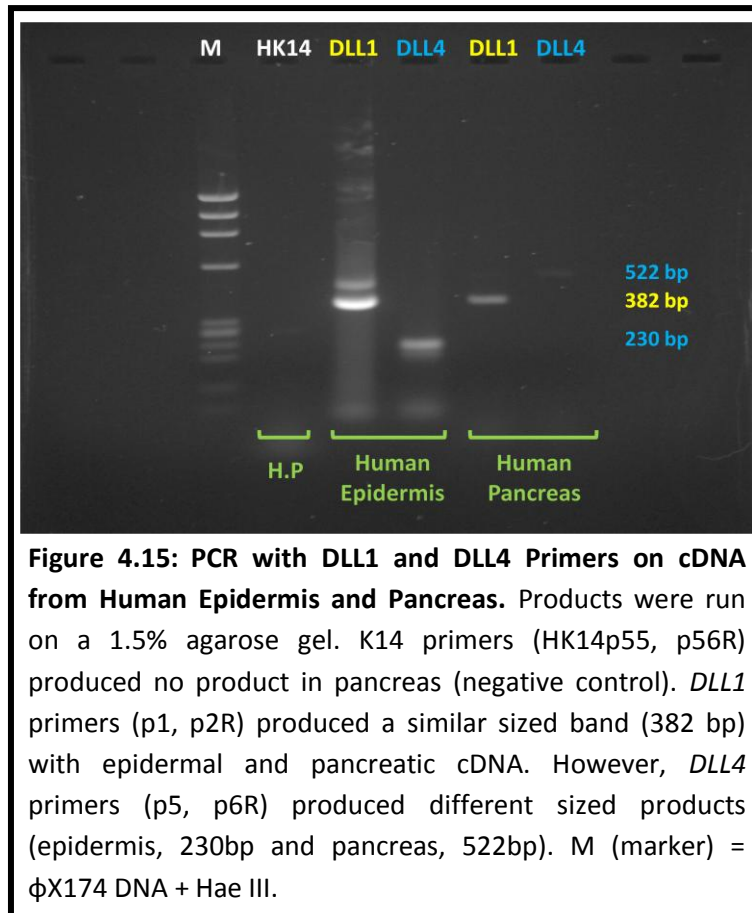
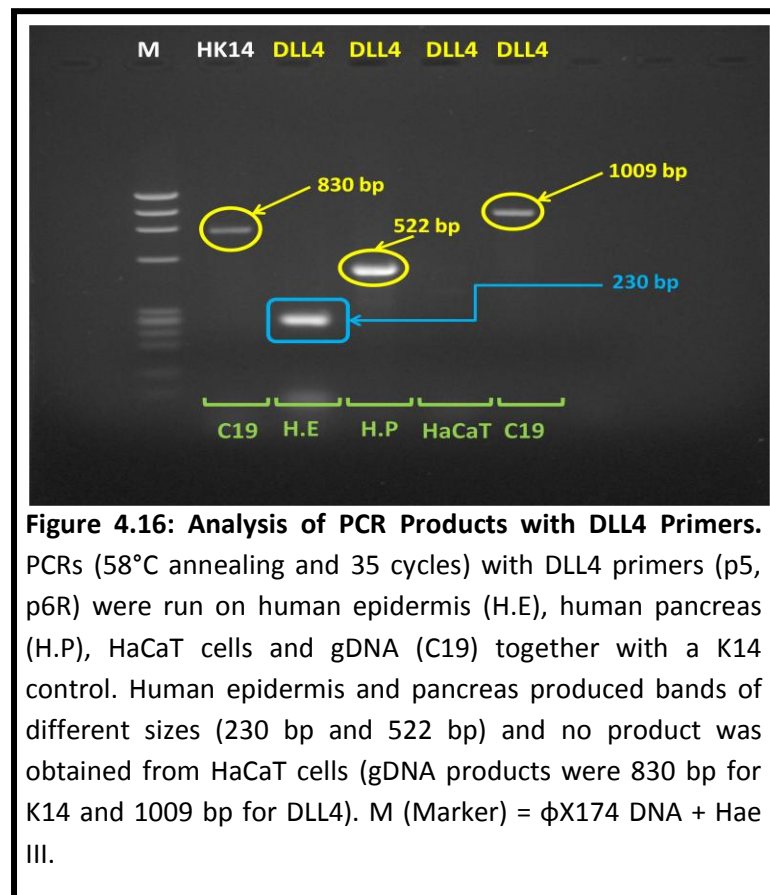


Figure 4.15: PCR with DLL1 and DLL4 Primers on cDNA from Human Epidermis and Pancreas. Products were run on a 1.5% agarose gel. K14 primers (HK14p55, p56R) produced no product in pancreas (negative control). *DLL1* primers (p1, p2R) produced a similar sized band (382 bp) with epidermal and pancreatic cDNA. However, *DLL4* primers (p5, p6R) produced different sized products (epidermis, 230bp and pancreas, 522bp). M (marker) = ϕ X174 DNA + Hae III.

All of the PCR products were sequenced and while *DLL1* products were correct, only the larger *DLL4* product from the pancreatic cDNA was correct. The smaller product from the epidermal cDNA was a partial sequence only. Thus, only the *DLL1* product was used to make a set of serial dilutions for qPCR. While *DLL4* was strongly expressed in human pancreas, little was found in human epidermis. The *DLL4* PCR was repeated with another sample of human epidermis and cDNA from HaCaT cells but again no bands were detected except in the pancreatic cDNA (**Figure 4.16**). This observation concurred with published research and other work in the laboratory (Dr. Paul

Bowden, unpublished data) that indicated that very little, if any, DLL4 was expressed in human epidermis. Thus, the investigations into DLL4 expression were halted.



A summary of all the data for DLL1 and DLL4 analysed by standard PCR showing expression in different samples such as human epidermis, human pancreas and HaCaT cell cultures is shown in **Table 4.13**. DLL1 was made the main focus for the research on HaCaT cell cultures and no further work was done with DLL4.

Table 4.13: Summary of *DLL1* and *DLL4* data experiments was conducted using standard PCR.

Primers	gDNA	Human Pancreas	Human Epidermis	HaCaT
DLL1 (p1, 2R)	Strong	Strong	Faint	Strong
DLL1 (p1, p8R)	Strong	?	?	Strong
DLL1 (p3, p4R)	Good	?	?	Good
DLL1 (p5, p6R)	Good	?	?	Good
DLL1 (p7, p2R)	Strong	?	?	Strong
DLL1 (p7, p8R)	Strong	?	?	Strong
DLL4 (p1, p3R)	Strong	Strong	?	No Band
DLL4 (p4, p2R)	Strong	Strong	?	No Band
DLL4 (p5, p6R)	Strong	Strong	Wrong size	No Band

The optimum DLL1 primer pair was used to generate a good PCR product for ligation into the pGEM-T easy vector and subsequent bacterial cloning. DLL1 PCR amplicons were sequenced to confirm their identity prior to use and then the inserts ligated into separate pGEM-T easy vectors (**see Chapter 2 for details of the methods**).

Once ligated into the pGEM-T easy vectors and cloned, the relevant bacterial clones were grown in batch culture and the plasmid carrying the vector and insert isolated. Six clones were selected for each insert and the plasmids extracted using a Qiagen mini plasmid kit (details in methods chapter). The DLL1 inserts were released from the pGEM-T easy vectors by digestion with Eco RI, and the products were run on a 1.5% agarose gel (**Figures 4.17**).

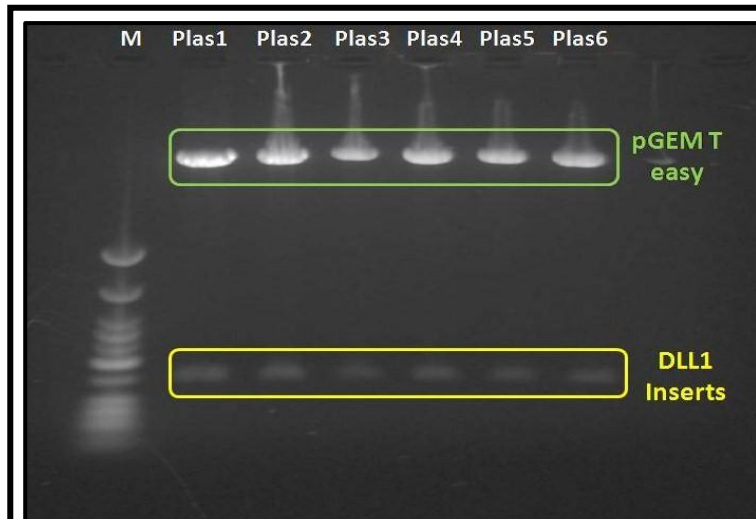


Figure 4.17: Gel Analysis of Cloned Plasmids cut with EcoRI to Release the pGEM-T vector and DLL1 Insert. The pGEM-T easy vector (3015bp, in green) lies at the top of the gel and the *DLL1* insert (126bp, in yellow) below. All plasmids (Plas1-6) were sequenced to confirm the presence of *DLL1* and one was selected to make a serial dilution series. M (marker) = low molecular weight mix.

The concentration of stock *DLL1* plasmid DNA (0.4 ng/ μ l) was determined by spectrophotometric analysis. The standard dilution series was made as before (see **Chapter 2** for details). Initially, the mass (m) of a single plasmid was calculated (depends on size of vector plus insert in bp). This was $3.44e-18$ g for the *DLL1* stock plasmid. The mass of 300,000 copies of the plasmid can then be calculated ($1.032e-12$) and the concentration of plasmid required determined ($2.1e-13$ g/ μ l). This allows calculation of the dilution required to make a total of 100 μ l at 300,000 copies per 5 μ l (add 45.65 μ l stock to 54.35 μ l sterile water). From the initial accurate plasmid dilution, a series can be generated by diluting the 300,000 copy stock serially by 1:10 (see **Table 4.14**).

Table 4.14: Dilution Series for DLL1 Cloned PCR Product. The stock plasmid (0.4 ng/ μ l) was diluted to 1 in 10^6 initially and this was diluted to 300,000 copies per 5 μ l. A 1 in 10 series dilution was then made and dilutions 4 to 8 were used for qPCR experiments (sterile nuclease free water was used as the diluent).

Dilution	Source of Plasmid DNA	Initial Conc (g/ μ l) C_1	Volume of Plasmid DNA (μ l) V_1	Volume of Diluent (μ l)	Final Vol (μ l) V_2	Final Conc (g/ μ l) C_2	Resulting Copy # per 5 μ l
1	Stock	4.6e-7	10 μ l	990 μ l	1000 μ l	4.6e-9	N/A
2	Dilution 1	4.6e-9	10 μ l	990 μ l	1000 μ l	4.6e-11	N/A
3	Dilution 2	4.6e-11	10 μ l	990 μ l	1000 μ l	4.6e-13	N/A
4	Dilution 3	4.6e-13	45.65 μ l	54.35 μ l	100 μ l	2.1e-13	300,000
5	Dilution 4	2.1e-13	10 μ l	90 μ l	100 μ l	2.1e-14	30,000
6	Dilution 5	2.1e-14	10 μ l	90 μ l	100 μ l	2.1e-15	3000
7	Dilution 6	2.1e-15	10 μ l	90 μ l	100 μ l	2.1e-16	300
8	Dilution 7	2.1e-16	10 μ l	90 μ l	100 μ l	2.1e-17	30

The amplification plot from the qPCR of the dilution series of DLL1 plasmids showed well spaced fluorescence curves and Ct values of 18 - 32 cycles (**Figure 4.18**).

The standard curve that was generated from this qPCR data was a reasonable straight line fit with an efficiency of 100.6% and an Rsq (R^2) value of 0.990 (**Figure 4.19**).

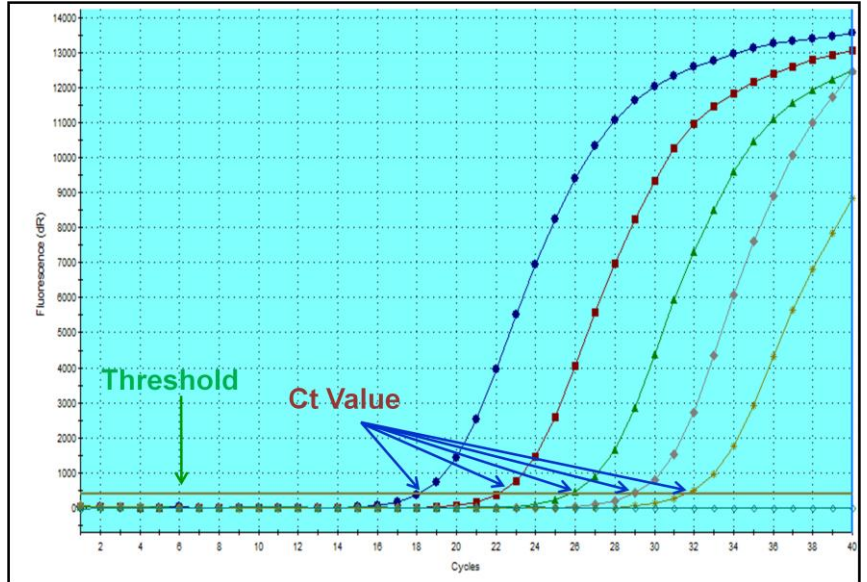


Figure 4.18: Amplification Plot of *DLL1* Plasmid Serial Dilutions. Data calculated by MxPro Software. Each fluorescence curve represents a different *DLL1* copy number (blue line: fluorescence with 300,000 copies; red: 30,000; green: 3,000; grey: 300 and yellow: 30). The distance between each fluorescence amplification plot was constant (about 4 cycles starting at 18 cycles) indicating the PCR reaction was efficient. Ct values represent the cycles at which the fluorescence crosses the threshold (each point average of 3 measurements).

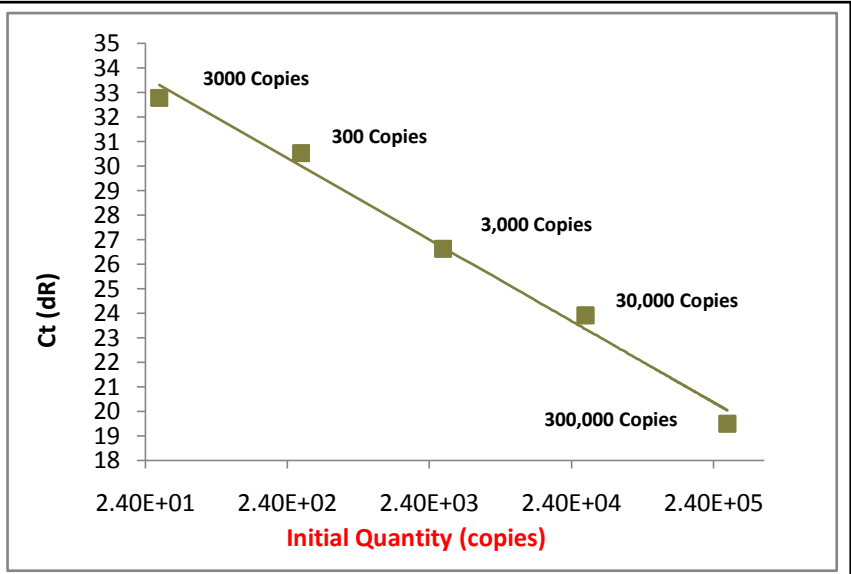
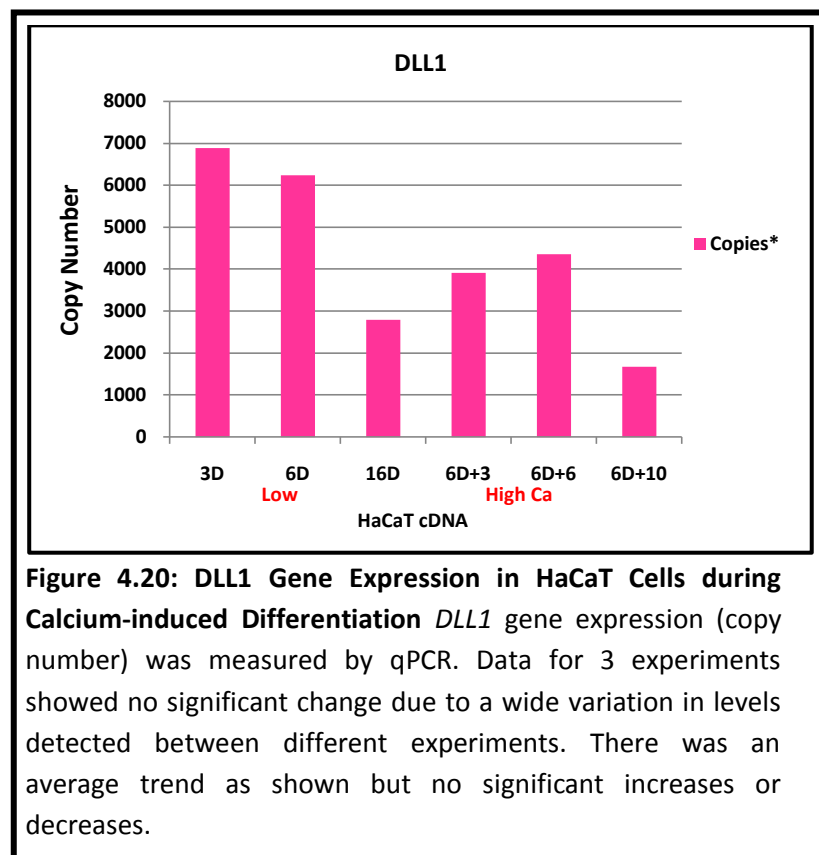


Figure 4.19: Standard Curve of *DLL1* Plasmid Dilution Series. Ct values plotted against copy number and efficiency of PCR reaction estimated as 100.6% (calculated from slope: $-3.308 \log X$). R^2 value was 0.990 indicating data was close to linear. Note scale on x-axis does not signify copy number (y-axis) data but an arithmetic range.

The DLL1 plasmid dilution series was then used to estimate copy number levels of DLL1 in various stages of HaCaT cell culture. The qPCR data showed that DLL1 levels were low, variable from culture to culture and that no significant alterations were found between proliferating cells and those that were undergoing terminal differentiation. This was true for the copy number data (**Figure 4.20**) and the data expressed as fold change (**Figure 4.21**).



Therefore, in conclusion, DLL1 expression levels were low and while some changes appeared to take place during HaCaT keratinocyte proliferation or differentiation, none of these were statistically significant. This was probably

due to the low transcript levels and variable results between different culture experiments. Expression of DLL1 at the protein level using western blotting was also inconclusive due to weak expression and the poor quality of antibodies available at the time this research was done (**data not shown**).

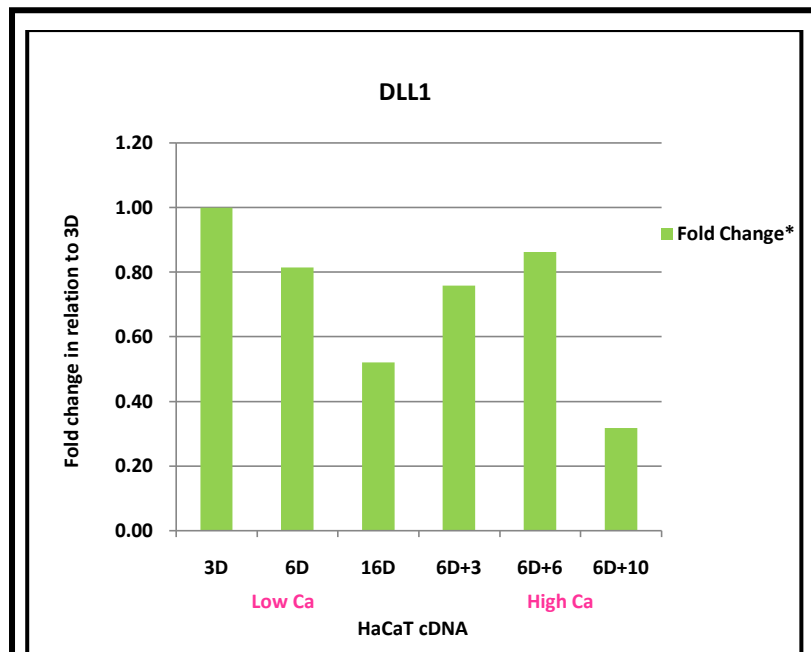


Figure 4.21: DLL1 Gene Expression in HaCaT Cells during Calcium-induced Differentiation. *DLL1* expression (fold change) was measured by qPCR in 3 experiments. The average data showed variation in fold change between cultures but none of the data reached significance.

Statistical (INSTAT version 1.0) software was used to analyse the qPCR data but no significant changes could be found (**Table 4.15**). The data was also analysed a different way, comparing fold change using the Tukey-Kramer Multiple Comparison Test (**Table 4.16**). This also showed no significant change

in DLL1 expression even when the largest changes (3D versus 6D+10) were considered.

Table 4.15: Statistical Analysis of DLL1 Expression Data. Values of Q >4.495 significant ($p < 0.05$) but no data reached this value in any of comparisons made in relation to copy number.

Comparison	Mean Difference	Q	P value
3D vs 6D	651.33	0.2816	ns $P > 0.05$
3D vs 16D	4088.3	1.768	ns $P > 0.05$
3D vs 6D+3	2967.3	1.283	ns $P > 0.05$
3D vs 6D+6	2525.7	1.092	ns $P > 0.05$
3D vs 6D+10	5202.0	2.249	ns $P > 0.05$
6D vs 16D	3437.0	1.486	ns $P > 0.05$
6D vs 6D+3	2316.0	1.001	ns $P > 0.05$
6D vs 6D+6	1874.3	0.8105	ns $P > 0.05$
6D vs 6D+10	4550.7	1.968	ns $P > 0.05$
16D vs 6D+3	-1121.0	0.4847	ns $P > 0.05$
16D vs 6D+6	-1562.7	0.6757	ns $P > 0.05$
16D vs 6D+10	1113.7	0.4816	ns $P > 0.05$
6D+3 vs 6D+6	-441.67	0.1910	ns $P > 0.05$
6D+3 vs 6D+10	2234.7	0.9663	ns $P > 0.05$
6D+6 vs 6D+10	2676.3	1.157	ns $P > 0.05$

Table 4.16: Statistical Analysis of DLL1 Expression Data. Values of Q greater than 4.495 are significant ($p < 0.05$) but no significant values were found in any of the comparisons made in relation to *DLL1* fold change.

Comparison	Mean Difference	Q	P value
3D vs 6D	0.1867	0.4224	ns $P > 0.05$
3D vs 16D	0.4767	1.079	ns $P > 0.05$
3D vs 6D+3	0.2400	0.5431	ns $P > 0.05$
3D vs 6D+6	0.1333	0.3017	ns $P > 0.05$
3D vs 6D+10	0.6833	1.546	ns $P > 0.05$
6D vs 16D	0.2900	0.6563	ns $P > 0.05$
6D vs 6D+3	0.05333	0.1207	ns $P > 0.05$
6D vs 6D+6	-0.05333	0.1207	ns $P > 0.05$
6D vs 6D+10	0.4967	1.124	ns $P > 0.05$
16D vs 6D+3	-0.2367	0.5356	ns $P > 0.05$
16D vs 6D+6	-0.3433	0.7770	ns $P > 0.05$
16D vs 6D+10	0.2067	0.4677	ns $P > 0.05$
6D+3 vs 6D+6	-0.1067	0.2414	ns $P > 0.05$
6D+3 vs 6D+10	0.4433	1.003	ns $P > 0.05$
6D+6 vs 6D+10	0.5500	1.245	ns $P > 0.05$

Also, several statistical tests were used to analyse the results but the outcome was the same. These included Tukey-Kramer Multiple Comparison Test and One-way Analysis of Variance (ANOVA) but none of the predicted values were significantly changed when comparing any cultures (low or high Ca²⁺).

Overall, the DLL1 gene was expressed at a constant level in keratinocyte cultures when examined by standard PCR. Similar results were obtained with qPCR in that no significant change in DLL levels could be found when comparing proliferating cells and differentiating cells. Previous experiments done on DLL1 expression at the protein level in epidermal tissue were also inconclusive due to a lack of good antibodies at the time this research was done. This was true for western blotting and direct immunofluorescence on cultured cells. Thus, the current research strategies have failed to reveal any significant information regarding DLL1 expression in HaCaT keratinocyte cultures.

Two other notch ligands, JAG1 and JAG2 had been investigated at the proteins level with some success and the current project was done to examine expression at the mRNA level. JAG1 and JAG2 primer pairs had already been designed and were available in the laboratory (sequences given in **Table 4.17**).

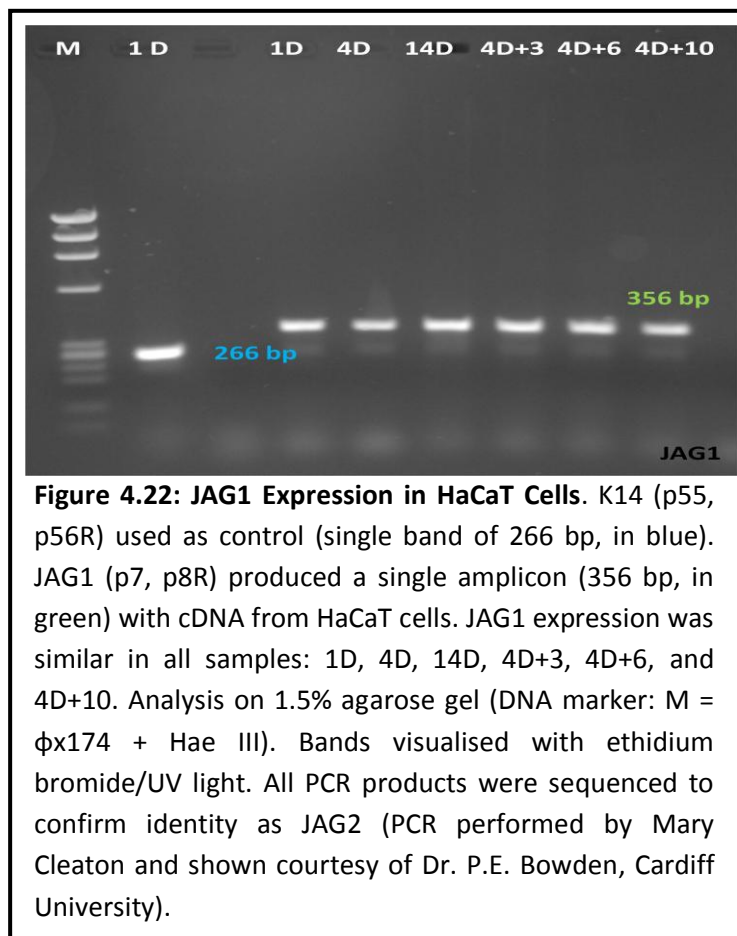
Table 4.17: Sequence of Oligonucleotide Primers for JAG1 and JAG2. All primers were designed by Dr. P.E. Bowden (Dermatology Department, Cardiff University). Those ending 'R' are reverse primers. Oligonucleotide primers in dark red were only used for standard PCR while the primers in green were used in qPCR.

Primers	Sequence
Jag1p7	[5' – GAT ATA CGG GAT GAT GGG AAC CCG – 3'] Exon 25
Jag1p8R	[5' – ATC CTT GAT GGG GAC CGT GTT GGC – 3'] Exon 26
Jag1p11	[5' – AGC CTA ATC CCT GCC AGA ACG GTG – 3'] Exon 13
Jag1p12R	[5' – TCA GGT GTG AGC AGT TCT TGC CCT – 3'] Exon 13
Jag2p14	[5'- AGG ATG AGG AGG ACG AGG ATC TGG-3'] Exon 26
Jag2p9R	[5' – CTA CTC CTT GCC GGC GTA GCG – 3'] 3'nc
Jag2p11R	[5'- GCC TCA TTG ATG CTC CTG ACC -3'] Exon 26

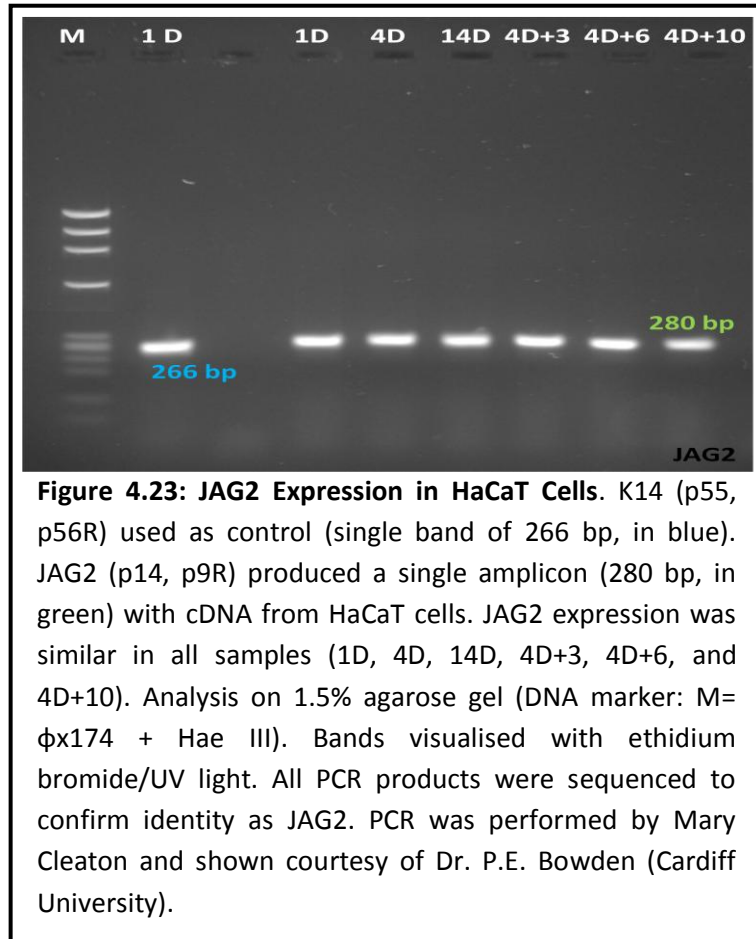
One primer pair (Jag1p7 and p8R) was designed across exons 25 and 26 and produced an amplicon of 356 bp with a cDNA template. This was used to detect expression of Jagged 1 (JAG1) in a standard PCR. However, this was too long for use in qPCR so another primer pair was made (Jag1p11 and p12R) within exon 13 producing a smaller fragment (102 bp) with a cDNA template, ideal for qPCR.

Two sets of Jagged 2 primers had previously been used for standard PCR. One primer pair (Jag2p14 and p9R) was designed from exon 26 to the 3' non-coding region of the Jagged 2 (JAG2) gene and produced an amplicon of 240 bp with a cDNA template. The other pair were made within exon 26 (Jag2p14 and p11R) and produced an amplicon of 168 bp with a cDNA template, sufficient for qPCR.

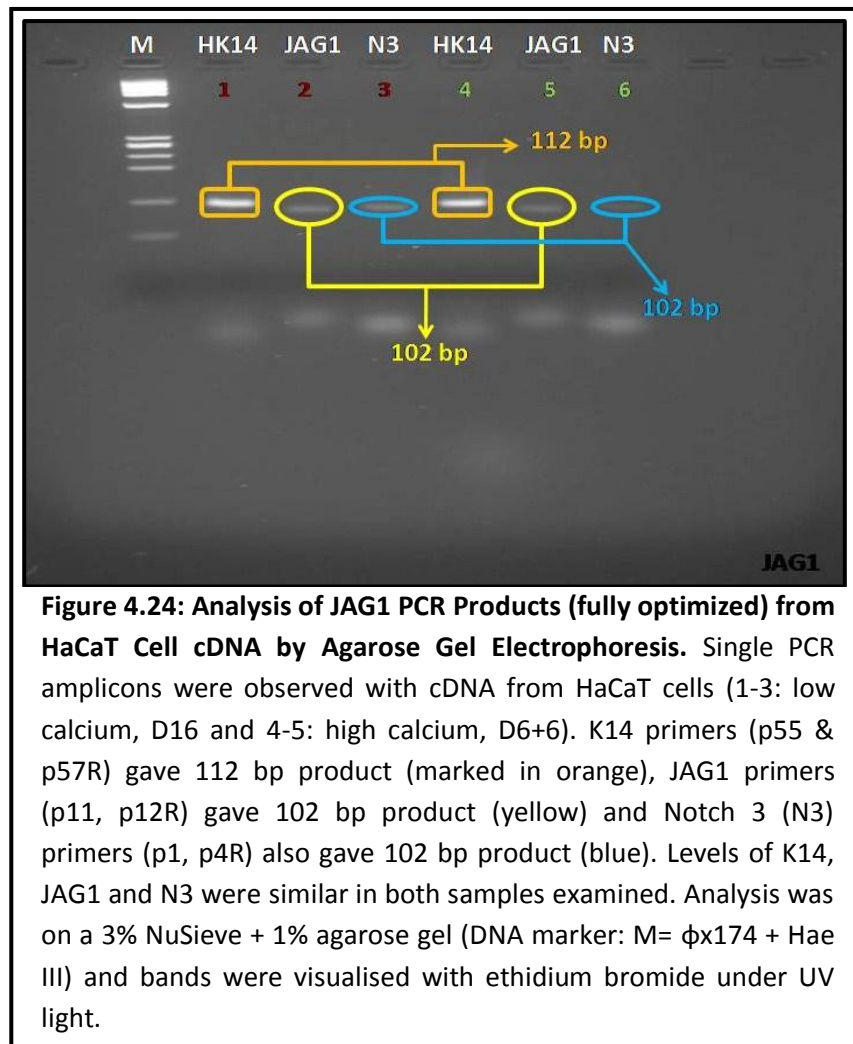
JAG1 and JAG2 expression in HaCaT cells during proliferation (low Ca^{2+}) and differentiation (high Ca^{2+}) was examined using the larger primer sets by standard PCR (60°C annealing and 35 cycles). The PCR products were then run on a 1.5% agarose gel and the DNA visualised on a UV light box (**Figure 4.22**). JAG1 showed strong bands throughout the whole range of HaCaT cell culture and similar levels were detected during proliferation (low Ca^{2+}) and differentiation (high Ca^{2+}). No genomic contamination was detected in this gel.



The results were similar for JAG2 with approximately equal expression in low calcium cultures (proliferating cells) and high calcium cultures (differentiating cells). The PCR products were analysed on a 1.5% agarose gel (**Figure 4.23**).



JAG1 and JAG2 PCR products were too big for qPCR, so the other primers were used. However, it was necessary to optimize these primer pairs before starting qPCR experiments. A summary agarose gel was run to show the products produced under optimal primer concentrations (**Figure 4.24**).



The JAG2 primer pair intended for qPCR (p14 & p11R) was also used with cDNA from various HaCaT cultures in a standard PCR (**Figure 4.25**). Again similar levels were seen in proliferating and differentiating cells.

The JAG1 and JAG2 PCR amplicons were sequenced to confirm their identity and then the inserts were cloned into separate pGEM-T easy vectors (see methods chapter for details). PCR samples were selected for cloning as before. However, JAG1 cloning was problematic even though the PCR product

was strong, ligation into pGEMT- easy and cloning gave the wrong product.

This was repeated without any problems. JAG2 worked well.



Figure 4.25: JAG2 PCR Products with cDNA from HaCaT Cells Analysed by Agarose Gel Electrophoresis. JAG2 primers (p14 & p11R) produced a single PCR amplicon (168 bp) with cDNA from HaCaT cells. Levels of JAG2 expression were similar in all samples examined (low calcium: D2 and high calcium: D4+1, D4+3 and D4+10). Analysis was done on a 3% NuSieve + 1% agarose gel (DNA marker: M= ϕ x174 + Hae III) and bands were visualised with ethidium bromide under UV light.

Once ligated into the pGEM-T easy vectors and cloned, the relevant bacterial clones were grown in batch culture and the plasmids carrying vector and insert isolated. Six clones were selected for each insert and the plasmids extracted using a Qiagen mini plasmid kit (details in **Chapter 2**). JAG1 and JAG2 inserts were released from the pGEM-T easy vectors by digestion with Eco RI, and the products were run on a 1.5% agarose gel (**Figure 4.26**, JAG2 data only).



Figure 4.26: Analysis of JAG2 Plasmid Digests by Gel Electrophoresis. Cloned JAG2 plasmids (Plas 1-6) were digested with EcoR1 and run on 1.5% agarose gel. The pGEM-T easy vector is larger band (3015 bp) and the lower band (168 bp) is JAG2 insert. Plasmids 1, 2, 4, 5 and 6 were selected and sequenced to confirm JAG2 identity. M (DNA marker): low molecular weight mix (755 bp - 21 bp).

Bacterial clones containing plasmids were stored as glycerol stocks at -80°C and isolated plasmid DNA was stored at -20°C . One plasmid was then selected based on the quality of the insert (Plasmid 3 for JAG1 and plasmid 6 for JAG2) and a set of serial dilutions (300,000 to 30 copies) were made for the qPCR experiments (**Tables 4.18 and 4.19**. Also see **Chapter 2** for further details).

Table 4.18: Serial Dilutions of JAG1 Plasmid 3 for qPCR Standards. Sterile nuclease free H₂O was used as the diluent.

Dilution	Source of plasmid DNA for dilution	Initial Conc. (g/μl) C ₁	Volume of plasmid DNA (μl) V ₁	Volume of diluents (μl)	Final Vol. (μl) V ₂	Final conc. (g/μl) C ₂	copy#
1	Stock	7.2e-7	10μl	990μl	1000μl	7.2e-9	N/A
2	Dilution1	7.2e-9	10μl	990μl	1000μl	7.2e-11	N/A
3	Dilution2	7.2e-11	10μl	990μl	1000μl	7.2e-13	N/A
4	Dilution3	7.2e-13	142.35	357.65	500μl	2.049e-13	300,000
5	Dilution4	2.049e-13	50μl	450μl	500μl	2.049e-14	30,000
6	Dilution5	2.049e-14	50μl	450μl	500μl	2.049e-15	3000
7	Dilution6	2.049e-15	50μl	450μl	500μl	2.049e-16	300
8	Dilution7	2.049e-16	50μl	450μl	500μl	2.049e-17	30

The serial dilutions of JAG1 plasmid were initially tested by standard PCR and analyzed on a high definition (3% NuSieve and 1% agarose) gel (**Figure 4.27**).

The only bands visible were those that started with higher copy numbers.

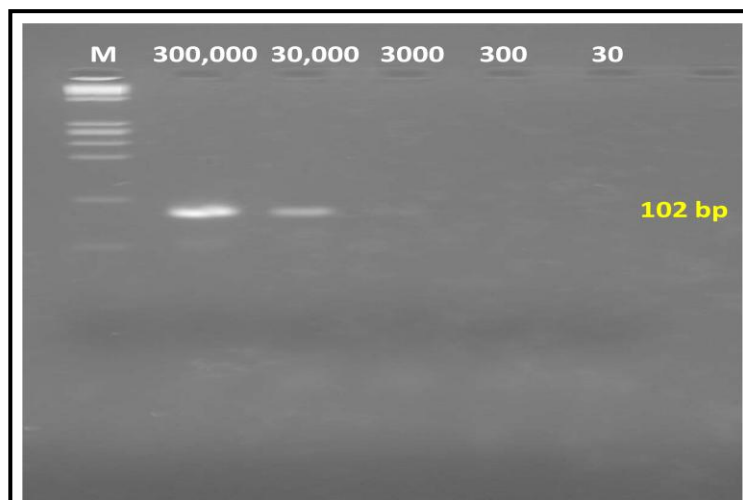


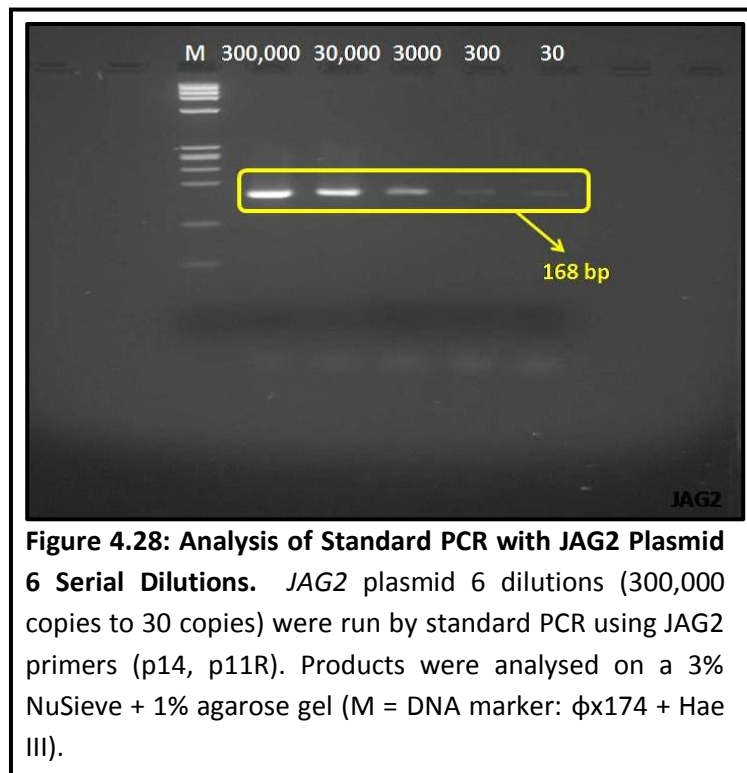
Figure 4.27: Analysis of Standard PCR with JAG1 Plasmid 3 Serial Dilutions. JAG1 plasmid 3 dilutions (300,000 copies to 30 copies) were amplified by PCR using JAG1 primers (JAG1p11, p12R). Products analysed on 3% NuSieve + 1% agarose gel (M = DNA marker: φx174 + Hae III).

Table 4.19: Serial Dilutions of Jag 2 Plasmid 6 for qPCR Standards. Sterile nuclease free H₂O was used as diluents.

Dilution	Source of plasmid DNA for dilution	Initial Conc. (g/μl) C ₁	Volume of plasmid DNA (μl) V ₁	Volume of Diluent (μl)	Final Vol. (μl) V ₂	Final conc. (g/μl) C ₂	copy#
1	Stock	3.15e-7	10μl	990μl	1000μl	5e-9	N/A
2	Dilution1	3.15e-9	10μl	990μl	1000μl	5e-11	N/A
3	Dilution2	3.15e-11	10μl	990μl	1000μl	5e-13	N/A
4	Dilution3	3.15e-13	66.45	33.55	100μl	2.093e-13	300,000
5	Dilution4	2.093e-13	10μl	90μl	100μl	2.093e-14	30,000
6	Dilution5	2.093e-14	10μl	90μl	100μl	2.093e-15	3000
7	Dilution6	2.093e-15	10μl	90μl	100μl	2.093e-16	300
8	Dilution7	2.093e-16	10μl	90μl	100μl	2.093e-17	30

The serial dilutions of JAG2 plasmid were initially tested by standard PCR and analyzed on a high definition (3% NuSieve and 1% agarose) gel (**Figure 4.28**). The larger product size (168 bp) was visible across the whole range showing that the dilution series was reliable.

JAG1 expression was measured in HaCaT cultures by qRT-PCR both estimating the copy numbers of cDNA (and mRNA by inference) and also the fold change relative to the initial culture conditions (Day 1-3, varies between difference experiments).



The *JAG1* standard dilution series was run at the same time as the experimental samples and this data was used to calculate the copy number from the individual sample Ct values (number of cycles to reach the threshold). The *JAG1* dilution series data was analysed first and a standard curve drawn as before.

The amplification plot of the *JAG1* dilution series (**Figure 4.29**) showed evenly spaced curves (fluorescence vs cycle number), shown in different colours for each dilution (blue = 300,000; red= 30,000; green = 3,000; grey = 300 and yellow = 30 copies). As the dilution increased, the threshold copy number (Ct

value) increased and this data was used to calculate a standard curve, Ct values versus copy number (**Figure 4.30**).

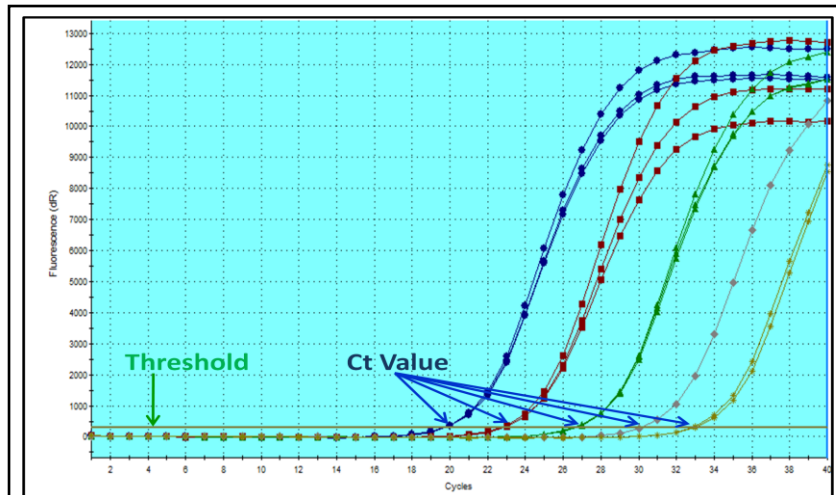
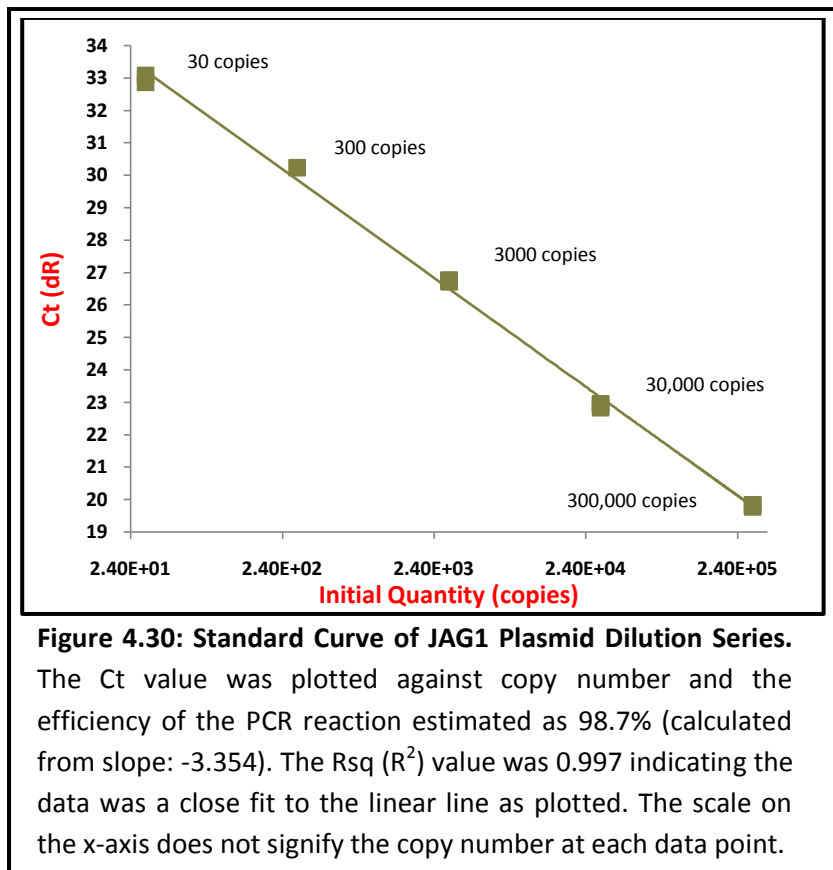


Figure 4.29: Amplification Plot of JAG1 Plasmid Dilution Series. Amplification plots were calculated by qPCR MxPro Software. Each colour represents the fluorescence values for a different JAG1 plasmid dilution: blue represents 300,000 copies, red (30,000), green (3,000), grey (300) and yellow (30). The distance between each fluorescence amplification plot was approximately constant (3-4 cycles). The Ct values are shown for each curve (blue arrows). Note: The data is an average of 3 measurements (triplicate samples).

The Ct values for the JAG1 dilution series ranged from 20 to 33 and this produced a linear plot (**Figure 4.30**) with an efficiency of 98.7% (ideal = 100%) , an Rsq (R^2) value of 0.997 (ideal = 1.000) and a slope of -3.354 $\log(X)$ (ideal = -3.2 to -3.6). This represents a good standard curve for JAG1 and this was used to estimate the copy number in experimental samples from the measured Ct value.



The data from 3 consecutive JAG1 qPCR runs (triplicate) with cDNA from HaCaT cultures was analysed using this JAG1 standard curve and INSTAT software. The raw qPCR data was then analysed using different statistical methods (e.g. Tukey-Kramer Multiple Comparison Test and One-way Analysis of Variance, ANOVA). The JAG1 experimental data was analysed in two different ways. Initially calculating the level of JAG1 expression in relation to copy number and then calculating the fold change in expression. Proliferating cultures (day 3 in low calcium medium) did have a low average copy number (1,028) of JAG1 transcripts (**Table 4.20**). Even though very little if any JAG1 protein was observed in these cells, there was a dramatic increase in copy

number (38,736) in cells grown for 6 days in low calcium medium. Cultures that showed distinct stratification and cornification (6D+3 in high calcium medium) showed a further increase in JAG1 copy number (65,406). Both the individual and average values of the 3 experiments are shown in **Table 4.20**.

Table 4.20: JAG1 Gene Expression (Copy Number) during HaCaT Cell Culture.

Data for 3 experiments showed the same general trend with an increase in K10 expression as the cultures differentiated. There was a significant increase in copy number as cells differentiated (16D, 6D+3, 6D+6 and 6D+10) relative to proliferating cultures (3D, 6D).

Experiment	3D	6D	16D	6D+3	6D+6	6D+10
1	800	27,120	15,870	56,280	30,190	34,930
2	455	21,370	13,170	35,240	28,800	42,120
3	1,830	67,720	54,650	104,700	80,630	47,430
Average	1,028	38,736	27,896	65,406	46,540	41,493

In terms of fold change, JAG1 expression increased a cell density increased so day 6 levels were on average 39.30 fold higher but did fall slightly by day 16 (**Table 4.21**). Differentiating cells had even higher levels (68.35 fold increase 3 days after switching to high calcium falling to 48.37 fold at 6 days).

Table 4.21: JAG1 Gene Expression (Fold Change) in HaCaT Cell Cultures. JAG1 gene expression increased significantly while cells were proliferating (39.30 fold average) but larger increases were seen as cells differentiated (68.35 fold maximum average). Fold change data relative to 3D culture levels and average values are shown in blue.

Experiment	3D	6D	16D	6D+3	6D+6	6D+10
1	1.00	33.92	19.85	70.39	37.76	43.68
2	1.00	46.97	28.95	77.45	63.30	92.57
3	1.00	37.01	29.86	57.21	44.06	25.92
Average	1.00	39.30	26.22	68.35	48.37	54.06

Comparisons were then made between levels of JAG1 expression at each time point in the HaCaT culture experiments using the Tukey-Kramer Multiple Comparison Test (**Table 4.22**). In all cases when comparing cultures that showed signs of differentiation with proliferating cultures (either 3D or 6D), the increases were not significant, as the value of q was always <4.8. Even though there was a large difference between JAG1 levels in 3D and 6D cultures (both low calcium) this was not statistically significant. The cultures that differentiated generally had higher levels of JAG1 but these were variable. The largest difference observed (comparing 3D and 6D+3) was almost significant (q=4.714).

Table 4.22: Comparison of JAG1 Expression Levels (Copy Number) in Different HaCaT Cultures. The mean difference in copy number between the cultures compared was calculated and a Q value assigned. Where the value of Q was <3.00, the data was not significant otherwise as stated below.

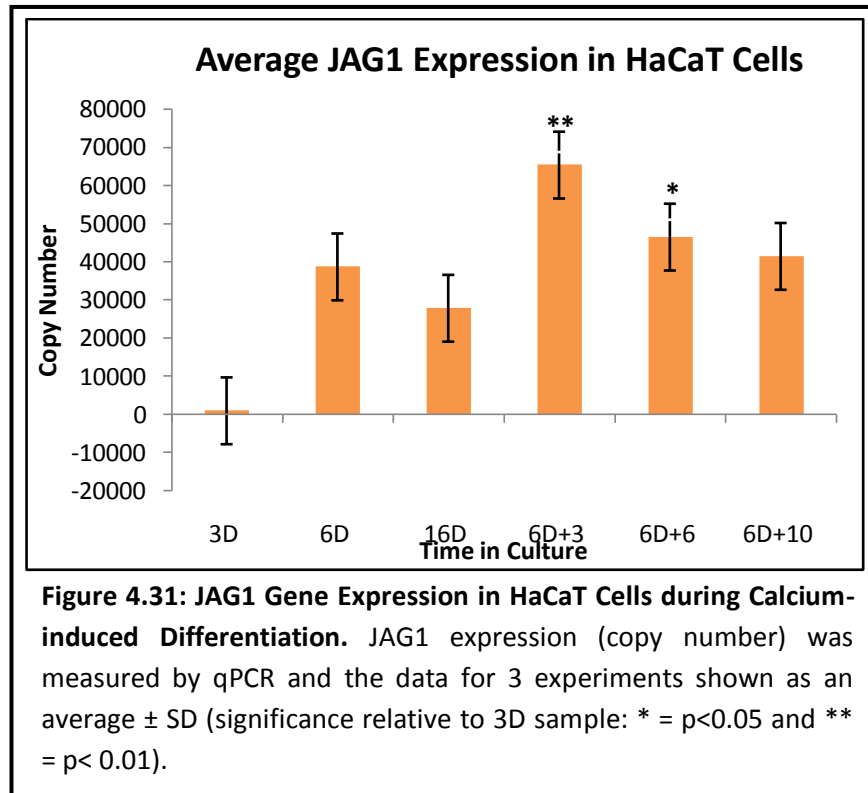
Comparison	Mean Difference	Q	P value
3D vs 6D	-37708	2.761	ns P>0.05
3D vs 16D	-26868	1.967	ns P>0.05
3D vs 6D+3	-64378	4.714	** P<0.01
3D vs 6D+6	-45512	3.332	* P<0.05
3D vs 6D+10	-40465	2.963	ns P>0.05
6D vs 16D	10840	0.7937	ns P>0.05
6D vs 6D+3	-26670	1.953	ns P>0.05
6D vs 6D+6	-7803.3	0.5714	ns P>0.05
6D vs 6D+10	-2756.7	0.2018	ns P>0.05
16D vs 6D+3	-37510	2.746	ns P>0.05
16D vs 6D+6	-18643	1.365	ns P>0.05
16D vs 6D+10	-13597	0.9955	ns P>0.05
6D+3 vs 6D+6	18867	1.381	ns P>0.05
6D+3 vs 6D+10	23913	1.751	ns P>0.05
6D+6 vs 6D+10	5046.7	0.3695	ns P>0.05

Interestingly, the data expressed as fold change in JAG1 expression levels was significant in comparison to the copy number data (**Table 4.23**). This was also analysed using the Tukey-Kramer Multiple Comparison Test. Values of q greater than 4.495 were significant ($p < 0.05$) with larger values ($q=7.255$) being more significant ($p < 0.01$). The only data that reached significance was the comparison between early proliferating cultures (3 days in low calcium) and differentiating cultures in high calcium (6D+3, 6D+6 and 6D+10).

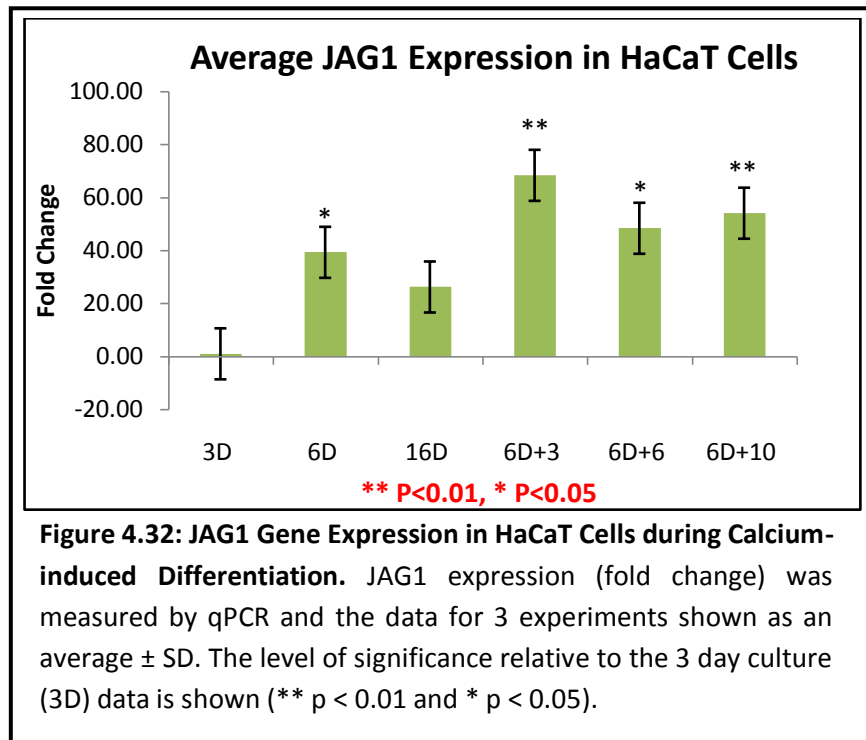
Table 4.23: Comparison of JAG1 Expression Levels (Fold Change) in HaCaT Cultures. The mean difference in JAG1 fold change between certain cultures was compared and where the value of Q was greater than 3.495, the difference was significant ($p < 0.05$ or $p < 0.01$, marked in red).

Comparison	Mean Difference	Q	P value
3D vs 6D	-38.300	4.126	* $P < 0.05$
3D vs 16D	-25.220	2.717	ns $P > 0.05$
3D vs 6D+3	-67.350	7.255	** $P < 0.01$
3D vs 6D+6	-47.373	5.103	* $P < 0.05$
3D vs 6D+10	-53.057	5.716	** $P < 0.01$
6D vs 16D	13.080	1.409	ns $P > 0.05$
6D vs 6D+3	-29.050	3.129	ns $P > 0.05$
6D vs 6D+6	-9.073	0.9774	ns $P > 0.05$
6D vs 6D+10	-14.757	1.590	ns $P > 0.05$
16D vs 6D+3	-42.130	4.539	* $P < 0.05$
16D vs 6D+6	-22.153	2.387	ns $P > 0.05$
16D vs 6D+10	-27.837	2.999	ns $P > 0.05$
6D+3 vs 6D+6	19.977	2.152	ns $P > 0.05$
6D+3 vs 6D+10	14.293	1.540	ns $P > 0.05$
6D+6 vs 6D+10	-5.683	0.6123	ns $P > 0.05$

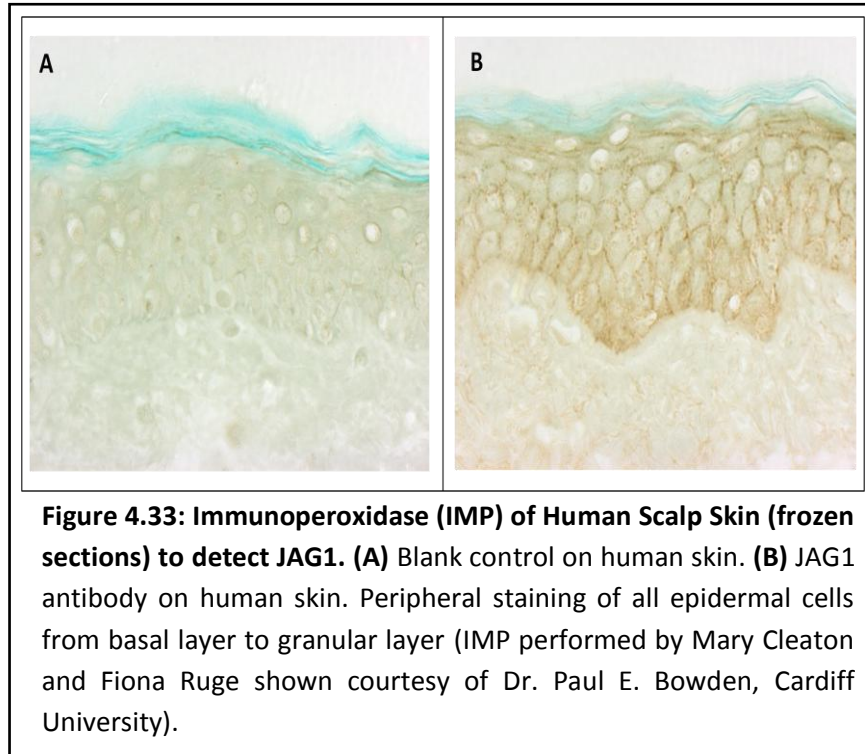
The copy number data for JAG1 expression in different HaCaT cultures was made into a bar chart that showed the standard deviation (SD) and the significance relative to 3D cultures (**Figure 4.31**). Low levels of JAG1 expression were found in early cultures in low calcium medium (3D) but this increase as the cell density increased and JAG1 expression was further increased in cultures that had stratified and differentiated (6D+3, 6D+6 and 6D+10).



Expressing the JAG1 data as fold change produced a bar chart with the same overall trends but higher levels of significance (**Figure 4.32**). The only increases that were significant were those in late differentiation (6D+3, 6D+6 and 6D+10) as these were greater than 10 fold over the levels seen in the 3D cultures ($p < 0.01$ and $p < 0.05$ respectively).

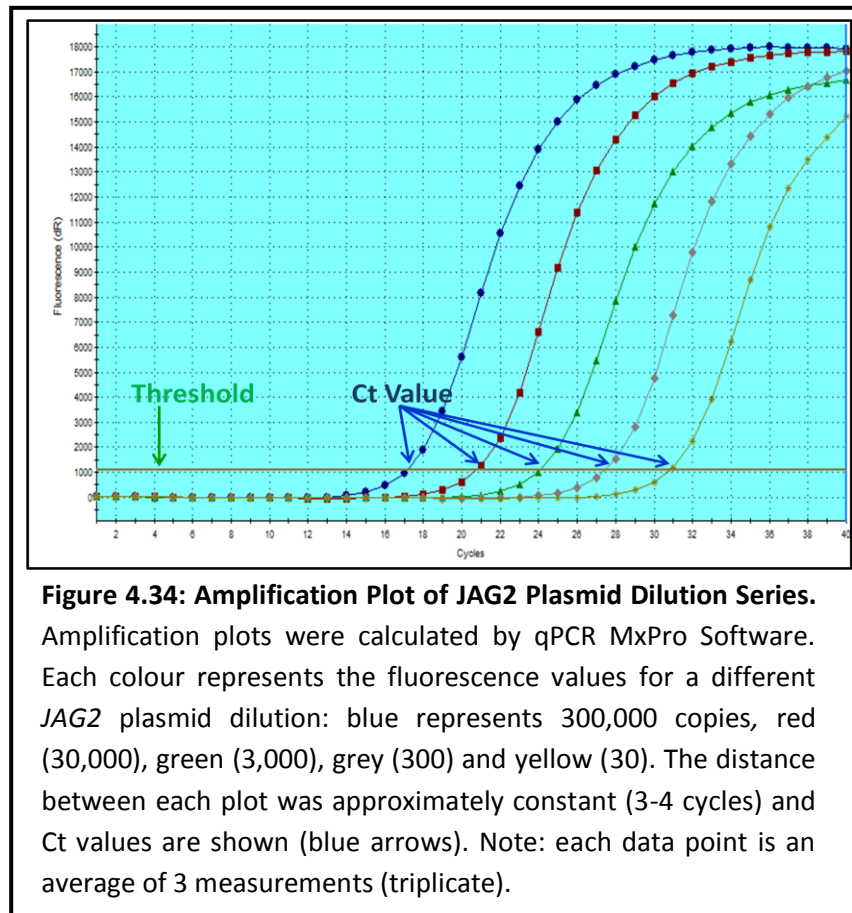


Overall, JAG1 was not expressed at a constant level in cultured HaCaT keratinocytes undergoing calcium-induced differentiation. In fact, JAG1 expression was significantly higher in differentiating cells compared to early cultures in low calcium. However, when compared to more mature cultures in low calcium (6 days or 16 days), the increase was much less and not significant. Earlier data from the dermatology laboratory using western blotting showed a constant expression of JAG1 in all epidermal layers although there was some variation (**data not shown**). Experiments using immunoperoxidase (IMP) and immunofluorescence (IMF) techniques on human skin and cultured cells also showed that JAG1 expression was similar across the whole epidermis (**Figure 4.33**). Thus, the small changes seen in JAG1 expression probably only represent variations in the level in culture.

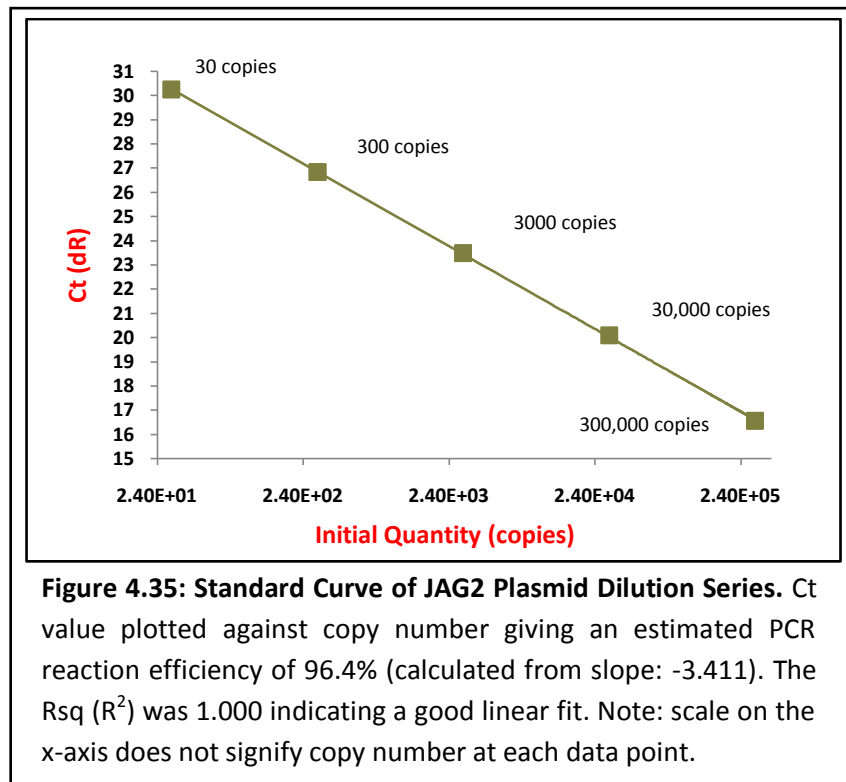


JAG2 levels were also measured in HaCaT cells undergoing calcium-induced differentiation. The same experimental procedure was used for qRT-PCR measurements and analysis of the data using MxPro software. This required cloning a segment of JAG2 into pGEM-T easy, using this to construct a set of serial dilution standards of known copy number and then relating the sample fluorescence and Ct value back to starting copy number. The amplification plot data for the serial dilutions was quite as good as that for JAG1 with evenly spaced Ct values between dilutions (**Figure 4.34**). The amplifications were shown in different colours for each dilution (blue = 300,000; red= 30,000; green = 3,000; grey = 300 and yellow = 30 copies). As the dilution

increased, the threshold copy number (Ct value) increased and this data can be used to calculate a standard curve of Ct value versus copy number.



The Ct values for the JAG2 dilution series ranged from 17 to 31 and this produced a linear plot (**Figure 4.35**) with an efficiency of 96.4% (ideal = 100%), an R^2 value of 1.000 (ideal = 1.000) and a slope of $-3.411 \log X$ (ideal values = -3.2 to -3.6). This represents a very good standard curve and this was used to estimate the JAG2 copy number in experimental samples from the measured Ct value.



The JAG2 data from 3 consecutive qPCR runs (triplicate) was interpreted with the JAG2 standard curve and INSTAT software. The raw qPCR data was then analysed using different statistical methods (e.g. Tukey-Kramer Multiple Comparison Test and One-way Analysis of Variance, ANOVA). This software was used to analyse the JAG2 experimental data and to calculate JAG2 expression in terms of copy number and fold change values. JAG2 levels showed reduction in early proliferating cultures and were reduced by about half at day 6 compared to day 3 (**Table 4.24**). However, after cultures were left in low calcium for 16 days, JAG2 levels increased (16 day cultures almost 3 fold higher than 3 day cultures). After calcium-induced differentiation, JAG2 levels were similarly increased (day 6+6 was 5 fold higher than day 3 cultures) but a slight reduction was seen later (day 6+10). This data was not related to

the amount of starting cellular material so the initial increase JAG2 expression probably reflected the 4 fold increase in cell density typically seen between 6 and 16 days and the subsequent reduction in JAG2 levels as cellular material increased further reflected a fall in JAG2 expression in real terms.

Table 4.24: JAG2 Gene Expression (Copy Number) during HaCaT Cell Culture. Data for 3 experiments showed the same general trend with an increase in JAG2 expression as the cultures initially proliferated and then a subsequent decrease as cells differentiated. An average value for the three experiments is shown in blue.

Experiment	3D	6D	16D	6D+3	6D+6	6D+10
1	5,546	7,133	2,446	3,784	1,872	3,981
2	17,060	3,604	35,370	26,660	48,170	13,940
3	9,500	2,213	50,670	51,960	51,880	15,970
Average	10,702	4,316	29,495	27,468	33,974	11,297

JAG2 levels were reduced halved during early proliferation (day 6 compared to day 3) but did increase later (2.61 fold higher at day 16) as cells in low calcium differentiated due to contact inhibition (**Table 4.25**). Cells that were forced into differentiation by increasing calcium levels showed similar increase in JAG2 levels (2.87 fold higher in 6D+6 cultures was typical).

Table 4.25: JAG2 Gene Expression (Fold Change) during HaCaT Cell Culture. JAG2 gene expression increased almost 3 fold in late proliferating cultures and then increased as cells differentiated (2.61 to 2.87 fold). But by day 6+10 (6D+10) a major reduction in fold change. Fold change data relative to 3D culture levels and average values of 3 experiments are shown in blue.

Experiment	3D	6D	16D	6D+3	6D+6	6D+10
1	1.00	1.29	0.44	0.68	0.34	0.72
2	1.00	0.21	2.07	1.56	2.82	0.82
3	1.00	0.23	5.33	5.47	5.46	1.68
Average	1.00	0.57	2.61	2.57	2.87	1.07

The levels of JAG2 expression at each time point in the HaCaT culture experiments were analysed using the Tukey-Kramer Multiple Comparison Test. Here, values of q greater than 5.837 were just significant ($p < 0.05$). Large differences were only found when comparing 6D cultures to other time points and the data was in general significant in all cases ($p < 0.05$). This was true whether the data was expressed in terms of copy number (**Table 4.26**) or fold change (**data not shown**).

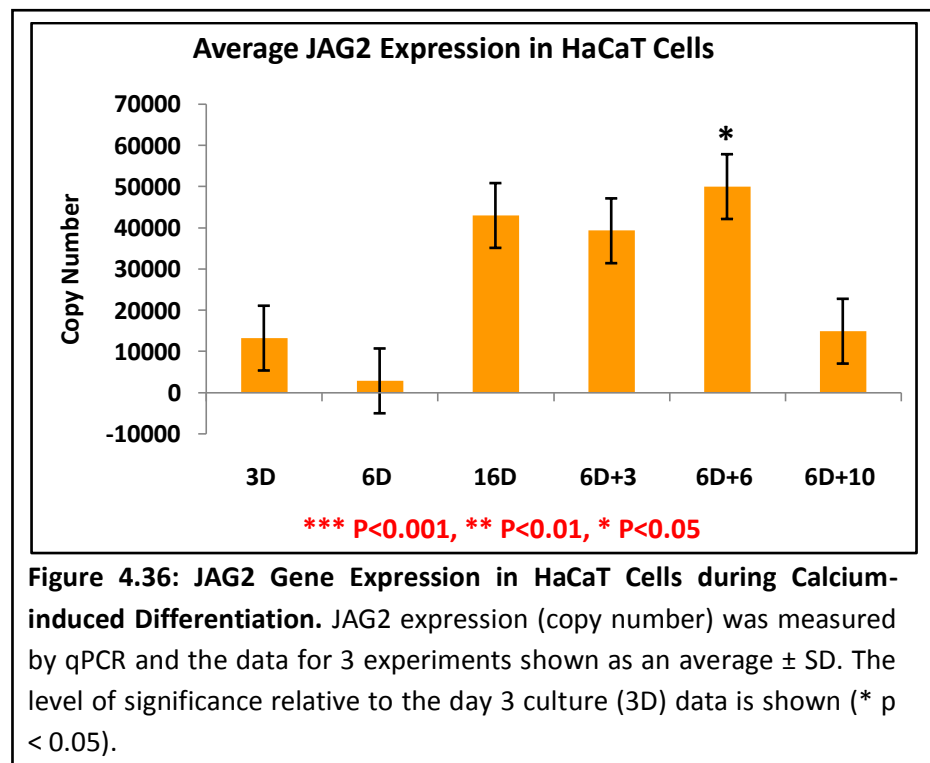
Table 4.26: Comparison of JAG2 Levels (Copy Number) in Different HaCaT Cultures. Mean difference in JAG2 copy number comparing various HaCaT cultures (as listed) was calculated and a Q value assigned. Where the value of q was >4.495 , the data was significant (significant p values shown in red).

Comparison	Mean Difference	Q	P value
3D vs 6D	10372	1.647	ns $P>0.05$
3D vs 16D	-29740	4.724	ns $P>0.05$
3D vs 6D+3	-26030	4.135	ns $P>0.05$
3D vs 6D+6	-36745	5.837	* $P<0.05$
3D vs 6D+10	-1675.0	0.2661	ns $P>0.05$
6D vs 16D	-40112	6.372	* $P<0.05$
6D vs 6D+3	-36402	5.782	* $P<0.05$
6D vs 6D+6	-47117	7.484	* $P<0.05$
6D vs 6D+10	-12047	1.914	ns $P>0.05$
16D vs 6D+3	3710.0	0.5893	ns $P>0.05$
16D vs 6D+6	-7005.0	1.113	ns $P>0.05$
16D vs 6D+10	20865	4.458	ns $P>0.05$
6D+3 vs 6D+6	-10715	1.702	ns $P>0.05$
6D+3 vs 6D+10	24355	3.869	ns $P>0.05$
6D+6 vs 6D+10	35070	5.571	ns $P>0.05$

As day 3 (3D) levels of JAG2 were relatively high compared to day 6, comparison of the 3D data and most other time points (6D, 16D, 6D+3, and 6D+10) showed no significant difference. However, the levels 6 days after

shifting to high calcium (6D+6) were significantly higher. This was also true whether the data was expressed as copy number or fold change.

The JAG2 data from individual experiments was also analysed by the INSTAT statistical software as an overall average. This was presented as a bar chart showing mean plus standard deviation and any significant p values were shown. This data was expressed in terms of total copy number (**Figure 4.36**) and while there was a general trend for higher levels of JAG2 in differentiated cultures, the data was only significant at 6D+6.



In conclusion, JAG2 levels increased in 16 day cultures left in low calcium but these cannot be considered as proliferating as contact inhibition in a cell mass of this size induces differentiation. After calcium induced differentiation, JAG2 levels increased in all cultures initially (6D+3 and 6D+6) but levels did decline in older cultures (6D+10). As the cell volume continued to increase, then an increase in JAG2 expression per unit cell seemed likely, agreeing with the increase seen as cells differentiated *in vivo*.

Jagged 2 (JAG2) levels had been previously estimated at the protein level by analysis of HaCaT cell extracts (Dr. P.E Bowden, unpublished data). Total protein extracts were analysed by SDS-PAGE (visualised with Coomassie Blue R250) and western blotted using JAG2 specific antisera (**data not shown**). Also, cultured cells were directly stained with JAG2 specific antisera that were labelled with fluorescent tags and visualised by immunofluorescence (IMF) microscopy (see **Figure 4.37**). This indicated that JAG1 and JAG2 levels were not constant but varied in different culture conditions. JAG1 and JAG2 levels were low (or even absent) in early cultures (3D) in low calcium medium but then significantly increased as cells differentiated. This protein data was in broad agreement with the quantitative mRNA data.

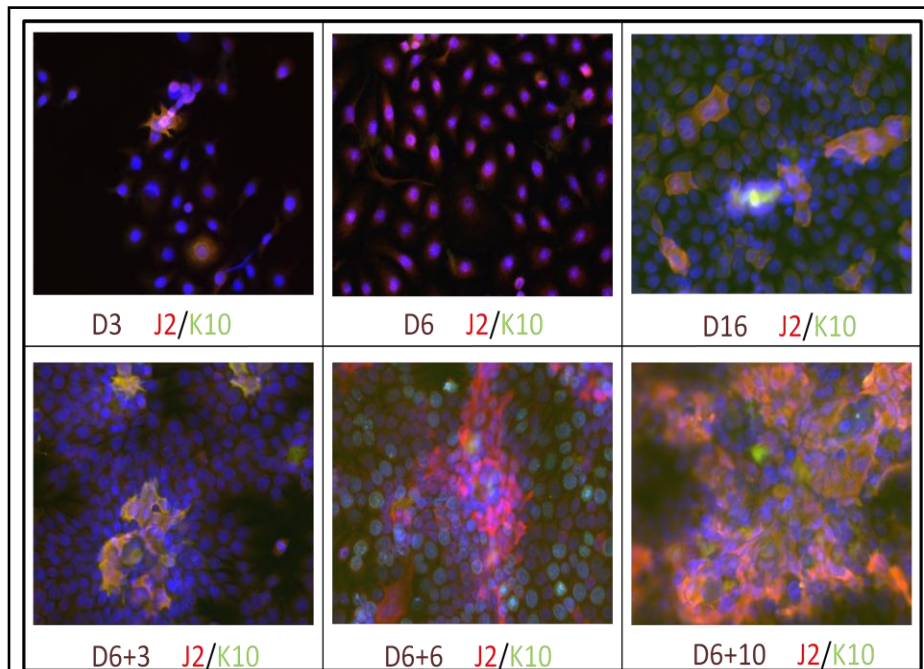


Figure 4.37: Expression of Jagged 2 (J2) and K10 (Differentiation Marker) in HaCaT Cells. HaCaT cells were grown in low calcium KGM for 3 days (D3), 6 days (D6) or 16 days (D16) or shifted to high calcium KGM at 6 days and growth for another 3 days (D6+3), 6 days (D6+6) or 10 days (D6+10). J2 (red) was expressed late in proliferation and throughout differentiation. K10 (in green) not expressed in early low calcium cultures and only poorly expressed at 16 days. K10 expression increased dramatically as differentiation was induced by high calcium levels. Nuclei were stained blue with DAPI (courtesy of Dr. Paul E. Bowden, Department of Dermatology, Cardiff University).

Overall, JAG2 showed variable expression in early proliferating cultures (low calcium) with an increase after 16 days where low calcium cultures undergo a certain level of differentiation. Levels did increase slightly (about 2-3 fold) in cells undergoing calcium-induced differentiation but this was not sustained over time and only significant at some points (e.g. 6D+6 data). This infers a possibly biphasic action of JAG2 both in early proliferation and late differentiation, a situation that agrees with some of the in vivo observations.

However, this data is not robust enough and needs to be repeated to see if these changes are real or not.

Earlier immunoperoxidase (IMP) and immunofluorescence (IMF) work in the dermatology laboratory using various JAG2 antibodies with human skin sections did reveal that JAG2 was prominent in both the basal layer and granular layer of the epidermis but the antibodies were of low titre and the results were not robust (**Figure 4.38**). Thus, more work is required to fully assess the role of JAG2 in terminal differentiation of keratinocytes.

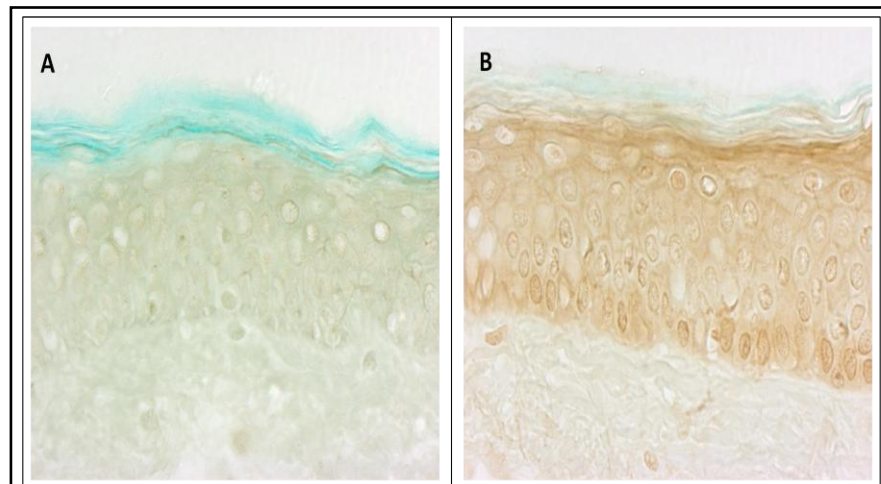


Figure 4.38: Immunoperoxidase (IMP) of Human Scalp Skin (Frozen Sections). (A) Blank Control of Human epidermis. (B) JAG2 staining of human epidermis. JAG2 was more prominent in basal cells and again in granular cells of human epidermis (data courtesy of Dr. Paul E. Bowden). Note: sections were counterstained with Light Green (histology dye).

In conclusion, levels of JAG1 and JAG2 expression in HaCaT cell cultures were broadly similar (**Figure 4.39**). While differentiating cells appeared to express a higher level of both JAG1 and JAG2, levels measured between experiments were variable and the increases were not always statistically significant.

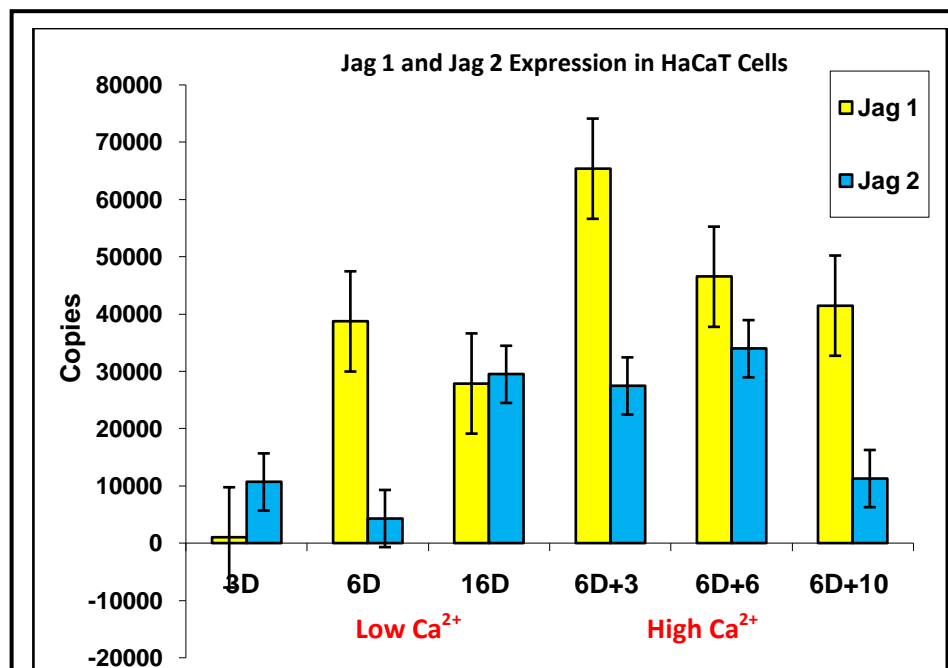


Figure 4.39: Alterations in JAG1 and JAG2 Expression (Copy Number) in HaCaT Cells during Calcium-Induced Differentiation. JAG1 (yellow) and JAG2 (blue) expression in terms of copy number was measured by qPCR and analysed using MxPro software. JAG1 expression increased in low calcium medium (3D, 6D, 16D) and increased further with calcium-induced differentiation (6D+3, 6D+6, 6D+10). JAG2 levels were similar, with the small but not significant decrease in early low calcium cultures being followed by a small increase in differentiating cells.

4.4 Expression of Notch Target Genes (HES and HERT) in HaCaT Cells

Notch target genes form two broad families (HES and HERT) and within these multigene families only certain members are thought to be expressed in human skin. From data in the literature, we focussed on HES1, HES5, HES7, HEYL, HEY1 and HEY2 as possible Notch signalling targets in skin. Primers were designed to specifically detect cDNA for these six genes using standard PCR to confirm that they were expressed in human epidermis (**Table 4.27**).

Table 4.27: Sequence of HES & HEY Primer Pairs. All oligonucleotide primers were designed by Dr. P.E. Bowden (Dermatology, Cardiff University) and supplied by Sigma-Aldrich Company Ltd (Poole, UK). Reverse primers were designated 'R'. Location of primers within each gene is shown.

Primers	Sequence
Hes 1 p1	[5'- GGT GCT GAT AAC AGC GGA AT -3'] (5'nc)
Hes 1 p2R	[5'- TGA GCA AGT GCT GAG GGT TT -3'] (5'nc)
Hes 5 p1	[5'- GGT GCC TCC ACT ATG ATC CTT A -3'] (3'nc)
Hes 5 p2R	[5'- ATT GAA CTC TCA GTC ACG TGG A -3'] (3'nc)
Hes 7 p1	[5'- AAC CCG AAG CTG GAG AAA GCG GAG -3'] Exon 3
Hes7 p2R	[5'- AAA CCG GAC AAG TAG CAG CTG GCG -3'] Exon 4
Hey1 p3	[5'- CCA TGT CCC CCA CTA CAT CTT CCC -3'] Exon 2
Hey 1 p4R	[5'- ACG GTC ATC TGC AGG ATC TCG GCT -3'] Exon 4
Hey 2 p3	[5' - ACG TGG CTG ATA CTG ACA AGG GCG -3'] Exon 5
Hey2 p4R	[5' - ACG TTT GCC CAT GCG GAT TCA GCC -3'] Exon 5
Hey L p1	[5' – CGG AGG AAT GTG CTG CCC AGT CGA -3'] Exon 5
Hey L p2R	[5' – TCG ACT GGG CAG CAC ATT CCT CCG -3'] Exon 5

The HES1 primers (p1 and p2R) produced an amplicon of 108 bp from the 5' non-coding region of the gene. HES5 primers (p1, p2R) were designed to amplify the 3' non-coding region and produced an amplicon of 96 bp. HES7 primers (p1, p2R) was designed across exons 3 and 4 to produce an amplicon of 140 bp with cDNA (and a larger amplicon with gDNA due to the inclusion of intron sequences).

HEY1 (p3, p4R) and HEY2 (p3, p4R) primers were made to exon 5 of the appropriate gene and produced amplicons of 181 bp and 250 bp respectively using cDNA. Finally, HEYL primers (p1 and p2R) were also made to exon 5 sequences and produced an amplicon of 185 bp on cDNA.

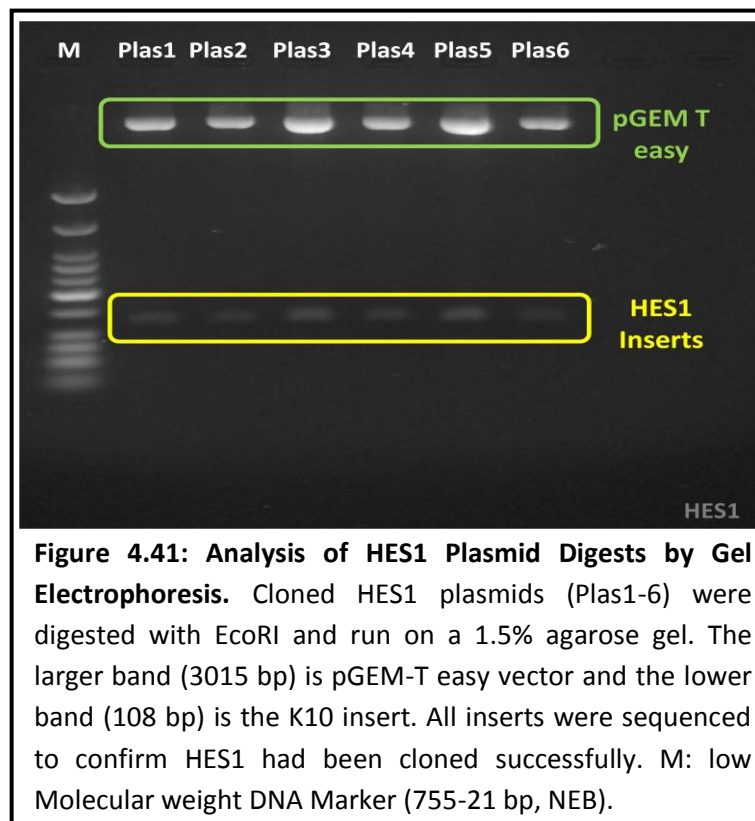
Standard PCRs were carried out to investigate the expression of HES1, HES5, HES7, HEY1, HEY2 and HEYL in HaCaT cells during proliferation (low Ca^{2+}) and differentiation (high Ca^{2+}). cDNA was prepared by reverse transcription of total RNA extracted from the relevant cells (see **Chapter 2** for details). PCR were run at an annealing temperature of 60°C for 35 cycles, the products separated on 3% NuSieve plus 1% agarose gels (see **Table 4.3** for details) and DNA visualised under UV light in the presence of ethidium bromide.

HES1 amplicons showed as relatively strong bands across the whole gel, changing throughout the experiment (**Figure 4.40**). Thus, levels were similar in proliferating HaCaT cells (low Ca²⁺ KGM) and differentiating cells (high Ca²⁺ KGM). The amplicons were sequenced to confirm their identity as products of the HES1 gene. The level of expression was highest in the D4, D4+1 and D4+3 cultures and these were selected for cloning.



Figure 4.40: Expression of HES1 in HaCaT cell differentiation. HES1 primers (p1, p2R) produced an amplicon of 108 bp with cDNA from HaCaT keratinocytes. Levels were low in early proliferation (D2) but increased later (D4) and in differentiating cells (D4+1, D4+3 and D4+10). Products separated on a 3% NuSieve plus 1% agarose gel. Human K14 (HK14) primers (p55, p56R) used as a positive control (amplicon 266bp). All PCR products were confirmed by sequencing. M (DNA Marker) = ϕ x174 DNA +Hae III.

HES1 PCR products were inserted into pGEM-T easy vectors by ligation and then cloned in bacterial cells (see **Chapter 2** for details). Bacterial clones were selected, grown in bulk and the plasmids purified using a Qiagen plasmid Miniprep kit. The HES1 inserts were released by restriction enzyme digestion (Eco RI) and analysed by electrophoresis on 1.5% agarose gels (**Figure 4.41**).



HES1 Plasmid 5 was selected to make a set of serial dilutions (300,000 to 30 copies) for qPCR. The calculations were done as before (see **Chapter 2** for details) and all the dilutions are given in **Table 4.28**.

Table 4.28: Serial Dilutions of HES1 Plasmid 5 for qPCR. Sterile nuclease free H₂O was used as the diluent.

Dilution	Source of plasmid DNA for dilution	Initial Conc. (g/μl)	Volume of plasmid DNA (μl)	Volume of diluents (μl)	Final Vol. (μl)	Final conc. (g/μl)	copy#
		C ₁	V ₁		V ₂	C ₂	
1	Stock	2.3e-7	10μl	990μl	1000μl	2.3e-9	N/A
2	Dilution1	2.3e-9	10μl	990μl	1000μl	2.3e-11	N/A
3	Dilution2	2.3e-11	10μl	990μl	1000μl	2.3e-13	N/A
4	Dilution3	2.3e-13	89.26μl	10.74μl	100μl	2.05e-13	300,000
5	Dilution4	2.05e-13	10μl	90μl	100μl	2.05e-14	30,000
6	Dilution5	2.05e-14	10μl	90μl	100μl	2.05e-15	3000
7	Dilution6	2.05e-15	10μl	90μl	100μl	2.05e-16	300
8	Dilution7	2.05e-16	10μl	90μl	100μl	2.05e-17	30

HES1 expression was measured in HaCaT cell cultures by qPCR and both the copy number and fold change relative to the initial culture conditions (Day 1-3, varies between difference experiments) were calculated. The HES1 standard dilution series was run at the same time as the experimental samples and this data was used to calculate the copy number from the individual sample Ct values (number of cycles to reach the threshold). The HES1 dilution series data was analysed first and a standard curve drawn. The amplification plot (**Figure 4.42**) of the HES1 dilution series showed evenly spaced curves (fluorescence vs cycle number) and each dilution was shown in a different colour (blue = 300,000; red= 30,000; green = 3,000; grey = 300 and yellow = 30 copies).

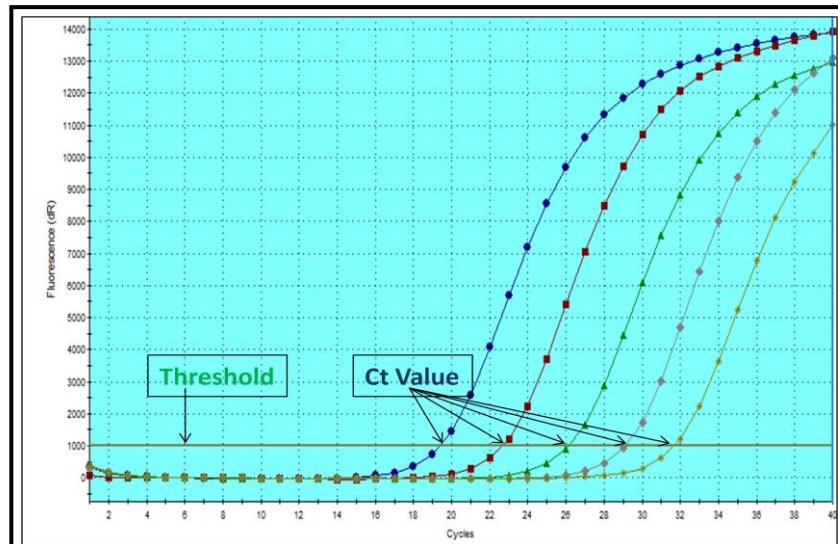


Figure 4.42: Amplification Plot of *HES1* Plasmid serial dilutions. Data calculated by MxPro Software. Each coloured line represents fluorescence with different *HES1* copy numbers. Blue line represents 300,000 copies, red (30,000), green (3,000), grey (300) and yellow (30). The distance between each fluorescence amplification plot was constant (about 4 cycles starting at 20 cycles) indicating the PCR reaction was efficient.

As the dilution increased, the threshold copy number (Ct value) increased and this data can be used to calculate a standard curve of Ct value versus copy number. The Ct values for the *HES1* dilution series ranged from 18 to 32 and this produced a linear plot (**Figure 4.43**) with an efficiency of 92.0% (ideal = 100%), an Rsq (R^2) value of 0.996 (ideal = 1.000) and a slope of -3.351 (ideal = -3.2 to -3.6). This represents a very good standard curve for *HES1* and this was used to estimate the copy number in experimental samples from the measured Ct value.

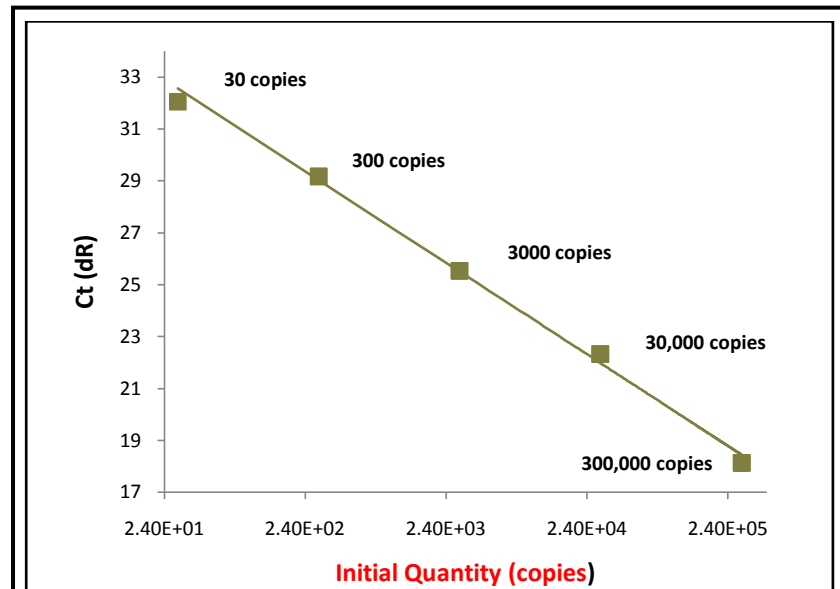


Figure 4.43: Standard Curve of HES1 Plasmid Dilution Series. The Ct value was plotted against copy number and the efficiency of the PCR reaction estimated as 92.0% (calculated from the slope which was -3.531). The Rsq (R^2) value was 0.996 indicating the data is a close fit to the linear line as plotted. The scale on the x-axis does not signify the copy number at each data point.

The data from 5 consecutive qPCR experiments with HES1 primers and HaCaT cell cDNA was then analysed using the HES1 standard curve and INSTAT software. This analysed the raw qPCR data using different statistical methods such as Tukey-Kramer Multiple Comparison Test and One-way Analysis of Variance (ANOVA). This software was used to analyse the HES1 experimental data in two different ways: initially calculating the level of HES1 expression in relation to copy number and then calculating the fold change in expression relative to one set of culture conditions (**Table 4.29**). Proliferating cultures (3D and 6D in low calcium medium) did have a reasonable number of HES1 transcripts (average of 28,779 and 92,130 respectively) but cultures that

showed distinct stratification and cornification (16D in low calcium and all high calcium cultures) showed greater levels of HES1 (105,000 – 795,000 copies). The data is given for individual experiments as well as an overall average value (**Table 4.29**).

Table 4.29: HES1 Gene Expression (Copy Number) during HaCaT Cell Culture. Data for 5 experiments showed almost the same general trend with an increase in HES1 expression as the cultures differentiated. There was a significant increase in copy number as cells differentiated (16D, 6D+3, 6D+6, and 6D+10) relative to proliferating cultures (3D, 6D).

Experiment	3D	6D	16D	6D+3	6D+6	6D+10
1	28,000	15,110	27,090	24,790	7,685	23,700
2	24,250	10,950	30,330	34,990	67,060	23,490
3	4,137	36,370	123,000	346,600	65,070	112,100
4	60,180	357,300	718,900	795,000	647,500	428,100
5	27,330	40,920	105,000	325,600	307,800	391,700
Average	28,779	92,130	200,864	305,396	219,023	195,818

In terms of fold change, the increase in HES1 expression during differentiation represented a 3.18 (min) to 13.92 (max) fold increase over the level observed in 3D cultures (**Table 4.30**).

Table 4.30: HES1 Gene Expression (Fold Change) in HaCaT Cell Cultures. HES1 gene expression increased gradually while cells were proliferating (6D average 4.7 fold) but much larger increases were seen as cells differentiated (10.8-26.9 fold on average). Fold change data was expressed relative to 3D culture levels and average values of 5 experiments are shown in blue.

Experiment	3D	6D	16D	6D+3	6D+6	6D+10
1	1.0	5.94	11.95	13.21	10.76	7.11
2	1.0	1.5	3.84	11.91	11.26	14.33
3	1.0	3.44	3.32	17.94	7.83	3.03
4	1.0	3.83	5.35	7.74	8.84	6.51
5	1.0	8.79	29.73	83.78	15.73	27.10
Average	1.0	4.7	10.83	26.91	10.88	11.61

The range of values in different experiments varied widely but the overall trend was similar. Comparisons were made between levels of HES1 expression at each time point in the HaCaT culture experiments using the Tukey-Kramer Multiple Comparison Test (**Table 4.31**). Values of q less than 2.691 were not statistically significant (ns). In all cases when comparing cultures that showed signs of differentiation with proliferating cultures (either 3D or 6D), the increases observed were not statistically significant, generally due to the large variance in the individual values. Larger numbers of cultures would have to be analysed to get a robust set of average data values.

Table 4.31: Comparison of HES1 Expression Levels (Copy Number) in Different HaCaT Cultures. The mean difference in copy number between the cultures compared was calculated and Q values assigned (values of Q <2.000 were not significant, ns).

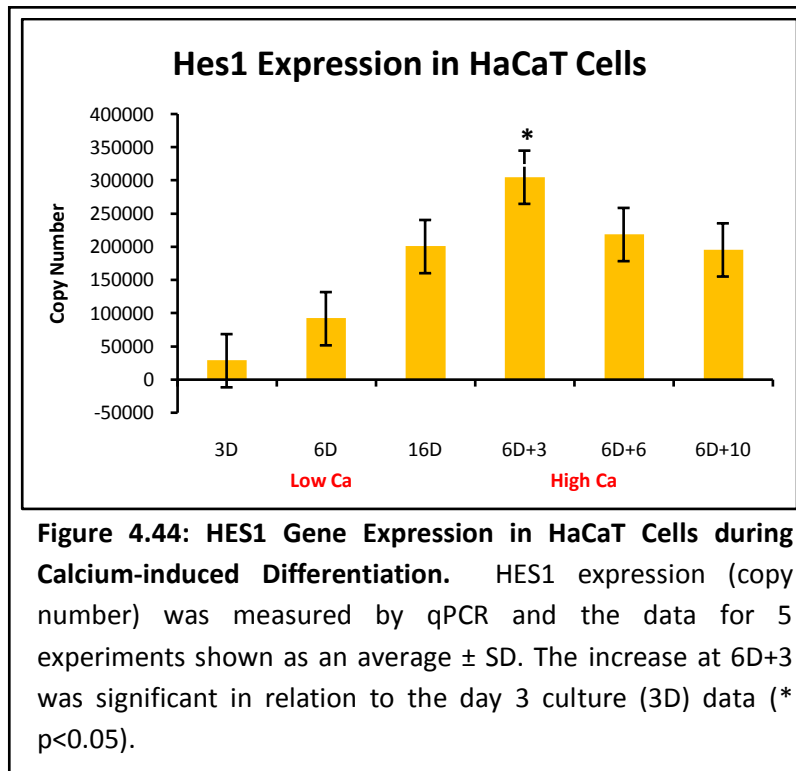
Comparison	Mean Difference	Q	P value
3D vs 6D	-63,351	0.6162	ns P>0.05
3D vs 16D	-172,085	1.674	ns P>0.05
3D vs 6D+3	-276,617	2.691	* P<0.05
3D vs 6D+6	-190,244	1.850	ns P>0.05
3D vs 6D+10	-167,039	1.625	ns P>0.05
6D vs 16D	-108,734	1.058	ns P>0.05
6D vs 6D+3	-213,266	2.074	* P<0.05
6D vs 6D+6	-126,893	1.234	ns P>0.05
6D vs 6D+10	-103,688	1.009	ns P>0.05
16D vs 6D+3	-104,532	1.017	ns P>0.05
16D vs 6D+6	-18,159	0.1766	ns P>0.05
16D vs 6D+10	5,046	0.04908	ns P>0.05
6D+3 vs 6D+6	86,373	0.8401	ns P>0.05
6D+3 vs 6D+10	109,578	1.006	ns P>0.05
6D+6 vs 6D+10	23,205	0.2257	ns P>0.05

Interestingly, the data expressed as fold change in HES1 expression levels was significant (**Table 4.32**). This was also analysed using the Tukey-Kramer Multiple Comparison Test and values of q that were 5.398 or greater were significant ($p < 0.05$) and larger values (>7.281) were very significant ($p < 0.001$). This analysis did show that the levels of HES1 observed in 6D+3 and 6D+6 cultures was significantly higher than the level in proliferating cells in low calcium medium (3D and 6D).

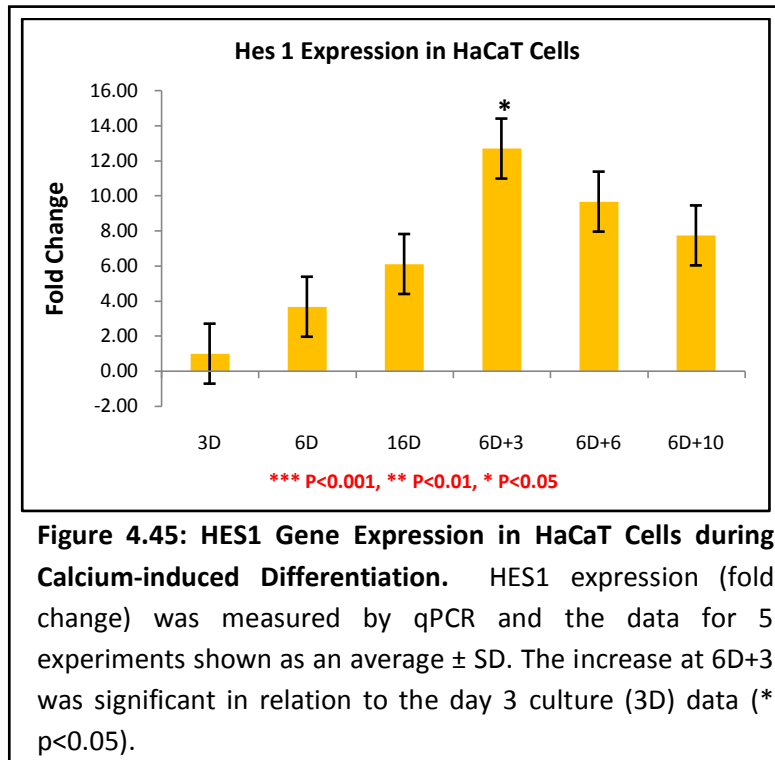
Table 4.32: Comparison of HES1 Expression Levels (Fold Change) in HaCaT Cultures. The mean difference in HES1 fold change between certain cultures was compared and where the value of Q was greater than 4.195, the difference were significant ($p < 0.05$).

Comparison	Mean Difference	Q	P value
3D vs 6D	-2.678	1.667	ns $P > 0.05$
3D vs 16D	-5.115	3.184	ns $P > 0.05$
3D vs 6D+3	-11.700	7.283	* $P < 0.05$
3D vs 6D+6	-8.672	5.398	ns $P > 0.05$
3D vs 6D+10	-6.745	4.199	ns $P > 0.05$
6D vs 16D	-2.437	1.517	ns $P > 0.05$
6D vs 6D+3	-9.023	5.616	ns $P > 0.05$
6D vs 6D+6	-5.995	3.732	ns $P > 0.05$
6D vs 6D+10	-4.068	2.532	ns $P > 0.05$
16D vs 6D+3	-6.585	4.099	ns $P > 0.05$
16D vs 6D+6	-3.557	2.214	ns $P > 0.05$
16D vs 6D+10	-1.630	1.015	ns $P > 0.05$
6D+3 vs 6D+6	3.028	1.885	ns $P > 0.05$
6D+3 vs 6D+10	4.955	3.084	ns $P > 0.05$
6D+6 vs 6D+10	1.927	1.200	ns $P > 0.05$

The copy number data for HES1 expression in different HaCaT cultures was made into a bar chart and the standard deviation (SD) was shown for each value as well as the significance relative to 3D cultures (**Figure 4.44**). Low levels of HES1 expression were found in early cultures in low calcium medium (3D & 6D) but while levels in cultures that had stratified and differentiated (16D, 6D+3, 6D+6, 6D+10) were higher, none of the values was statistically significant.

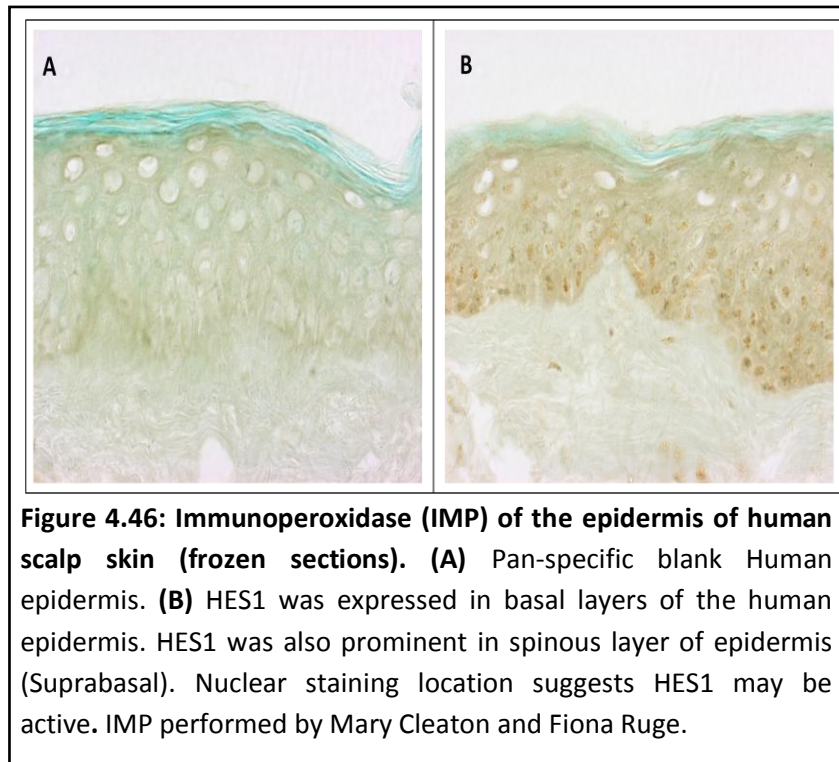


Expressing the HES1 data as fold change produced a bar chart with the same overall trends but higher levels of significance (**Figure 4.45**). The increases that were significant were those in late differentiation (6D+3 and 6D+6) as these were greater than 12 fold over the levels seen in the 3D cultures ($p < 0.001$ and $p < 0.05$ respectively).



Overall, HES1 was not expressed at a constant level in cultured HaCaT keratinocytes undergoing calcium-induced differentiation. Levels were higher in differentiating cells and in some cases this was significant.

The qPCR data did not agree with preliminary work on Hes-1 protein expression using immunoperoxidase (IMP) and immunofluorescence (IMF). While the available antibodies were not always of high titre, expression of HES1 appeared more prominent in basal layer of epidermis (**Figure 4.46**).



Observations of HES1 expression indicated that the notch pathway is active in HaCaT cells but a specific link with proliferation or differentiation was not apparent.

Several problems were encountered with the HES5 (p1, p2R) PCR primers and HaCaT cell cDNA. Not all PCRs gave a product but where a product was obtained, this was the correct size and sequence (**Figure 4.47**). However, the PCR generated HES5 DNA failed to clone properly and inserts released after cloning were not the correct size and were of random sequence (**Figures 4.48**). HES5 cloning was repeated several times but none of the attempts was successful.

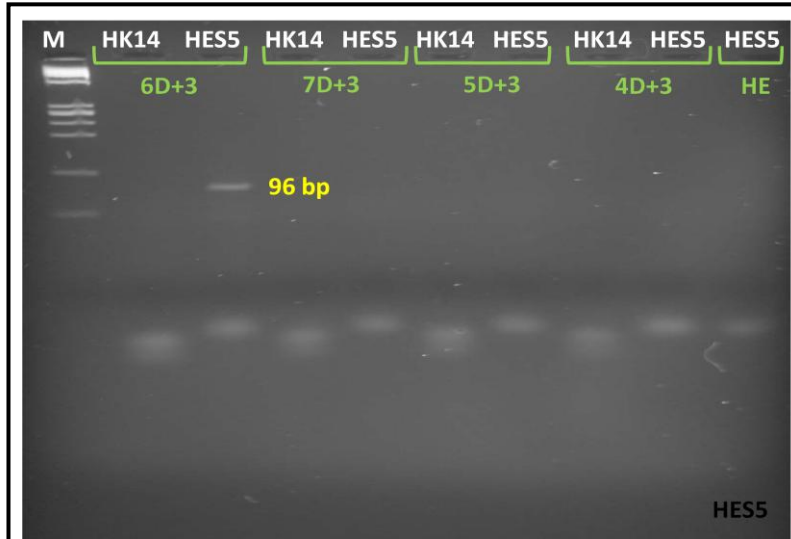
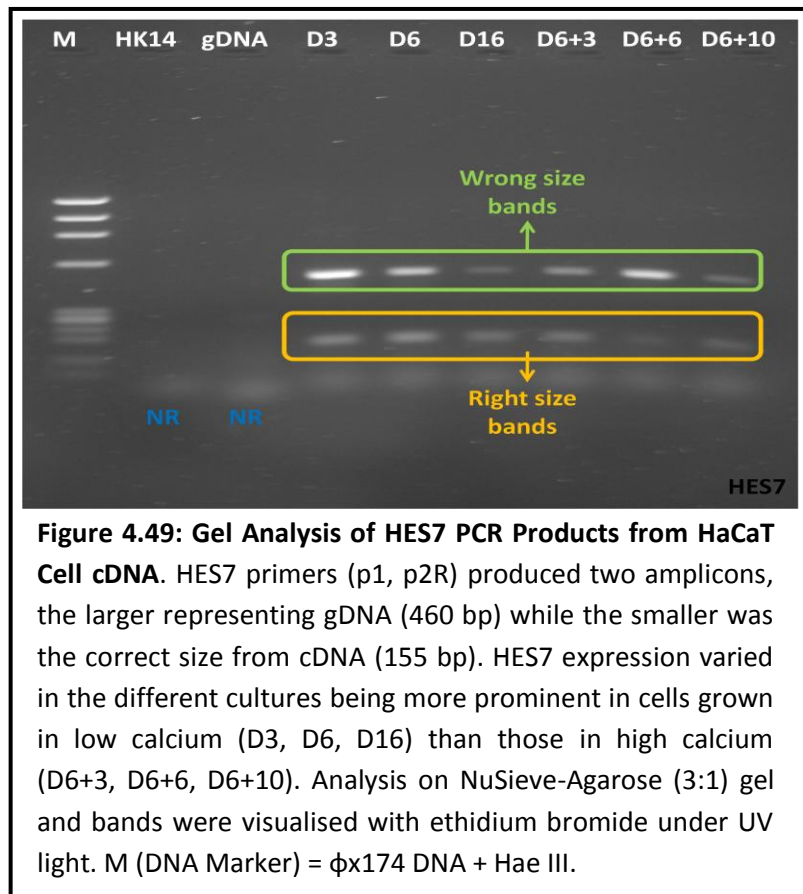


Figure 4.47: HES5 Expression in HaCaT Cells. HES5 primers (p1 & p2R) produced a single PCR amplicon (96 bp) with cDNA from HaCaT cells (high calcium cultures: 6D+3, 7D+3, 5D+3 and 4D+3). K14 control primers (HK14p55, p57R) produced no product and a HES5 product was only found in one set of cultures (6D+3) and not in human epidermis (HE). Analysis on Nusieve:Agarose (3:1) gel (M (DNA Marker) = ϕ x174 DNA + Hae III and bands visualised with ethidium bromide under UV light.



Figure 4.48: Analysis of HES5 Plasmid Digested with EcoRI. Cloned HES5 plasmids (Plas1-6) were digested with EcoRI and run on a 1.5% agarose gel. The larger band (3,015 bp) is pGEM-T easy vector (blue) but the lower band is too large for HES5. Inserts were sequenced and were not HES5. M: low molecular weight DNA Marker (755-21 bp).

Problems were also experienced with HES7. The PCR primers used (p1, p2R) produced two amplicons of different size (**Figure 4.49**), the larger of which was from genomic DNA (460 bp) and the smaller, the correct cDNA amplicon (155 bp). This genomic contamination meant that the PCR products were no good for cloning and there was not sufficient time to repeat the experiments with better samples of HaCaT cell cDNA.



Thus, only HES1 data was generated by qPCR and further work would be needed to optimise the primers and PCR conditions to obtain good levels of HES5 and HES7 so these could be cloned and further investigated.

PCRs were then run with HEY1 primers (p3, p4R) using cDNA from HaCaT cell cultures. Standard PCR conditions (58°C annealing and 35 cycles) were used and the HEY1 amplicons (181 bp) were run on a 1.5% agarose gel. In addition, their identity was confirmed by sequence analysis. However, only very low levels of HEY1 were found in HaCaT cells (**Figure 4.50**) and the highest levels appeared to be in moderately confluent cultures in low calcium medium (6D).

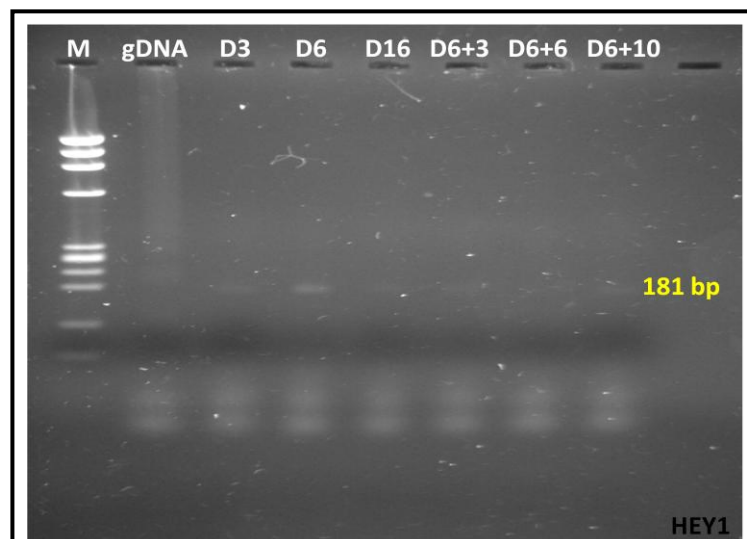


Figure 4.50: HEY1 Expression in HaCaT Cells. HEY1 primers (p3 & p4R) produced a single PCR amplicon (181 bp) from cDNA. No gDNA product was found (583 bp) and the level of HEY1 expression was very faint in all samples: (low calcium: D3, D6, D16 and high calcium: D6+3, D6+6, D6+10). Analysis was on a 1.5% agarose gel and bands were visualised with ethidium bromide under UV light. M (Marker DNA) = ϕ x174 DNA + Hae III.

The very low levels of HEY1 PCR product obtained meant this PCR product was difficult to clone. This was repeated twice but no clones of the HEY1 gene product were obtained. Results with HEY2 and HEYL were similar. Only low levels of PCR product were obtained using cDNA from HaCaT cells but the products were correct (confirmed by sequencing). Also, there did appear to be some changes in expression level at different times in culture but insufficient material was obtained for cloning (**Figures 4.51 and 4.52**) so no further work was done with HEY2 and HEYL.

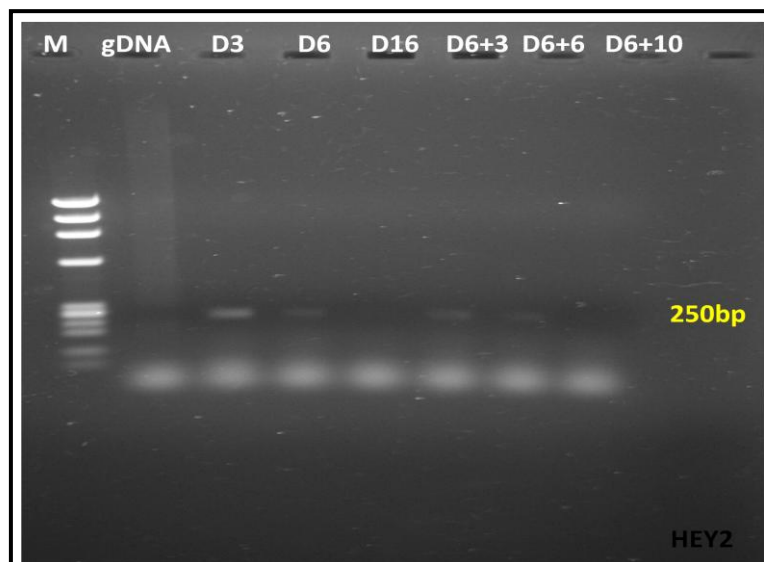
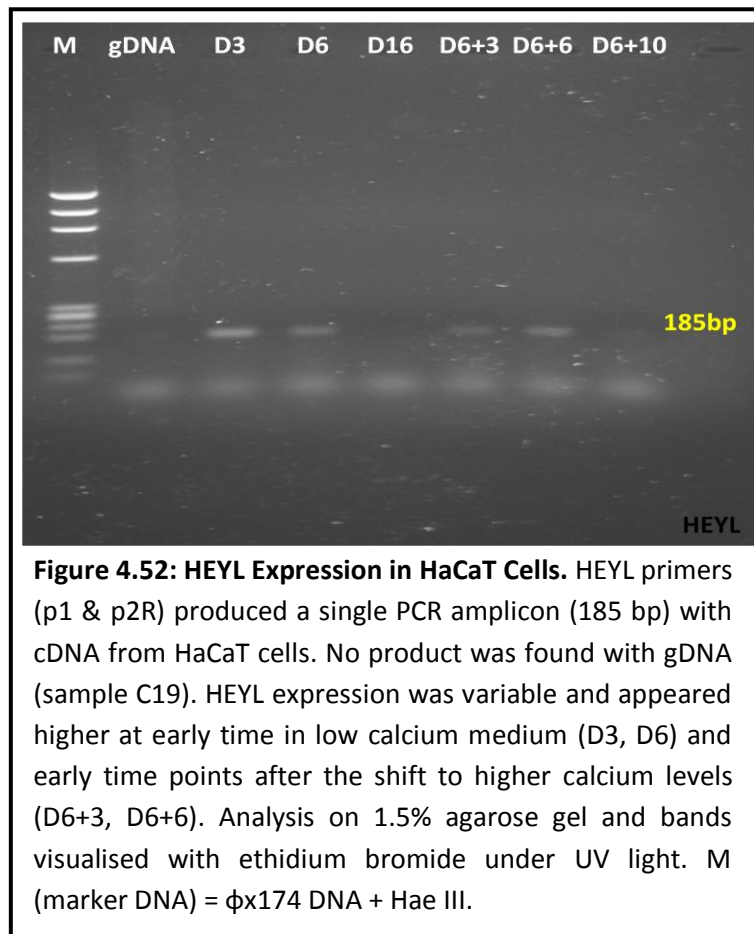


Figure 4.51: HEY2 Expression in HaCaT Cell Cultures. HEY2 primers (p3 & p4R) produced a single PCR amplicon (250 bp) with cDNA from HaCaT cells. However, no product was obtained from a gDNA sample (C19). The level of HEY2 expression varied and was higher in early low calcium cultures (D3) and at early time points after shifting to high calcium (D6+3, D6+6). Analysis on 1.5% agarose gel and bands visualised with ethidium bromide under UV light. M (marker DNA) = ϕ x174 DNA + Hae III.



4.5 Summary

It is clear from the research literature that cultured keratinocytes grown in low calcium medium do exhibit many properties of epidermal basal cells, including proliferation and the ability to undergo terminal differentiation. The structural and biochemical changes that occur during terminal differentiation can be re-iterated in cultured keratinocytes and the process observed does closely resemble that occurring *in vivo*. The expression of terminal differentiation markers such as keratin K10 provides a good indicator of which

cells are differentiating but this does not necessarily mean that all cellular signalling systems are behaving the same way in cell cultures as they are *in vivo*. Thus, while some changes did appear to be significant in differentiating HaCaT cells and these could be related to changes observed *in vivo*, many of the observations failed to reach significance and more work is required to obtain a more complete set of data on notch signalling pathways in HaCaT cells.

The data obtained from this project suggested that Notch receptors, ligands and target genes differ when comparing keratinocyte proliferation and calcium-induced differentiation in HaCaT cells. While expression levels of Notch3, JAG1, JAG2, DLL1 and HES1 differed between cells growing in low and high calcium, the differences were often variable in different cultures which prevented the average data from being statistically significant. Levels of HES1 expression were much higher in terms of copy number than the other genes examined but high standard deviation in the data prevented any of the changes from being significant (**Figure 4.53**). Notch receptor and ligand levels were much lower and DLL1 levels were the lowest.

When the data was expressed in terms of fold change (**Figure 4.54**), HES1 and K10 did show significantly higher levels in differentiating cells than in proliferating cells. As HES1 is a notch signalling responsive gene, this would

indicate that notch signalling is active during terminal differentiation of HaCaT cells.

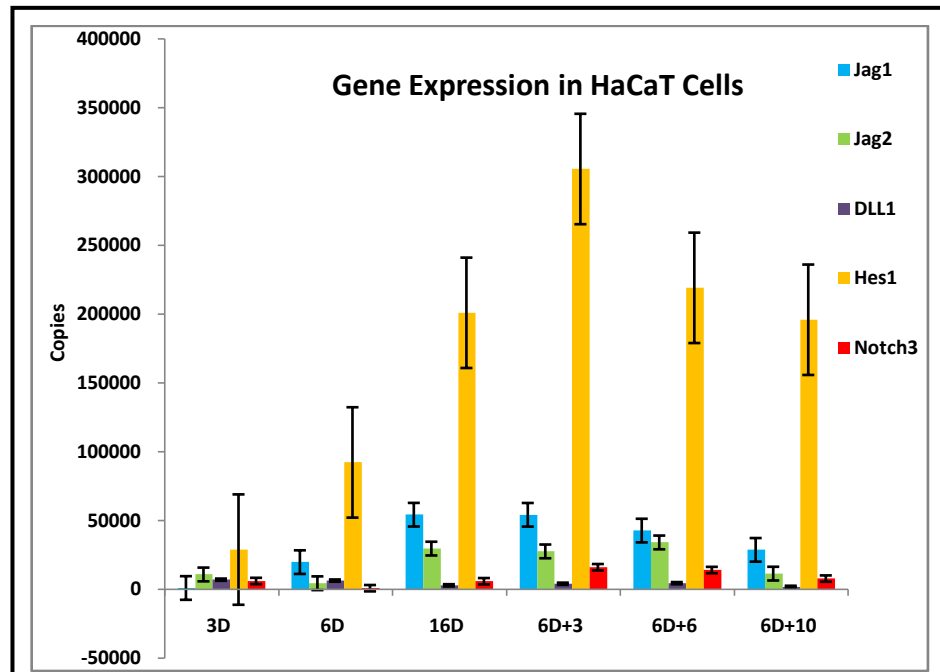


Figure 4.53: Expression of JAG1, JAG2, DLL1, HES1 and Notch3 in HaCaT Cells during Calcium-Induced Differentiation. Relative copy number for all Notch family genes examined (JAG1, blue; JAG2, green; DLL1, purple; HES1, yellow and Notch3, red). qPCR data was analysed using MxPro software. HES1, JAG1 and JAG2 expression increased in low calcium medium (6D, 16D) with a further increase during calcium-induced differentiation (6D+3, 6D+6). Notch3 levels were much lower but a similar trend was observed. Little change was apparent in DLL1 levels.

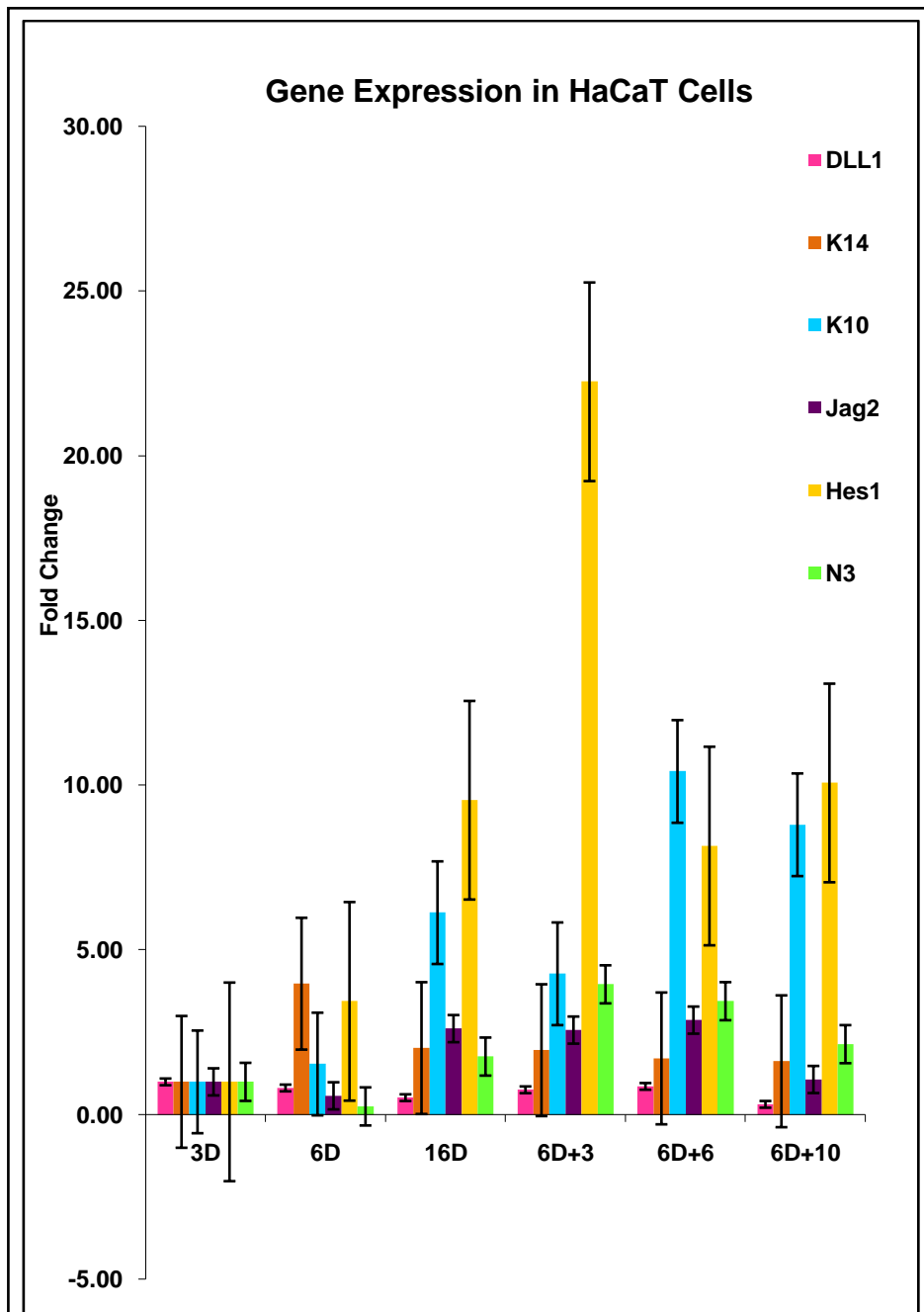


Figure 4.54: Expression Levels of *DLL1*, *K14*, *K10*, *JAG2*, *HES1* and *NOTCH3* in HaCaT Cells during Calcium-Induced Differentiation. All qPCR measurements were made in triplicate and analysed using MX3000 software. Total RNA was isolated from HaCaT cells at different stages of differentiation, converted to total cDNA and used qPCR. The fold change relative to 3 day cultures was then calculated.

CHAPTER 5:

Discussion and Conclusions

5.1 Discussion

This study has examined Notch signalling during the switch from epidermal proliferation to terminal differentiation *in vitro*. This was done by observing the expression of notch receptors, ligands and target genes at the mRNA level in immortalized human keratinocyte cultures (HaCaT). It examined changes in gene expression using PCR based methods (standard PCR, RT-PCR and qPCR) as well as having to clone and sequence various notch receptor, ligand and target gene probes. Levels of notch receptors, ligands and target genes at different time points in calcium-induced keratinocyte differentiation were examined in the HaCaT cell culture model. In addition, the results were compared to earlier preliminary work done in the laboratory that was largely based on protein methods (IMP, IMF, SDS-PAGE and western blotting).

Notch signalling is considered a highly conserved pathway essential for cell fate determination in embryonic development but less is known about the function in adult tissues. Human epidermis is regulated by notch signalling and this is required for the maintenance of stem cells, for proliferation and for differentiation into mature keratinocytes

(*Blanpain et al, 2006*). However, some details of how this complex terminal differentiation programme is regulated in keratinocytes still remain unclear (*Nickoloff et al., 2002*). While notch signalling in human epidermis may initially promote differentiation, loss of notch signalling in the skin may potentiate skin tumour development or result in a defect of interfollicular epidermal differentiation (*Rangarajan et al., 2001 and Nicolas et al., 2003*). However, there is still very little evidence of any dynamic regulatory function of notch signalling in terms of epidermal differentiation.

Several studies have examined notch signalling in human epidermis at the protein level. *Lowell et al* (2000) suggested that Notch1 was expressed in all living epidermal cells throughout differentiation but delta 1 was confined to the basal layer. On the other hand, *Wilson and Radtke* (2006) provided evidence that mRNA encoding Notch1-3 was expressed in the basal layer of human epidermis. *Estrach et al* (2008) also detected suprabasal expression of JAG1 and JAG2. In addition, *Powell et al* (1998) detected expression of Notch1 and JAG1 at the protein level in hair follicles with Notch1 expression in the bulb and ORS while JAG2 was restricted to the bulb and basal layer of the ORS.

In this project, a detailed study of notch receptors, ligands and target genes was made a human keratinocyte cell line (HaCaT) and where possible the results related back to earlier results obtained on human epidermis.

As part of this study, it was necessary to clone PCR generated cDNA probes of the genes being studied so that standard curves could be generated for each gene so that quantitative assessment of the copy number could be made by qPCR. In total probes were cloned for two Notch receptors (Notch1 and Notch3), three ligands (DLL1, JAG1 and JAG2) and one target gene (HES1) as well as the keratins (K10 and K14) required to define the level of differentiation in the HaCaT cells.

When the project began, there were few published papers that investigated Notch1 expression in human adult epidermis. *Okuyama* and colleagues (2008) reported that Notch1 was differentially localized in various layers of hair follicles, a finding largely supported by *Powell et al* (1998) who detected Notch1 expression in the hair bulb and ORS of the hair follicle. This concurred with the findings of *Watt et al* (2008) suggesting that notch receptors are expressed at the base of the hair follicle. Notch1 was also thought to be up-regulated in suprabasal layers

of interfollicular epidermis (*Pan et al.*, 2004 and *Kopan and Weintraub*, 1993).

However, other work was contradictory and investigations by *Thelu et al* (2002) showed weak expression of Notch1 in differentiating skin. Similar results were also observed by *Dhouailly et al* (2000) and *Favier et al* (2000). Interestingly, *Blanpain et al* (2006) claimed that Notch1 expression was restricted to suprabasal layers of the epidermis while *Wilson and Radtke* (2006) suggested Notch1 was highly expressed in the basal layer, agreeing with observations by *Nickoloff et al* (2002) providing evidence for strong staining of the lower and middle layers of the epidermis.

In the present study, our evidence suggests that Notch1 has a somewhat uniform pattern of expression across the epidermis based on qPCR estimation of mRNA copy number. The data obtained with standard PCR was more variable and earlier obtained using Notch1 antibodies varied depending on which antibody was used. This implies that there was no significant change in Notch1 expression during the transition from proliferation to differentiation in HaCaT cell cultures. Thus, our evidence suggests that Notch1 may be required to maintain

the epidermal phenotype but it is unlikely that signalling via Notch1 is driving the shift from epidermal proliferation to differentiation.

Less work has been published on Notch3 expression in human epidermis. *Wilson and Radtke (2006)* suggested that mRNA levels were high in basal cells and lower in suprabasal cells. Similar observations were reported by *Thelu et al (2002)* but *Blanpain et al (2006)* claimed that Notch3 expression was restricted to suprabasal cells agreeing with earlier evidence from *Nickoloff et al (2002)*. In this study, Notch3 was expressed in mid and upper epidermal cells by immunoperoxidase staining. Our investigations of Notch3 showed predominant expression during epidermal differentiation rather than proliferation based on data from standard PCR and qPCR analysis confirmed this by showing there was a significant fourfold increase in copy number. Again these findings agree with some but not all of the earlier work on Notch3 expression. It is important to point out that there was no preliminary investigation of Notch3 as reliable antibodies were not available for western blotting and tissue immunofluorescence studies. The current work would suggest that Notch3 is likely to play a role switching human keratinocytes from proliferation to differentiation, agreeing with earlier work that suggests Notch3 may promote the switch towards terminal differentiation.

Previous studies on DLL1 expression have indicated that it is confined to basal cells. According to *Wilson and Radtke (2006)*, DLL1 mRNA levels are high in basal cells and appear to be mainly localised at the tip of dermal papillae. This observation agreed with earlier studies by *Thelu et al (2002)*, *Nickoloff et al (2002)*, *Pourquie (2000)* and *Lowell et al (2000)*. Our data showed that DLL1 expression was low in HaCaT cells and somewhat uniform across all the cultures (similar to Notch1). However, DLL1 expression was also variable in both low and high calcium cultures and no significant differences were found in qPCR experiments. This implies that DLL1 expression did not significantly change in relation to keratinocyte differentiation. These findings disagree with earlier published work that suggests DLL1 is localised to epidermal basal cells and more work is needed to reconcile these differences. However, it still remains unclear how DLL1 expression in the human epidermis is initiated or maintained and what role this has in notch signalling.

Preliminary investigations on DLL4 expression showed that while this was expressed in pancreatic tissue, there was no expression in human epidermis or HaCaT cell cultures. Thus, this ligand does not play a role in notch signalling in human epidermal keratinocytes.

Jagged 1 (JAG1) expression in human adult epidermis has been previously investigated. Thelu *et al* (2002) reported that JAG1 mRNA was found in proliferating cells and transcribed to a lesser extent in suprabasal differentiating cells. Wilson and Radtke (2006) supported this with their observation that JAG1 expression was confined to the basal layer. However, Nickoloff *et al* (2002) reported that JAG1 showed strong and diffuse staining from the basal layer to the lower suprabasal layers but there was no stain detectable in the granular layer. In contrast others reported that JAG1 expression increased as keratinocytes differentiated and levels were highest in the suprabasal layers (Blanpain *et al.*, 2006; Dotto, 2008 and Watt *et al.*, 2008). At the same time, Estrach *et al* (2006) reported JAG1 expression in suprabasal layers of upper ORS.

Our earlier research investigated JAG1 expression in the peripheral matrix cells of the hair bulb indicating a possible regulatory function in cell fate decisions during hair differentiation. In human epidermis, JAG1 was found at the cell periphery of basal, spinous and granular cells both by immunoperoxidase and immunofluorescence. However, clear differences appear to exist amongst all of this evidence and it is not clear how much of this variability is due to the use of different techniques. It is clear that JAG1 antibodies vary in the ability to stain

human epidermis and results at the protein level do not always concur with those at the mRNA level.

The current findings show that HaCaT cells expressed JAG1 uniformly throughout HaCaT cell culture. The qPCR data did highlight slight variations in JAG1 levels with a trend towards higher levels in differentiating cells but in terms of copy number, none of the findings were significant. In terms of fold change, comparisons of the early proliferating cells and the most differentiated cells did show a 5 fold significant difference, supporting the evidence that JAG1 levels are higher in differentiating cells. These findings suggest that JAG1 may contribute to the shift of keratinocytes from proliferation to differentiation but strong evidence for this suggestion is still not forthcoming.

There is very little published work on JAG2 expression in human adult epidermis. Nickoloff et al (2002) did include JAG2 in his study but found weak to undetectable staining in suprabasal cells and concluded that the antibody was not working well enough. Preliminary work done in the laboratory on JAG2 was variable and poor due to the lack of good reagents. The only antibody that did work well gave strong suprabasal staining of human epidermis but this was later found to cross-react with

K10 making the data worthless (Dr. P.E. Bowden, unpublished data). The current research on JAG2 levels in HaCaT cell cultures showed similar findings to JAG1. In overall terms, the level of expression did not change much in the different culture conditions but the qPCR data did show a 2 fold increase of JAG2 in differentiating cells but again this was not significant. Thus, while there was a trend for JAG2 levels of expression to be higher in differentiating keratinocytes, the data was not conclusive so the role played by JAG2 is currently unclear. Thus, further investigations are required on JAG2 expression to obtain a better understanding of the nature of JAG2 function in human epidermis.

Notch target genes have received less attention and the only research published at the beginning of this study was restricted to investigations of the hair follicle. Blanpain *et al* (2006) reported that HES1 was expressed in the inner root sheath (IRS) during hair follicle development. In addition, Ambler and Watt (2007) found that HES1 expression was low in telogen and high in the matrix of mouse hair bulbs.

Preliminary work done in the laboratory had already established that HES1, HES5 and HEY1 were expressed in HaCaT cells. However, these

target genes were difficult to in human epidermis. HES1 was detected at the protein level in human epidermis using IMP but again the antibodies were poor and the data not conclusive. However, the current work with qPCR found high levels of HES1 expression in cultured HaCaT cells that were differentiating and levels were significantly above those measured in proliferating cultures. These findings imply that HES1 is up-regulated in HaCaT cells during the induction of terminal differentiation. This provides good evidence for notch signalling and from the present data, it would appear that the molecules involved in this signalling pathway are Notch3, JAG1 and JAG2. However, these results are far from conclusive and more research is needed to confirm if this signalling pathway is indeed active in differentiating keratinocytes. The other notch target genes (HES5, HES7, HEY1, HEY2, and HEYL) provided no data due to various technical difficulties and this work needs to be repeated at later date.

Even though several epidermal markers were used as controls in our study of keratinocyte differentiation in a HaCaT cell culture model, the expression of Notch receptors, ligands and target genes was more variable than anticipated, This raises the question as to whether the HaCaT cell culture model was mimicking normal keratinocytes or not. Despite trying to standardise the HaCaT cells cultures and keep the extraction of total RNA and making of cDNA as reproducible as possible,

some variation in expression was inevitable. Nevertheless, HaCaT cells currently remain the best choice of system to study human epidermis.

More studies still need to be done and a better clarity between the data obtained at the protein level and that obtained at the mRNA levels needs to be sought. Other approaches are also needed including the use of other keratinocytes (e.g. Ntert, primary cells) and other methods such as siRNA knock down of notch receptors and ligands. Once knocked down, the effect on the target genes and on keratinocyte differentiation can be assessed.

5.2 Conclusions

It is well documented that Notch signalling pathways are essential for the normal development of human tissues and that they are involved in manipulating cell fate, survival, cell proliferation and differentiation. Despite recent efforts, many questions concerning notch signalling and the skin remain obscure. More work is needed on establishing which pathway components are required for normal epidermal growth and differentiation and what receptor-ligand interactions are required. The importance of non-canonical signalling and the effect of *cis* and *trans* interactions cannot be underestimated.

The two main points where notch signalling could influence human epidermis are at the basal-spinous interface and then again at the level of the granular layer where a host of late differentiating events are taking place. The HaCaT cell model as used in these studies has focused on the switch from a basal to suprabasal phenotype and studies of later differentiation would require more advanced systems such as the organotypic culture system.

Studies have also linked another signalling pathway (Wnt) to epidermal differentiation. Interestingly, DLL1 and JAG1 are both transcriptional targets of canonical Wnt signalling (Estrach et al, 2006). Thus, it is likely that Notch and Wnt signalling pathways may integrate together to influence self renewal, proliferation survival, suppression of cell fate commitment and lineage determination. Therefore, it would also be interesting to investigate how notch ligands impact on other signalling pathways.

In the coming years, notch signalling pathways may become a major focus in terms of delivering therapy to patients with skin disorders. Biological therapies are gathering pace and having many successful outcomes so understanding the role of notch signalling in the human epidermis may be of potential benefit to patients with disorder of keratinisation such as eczema and psoriasis. This will remain a major challenge for future research.

References

1. Acar, M., H. Jafar-Nejad, et al. (2008). "Rumi is a CAP10 domain glycosyltransferase that modifies notch and is required for notch signalling." Cell **132**(2): 247-258.
2. Amagai, M. and J. R. Stanley (2011). "Desmoglein as a Target in Skin Disease and Beyond." J Invest Dermatol.
3. Ambler, C. A. and F. M. Watt (2007). "Expression of notch pathway genes in mammalian epidermis and modulation by beta-catenin." Developmental Dynamics **236**(6): 1595-1601.
4. Andl, T., K. Ahn, et al. (2004). "Epithelial Bmpr1a regulates differentiation and proliferation in postnatal hair follicles and is essential for tooth development." Development **131**(10): 2257-2268.
5. Artavanis-Tsakonas, S., M. D. Rand, et al. (1999). "Notch signalling: Cell fate control and signal integration in development." Science **284**(5415): 770-776.
6. Barai, N. D., S. T. Boyce, et al. (2008). "Improved barrier function observed in cultured skin substitutes developed under anchored conditions." Skin Research and Technology **14**(4): 418-424.
7. Baron, M. (2003). "An overview of the Notch signalling pathway." Seminars in Cell & Developmental Biology **14**(2): 113-119.
8. Bianchi, S., M. T. Dotti, et al. (2006). "Physiology and pathology of notch signalling system." Journal of Cellular Physiology **207**(2): 300-308.
9. Bickenbach, J. R. and K. L. Grinnell (2004). "Epidermal stem cells: interactions in developmental environments." Differentiation **72**(8): 371-380.
10. Bikle, D. D., A. Ratnam, et al. (1996). "Changes in calcium responsiveness and handling during keratinocyte differentiation - Potential role of the calcium receptor." Journal of Clinical Investigation **97**(4): 1085-1093.
11. Bikle, D. D. (2004). "Vitamin D regulated keratinocyte differentiation." Journal of Cellular Biochemistry **92**(3): 436-444.

12. Blanpain, C., W. E. Lowry, et al. (2006). "Canonical Notch signalling functions as a commitment switch in the epidermal lineage." Genes & Development **20**(21): 3022-3035.
13. Blanpain, C. and E. Fuchs (2006). "Epidermal stem cells of the skin." Annual Review of Cell and Developmental Biology **22**: 339-373.
14. Boukamp, P., R. T. Petrussevska, et al. (1988). "Normal Keratinisation in a Spontaneously Immortalized Aneuploid Human Keratinocyte Cell-Line." Journal of Cell Biology **106**(3): 761-771.
15. Bowden, P.E., Quinlan, R., Breitkreutz, D., Fusenig, N.E. (1984). "Proteolytic modification of acidic and basic keratins during terminal differentiation of mouse and human epidermis." Europ. J. Biochem. **142**: 29-36.
16. Bowden, P.E., Stark, H.-J., Breitkreutz, D., Fusenig, N.E. (1987). "Expression and modification of keratins during terminal differentiation of mammalian epidermis." Current Topics in Developmental Biology. The Molecular and Developmental Biology of Keratins. Chapter 22: 35-68. Academic Press, Orlando, Florida, USA.
17. Bray, S. J. (2006). "Notch signalling: a simple pathway becomes complex." Nature Reviews Molecular Cell Biology **7**(9): 678-689.
18. Bruckner, K., L. Perez, et al. (2000). "Glycosyltransferase activity of fringe modulates notch-delta interactions." Nature **406**(6794): 411-415.
19. Chitnis, A. (2006). "Why is Delta endocytosis required for effective activation of Notch?" Developmental Dynamics **235**(4): 886-894.
20. Christophers, E.H., K. Wolff, et al. (1974). "Formation of Epidermal-Cell Columns." Journal of Investigative Dermatology **62**(6): 555-559.
21. Chu AC and Morris JF. The keratinocyte. In: Bos JD, ed. Skin Immune System (SIS): Cutaneous Immunology and Clinical Immunodermatology, 3rd edition. Boca Raton, FL: CRC Press, 2005:77–99.
22. Chuong, C., L. Ma, et al. (2002). "Cycling alopecia in Msx2 mutants: Defects in hair shaft differentiation and hair cycling." Journal of Investigative Dermatology **119**(1): 285.

23. Clayton, E., D. P. Doupe, et al. (2007). "A single type of progenitor cell maintains normal epidermis." Nature **446**: 185-189.
24. Collin, C., R. Moll, et al. (1992). "Characterization of Human Cytokeratin-2, an Epidermal Cytoskeletal Protein Synthesized Late During Differentiation." Experimental Cell Research **202**(1): 132-141.
25. Collins, C. A., K. Kretzschmar, et al. (2011). "Reprogramming adult dermis to a neonatal state through epidermal activation of beta-catenin." Development **138**(23): 5189-5199.
26. Compton, C. C., J. M. Gill, et al. (1989). "Skin Regenerated from Cultured Epithelial Autografts on Full-Thickness Burn Wounds from 6 Days to 5 Years after Grafting - a Light, Electron-Microscopic and Immunohistochemical Study." Laboratory Investigation **60**(5): 600-612.
27. De Luca, M., G. Pellegrini, et al. (1994). "Role of integrins in cell adhesion and polarity in normal keratinocytes and human skin pathologies." Journal of Dermatology (Tokyo) **21**(11): 821-828.
28. Del Alamo, D. and F. Schweisguth (2009). "Notch Signalling: Receptor cis-Inhibition To Achieve Directionality." Current Biology **19**(16): R683-R684.
29. Delva, E., D. K. Tucker, et al. (2009). "The Desmosome." Cold Spring Harbour Perspectives in Biology **1**(2).
30. Demehri, S., A. Turkoz, et al. (2009). "Epidermal Notch1 Loss Promotes Skin Tumorigenesis by Impacting the Stromal Microenvironment." Cancer Cell **16**(1): 55-66.
31. Denecker, G., P. Ovaere, et al. (2008). "Caspase-14 reveals its secrets." Journal of Cell Biology **180**(3): 451-458.
32. Deyrieux, A. F. and V. G. Wilson (2007). "In vitro culture conditions to study keratinocyte differentiation using the HaCaT cell line." Cytotechnology **54**(2): 77-83.
33. Dotto, G. P. (2008). "Notch tumor suppressor function." Oncogene **27**(38): 5115-5123.
34. Dunwoodie, S. L., D. Henrique, S.M. Harrison and R.S. Boddington. (1997). "Mouse Dll3: a novel divergent Delta gene which may complement the function of other delta homologues

- during early pattern formation in the mouse embryo." Development **124**: 3065-3076.
35. Eckert, R. L. and E. A. Rorke (1989). "Molecular-Biology of Keratinocyte Differentiation." Environmental Health Perspectives **80**: 109-116.
 36. Egan, S. E., B. St-Pierre, et al. (1998). "Notch receptors, partners and regulators: From conserved domains to powerful functions." Current Topics In Microbiology And Immunology **228**: 273-324.
 37. Epstein, W. L. and H. I. Maibach (1965). "Cell Renewal in Human Epidermis." Archives of Dermatology **92**(4): 462- 468.
 38. Estrach, S., R. Cordes, et al. (2008). "Role of the Notch ligand Delta1 in embryonic and adult mouse epidermis." Journal of Investigative Dermatology **128**(4): 825-832.
 39. Fan, H. R. and P. A. Khavari (1999). "Sonic hedgehog opposes epithelial cell cycle arrest." Journal of Cell Biology **147**(1): 71-76.
 40. Favier, B., I. Fliniaux, et al. (2000). "Localisation of members of the notch system and the differentiation of vibrissae hair follicles: Receptors, ligands, and fringe modulators." Developmental Dynamics **218**(3): 426-437.
 41. Fior, R. and D. Henrique (2009). "'Notch-Off': a perspective on the termination of Notch signalling." International Journal of Developmental Biology **53**(8-10): 1379-1384.
 42. Fisher, A. and M. Caudy (1998). "The function of hairy-related bHLH repressor proteins in cell fate decisions." Bioessays **20**(4): 298-306.
 43. Fischer, A. and M. Gessler (2007). "Delta-Notch-and then? Protein interactions and proposed modes of repression by Hes and Hey bHLH factors." Nucleic Acids Research **35**: 4583-4596.
 44. Fiuza, U. M. and A. M. Arias (2007). "Cell and molecular biology of Notch." Journal of Endocrinology **194**: 459-474.
 45. Fiuza, U. M., T. Klein, et al. (2010). "Mechanisms of Ligand-Mediated Inhibition in Notch Signalling Activity in Drosophila." Developmental Dynamics **239**(3): 798-805.
 46. Fortini, M. E. (2001). "Notch and Presenilin: a proteolytic mechanism emerges." Current Opinion in Cell Biology **13**(5): 627-634.

47. Fortini, M. E. (2009). "Notch Signalling: The Core Pathway and Its Posttranslational Regulation." Developmental Cell **16**(5): 633-647.
48. Fryer, C. J., J. B. White, et al. (2004). "Mastermind recruits CycC : CDK8 to phosphorylate the notch ICD and coordinate activation with turnover." Molecular Cell **16**(4): 509-520.
49. Fuchs, E., T. Tumbar, et al. (2004). "Socializing with the neighbours: Stem cells and their niche." Cell **116**(6): 769-778.
50. Fuchs, E. (2008). "Skin stem cells: rising to the surface." Journal of Cell Biology **180**(2): 273-284.
51. Fuchs, E. and V. Horsley (2008). "More than one way to skin." Genes & Development **22**(8): 976-985.
52. Gallico, G. G., N. E. Oconnor, et al. (1984). "Permanent Coverage of Large Burn Wounds with Autologous Cultured Human Epithelium." New England Journal of Medicine **311**(7): 448-451.
53. Gambardella, L. and Y. Barrandon (2003). "The multifaceted adult epidermal stem cell." Current Opinion in Cell Biology **15**(6): 771-777.
54. Gandarillas, A. and F. M. Watt (1997). "c-Myc promotes differentiation of human epidermal stem cells." Genes & Development **11**(21): 2869-2882.
55. Garrod, D. and M. Chidgey (2008). "Desmosome structure, composition and function." Biochimica Et Biophysica Acta-Biomembranes **1778**(3): 572-587.
56. Ginsberg, M. H., A. Partridge, et al. (2005). "Integrin regulation." Current Opinion in Cell Biology **17**(5): 509-516.
57. Gordon, W. R., D. Vardar-Ulu, et al. (2009). "Effects of S1 Cleavage on the Structure, Surface Export, and Signalling Activity of Human Notch1 and Notch2." Plos One **4**(8).
58. Gray, G. E., R. S. Mann, et al. (1999). "Human ligands of the Notch receptor." American Journal of Pathology **154**(3): 785-794.
59. Green, K. J. and C. L. Simpson (2007). "Desmosomes: New Perspectives on a Classic." J Invest Dermatol **127**(11): 2499-2515.

60. Haines, N. and K. D. Irvine (2003). "Glycosylation regulates notch signalling." Nature Reviews Molecular Cell Biology **4**(10): 786-797.
61. Hall, P. A. and F. M. Watt (1989). "Stem-Cells - the Generation and Maintenance of Cellular Diversity." Development **106**(4): 619-633.
62. Haltiwanger, R. S. and P. Stanley (2002). "Modulation of receptor signalling by glycosylation: fringe is an O-fucose- β 1,3-N-acetylglucosaminyltransferase." Biochimica et Biophysica Acta (BBA) - General Subjects **1573**(3): 328-335.
63. Hansson, E. M., U. Lendahl, et al. (2004). "Notch signalling in development and disease." Seminars in Cancer Biology **14**(5): 320-328.
64. Hoath, S. B. and D. G. Leahy (2003). "The organization of human epidermis: Functional epidermal units and phi proportionality." Journal of Investigative Dermatology **121**(6): 1440-1446.
65. Heitzler, P. and P. Simpson (1993). "Altered Epidermal Growth Factor-Like Sequences Provide Evidence for a Role of Notch as a Receptor in Cell Fate Decisions." Development **117**(3): 1113-1123.
66. Heuss, S. F., D. Ndiaye-Lobry, et al. (2008). "The intracellular region of Notch ligands Dll1 and Dll3 regulates their trafficking and signalling activity." Proceedings of the National Academy of Sciences of the United States of America **105**(32): 11212-11217.
67. Hubbard, E. J. A., G. Y. Wu, et al. (1997). "sel-10 a negative regulator of lin-12 activity in *Caenorhabditis elegans*, encodes a member of the CDC4 family of proteins." Genes & Development **11**(23): 3182-3193.
68. Huelsken, J., R. Vogel, et al. (2001). "beta-catenin controls hair follicle morphogenesis and stem cell differentiation in the skin." Cell **105**(4): 533-545.
69. Hurlbut, G. D., M. W. Kankel, et al. (2007). "Crossing paths with Notch in the hyper-network." Current Opinion in Cell Biology **19**(2): 166-175.
70. Ishii, K., S. M. Norvell, et al. (2001). "Assembly of desmosomal cadherins into desmosomes is isoform dependent." Journal of Investigative Dermatology **117**(1): 26-35.
71. Iso, T., G. Chung, et al. (2002). "HERP1 is a cell type-specific primary target of Notch." Journal of Biological Chemistry **277**(8): 6598-6607.

72. Iso, T., L. Kedes, et al. (2003). "HES and HERP families: Multiple effectors of the Notch signalling pathway." Journal of Cellular Physiology **194**(3): 237-255.
73. Iversen, L., C. Johansen, et al. (2005). "Signal transduction pathways in human epidermis." European Journal of Dermatology **15**(1): 4-12.
74. Izon, D. J., J. C. Aster, et al. (2002). "Deltex1 redirects lymphoid progenitors to the B cell lineage by antagonizing Notch1." Immunity **16**(2): 231-243.
75. Jones, P. H. and F. M. Watt (1993). "Separation of human epidermal stem cells from transit amplifying cells on the basis of differences in integrin function and expression." Cell **73**(4): 713-724.
76. Jones, P. H., S. Harper, et al. (1995). "Stem cell patterning and fate in human epidermis." Cell **80**(1): 83-93.
77. Katoh, M. and M. Katoh (2007). "Integrative genomic analyses on HES/HEY family: Notch-independent HES1, HES3 transcription in undifferentiated ES cells, and Notch-dependent HES1, HES5, HEY1, HEY2, HEYL transcription in foetal tissues, adult tissues, or cancer." International Journal of Oncology **31**(2): 461-466.
78. Kaur, P., A. Li, et al. (2004). "Keratinocyte stem cell assays: An evolving science." Journal of Investigative Dermatology Symposium Proceedings **9**(3): 238-247.
79. Kaur, P. and C. S. Potten (2011). "The interfollicular epidermal stem cell saga: sensationalism versus reality check." Experimental Dermatology **20**(9): 697-702.
80. Kidd, S., M. R. Kelley, et al. (1986). "Sequence of the Notch Locus of *Drosophila-Melanogaster* - Relationship of the Encoded Protein to Mammalian Clotting and Growth-Factors." Molecular and Cellular Biology **6**(9): 3094-3108.
81. Kidd, S. and T. Lieber (2002). "Furin cleavage is not a requirement for *Drosophila* Notch function." Mechanisms of Development **115**(1-2): 41-51.
82. Kopan, R. and H. Weintraub (1993). "Mouse Notch - Expression in Hair-Follicles Correlates with Cell Fate Determination." Journal of Cell Biology **121**(3): 631-641.

83. Kopan, R. and M. X. G. Ilagan (2009). "The Canonical Notch Signalling Pathway: Unfolding the Activation Mechanism." Cell **137**(2): 216-233.
84. Koster, M. I. and D. R. Roop (2008). "Sorting out the p63 signalling network." Journal of Investigative Dermatology **128**(7): 1617-1619.
85. Le Borgne, R., A. Bardin, et al. (2005). "The roles of receptor and ligand endocytosis in regulating Notch signalling." Development **132**(8): 1751-1762.
86. Le Borgne, R. (2006). "Regulation of Notch signalling by endocytosis and endosomal sorting." Current Opinion in Cell Biology **18**(2): 213-222.
87. Lee, J. S., M. R. Kim, et al. (2010). "Expression Profiling of Calcium Induced Genes in Cultured Human Keratinocytes." Journal of Korean Medical Science **25**(4): 619-625.
88. Lechler, T. and E. Fuchs (2005). "Asymmetric cell divisions promote stratification and differentiation of mammalian skin." Nature **437**(7056): 275-280.
89. Lefort, K. and G. P. Dotto (2004). "Notch signalling in the integrated control of keratinocyte growth/differentiation and tumor suppression." Seminars in Cancer Biology **14**(5): 374-386.
90. Lefort, K., A. Mandinova, et al. (2007). "Notch1 is a p53 target gene involved in human keratinocyte tumor suppression through negative regulation of ROCK1/2 and MRCK alpha kinases." Genes & Development **21**: 562-577.
91. Lehmann, R., F. Jimenez, et al. (1983). "On the Phenotype and Development of Mutants of Early Neurogenesis in *Drosophila-Melanogaster*." Wilhelm Roux's Archives of Developmental Biology **192**(2): 62-74.
92. Louvi, A. and S. Artavanis-Tsakonas (2006). "Notch signalling in vertebrate neural development." Nature Reviews Neuroscience **7**(2): 93-102.
93. Lowell, S., P. Jones, et al. (2000). "Stimulation of human epidermal differentiation by Delta-Notch signalling at the boundaries of stem-cell clusters." Current Biology **10**(9): 491-500.

94. Lowell, S. and F. M. Watt (2001). "Delta regulates keratinocyte spreading and motility independently of differentiation." Mechanisms of Development **107**(1-2): 133-140.
95. Lyle, S., M. Christofidou-Solomidou, et al. (1998). "The C8/144B monoclonal antibody recognizes cytokeratin 15 and defines the location of human hair follicle stem cells." Journal of Cell Science **111**: 3179-3188.
96. Mackenzie I.C. (1970). "Relationship between Mitosis and Ordered Structure of Stratum Corneum in Mouse Epidermis." Nature **226**(5246): 653-&.
97. Mackenzie, I. C. (1975). "Ordered Structure of Epidermis." Journal of Investigative Dermatology **65**(1): 45-51.
98. Mackenzie, I. C. (1997). "Retroviral transduction of murine epidermal stem cells demonstrates clonal units of epidermal structure." Journal of Investigative Dermatology **109**(3): 377-383.
99. Massari, M. E. and C. Murre (2000). "Helix-loop-helix proteins: Regulators of transcription in eukaryotic organisms." Molecular and Cellular Biology **20**(2): 429-440.
100. Matoltsy, A. G. (1975). "Desmosomes, Filaments, and Keratohyalin Granules - Their Role in Stabilization and Keratinisation of Epidermis." Journal of Investigative Dermatology **65**(1): 127-142.
101. Micallef, L., F. Belaubre, et al. (2009). "Effects of extracellular calcium on the growth-differentiation switch in immortalized keratinocyte HaCaT cells compared with normal human keratinocytes." Experimental Dermatology **18**(2): 143-151.
102. Michel, M., N. Torok, et al. (1996). "Keratin 19 as a biochemical marker of skin stem cells in vivo and in vitro: Keratin 19 expressing cells are differentially localized in function of anatomic sites, and their number varies with donor age and culture stage." Journal of Cell Science **109**: 1017-1028.
103. Miller, A. C., E. L. Lyons, et al. (2009). "cis-Inhibition of Notch by Endogenous Delta Biases the Outcome of Lateral Inhibition." Current Biology **19**(16): 1378-1383.
104. Morgan, T. H. (1917). "The theory of the gene." American Naturalist **51**: 513-544.

105. Moriyama, M., A. D. Durham, et al. (2008). "Multiple roles of notch signalling in the regulation of epidermal development." Developmental Cell **14**(4): 594-604.
106. Morris, R. J., S. M. Fischer, et al. (1985). "Evidence That the Centrally and Peripherally Located Cells in the Murine Epidermal Proliferative Unit Are 2 Distinct Cell-Populations." Journal of Investigative Dermatology **84**(4): 277-281.
107. Murre, C., G. Bain, et al. (1994). "Structure and Function of Helix-Loop-Helix Proteins." Biochimica Et Biophysica Acta-Gene Structure and Expression **1218**(2): 129-135.
108. Nickoloff, B. J., J. Z. Qin, et al. (2002). "Jagged-1 mediated activation of notch signalling induces complete maturation of human keratinocytes through NF-kappa B and PPAR gamma." Cell Death and Differentiation **9**(8): 842-855.
109. Nicolas, M., A. Wolfer, et al. (2003). "Notch1 functions as a tumor suppressor in mouse skin." Nature Genetics **33**(3): 416-421.
110. Oda, Y., C. L. Tu, et al. (2000). "The calcium sensing receptor and its alternatively spliced form in murine epidermal differentiation." Journal of Biological Chemistry **275**(2): 1183-1190.
111. Ohtsuka, T., M. Ishibashi, et al. (1999). "Hes1 and Hes5 as Notch effectors in mammalian neuronal differentiation." Embo Journal **18**(8): 2196-2207.
112. Okajima, T. and K. D. Irvine (2002). "Regulation of Notch Signalling by O-Linked Fucose." Cell **111**(6): 893-904.
113. Okajima, T., A. G. Xu, et al. (2005). "Chaperone activity of protein O-fucosyltransferase 1 promotes Notch receptor folding." Science **307**(5715): 1599-1603.
114. Okuyama, R., H. Tagami, et al. (2008). "Notch signalling: Its role in epidermal homeostasis and in the pathogenesis of skin diseases." Journal of Dermatological Science **49**(3): 187-194.
115. Pan, Y. H., M. H. Lin, et al. (2004). "Gamma-secretase functions through notch signalling to maintain skin appendages but is not required for their patterning or initial morphogenesis." Developmental Cell **7**(5): 731-743.
116. Panelos, J. and D. Massi (2009). "Emerging role of Notch signalling in epidermal differentiation and skin cancer." Cancer Biology & Therapy **8**(21): 1986-1993.

117. Pellegrini, G., E. Dellambra, et al. (2001). "p63 identifies keratinocyte stem cells." Proceedings of the National Academy of Sciences of the United States of America **98**(6): 3156-3161.
118. Petrof, G., J. E. Mellerio, et al. (2011). "Desmosomal genodermatoses." British Journal of Dermatology **166**(1): 36-45.
119. Pillai, S., D. D. Bikle, et al. (1990). "Calcium Regulation of Growth and Differentiation of Normal Human Keratinocytes - Modulation of Differentiation Competence by Stages of Growth and Extracellular Calcium." Journal of Cellular Physiology **143**(2): 294-302.
120. Potten, C. S. (1974). "Epidermal Proliferative Unit - Possible Role of Central Basal-Cell." Cell and Tissue Kinetics **7**(1): 77-88.
121. Potten, C. S. and J. C. Bullock (1983). "Cell Kinetic-Studies in the Epidermis of the Mouse .1. Changes in Labelling Index with Time after Tritiated-Thymidine Administration." Experientia **39**(10): 1125-1129.
122. Potten, C. S. and R. J. Morris (1988). "Epithelial stem cells in vivo." Journal of cell science. Supplement **10**: 45-62.
123. Potten, C. S. and M. Loeffler (1990). "Stem-Cells - Attributes, Cycles, Spirals, Pitfalls and Uncertainties - Lessons for and from the Crypt." Development **110**(4): 1001-1020.
124. Poulson, D. F. (1945). "Chromosomal Control of Embryogenesis in Drosophila." American Naturalist **79**(783): 340-363.
125. Pourquie, O. (2000). "Skin development: Delta laid bare." Current Biology **10**(11): R425-R428.
126. Powell, B. C., E. A. Passmore, et al. (1998). "The Notch signalling pathway in hair growth." Mechanisms of Development **78**(1-2): 189-192.
127. Radtke, F., F. Schweisguth, et al. (2005). "The Notch /'gospel/'." EMBO Rep **6**(12): 1120-1125.
128. Rand, M. D., L. M. Grimm, et al. (2000). "Calcium depletion dissociates and activates heterodimeric notch receptors." Molecular and Cellular Biology **20**(5): 1825-1835.
129. Rangarajan, A., C. Talora, et al. (2001). "Notch signalling is a direct determinant of keratinocyte growth arrest and entry into differentiation." Embo Journal **20**(13): 3427-3436.

130. Ro, J., G. Odland, et al. (1964). "Hyperbaric Oxygen Therapy in Anaerobic Infection." Nordisk Medicin **72**: 1077-9.
131. Sasamura, T., H. O. Ishikawa, et al. (2007). "The O-fucosyltransferase O-fut1 is an extracellular component that is essential for the constitutive endocytic trafficking of Notch in Drosophila." Development **134**(7): 1347-1356.
132. Schallreuter, K. U. and J. M. Wood (1995). "The Human Epidermis." Proceedings of the Nutrition Society **54**(1): 191-195.
133. Scott, G. A. and L. A. Goldsmith (1993). "Homeobox Genes and Skin Development: A Review." J Invest Dermatol **101**(1): 3-8.
134. Seitz, C. S., H. Deng, et al. (1998). "NF-kappa B triggers cell cycle arrest in epidermis via specific induction of the cyclin-dependent kinase inhibitor p21(Cip1)." Journal of Investigative Dermatology **110**(4): 475-475.
135. Shutter, J. R., S. Scully, et al. (2000). "DII4, a novel Notch ligand expressed in arterial endothelium." Genes & Development **14**(11): 1313-1318.
136. Sporl, F., M. Wunderskirchner, et al. (2010). "Real-Time Monitoring of Membrane Cholesterol Reveals New Insights into Epidermal Differentiation." J Invest Dermatol **130**(5): 1268-1278.
137. Talora, C., A. F. Campese, et al. (2008). "Notch signalling and diseases: An evolutionary journey from a simple beginning to complex outcomes." Biochimica Et Biophysica Acta-Molecular Basis of Disease **1782**(9): 489-497.
138. Taniguchi, Y., Karlstrom H., et al. (2002). "Notch receptor cleavage depends on but not directly executed by presenilins." PNAS **99** (6): 4014-19.
139. Taylor, G., M. S. Lehrer, et al. (2000). "Involvement of Follicular Stem Cells in Forming Not Only the Follicle but Also the Epidermis." Cell **102**(4): 451-461.
140. Thelu, J., P. Rossio, et al. (2002). "Notch signalling is linked to epidermal cell differentiation level in basal cell carcinoma, psoriasis and wound healing." BMC Dermatol **2**: 7.
141. Tien, A.-C., A. Rajan, et al. (2009). "A Notch updated." Journal of Cell Biology **184**(5): 621-629.

142. Till, J. E. and E. A. McCulloch (1961). "Direct Measurement of Radiation Sensitivity of Normal Mouse Bone Marrow Cells." Radiation Research **14**(2): 213-&.
143. Tu, C. L., W. H. Chang, et al. (2001). "The extracellular calcium-sensing receptor is required for calcium-induced differentiation in human keratinocytes." Journal of Biological Chemistry **276**(44): 41079-41085.
144. Vassin, H., J. Vielmetter, et al. (1985). "Genetic Interactions in Early Neurogenesis of *Drosophila-Melanogaster*." Journal of Neurogenetics **2**(5): 291-308.
145. Wang, N. J., Z. Sanborn, et al. (2011). "Loss-of-function mutations in Notch receptors in cutaneous and lung squamous cell carcinoma." PNAS **108**: 17761-17766.
146. Wang, W. D. and G. Struhl (2004). "Drosophila epsin mediates a select endocytic pathway that DSL ligands must enter to activate notch." Development **131**(21): 5367-5380.
147. Wang, W. D. and G. Struhl (2005). "Distinct roles for Mind bomb, Neuralized and Epsin in mediating DSL endocytosis and signalling in *Drosophila*." Development **132**(12): 2883-2894.
148. Watt, F.M. (1989). "Terminal differentiation of epidermal keratinocytes." Current opinion in cell biology **1**(6): 1107-15.
149. Watt, F.M. and Driskell R.R. (2010). "The therapeutic potential of stem cells." Phil. Trans. R. Soc. B **365** (1537): 155-163
150. Watt, F. M., S. Estrach, et al. (2008). "Epidermal Notch signalling: differentiation, cancer and adhesion." Current Opinion in Cell Biology **20**(2): 171-179.
151. Wharton, K. A., K. M. Johansen, et al. (1985). "Nucleotide-Sequence from the Neurogenic Locus Notch Implies a Gene-Product That Shares Homology with Proteins Containing Egf-Like Repeats." Cell **43**(3): 567-581.
152. Wilson, A. and F. Radtke (2006). "Multiple functions of Notch signalling in self-renewing organs and cancer." Febs Letters **580**(12): 2860-2868.
153. Wu, L. and J. D. Griffin (2004). "Modulation of Notch signalling by mastermind-like (MAML) transcriptional co-activators and their

- involvement in tumorigenesis." Seminars in Cancer Biology **14**(5): 348-356.
154. Yin, L., O. C. Velazquez, et al. (2010). "Notch signalling: Emerging molecular targets for cancer therapy." Biochemical Pharmacology **80**(5): 690-701.
155. Yuspa, S. H., A. E. Kilkenny, et al. (1989). "Expression of Murine Epidermal Differentiation Markers Is Tightly Regulated by Restricted Extracellular Calcium Concentrations In vitro." Journal of Cell Biology **109**(3): 1207-1217.
156. Zhong, T. P., M. Rosenberg, et al. (2000). "Gridlock, an HLH Gene Required for Assembly of the Aorta in Zebra fish." Science **287**(5459): 1820-1824.
157. Zouboulis, C. C., J. Adjaye, et al. (2008). "Human skin stem cells and the ageing process." Experimental Gerontology **43**(11): 986-997.